Stress Response SCF Ubiquitin Ligase F-box Protein Fbx15 Controls Nuclear Co-repressor Localization and Virulence of the Opportunistic Human Fungal Pathogen *Aspergillus fumigatus*

Dissertation
for the award of the degree
"Doctor rerum naturalium"
Division of Mathematics and Natural Sciences
Georg-August-University Göttingen

within the doctoral program biology
of the Georg-August University School of Science (GAUSS)

submitted by
Bastian Jöhnk

from Eckernförde

Göttingen, 2016

Thesis Committee

Prof. Dr. Gerhard H. Braus, Department of Molecular Microbiology and Genetics, Georg-August University Göttingen.

Prof. Dr. Stefanie Pöggeler, Department of Genetics of Eukaryotic Microorganisms, Georg-August University Göttingen.

Members of the Examination Board

Reviewer:

Prof. Dr. Gerhard H. Braus, Department of Molecular Microbiology and Genetics, Georg-August University Göttingen.

Second Reviewer:

Prof. Dr. Stefanie Pöggeler, Department of Genetics of Eukaryotic Microorganisms, Georg-August University Göttingen.

Further members of the Examination Board:

Prof. Dr. Rolf Daniel, Department of Genomic and Applied Microbiology, Georg-August University Göttingen.

Prof. Dr. Ralf Ficner, Department of Molecular Structural Biology, Georg-August University Göttingen.

Jun.-Prof. Dr. Kai Heimel, Department of Molecular Microbiology and Genetics, Georg-August University Göttingen.

Prof. Dr. Michael S. Weig, Institute for Medical Microbiology, University Medical Center Göttingen.

Date of the oral examination: April 12th, 2016

Declaration

Hereby I declare that the Ph.D. Thesis entitled:

"Stress Response SCF Ubiquitin Ligase F-box Protein Fbx15 Controls Nuclear Co-repressor Localization and Virulence of the Opportunistic Human Fungal Pathogen *Aspergillus fumigatus*"

has been written independently with no other sources and aids than quoted.

Göttingen, 2016   Bastian Jöhnk

This work was accomplished in the group of Prof. Dr. Gerhard H. Braus, at the Department of Molecular Microbiology and Genetics, Institute of Microbiology and Genetics, Georg-August University Göttingen.

Parts of this work are published or under review for publication:

Jöhnk, B., Bayram, Ö., Valerius, O., Heinekamp, T., Jacobsen, I.D., and Braus G.H. (2016) SCF ubiquitin ligase F-box protein Fbx15 controls nuclear co-repressor localization, stress response and virulence of the human pathogen *Aspergillus fumigatus*. Under review.

Fajardo-Somera, R.A., **Jöhnk, B.**, Bayram, Ö., Valerius, O., Braus, G.H., and Riquelme, M. (2015) Dissecting the function of the different chitin synthases in vegetative growth and sexual development in *Neurospora crassa*. Fungal Genet Biol *75*, 30-45.

Terfrüchte, M., **Joehnk, B.**, Fajardo-Somera, R., Braus, G.H., Riquelme, M., Schipper, K., and Feldbrügge, M. (2014) Establishing a versatile Golden Gate cloning system for genetic engineering in fungi. Fungal Genet Biol *62*, 1-10.

Bayram, Ö., Bayram, Ö.S., Valerius, O., **Jöhnk, B.**, and Braus, G.H. (2012) Identification of protein complexes from filamentous fungi with tandem affinity purification. Humana Press *944*, 191-205.

Table of Contents

Abstract

Aspergillus fumigatus is the most prevalent cause for pulmonary infections in immuno-compromised patients. Virulence factors are often linked to developmental control mechanisms, which are often identified in the closely related model organism *Aspergillus nidulans*. This work presents the characterization of the F-box protein Fbx15 in *A. fumigatus*, which had been shown to have a crucial impact on development in *A. nidulans*. Deletion of *fbx15* resulted in severe growth defects under various stress conditions, including classical virulence factors like increased temperature, oxidative stress and amino acid starvation, whereas growth under standard conditions was not affected. Oxidative stress induces a transient peak of *fbx15* transcript expression leading to three-fold increased protein levels after 40 min. Fbx15 is a stable F-box protein with a half-life of more than 90 minutes. F-box proteins normally act as substrate adaptors for SCF E3 ubiquitin ligases. Fbx15 is phosphorylated during non-stress conditions and interacts with the Skp1/A linker subunit of SCF complexes, preferentially in smaller subpopulations in the cytoplasm. The phosphorylated form of Fbx15 preferentially incorporates into SCF complexes. Oxidative stress results in rapid dephosphorylation of Fbx15. Fbx15 variants, which are unable to be phosphorylated, interact with Skp1/A primarily in the nucleus. Fbx15 recruits three subunits of the COP9 signalosome and proteins involved in transcription, translation, signal transduction, morphology or metabolism. Fbx15 binds the Ssn6/SsnF subunit of the conserved Tup1/RcoA-Ssn6/SsnF co-repressor and is required for its nuclear localization. Dephosphorylated Fbx15 interacts with Ssn6/SsnF in the nucleus and Fbx15-SsnF mediated control of gene repression is required to reduce the biosynthesis of gliotoxin. *fbx15* deletion strains are unable to infect immunocompromised mice in a model of invasive aspergillosis, supporting that Fbx15 is essential for virulence. This work suggests that Fbx15 is not only part of SCF E3 ubiquitin ligases but carries a novel second molecular function, which includes the physical interaction with the co-repressor subunit Ssn6/SsnF and control of its localization. This dual function results in a crucial role for Fbx15 in the control of oxidative stress response, secondary metabolism and virulence in the opportunistic human pathogen *A. fumigatus*.

Zusammenfassung

Aspergillus fumigatus ist die häufigste Ursache für Lungeninfektionen in immunsuppri-
mierten Patienten. Virulenzfaktoren sind häufig an Kontrollmechanismen für Entwick-
lung gekoppelt, welche im verwandten Modellorganismus *Aspergillus nidulans* entdeckt
wurden. Diese Arbeit präsentiert die Charakterisierung des F-box Proteins Fbx15 in
A. fumigatus, welches einen starken Einfluss auf die Entwicklung in *A. nidulans* hat. Die
Deletion von *fbx15* resultierte in starken Wachstumsdefekten unter vielen Stress induzie-
renden Bedingungen, welche klassische Virulenz Faktoren beinhalten, wie erhöhte Tem-
peratur, oxidativer Stress und Aminosäuremangel, während das Wachstum unter Stan-
dardbedingungen nicht beeinflusst war. Oxidativer Stress induziert eine transiente
Erhöhung der *fbx15* Expression, welche nach 40 Minuten zu einer dreifach erhöhten Pro-
teinmenge führte. Fbx15 ist ein stabiles F-box Protein mit einer Halbwertszeit von
90 Minuten. Generell funktionieren F-box Proteine als Substratadapter für SCF-E3-
Ubiquitin-Ligasen. Fbx15 liegt unter normalen Bedingungen phosphoryliert vor und in-
teragiert mit der Skp1/A Untereinheit des SCF-Komplexes, vorzugsweise in kleineren
Subpopulationen im Zytoplasma. Phosphoryliertes Fbx15 wird bevorzugt in SCF-
Komplexe eingebaut. Oxidativer Stress führt zu einer schnellen Dephosphorylierung von
Fbx15. Fbx15 Varianten, welche nicht phosphoryliert werden können, interagieren mit
Skp1/A primär im Kern. Fbx15 rekrutiert drei Untereinheiten des COP9-Signalosoms und
Proteine welche in Transkription, Translation, Signalübertragung, Morphologie oder
Stoffwechsel involviert sind. Fbx15 bindet die Ssn6/F Untereinheit des konservierten
Ssn6/SsnF-Tup1/RcoA Co-Repressors und wird für dessen Kernlokalisation benötigt.
Dephosphoryliertes Fbx15 interagiert mit Ssn6/F im Kern und eine Fbx15-Ssn6/F be-
dingte Genrepression wird für die Reduzierung der Gliotoxin-Biosynthese benötigt. *fbx15*
Deletionsstämme sind nicht in der Lage immunsupprimierte Mäuse in einem Model für
invasive Aspergillose zu infizieren, was eine essentielle Funktion von Fbx15 für die Viru-
lenz bestätigt. Diese Arbeit zeigt, dass Fbx15 nicht nur Teil von SCF-E3-Ubiquitin-
Ligasen sein kann, sondern eine zweite neue molekulare Funktion aufweist, welche die
physische Interaktion mit der Co-Repressor Untereinheit Ssn6/F und dessen Lokalisa-
tionskontrolle beinhaltet. Diese duale Funktion resultiert in einer essentiellen Funktion
von Fbx15 für die Kontrolle der oxidativen Stressantwort, des Sekundärmetabolismus
und der Virulenz im opportunistischen Humanpathogen *A. fumigatus*.

Abbreviations

Δ	Deletion
λ	Wavelength
3-AT	3-amino-1,2,4-triazole
aa	Amino acid
Ala / A	Alanine
AMM	*Aspergillus* minimal medium
Asp / D	Aspartate
BiFC	Bimolecular fluorescence complementation
BLAST	Basic local alignment and search tool
bp	Base pairs
BSA	Bovine serum albumin
CBP	Calmodulin binding peptide
CCR	Carbon catabolite repression
CPA	Chronic pulmonary aspergillosis
CPC	Cross-pathway control
CRL	Cullin RING ligase
CSN	COP9-signalosome
C-sources	Carbon sources
C-terminal	Carboxy-terminal
DHN	1,8-dihydroxynaphthalene
DIC	Differential interference contrast
DNA	Deoxyribonucleic acid
DUB	Deubiquitinating enzyme
ER	Endoplasmic reticulum
ERAD	Endoplasmic reticulum-associated degradation
GFP	Green fluorescent protein
gDNA	Genomic deoxyribonucleic acid
GER	Germany
GPI	Glycosylphosphatidylinositol
GSH	Glutathione
GT	Gliotoxin
HECT	Homologous to the E6-AP carboxyl terminus
HPLC	High performance liquid chromatography
HRP	Horseradish peroxidase
IPA	Invasive pulmonary aspergillosis
IgG	Immunoglobulin G
JPN	Japan
kb	Kilo base pairs
kDa	Kilo Dalton

Lys / K	Lysine
LC	Liquid chromatography
M	Molar (mol/l)
m/z	Mass-to-charge ratio
Mb	Mega bases
min	Minute
mRNA	Messenger ribonucleic acid
MS	Mass spectrometry
NRPS	Non-ribosomal peptide synthetases
N-sources	Nitrogen sources
N-terminal	Amino-terminal
NLS	Nuclear localization signal
OE	Overexpression
ORF	Open reading frame
PAMP	Pathogen-associated molecular pattern
PCR	Polymerase chain reaction
PKA	cAMP-dependent protein kinase A
PTM	Posttranslational modification
RFP	Red fluorescent protein
RING	Really interesting new gene
RNA	Ribonucleic acid
ROI	Reactive oxygen intermediates
ROS	Reactive oxygen species
rpm	Revolution per minute
RT	Room temperature
SCF	SkpA/CulA/F-box
SEM	Scanning electron microscope
Ser / S	Serine
SOD	Superoxide dismutase
TAP	Tandem affinity purification
TEV	Tobacco etch virus
TF	Transcription factor
TMT	Tandem mass tag
Ub	Ubiquitin
UBD	Ubiquitin binding domain
UPS	Ubiquitin proteasome system
UTR	Untranslated region
v/v	Volume per volume
WT	Wild type
w/v	Weight per volume

Table of figures

List of tables

I   Introduction

1   The opportunistic human pathogen *Aspergillus fumigatus*

1.1   Biology of *A. fumigatus*

1.1.1   Nutritional versatility of the saprophytic mold *A. fumigatus*

The filamentous fungus *Aspergillus fumigatus* is a soilborne organism with a saprophytic life style. Its primary ecological niche is decaying plant material, which is found especially in composts and organic waste. A genome wide survey identified a large set of hydrolytic enzymes, encoded by the *A. fumigatus* genome, which are required for the degradation of plant cell wall oligomers (Miao et al., 2015; Tekaia and Latgé, 2005). Interestingly, comparable amounts of these enzyme families were also discovered in true phytopathogenic fungi like *Fusarium graminearum* or *Magnaporthe grisea*, corroborating the primary saprophytic mode of life for *A. fumigatus* (Perez-Nadales et al., 2014; Tekaia et al., 1999; Tekaia and Latgé, 2005). Therefore, *A. fumigatus* is considered to play an important role for the recycling of carbon and nitrogen sources (Adav et al., 2015; Bohlin et al., 2013; Brakhage and Langfelder, 2002; Wang et al., 2012).

A. fumigatus is a prototrophic organism and its recycling function is further illustrated by its high metabolic versatility. In the absence of its favored carbon-source glucose, *A. fumigatus* is able to utilize an extensive range of alternate carbon sources such as D-galactose, the pentoses L-arabinose and D-xylose or alcohols like glycerol and ethanol (Flipphi et al., 2009). Similarly, *A. fumigatus* is also able to utilize a variety of nitrogen-sources like nitrate, purines or amino acids, if the primary nitrogen sources ammonium, glutamate or glutamine are not accessible (Krappmann and Braus, 2005; Lee et al., 2013).

A. fumigatus is capable to synthesize all proteinogenic amino acids *de novo* (Amich et al., 2016). The biosynthesis of amino acids is an energy-consuming but also essential process, which is tightly controlled by a complex genetic network, called cross-pathway control (CPC). This system detects uncharged tRNAs, which finally leads to selective inhibition of a broad range of target genes, whereas the central activator of the CPC-system, CpcA remains active and coordinates the expression of hundreds of biosynthetic genes, leading to a global cellular response (Braus et al., 2006; Hoffmann et al., 2001; Sasse et al., 2008).

1.1.2   Asexual development and its effect on geographical distribution

A. fumigatus belongs to the most ubiquitously distributed fungi around the planet (Rocchi et al., 2015). A large survey of *A. fumigatus* isolates from Europe and the USA revealed that the fungus displays a very high genetic diversity, which could not be clustered to specific geographical regions (Debeaupuis et al., 1997). This phenomenon can be explained by its primary distribution route, which relies on the airborne spores, called conidia. The production of haploid, uninucleate conidiospores is the predominant form of reproductive development in *A. fumigatus* and requires the sequential activation of the transcription factors BrlA, AbaA and WetA (Park et al., 2012; Shin et al., 2015). During asexual propagation vegetative hyphae develop specialized foot-cells that mature into the conidiophore, the characteristic asexual reproductive structure of Aspergilli (Figure 1). Conidiophores are complex multicellular structures, which extend from the foot-cell with an elongated stalk that terminates in a clavate vesicle. The vesicle is covered with a single layer of green phialides that directly produces the green-pigmented conidia by mitotic division and subsequent constriction (Brakhage and Langfelder, 2002; Tao and Yu, 2011). This sets *A. fumigatus* apart from the model conidiophore of the closely related *A. nidulans*, that habours an additional specific cell-layer on the phialides called metulae, which produce the conidiospores (Yu, 2010). The small size of conidia of 2-3 μm facilitates their effective dispersal.

1.1.3   Characteristics of conidia

The asexual spores of filamentous fungi are long-term resting structures, which display a wide range of resistances against environmental stressors like heat, oxidative stress and desiccation (Hagiwara et al., 2014; Kwon-Chung and Sugui, 2013). Conidia are covered with a layer of hydrophobins, called the rodlet layer (Bayry et al., 2012; Beever and Dempsey, 1978). From the two hydrophobins that have been discovered so far in *A. fumigatus*, namely RodA and RodB, only RodA contributes to the conidial rodlet layer (Paris et al., 2003a; Wyatt et al., 2013). This proteinaceous structure seems to benefit the aerial dispersal of the spores, thus contributing to the wide distribution of *A. fumigatus* species. Below the rodlet layer the conidia are covered by a cell wall, which is characterized by an interwoven matrix of different glucan types, chitin and galactomannan (Amarsaikhan and Templeton, 2015; Hohl and Feldmesser, 2007; Samar et al., 2015; Valiante et al., 2015).
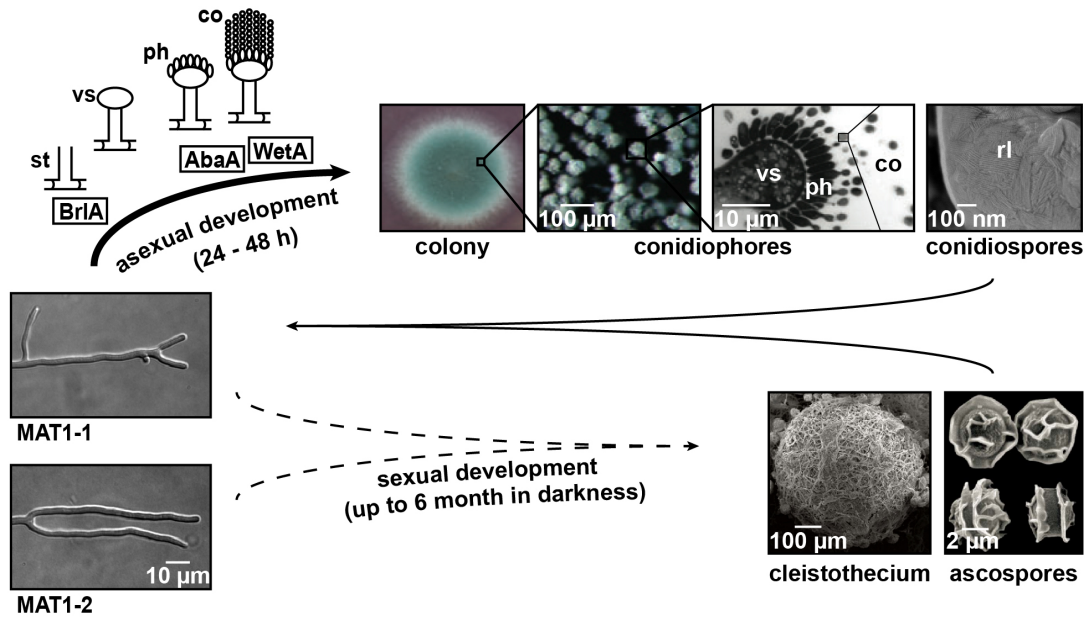
Figure 1: The life cycle of *A. fumigatus*. The primary developmental program of *A. fumigatus* is the asexual development (top). Vegetative hyphae form a stalk (st) with a terminal congealed vesicle (vs). Subsequently the vesicle is covered with a single layer of phialides (ph), which produce the conidiospores (co) via mitotic divisions. These developmental steps require the sequential action of the transcriptional activators BrlA, AbaA and WetA. Conidiospores are covered with bundles of the hydrophobin RodA, which build the characteristic rodlet layer (rl). Germination of conidiospores result in vegetative mycelium and developmental competence for another round of asexual development is achieved 16-20 hours after germination. In contrast sexual development is a rare and time-consuming event in *A. fumigatus*, which requires specialized media compositions and growth conditions as well as hyphal fusion with a compatible mating partner. The resulting fruiting body, called cleistothecium, is surrounded by a network of flattened hyphae and contains numerous asci, which inhabit the heat-resistant ascospores. SEM pictures of conidiophores and conidiospores from Tao et al., 2011 & Paris et al., 2003. SEM pictures of cleistothecium and ascospores from O'Gorman et al., 2009.

In addition the hyphal and conidial cell wall is decorated with a variety of glyco-sylphosphatidylinositol (GPI)-anchored proteins, which play a role in hyphal development and conidiation (Bruneau et al., 2001; Karkowska-Kuleta and Kozik, 2015). Furthermore, the cell wall of *A. fumigatus* harbors at least two types of pigments, called melanins. Melanins are secondary metabolites with a variety of protective functions against UV-light, reactive oxygen species (ROS) or elevated temperatures. One of the melanins produced by *A. fumigatus* is pyomelanin, a brown, water-soluble compound, which derives from the degradation of L-tyrosine and has protective functions against cell wall stress and ROS. The second pigment is 1,8-dihydroxynaphthalene (DHN)-melanin, which is responsible for the grey-green color of the conidia and also provides protection

against ROS (Heinekamp et al., 2012; Rambach et al., 2015; Schmaler-Ripcke et al., 2009; Sugareva et al., 2006).

1.1.4   The cryptic sexual cycle of *A. fumigatus*

For decades *A. fumigatus* was considered to propagate strictly asexually despite an early-discovered parasexual state. Parasexuality describes the fusion of haploid nuclei in a heterokaryon to form diploid nuclei, which finally undergo mitotic recombination during asexual sporulation (Stromnaes and Garber, 1963). Therefore, *A. fumigatus* has been classified as Deuteromycotina or *fungi imperfecti*, describing fungi with a lacking a sexual cycle. However, with the publication of the genome sequences of *A. fumigatus* and the sexually reproducing *A. nidulans* in 2005, evidence emerged that *A. fumigatus* might possess a sexual life cycle. Every gene, required for sexual development in *A. nidulans* is also present in *A. fumigatus* (Galagan et al., 2005; Nierman et al., 2005). In 2009 O'Gorman et al. discovered the sexual cycle for *A. fumigatus* by mixing and matching 12 *A. fumigatus* isolates with either mating type *MAT1-1* or *MAT1-2* on a variety of different growth media and incubation temperatures (Figure 1) (O'Gorman et al., 2009). In addition to its anamorphic (asexual) state, which is responsible for the Latin genus name *Aspergillus*, the second name *Neosartorya* was given for its teleomorphic (sexual) phase, resulting in two species affiliations, *Aspergillus fumigatus* and *Neosartorya fumigata* respectively. *Neosartorya* describes the morphology of the mature fruiting body, called cleistothecium, which is characterized by a network of interwoven flattened hyphae that build the cleistothecial wall (Dyer and O'Gorman, 2012). Although *A. fumigatus* has the ability to perform sexual propagation, this process requires highly specific growth media, incubation temperatures and extreme long incubation periods of up to six months. This does not only explain, why the sexual cycle has long remained undiscovered but also indicates that asexual development is the favored form of propagation, whereas sexual development seems to be a rare event in *A. fumigatus* (Dyer and O'Gorman, 2012; Ene and Bennett, 2014; O'Gorman et al., 2009).

1.1.5   Secondary metabolites produced by *A. fumigatus*

Besides melanins, *A. fumigatus* is able to produce a variety of secondary metabolites with different functions (Lind et al., 2015). Two prominent groups of secondary metabolites

produced by *A. fumigatus* are siderophores and mycotoxins. Since *A. fumigatus* lacks specific iron-uptake systems, intra- and extracellular siderophores, produced by nonribosomal peptide synthetases (NRPS) are able to chelate ferric iron for iron acquisition. These siderophores have an additional protective function against oxidative stress (Brandon et al., 2015; Schrettl and Haas, 2011; Schrettl et al., 2007).

Mycotoxins produced by *A. fumigatus* include Gliotoxin (GT) as one of the best studied. The genes involved in GT biosynthesis are organized in a cluster that comprises 13 genes. One of these genes encodes the zinc finger transcription factor GliZ, which regulates expression of the cluster (Dolan et al., 2015; Scharf et al., 2015; 2012). Gliotoxin production is further controlled by other transcription factors like GipA, MtfA or VeA and the methytransferase LaeA, which act as global secondary metabolite regulators. In contrast to *gliZ*, the corresponding global regulator genes are not embedded in the GT cluster (Dhingra et al., 2012; Perrin et al., 2007; Schoberle et al., 2014; Smith and Calvo, 2014). Environmental stimuli that induce the production of gliotoxin, remain to be discovered, though a recent study has identified bacterial pathogen-associated molecular patterns (PAMPs) to stimulate GT secretion in *A. fumigatus* (Scharf et al., 2012; Svahn et al., 2014). Like siderophores, gliotoxin has anti-oxidant functions as it was recently shown by Owens et al. (Owens et al., 2014). Secondary metabolite genes of filamentous fungi are often organized in clusters in the genome and are usually repressed under standard laboratory growth conditions (Gerke and Braus, 2014). 226 bioactive metabolites, belonging to 24 biosynthetic families have been identified during a metabolomics study with *A. fumigatus* (Frisvad and Larsen, 2016; Frisvad et al., 2009). Furthermore, the genome of *A. fumigatus* encodes 317 genes organized in 37 gene clusters with a proposed function in secondary metabolism (Lind et al., 2015). However, in most cases a direct connection between specific metabolites and their corresponding gene clusters remains to be identified.

1.1.6 Oxidative stress response mechanisms of *A. fumigatus*

In addition to secondary metabolites with protective function against oxidative stress, *A. fumigatus* possesses other ROS detoxification mechanisms (Brandon et al., 2015). Superoxide dismutases (SOD) reduce superoxides to hydrogen peroxide (H_2O_2) and provide a first line of defense against ROS (Aguirre et al., 2005). *A. fumigatus* harbors four SODs, of which one, namely Sod4, is essential. Deletion mutants lacking one of the

three other SODs were more susceptible to higher temperatures and ROS triggered by menadione (Lambou et al., 2010).

In a next step catalases protect cells from peroxides by converting them into water and oxygen. Three catalases have been characterized so far, of which CatA is exclusively localized in conidia, whereas Cat1 and Cat2 are hyphal catalases. Whereas the deletion of *catA* resulted in conidia with higher susceptibility to H_2O_2, single deletions of *cat1* or *cat2* showed similar phenotypes to wild type under oxidative stress. Only double deletions of both hyphal catalases led to slightly increased ROS sensitivity (Paris et al., 2003b).

Another anti-oxidant system is provided by the presence of reduced glutathione (GSH), which acts as a scavenger for oxidants by supplying electrons for reactive oxygen intermediates (ROI) (Grant et al., 2000).

These enzymatic ROS detoxifying systems are primarily controlled by the transcription factors AtfA, Yap1 and Skn7 and seem to comprise some redundancy since single mutations of ROS encountering enzymes only led to slightly enhanced oxidative stress sensitivity (Abad et al., 2010; Chauhan et al., 2006; Emri et al., 2015).

1.1.7   Adaption to high temperatures and broad pH ranges

Another remarkable characteristic that provides a competitive advantage for *A. fumigatus* is its ability to adapt to extreme environmental conditions. *A. fumigatus* is able to grow at temperatures up to 55 °C, with a growth optimum between 37 °C and 42 °C, while conidia can survive temperatures up to 75 °C (McCormick et al., 2010; Perez-Nadales et al., 2014; Sueiro-Olivares et al., 2015). Germination and growth rates of *A. fumigatus* conidia are significantly higher at 37 °C than the corresponding growth rates of other *Aspergillus* species such as *A. flavus* and *A. niger*. This effect was even more pronounced at elevated temperatures of 41 °C, where *A. fumigatus* conidia had a slightly enhanced conidiation rate compared to 37 °C, whereas the germination of *A. flavus* was decreased by 45% and conidia from *A. niger* did not germinate at all (Araujo and Rodrigues, 2004). Similar to its high thermo tolerance, *A. fumigatus* also withstands a broad pH range of pH 3.7 to 7.6 without inhibition of growth (Kwon-Chung and Sugui, 2013).

Taken together, its nutritional versatility, the ability for fast asexual propagation and efficient dispersion of the conidia and the capacity to adapt and withstand extreme envi-

ronmental conditions makes *A. fumigatus* a highly competitive member of the compost microbiota.

1.2 Pathogenicity of *A. fumigatus*

Beside its saprophytic life style *A. fumigatus* also acts as an opportunistic pathogen, which can infect humans and animals. Among the more than 200 *Aspergillus* species only a small subset of approximately 10% have been associated with human pathogenicity, with *A. fumigatus* as the most important cause for life-threatening mycoses (Horn et al., 2012; Lamoth et al., 2016). The infective agents are the conidia, which are inhaled and because of their small size easily reach the lung alveoli. On average every human inhales several hundreds of *A. fumigatus* conidia per day (Kwon-Chung and Sugui, 2013). In immunocompetent hosts this rarely causes problems since the conidia are efficiently eliminated by the innate immune response (Denning, 1998; Gazendam et al., 2016). However, especially in patients with structural lung diseases like tuberculosis or patients suffering from cystic fibrosis or asthma, conidia are able to cause allergic reactions and aspergilloma, which refers to growing mycelia in the lung cavities, called chronic pulmonary aspergillosis (CPA) with the potential to disrupt surrounding blood vessels (Agarwal et al., 2013; Hedayati et al., 2015; Latgé, 1999). The most severe disease caused by *A. fumigatus* is the life threatening invasive pulmonary aspergillosis (IPA), which affects predominantly patients with a disturbed immune system. IPA is typified by growing mycelia, which penetrates the surrounding tissues with the potential to spread to other tissues with the blood stream, leading to mortality rates of 40% to 90% (Dagenais and Keller, 2009; Lamoth et al., 2016). Particularly patients with the auto-immune deficiencies like chronic granulomatous disease (CGD), characterized by dysfunctional neutrophils, patients suffering from leukemia or patients with heart and lung transplantation carry high risks for IPA, with an incidence of 25-40%, 48% and 19-26% respectively (Denning, 1998; Georgiadou and Kontoyiannis, 2012). The number of high-risk patients for IPA has increased during recent decades for reasons like intensified usage of chemotherapy during cancer treatment, an increasing number of patients with solid organ transplantations or the appearance and rise of AIDS (Cramer, 2016; Steinbach, 2013). Treatment of IPA patients is complicated by poor diagnosis methods and the limited availability of antifungal agents. Commonly used antifungals like

voriconazole or amphotericin B may have toxic side-effects for the host, whereas second line agents like echinocardins exhibit fungi-static properties instead of being fungicidal (Lamoth et al., 2016; Smith and Kauffman, 2012). Therefore, severity and increasing incidence of IPA yield in a growing interest into this medical important fungus.

1.2.1   Virulence determinants

The identification of specific virulence factors, which set *A. fumigatus* apart from other Aspergilli, thus making it the most prevalent cause for aspergillosis in humans, has gained an increasing interest during recent decades. Consequently more than 400 *A. fumigatus* mutant strains have been constructed and assessed for their virulence (Horn et al., 2012). Especially the availability of genome sequences for *A. oryzae*, *A. nidulans* and *A. fumigatus*, which allowed comparative studies among these Aspergilli and the addition of new genetic tools like extended genetic marker availability, new mutagenesis systems and *akuA/akuB*-mutant strains that allow a more efficient transformation procedure led to a substantial progress in the determination of virulence traits for *A. fumigatus* (da Silva Ferreira et al., 2006; Galagan et al., 2005; Krappmann, 2006; Krappmann et al., 2006b; Machida et al., 2005; Nierman et al., 2005; Zhang et al., 2016). Although specific virulence determinants could be identified (see Table 1), the largely accepted hypothesis claims that virulence of *A. fumigatus* is based on a multifactorial basis. The ability of *A. fumigatus* to grow and adapt to the harsh conditions of compost piles, its nutritional versatility, a sophisticated system to prevent damage from oxidative stress and the ability to produce a variety of secondary metabolites including mycotoxins are the main reasons for its success as a human pathogen (Brandon et al., 2015; Frisvad and Larsen, 2016; Hillmann et al., 2015; Miao et al., 2015; Rhodes, 2006).

Table 1: Putative virulence determinants, involved genes and their impact on *A. fumigatus* pathogenicity.

Virulence determinants	Genes involved	Function	Involved in pathogenicity
Conidial size and surface	*rodA*, *rodB*	Rodlet layer, oxidative stress resistance, dispersion of spores, prevents immune-recognition	Yes (*rodA*) (Aimanianda et al., 2009; Paris et al., 2003a)
	pksP	PKS, key enzyme for DHN-melanin biosynthesis, ROS protection, prevents phagocytical killing of conidia	Yes (Heinekamp et al., 2012)
Thermotolerance	*thtA*, *pmt1*	Required for growth above 37 °C (*pmt1*) or 42 °C (*thtA*)	No (Chang et al., 2004; Zhou et al., 2007)
	mnt1, *cgrA*	Required for growth above 25 °C (*cgrA*) and 30 °C (*mnt1*), essential for conidial germination at 48 °C	Yes (Bhabhra and Askew, 2005; Wagener et al., 2008)
Nutritional versatility	*cpcC*, *cpcA*	Sensor kinase and transcriptional activator of cross-pathway control of amino acid biosynthesis	Yes (only ΔcpcA showed attenuated virulence) (Krappmann et al., 2004; Sasse et al., 2008)
	pkaC, *pkaR*	Cyclic AMP-dependent protein kinase, regulation of carbon catabolite expression, adaption to different C-sources	Yes (Liebmann et al., 2004b; Rhodes, 2006)
	pyrG, *pabaA*, *lysF*	Prototrophy for uracil (*pyrG*), folate (*pabaA*), lysine (*lysF*)	Yes (Rhodes, 2006)
Oxidative stress resistance	*catA*, *cat1*, *cat2*	Catalases for scavenging H_2O_2	No (*cat1*/*cat2* double mutants exhibit slower growth in rat lungs) (Paris et al., 2003b)
	sod1, *sod2*, *sod3*, *sod4*	Superoxide dismutases for detoxification of superoxide anions	No (*sod4* is essential) (Lambou et al., 2010)
	yap1, *skn7*	Transcriptional regulators for oxidative stress response	No (Lamarre et al., 2007; Lessing et al., 2007)
Secondary metabolites	*sidA*, *sidC*, *sidD*, *sidF*, *sidG*	Siderophor biogenesis, iron uptake	Yes (Schrettl et al., 2007)
	gliZ, *gliP*	Transcription factor and core NRPS enzyme of the gliotoxin biosynthesis cluster, antiphagocytic properties and ROS protection	Yes (only in non-neutropenic mice) (Kwon-Chung and Sugui, 2009; Scharf et al., 2012)
	veA, *laeA*	global regulators for morphology and secondary metabolism	Yes (Bok et al., 2005; Dhingra et al., 2012)

1.2.2   Development and virulence in Aspergilli

The rapid responses to environmental changes are subject to distinct mechanisms that seem to be evolutionary conserved in *A. fumigatus* due to its natural habitat (Cramer, 2016; Latgé, 1999; Rhodes, 2006; Tekaia and Latgé, 2005). Several of these stress response mechanisms are linked to development regulating processes, which were thoroughly described for the related model organism *A. nidulans* (Cramer, 2016; Dhingra et al., 2013; Smith and Calvo, 2014). A key element for the regulation of asexual/sexual development in *A. nidulans* is the velvet protein VeA, which is known to promote sexual development and secondary metabolism while it delays the formation of asexual conidiospores (see also Discussion section 2) (Bayram et al., 2016; Gerke and Braus, 2014; Sarikaya Bayram et al., 2014; Terfrüchte et al., 2014). In *A. fumigatus*, however, the deletion of *veA* just merely affects asexual sporulation on nitrate containing medium, but has significant effects on the production of secondary metabolites like gliotoxin, fumagillin and many more (Alkhayyat et al., 2015; Dhingra et al., 2012; 2013; Dolan et al., 2015; Krappmann et al., 2005).

This example emphasizes possible connections between essential developmental regulators of *A. nidulans*, which play only minor roles for development in *A. fumigatus*, but instead have evolved as prominent virulence contributing factors.

2   Targeted protein degradation

2.1   Eukaryotic protein degradation systems

A rapid response to environmental changes as well as the maintenance and coordination of growth and cell division during the cell cycle requires a well-balanced system of production and degradation of proteins. While the rates of protein synthesis are controlled by transcriptional mechanisms, two major pathways for their degradation exist in eukaryotes. Autophagy is an unspecific or highly specific degradation pathway for single proteins, larger complexes or even whole organelles under starvation conditions and finally ends in the lysosome (animals) or its equivalent, the vacuole (fungi and plants) (He and Klionsky, 2009).

The other major pathway for protein degradation relies on the small modifying protein ubiquitin, which can be attached to other proteins to mark them for degradation via the 26S proteasome. This so called ubiquitin proteasome system (UPS) is highly conserved from unicellular yeasts to humans and affects various processes like cell cycle regulation, differentiation and development, stress response, transcriptional regulation, signal transduction and DNA damage repair (Glickman and Ciechanover, 2002; Kleiger and Mayor, 2014; Li and Jin, 2012). The UPS can be divided into two subsystems. The first mechanism refers to the quality control of newly synthesized proteins and is called endoplasmic reticulum-associated degradation (ERAD). Potentially misfolded or mutated proteins are recognized and ubiquitinated by ubiquitin ligases, which are embedded in the endoplasmic reticulum (ER) and transported to the 26S proteasome for degradation (Christianson and Ye, 2014; Hirsch et al., 2009). The second system is responsible for the ubiquitination and subsequent degradation of specific proteins, which contribute to highly regulated processes like development and stress responses.

Although ubiquitin is primarily associated with the UPS, recent studies provided evidence that ubiquitin also plays a role in selective autophagy processes (Ashida et al., 2014; Kleiger and Mayor, 2014). Generally proteins have to be linked to a chain of ubiquitin moieties to be marked for degradation. The way single ubiquitin proteins are attached to each other determines the further degradation pathway. Ubiquitin chains, where single ubiquitins are linked to the internal lysine residue 48 of the preceding ubiquitin moiety, are targeted to the 26S proteasome, whereas lysine 63 linked ubiquitin chains are preferential recognized by ubiquitin binding autophagy receptors and therefore serve as a signal for the autophagy-lysosomal degradation pathway (Kirkin et al., 2009; Komander and Rape, 2012). In addition, an ubiquitin-like conjugation system has been described for selective autophagy pathways. It requires the attachment of the ubiquitin-like proteins Atg5 and Atg8 to form double-layered membranes called autophagosomes, which engulf the degradable cytosolic structures and subsequently fuse with lysosomes for their degradation. Selective autophagy has emerged as an important mechanism for the removal of excessive or toxic cytosolic compounds and plays crucial roles for developmental pathways as well as diseases like cancer or neurodegenerative disorders (Rogov et al., 2014; Voigt and Pöggeler, 2013; Wurzer et al., 2015).

2.1.1   The ubiquitin proteasome system

In order to promote the proteasomal recognition and subsequent degradation of specific proteins, they have to be linked to a chain of at least four monomeric ubiquitins (Glickman and Ciechanover, 2002). Ubiquitin is a 76 amino acid comprising protein, which is highly conserved among all eukaryotes. It is encoded as a several repeats containing precursor form in the genome and has to be processed posttranslational by specific peptidases belonging to the deubiquitinase family (Clague et al., 2015; Monia et al., 1989). The mature monomeric ubiquitin is attached to the respective target protein in an enzymatic cascade, which involves three successive steps catalyzed by enzymes termed E1, E2 and E3 (Figure 2). First ubiquitin is activated in an ATP-dependent manner by the E1 enzyme also known as ubiquitin-activating enzyme. In this process the C-terminal glycine residue of ubiquitin is bound to a cysteine residue of the E1 enzyme through a high-energy thioester linkage. The activated ubiquitin is then transferred to the ubiquitin-carrier enzyme E2. In a final step the ubiquitin gets covalently linked to the target substrate within the E3 ubiquitin ligase. Due to successive rounds of E1-E2-E3 cascades ubiquitin chains are assembled, where a new ubiquitin is covalently linked to a previous attached ubiquitin via its internal lysine residue 48. The transfer mechanism of ubiquitin to the target protein depends on architecture of the E3 ligase. In (<u>r</u>eally <u>i</u>nteresting <u>n</u>ew <u>g</u>ene) RING-E3 ligases the ε-amino group of a lysine residue of the target or a previously attached ubiquitin attacks the thioester bond between the E2 enzyme and its attached ubiquitin and thereby directly forms an isopeptide bond with the C-terminal glycine residue of the new ubiquitin. In contrast, the ubiquitin transfer in (<u>h</u>omologous to the <u>E</u>6-AP <u>c</u>arboxyl <u>t</u>erminus) HECT-type E3 ligases is catalyzed through an intermediate state, where the activated ubiquitin is transferred to an active cysteine residue within the HECT-domain of the E3 ligase prior to its connection to the target (Glickman and Ciechanover, 2002).

Proteins that are covalently linked to polyubiquitin chains of at least 4 ubiquitin moieties are subsequently recognized and degraded by the 26S proteasome (Figure 2). The proteasome is a massive 2.5 MDa spanning multi-subunit complex, which can be divided into two sub-complexes. The center is comprised by the barrel-shaped 20S proteasome that harbors the proteolytic active sites. This 700 kDa core particle features two entrance pores with restricted size to the proteolytic center, which allow the entry of unfolded proteins whereas native proteins cannot pass these pores (Bhattacharyya et al., 2014). Addi-

tional regulation is achieved by the 19S regulatory particles that are connected to the ends of the 20S core particle. The 19S particle itself is comprised of two subcomplexes. The base contains six ATPases and two ubiquitin receptors with ubiquitin binding domains (UBD), which are used to identify and unfold ubiquitinated proteins to grant them access to the proteolytic core. On the contrary the lid contains a deubiquitinating enzyme (DUB), which allows the cleavage and recycling of ubiquitin from the target proteins (Bhattacharyya et al., 2014; Gu and Enenkel, 2014).
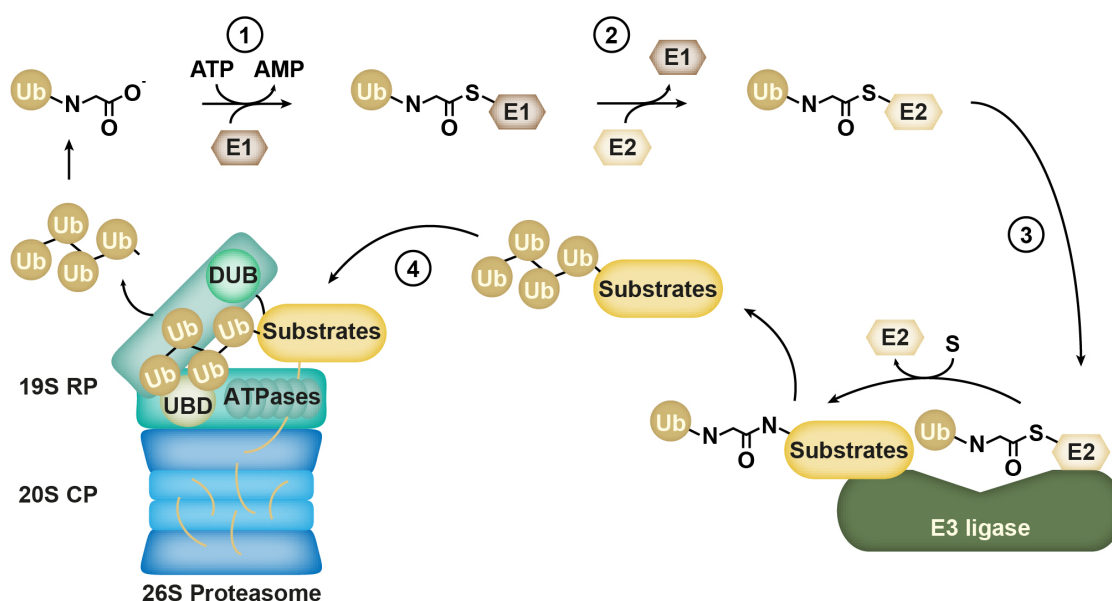
Figure 2: The Ubiquitin proteasome system (UPS). The ubiquitin dependent proteasomal degradation of specific proteins starts with free monomeric ubiquitin (Ub), which gets activated and bound to the E1 ubiquitin-activating enzyme in an energy-dependent step (1). Subsequently ubiquitin is transferred to an internal cysteine residue of the ubiquitin-conjugating enzyme E2 (2). The E2 enzyme with the activated ubiquitin as well as the target substrate is bound by the E3 ubiquitin ligase, which catalyzes the transfer of the ubiquitin to a lysine residue of the target protein (3). Successive rounds of ubiquitin transfer, where a single ubiquitin is attached to a previous one via its internal lysine residue 48, result in a polyubiquitin chain, which finally is recognized by ubiquitin binding domains (UBD) in the 19S proteasomal regulatory particle (RP) (4). Here a ring of six ATPases unfolds the substrate protein and permits its entry into the proteolytic chamber of the 20S core particle (CP), whereas a deubiquitinating enzyme (DUB), removes the ubiquitin-tag from the substrate to allow its recycling.

2.1.2 Non-proteolytic functions of ubiquitin modifications

Beside its canonical function as a marker for proteasomal degradation, recent studies demonstrated a wide variety of cellular functions for ubiquitin modifications, which is

dictated by the specificity of ubiquitin assembly on the target protein and the respective recognition proteins, which harbor a broad range of ubiquitin binding domains.

Ubiquitin can be attached to an internal lysine residue of the target substrate either as a monomer or as a multimeric chain in which the specificity is primarily determined by the E2 ubiquitin-conjugating enzyme (Clague et al., 2015). Monoubiquitination is often not associated with proteasomal degradation, but displays a variety of functions like transcriptional silencing or the activation of DNA damage response mechanisms (Chen and Sun, 2009; Wang et al., 2004). Ubiquitin can also be assembled in multimeric chains due to its seven internal lysine residues. Linear ubiquitin chains may also be assembled in a head to tail direction, where the aminoterminal methionine (Met1) serves as an acceptor for additional ubiquitin. Lys48 linked ubiquitin chains and, to less extent Lys11 linked polyubiquitins confer the signal for proteasomal degradation. In contrast Lys63 linked ubiquitin chains exhibit a linear conformation and play a role in kinase activation, DNA maintenance and lysosomal targeting (Ye and Rape, 2009). Homogeneous Lys6, Lys27, Lys29 and Lys33 linked ubiquitin chains as well as branched polyubiquitins have also been detected, but their cellular function remains to be identified (Park and Ryu, 2014).

2.2   Ubiquitin E3 ligases

E1 and E2 enzymes are characterized by a conserved domain containing a cysteine residue as acceptor site for ubiquitin. In contrast E3 ligases represent a highly diverse group characterized by several distinct motifs. This is also represented in total numbers. Whereas the human genome encodes only two E1 and approximately 40 E2 enzymes, the estimated amount of E3 ligases exceed 600, although most of them remain to be characterized (Clague et al., 2015; Li and Jin, 2012).
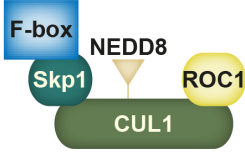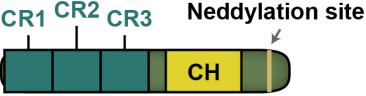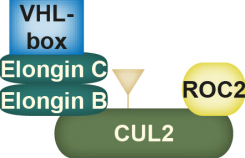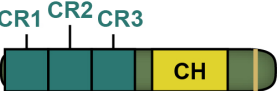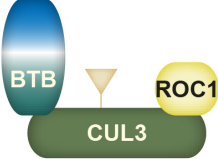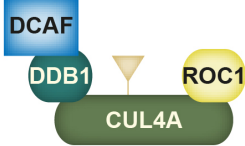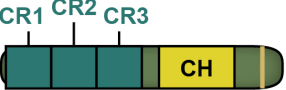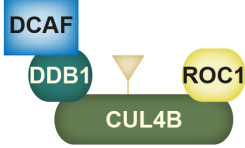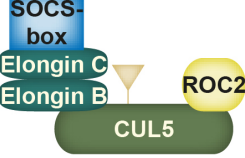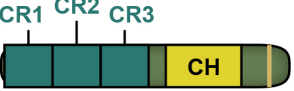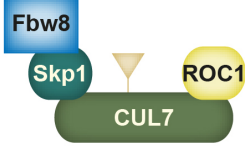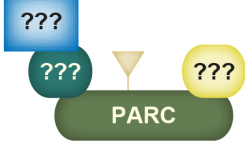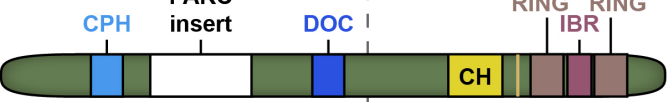
The majority of E3 ligases are no real ligases but act as scaffolding enzymes to mediate ubiquitination. They bind to the E2 enzyme with the conjugated ubiquitin moiety and the target substrate and thereby bringing both components into close proximity. This finally allows an efficient transfer of the activated ubiquitin to a lysine residue of the target protein. These E3 ligases often carry either a RING finger domain, or a structural similar U-box domain, which serves as a binding site for their partner E2s (Aravind and Koonin, 2000; Ardley and Robinson, 2005; Glickman and Ciechanover, 2002). RING and U-box containing E3 ligases have in common that they can either be monomeric or multi-

subunit complexes, with an ability to facilitate the transfer of ubiquitin to their target substrate.

Another class of E3 ligases is characterized by the HECT domain. HECT ligases were initially discovered for the human E6-AP ubiquitin ligase that targets the p53 tumor-suppressor protein for ubiquitination (Huibregtse et al., 1995). The 350 amino acids spanning HECT domain contains a conserved cysteine residue, which serves as acceptor for the activated ubiquitin. In this case the E3 ligase forms an intermediate complex with the ubiquitin, which is subsequently transferred to the target substrate and therefore comprises a catalytic function (Glickman and Ciechanover, 2002; Scheffner et al., 1995).

2.2.1   Diversity of Cullin-RING E3 ubiquitin ligases

The best characterized and probably largest family of E3 ligases is the cullin-based RING ligases (CRL), which comprise approximately half of the human E3 ligases (Sarikas et al., 2011). Cullin-based E3 ligases are generally multi-subunit enzymes that contain a cullin, which serves as a scaffold. As a common feature their cullin subunit is able to bind through its cullin homology domain (CH) to the RING-domain containing protein ROC1/Rbx1 that provides adaptor functionality for the E2 enzyme. In the N-terminal part different cullins can bind to a specific subset of substrate adaptors, which confer the substrate specificity of the respective CRLs. Mammals contain eight different cullins, whereas the amount of cullins in lower eukaryotes varies from five in *Drosophila* down to three in most fungi (Figure 3) (Sarikas et al., 2011). Apart from different cullin subunits used for CRL assembly the large variety of CRLs is conferred by a vast amount of different substrate adaptor subunits, which in case of F-box proteins can reach from 69 in humans to nearly 700 in *Arabidopsis thaliana* (Hua and Vierstra, 2011). Thus, it is has been estimated that 20% of proteasomal protein degradation in mammalian cells is mediated by ubiquitinating functions of CRLs (Soucy et al., 2009).

Molecular CRL composition	Cullin structures	present in Aspergilli / *S. cerevisiae*
F-box, Skp1, NEDD8, ROC1, CUL1	CUL1 (776 aa) — CR1 CR2 CR3, CH, Neddylation site	yes (CulA) / yes (Cdc53)
VHL-box, Elongin C, Elongin B, ROC2, CUL2	CUL2 (745 aa) — CR1 CR2 CR3, CH	no / no
BTB, ROC1, CUL3	CUL3 (768 aa) — CR1 CR2 CR3, CH	yes (CulC) / yes (Cul3)
DCAF, DDB1, ROC1, CUL4A	CUL4A (759/659 aa) — CR1 CR2 CR3, CH	yes (CulD) / (no) but similar to CUL4, yeast Rtt101/Cul8 also binds to DDB1-like Mms1
DCAF, DDB1, ROC1, CUL4B	CUL4B (913/895 aa) — CR1 CR2 CR3, CH	
SOCS-box, Elongin C, Elongin B, ROC2, CUL5	CUL5 (780 aa) — CR1 CR2 CR3, CH	no / no
Fbw8, Skp1, ROC1, CUL7	CUL7 (1782/1698 aa) — CPH, DOC, CH	no / no
???, ???, ???, PARC	PARC (2517 aa) — CPH, PARC insert, DOC, CH, RING IBR RING	no / no

Figure 3: Diversity of eukaryotic cullin ring ligases (CRL). Subunit composition of human cullin ring ligases. Based on the cullin scaffold protein different adaptor subunits confer the substrate specificity of the respective CRL. Except of CUL3-BTB ligase complexes, all CRLs bind in the N-terminal part to an additional adaptor protein, which links the exchangeable substrate adaptor to the cullin scaffold. In case of CUL3-BTB ligases the BTB-protein comprises cullin- and substrate binding activity. All isoforms of cullin proteins share a similar domain pattern that consists of a cullin homology (CH) domain for binding to the E2 adaptor protein ROC1/RBX1 and a conserved site for posttransla-

tional modification with NEDD8. The N-terminal parts of CUL1 - CUL5 contain three cullin repeat (CR) domains, which bind to the respective substrate adaptors. CUL7 and PARC share a conserved domain, present in CUL7, PARC and HERC2 (CPH) and a domain similar to the destruction of cyclin B (DOC) domain found in subunits of the anaphase-promoting complex. PARC has additional RING and in between RING (IBR) motifs, which might serve as interacting domains for further CRLs (Ardley and Robinson, 2005). Whereas CUL7 and PARC CRLs are only present in mammalians, especially CUL1, CUL3 and CUL4 are conserved from fungi to human. Modified after Sarikas et al., 2011.

2.2.2 Regulation of Cullin RING ligases

The activity of CRLs is controlled on different levels. First and foremost cullin scaffolds have to be activated by covalent linkage to the ubiquitin-like modifier NEDD8/NeddH. The attachment of NEDD8/NeddH provokes a conformational rearrangement of the cullin scaffold, which facilitates a close proximity of the substrate and the ubiquitin-charged E2 enzyme and thereby enhances the ubiquitination activity of CRLs (Enchev et al., 2012). Similar to ubiquitination, neddylation of cullins requires the sequential action of E1, E2 and E3 enzymes. First mature NEDD8/NeddH has to be activated by the heterodimeric E1 enzyme NAE1-UBA3 in an ATP dependent step. It is subsequently transferred to the conjugating E2 enzyme UBC12 (Watson et al., 2011). Finally an E3 ligase catalyzes the covalent linkage of NEDD8/NeddH to a conserved C-terminal lysine residue on the cullin, which promotes CRL activity (Merlet et al., 2009). The nature of the E3 NEDD8/NeddH ligase is not yet clear. The CRL subunit ROC1/RbxA is able to directly interact with cullins and the UBC12 E2 enzyme and therefore might serve as NEDD8/NeddH E3 ligase in addition to its function as adaptor for ubiquitin-conjugating E2s. However, other studies refer to the conserved DCN1 protein (deficient in cullin neddylation), which plays a crucial role for cullin neddylation (Duda et al., 2008). Comparisons of crystal structures of neddylated and unneddylated CRLs indicate a drastic conformational change in the C-terminal region of the cullin upon neddylation, which brings the ROC1/RbxA adaptor with the ubiquitin-charged E2 enzyme in close proximity to the substrate, allowing the ubiquitin transfer to the target protein (Duda et al., 2008; Gerke and Braus, 2014).

CRL activity is counteracted by deneddylation of the cullin subunit, which not only inactivates respective CRLs but also facilitates the exchange of their substrate adaptor subunits (Schmidt et al., 2009). Cullin deneddylation is primarily linked to the conserved eukaryotic COP9 signalosome (CSN) complex, which was initially identified in plant

mutants that exhibit a constitutive photomorphogenic phenotype (Meister et al., 2015; Wei et al., 1994). The prototype CSN complex harbors eight subunits, six of them with a PCI domain (Proteasome–COP9 signalosome–Initiation factor 3) and another two with MPN domains (MPR1–PAD1–N-terminal). Both, PCI and MPN domains are defined by their sequence homology to either components of the proteasomal lid or the eukaryotic translation initiation complex eIF3 (Beckmann et al., 2015; Enchev et al., 2010; Wei et al., 2008). Since its discovery homologues of CSN complexes have been identified from fungi to humans, although some fungal model organisms like *Neurospora crassa* or *Schizosaccharomyces pombe* only contain partial CSN complexes of seven or six subunits respectively, whereas the baker's yeast *Saccharomyces cerevisiae* harbors an alternative CSN version (Braus et al., 2010). Although the CSN complex is primarily responsible for the deneddylation of cullins, another deneddylase, DEN1/DenA, which physically inter-acts with the CSN complex, has recently been shown to be involved in cullin deneddyla-tion in the filamentous fungus *A. nidulans* (Christmann et al., 2013).

Deneddylation of the cullin subunit of a CRL is accompanied by the binding to another conserved protein, termed CAND1 (cullin associated NEDD8 dissociated protein 1). CAND1 exists in most eukaryotes as a single protein, whereas filamentous ascomycetes from the genus Aspergilli harbor a split-CandA protein, divided into a smaller N-terminal and a larger C-terminal part, which can interact and resemble the full lengths CAND1 protein of other organisms (Helmstaedt et al., 2011). CAND1 binds exclusively to deneddylated cullins and thus was believed to act as CRL inhibitor by competing with CRL substrate adaptor proteins (Petroski and Deshaies, 2005). However functional CSN and CAND1 proteins are required for efficient CRL-mediated ubiquitination (Bosu and Kipreos, 2008). Recent studies have shown that CAND1 rather acts as a protein exchange factor, which facilitates the interchange of substrate adaptor subunits on CRL cullin-ROC1/RbxA core complexes and thereby prevents these substrate adaptors from auto-ubiquitination and eventual proteasomal degradation (Chua et al., 2011; Pierce et al., 2013).

Further control mechanisms for the activity of some CRLs are dimeriza-tion/multimerization of either whole CRL complexes or substrate adaptors, which sub-stantially enhance their ubiquitination activity (Bosu and Kipreos, 2008; Petroski and Deshaies, 2005). For some CRLs also co-factors have been identified, such as mammali-an Cks1, which binds to the F-box substrate adaptor Skp2 inside E3 SCF^{Skp2} ubiquitin

ligases and plays an essential role for the recognition of the target substrate p27^{Kip1}, an inhibitor of G_1/S cell cycle progression (Spruck et al., 2001).

2.2.3 SCF-ubiquitin ligase complexes

One of the best-characterized CRL families are the SCF complexes, which are comprised of a CUL1/CulA scaffold and a ROC1/RbxA adaptor protein, building the core enzyme. In the N-terminal part CUL1/CulA binds to SKP1/SkpA, which serves as adaptor protein for the exchangeable substrate specificity determining F-box protein (Figure 3). The adaptor subunits ROC1/RbxA and SKP1/SkpA are unique in each organism. In contrast, their binding partners, E2 enzymes and F-box proteins are exchangeable, which lead to SCF specificity not only for the substrates but also for the ubiquitin chain linkage that determines the subsequent fate of the target protein. Like in other CRLs the cullin scaffold has to be modified with an additional ubiquitin-like modifier called NEDD8/NeddH in order to be assembled.

2.2.4 F-box proteins

F-box proteins are characterized by the presence of the SKP1/SkpA binding surface, called F-box domain. This 40-45 amino acids comprising domain was initially discovered in the mammalian F-box protein cyclin F, which originated the name (Bai et al., 1996). Inside the F-box domain almost every F-box protein from yeast to human contains a highly conserved proline residue at position seven, which is often accompanied by a prior leucin residue at position six (Figure 4). This proline residue exhibits a crucial function for the binding capacity of F-box proteins into SCF complexes via the SKP1/SkpA adaptor (Schmidt et al., 2009).

F-box proteins can be subdivided into three groups based on the presence of additional protein interaction domains, which serve as substrate binding sites (Cardozo and Pagano, 2004; Skaar et al., 2013):

– **FBXW**: F-box proteins that contain one or more WD40 domains, β-propeller structures that recognize a specific consensus sequence (D**S**GXXX(X)**S**), which have to be phosphorylated on its serine residues.

– **FBXL**: F-box proteins that contain l̲eucine r̲ich r̲epeats (LRR), α-β-repeat struc-
ture, which often require the phosphorylation of target proteins for efficient bind-
ing affinity, also it is not a general prerequisite.

– **FBXO**: F-box proteins that were initially described without an additional domain,
although most of them contain C-terminal motifs, which were either not known at
the time of their discovery or very unique to specific F-box proteins and thus did
not assemble into a larger group. These additional motifs include CASH (c̲arbo-
hydrate-binding proteins a̲nd s̲ugar h̲ydrolases), Kelch-repeats (double glycine re-
peats, that form β-propellers), zinc finger or proline rich domains.
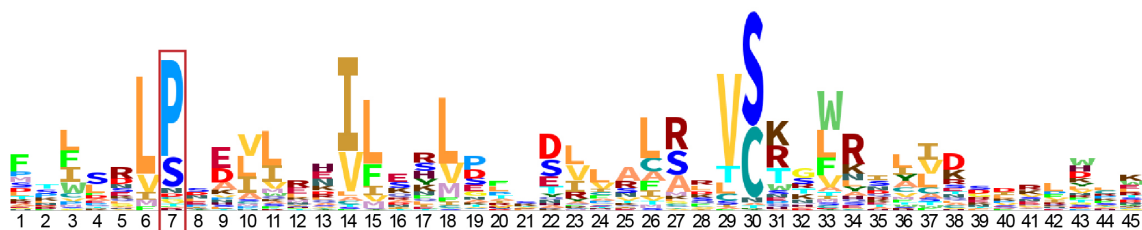
Figure 4: HMM model of the F-box domain. H̲idden M̲arkov m̲odel (HMM) of the F-
box domain (PF00646), which is stored at the Pfam database for protein families
(http://pfam.xfam.org) (Finn et al., 2014; Schuster-Böckler et al., 2004). The stack height
of the amino acid letters indicates the probability to find them in any given F-box protein.
The proline residue at position seven, which plays a crucial role for Skp1/A binding, is
highlighted with a red box.

The general functions of these additional protein interaction domains are thought to be
substrate recognition sites. However, especially for the WD40 repeats it has been shown
that this domain also serves as an ubiquitin acceptor site. The F-box protein Cdc4 was
shown to be ubiquitinated on its WD40 repeats within its own SCF^{Cdc4}-ligase complex,
leading to its proteasomal degradation (Pashkova et al., 2010). This reflects an autocata-
lytic mechanism, which results in the rapid degradation of specific F-box proteins in the
absence of their substrates and thus allows a fast exchange of the substrate adaptor on
otherwise stable SCF components (Galan and Peter, 1999).

Beside its canonical function as SCF subunit, F-box proteins have been shown to
exhibit SCF independent functions as well. An example is the mammalian Fbxo38
(MoKA), which binds to the K̲ruppel-l̲ike transcription f̲actor 7 (Klf7) and acts as a co-
factor for *p21$^{WAF1/Cip1}$* expression and thus plays a key role for neuronal development
(Nelson et al., 2013). Other F-box proteins like hFbh1 (Fbxo18) can perform DNA-
helicase functions and thereby promote genome maintenance. These examples provide

evidence for the vast amount of molecular functions, where F-box proteins are involved in.

3   Transcriptional regulation through the Ssn6-Tup1 co-repressor

3.1   Active transcriptional repression through Ssn6-Tup1

Transcriptional regulation of gene expression can be divided into activating and repressing functions. Whereas the activation of gene expression usually involves the recruitment of specific transcription factors to the target promoter sites accompanied by assembly of the RNA-polymerase holoenzyme and the initiation of transcription, transcriptional repression can be achieved either passively by the absence of specific transcription factors or due to active gene repression even in the presence of their respective activators. The conserved transcriptional co-repressor complex known as Ssn6(Cyc8)-Tup1 from *S. cerevisiae* is a highly efficient active transcriptional repressor, which coordinates the expression of approximately 3-5% of the whole yeast genome (Figure 5) (DeRisi et al., 1997; Parnell and Stillman, 2011). Mutations in the genes for either Ssn6 or Tup1 could be attributed to various phenotypes with defects in mating, glucose repression, DNA damage response and adaption to environmental stressors (Asada et al., 2015; Hanlon et al., 2011; Smith and Johnson, 2000). Especially its versatility with regard to number and function of its target genes highlights transcriptional repression through Ssn6-Tup1 as a key element for yeast biology.

3.2   Molecular mechanisms of Ssn6-Tup1 mediated gene expression

The Ssn6-Tup1 co-repressor is composed of a homo-tetramer of Tup1 subunits, which can access a pocket-like fold in the Ssn6 subunit that is formed by three tetratricopeptide repeat (TPR) motifs (Gounalaki et al., 2000; Palaiomylitou et al., 2008). Neither Ssn6 nor Tup1 comprise any DNA-binding domains. The Ssn6-Tup1 complex therefore needs to bind to additional DNA-binding proteins, which finally confers its versatility with respect to the various target genes (Hanlon et al., 2011; Roy et al., 2013).
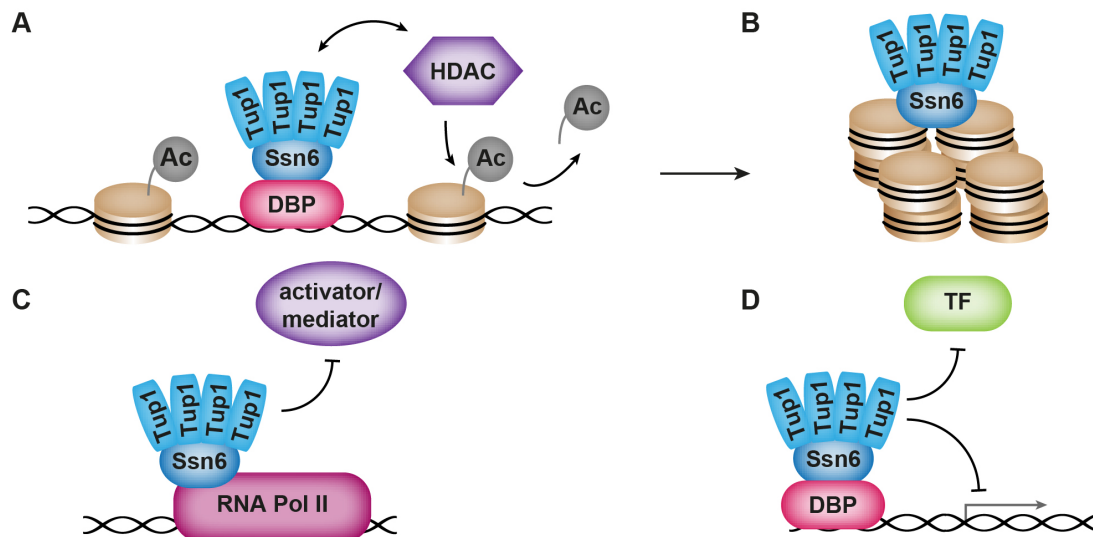
Figure 5: Proposed mechanisms of Ssn6-Tup1 mediated transcriptional repression.
(A) A homotetramer of Tup1 subunits is bound by Ssn6 that connects the co-repressor complex through a <u>D</u>NA <u>b</u>inding <u>p</u>rotein (DBP) to the respective target DNA. Subsequently, the Ssn6-Tup1 complex recruits histone deacetylases (HDAC) to the target sites, which remove acetyl groups (Ac) from adjacent histones, finally resulting in the positioning of nucleosomes with limited accessibility for the transcriptional machinery (B). (C) Furthermore the Ssn6-Tup1 complex is able to interact with the RNA polymerase II holoenzyme and blocks co-activators/mediators from binding and thus blocking the transcription initiation. (D) Ssn6-Tup1 is also able to bind through a variety of DNA binding proteins to specific promoter regions, inhibiting transcription factors from DNA binding. Models based on data from various publications, outlined in Introduction, section 3.2.

Both subunits have different functions inside the repressor complex. Whereas Ssn6 acts as an adaptor protein between the Tup1 tetramer and specific DNA-binding proteins, Tup1 is responsible for the repressing function of the co-repressor (García-Sánchez et al., 2005; Liu and Karmarkar, 2008; Tzamarias and Struhl, 1994). Several mechanisms for Ssn6-Tup1 mediated gene repression have been proposed, which are supposed to be used redundantly on different genes (Figure 5). First Ssn6-Tup1 has the ability to recruit <u>his</u>tone <u>deace</u>tylases (HDACs) to DNA target sites, which results in hypoacetylation of H3 and H4 histone tails (Davie et al., 2003; Fleming et al., 2014; Watson et al., 2000; Wong and Struhl, 2011). In addition Ssn6-Tup1 is required for the positioning of nucleosomes at repressed DNA-loci (Asada et al., 2015; Rizzo et al., 2011). Both functions lead to the formation of a repressive chromatin structure and thus play a key role for transcriptional repression. Furthermore, Ssn6-Tup1 has been shown to compete with either transcription factors or essential components at the RNA polymerase II holoenzyme, which leads to the inhibition of transcription initiation (Figure 5) (Merhej et al., 2015; Paul et al., 2015). This effect seems to be enhanced by modification of Tup1 with the ubiquitin-like modi-

fier SUMO, which leads to a prolongation of sumoylated Tup1 at promoter target sites and eventual removal of the RNA polymerase II holoenzyme (Ng et al., 2015; Texari et al., 2013).

3.3 Tup1-like gene repression in higher eukaryotes

The Ssn6 and Tup1 co-repressor subunits of yeast are belonging to orthologous protein groups OG5_128428 and OG5_131310 respectively, which are conserved across the fungal kingdom (http://orthomcl.org) (Li et al., 2003). However, the fungal Ssn6-Tup1 co-repressor complex does not share significant sequence homology with proteins from higher eukaryotes. The proteins of the Groucho/TLE family of proteins are considered as functional homologues of Tup1, since they have a comparable C-terminal domain structure comprising seven WD repeats and similar repression mechanisms in common (Chen and Courey, 2000; Liu and Karmarkar, 2008). Groucho (Gro) represents the single Tup1-like protein of the genetic model organism *Drosophila melanogaster*, whereas mammalians encode four Gro-like proteins termed TLE1-4 (transducing like enhancer of split). Similar to yeast Tup1, Gro/TLE repressors lack an intrinsic DNA-binding activity and thus need to bind to specific DNA-binding proteins to access respective DNA-target sites. In contrast to Tup1, which requires the Ssn6 adaptor protein, Gro/TLE proteins can directly bind to DNA-binding proteins through their WD repeats. The general mechanism of transcriptional repression seems to be conserved in Gro/TLE repressors, since they also compete with transcriptional activators, recruit HDACs and build tetramers which are required for nucleosome positioning (Figure 5) (Agoston and Schulte, 2009; Sekiya and Zaret, 2007).

4   Scope and aim of this study

The ubiquitin proteasome system plays a vital role for development and secondary metabolism in the filamentous ascomycete *A. nidulans* (Busch et al., 2003; 2007; Helmstaedt et al., 2011; Nahlik et al., 2010). The deletion of the gene for the catalytic subunit of the COP9 signalosome, *csnE*, which is vital for disassembly/reassembly cycles of CRLs, led to impaired sexual fruiting body formation and altered secondary metabolism (Busch et al., 2007; Gerke et al., 2012). In a screen for NeddH interacting proteins in Δ*csnE* mutants of *A. nidulans* five distinct F-box proteins were enriched, suggesting a stabilization of neddylated SCF complexes incorporating these F-box proteins. Among them Fbx15 was identified with a crucial role for asexual and sexual development as well as secondary metabolite production (Zeska Kress et al., 2012). A previous work has characterized the Fbx15 homolog in the opportunistic human pathogen *A. fumigatus* as an essential component of various stress response mechanisms, whereas asexual development was not influenced in the absence of *fbx15* under standard growth conditions (Jöhnk, 2009). This study aims to identify the role of the F-box protein Fbx15 for fungal stress response, secondary metabolism and virulence of the human opportunistic pathogen *A. fumigatus*.

The first part of this work addresses a detailed molecular characterization of Fbx15 in *A. fumigatus*. For this purpose *in silico* and *in vivo* studies of Fbx15 expression kinetics, protein stability, posttranslational modifications and subcellular localization are analyzed and compared with well-characterized F-box proteins such as SconB or GrrA. Furthermore, the ability of Fbx15 to interact within SCF-complexes is investigated. The second part of this work focuses on the identification and characterization of potential interacting proteins of Fbx15. The last part of this study is dedicated to the connection of Fbx15 towards secondary metabolism and virulence of *A. fumigatus*.

II Materials and Methods

1 Materials

1.1 Chemicals and laboratory hardware

Chemicals used for solutions, buffers and media were obtained from Merck KGaA (Darmstadt, GER), Roche GmbH (Mannheim, GER), Carl Roth GmbH & Co KG (Karlsruhe, GER), Sigma-Aldrich Chemie GmbH (München, GER) and Life Technologies GmbH (Darmstadt, GER). Restriction enzymes DNA-modifying enzymes and polymerases were purchased from Thermo Scientific (St. Leon-Rot, GER) and New England Biolabs GmbH (Frankfurt am Main, GER). RNAse A was used from Roche GmbH (Mannheim, GER). *A. fumigatus* mycelium, grown in liquid medium was harvested with Calbiochem® Miracloth from Merck Millipore (Darmstadt, GER). Plasmid DNA from *Escherichia coli* and DNA from agarose gels were prepared with Kits from Qiagen (Hilden, GER). Synthetic oligonucleotides were obtained from Thermo Scientific (St. Leon-Rot, GER) and Eurofins Genomics (Ebersberg, GER). PCR-reactions were done in PCR-cyclers primus96 cycler from MWG-Biotech (Ebersberg, GER), TProfessional Thermocycler from Biometra GmbH (Göttingen, GER) or Mastercycler® gradient from Eppendorf AG (Hamburg, GER). GeneRuler 1kb DNA Ladder from Thermo Scientific (St. Leon-Rot, GER) was used as DNA size standard for gel electrophoresis. Agarose was purchased from Biozyme Scientific GmbH (Oldendorf, GER). Gel electrophoresis was carried out in the Sub-Cell® GT Cell gel chamber powered by the Power Pac 300 from Bio-Rad Laboratories GmbH (München, GER). DNA-amounts were measured with the NanoDrop ND-1000 spectrophotometer from Peqlab Biotechnologie GmbH (Erlangen, GER). DNA-probes for Southern hybridization were labeled either radioactive with $[\alpha\text{-}^{32}P]$-dATP from Hartmann Analytic GmbH (Braunschweig, GER) and the DecaLabel DNA Labeling Kit from Thermo Scientific (St. Leon-Rot, GER) or non-radioactive with the Amersham Gene Images AlkPhos Direct Labeling and Detection System with CDP-Star Detection Reagent from GE Healthcare Europe GmbH (Freiburg, GER). Nucleic acids were transferred to Amersham Hybond-N nylon membrane and for detection either Amersham Hyperfilm MP for autoradiography

or Amersham Hyperfilm ECL for chemiluminescent signals from GE Healthcare Europe GmbH (Freiburg, GER) were used.

For Real-time-PCR fungal DNA was extracted with the RNeasy Plant Mini Kit and transcribed into cDNA using the QuantiTect Reverse Transcription Kit from Qiagen (Hilden, GER). Real time PCR was done with the Light Cycler 2.0 System from Roche GmbH (Mannheim, GER) using the RealMasterMix SYBR ROX 2.5x from 5 PRIME GmbH (Hilden, GER).

Proteins for immunoblotting were transferred to the Amersham Hybond-P membrane from GE Healthcare Europe GmbH (Freiburg, GER) and chemiluminescent signals were detected with either the Amersham Hyperfilm ECL from GE Healthcare Europe GmbH (Freiburg, GER) or with the Fusion SL7 system from Peqlab Biotechnologie GmbH (Erlangen, GER). For signal quantification the Bio 1D imaging software from Peqlab Biotechnologie GmbH (Erlangen, GER) was used. The PageRuler Prestained Protein Ladder or the PageRuler Plus Prestained Protein Ladder from Thermo Scientific (St. Leon-Rot, GER) was used as protein size standard. SDS-PAGE and immunoblotting was carried out in the BIO-RAD Mini Protean II, which was powered by the BIO-RAD Power Pac 300 power supply from Bio-Rad Laboratories GmbH (München, GER). Protein amounts were measured with an Uvikon 922 spectrophotometer from Kontron Instruments (Zürich, SUI) during Bradford assays.

For protein purifications of GFP- or RFP-tagged proteins GFP-Trap_A or RFP-Trap_A agarose beads from ChromoTek GmbH (Planegg-Martinsried, GER) were used. Tandem affinity purification of TAP-tagged proteins was performed with IgG sepharose 6 Fast Flow from GE Healthcare Europe GmbH (Freiburg, GER) and Calmoduline Affinity Resin from Agilent Technologies (Santa Clara CA, USA). Washing steps were carried out in Poly-prep chromatography columns from Bio-Rad Laboratories GmbH (München, GER).

For LC-MS/MS protein identification proteins were digested with Sequencing Grade Modified Trypsin from Promega GmbH (Mannheim, GER) and separated with an RSLC-nano Ultimate 3000 system from Thermo Scientific (St. Leon-Rot, GER). Peptide identification with mass spectrometry was done using the Orbitrap Velos Pro from Thermo Scientific (St. Leon-Rot, GER). Tandem mass tag labeling of peptides prior to mass spectrometry was performed with the TMTduplex Isobaric Mass Tagging Kit from Thermo Scientific (St. Leon-Rot, GER) was utilized.

Fluorescence microscopy was conducted with an Axiovert Observer Z1 confocal microscope from Carl Zeiss Microscopy GmbH (Jena, GER) equipped with either a CoolSNAP ES2 CCD Camera from Photometrics (Tucson, AZ, USA) or the Confocal Scanner Unit CSU-X1 from Yokogawa Electric Corporation (Tokyo, JPN) with a QuantEM:512SC EMCCD Camera from Photometrics (Tucson, AZ, USA).

1.2   Strains

1.2.1   *Escherichia coli* strains

For plasmid preparation *Escherichia coli* strains DH5α [F⁻, Δ(*argF-lac*)*169*, φ80d*lacZ58*(M15), Δ*phoA8*, *glnX44*(AS), λ⁻, *deoR481*, *rfbC1*, *gyrA96*(NalR), *recA1*, *endA1*, *thiE1*, *hsdR17*] (Hanahan et al., 1985) and MACH1™ [F⁻, φ80(*lacZ*)ΔM15, Δ*lac*X74, *hsd*R(r$_K^-$m$_K^+$), Δ*recA*1398, *end*A1, *ton*A] from Life Technologies GmbH (Darmstadt, GER) were utilized.

1.2.2   *Aspergillus fumigatus* strains

A. fumigatus strains generated and used in this study are listed in Table 2. Details about their construction are given below. Plasmids and oligonucleotides used for the generation of *A. fumigatus* strains are listed in Table 3 and Table 4.

Table 2: *A. fumigatus* strains used in this study.

Strain	Genotype	Reference
D141	Clinical isolate	(Reichard et al., 1990)
AfS35	*akuA::loxP*	(Krappmann et al., 2006b)
AfGB5	Δ*akuA*, Δ*fbx15::ptrA*	(Jöhnk, 2009)
AfGB8	Δ*akuA*, Δ*fbx23::ptrA*	(Jöhnk, 2009)
AfGB10	Δ*akuA*, Δ*grrA::ptrA*	(Jöhnk, 2009)
AfGB15	Δ*akuA*, Δ*fbx15::ptrA*, *fbx15*, *hph*	(Jöhnk, 2009)
AfGB18	Δ*akuA*, Δ*fbx23::ptrA*, *fbx23*, *hph*	(Jöhnk, 2009)
AfGB20	Δ*akuA*, Δ*grrA::ptrA*, *grrA*, *hph*	(Jöhnk, 2009)
AfGB32	Δ*akuA*, Δ*fbx15::ptrA::^{P}gpdA::fbx15::gfp*	This study
AfGB33	Δ*akuA*, Δ*fbx15::ptrA::^{P}gpdA::fbx15::tap*	This study

Strain	Genotype	Reference
AfGB34	$\Delta akuA$, $\Delta sconB$::$ptrA$::$^{P}gpdA$::$sconB$::gfp	This study
AfGB35	$\Delta akuA$, $\Delta sconB$::$ptrA$::$^{P}gpdA$::$sconB$::tap	This study
AfGB40	$\Delta akuA$, $\Delta fbx15$::$ptrA$::$^{P}gpdA$::$fbx15$(P12S)::gfp	This study
AfGB41	$\Delta akuA$, $\Delta fbx15$::$ptrA$::$^{P}gpdA$::$fbx15$(P12S)::tap	This study
AfGB42	$\Delta akuA$, $\Delta sconB$::$ptrA$::$^{P}gpdA$::$sconB$(P200S)::gfp	This study
AfGB43	$\Delta akuA$, $\Delta sconB$::$ptrA$::$^{P}gpdA$::$sconB$(P200S)::tap	This study
AfGB57	$\Delta akuA$, $ptrA$, $^{P}gpdA$::$fbx15$::$^{T}his2A$	This study
AfGB64	$\Delta akuA$, $\Delta ssnF$::hph::$ssnF$::gfp	This study
AfGB65	$\Delta akuA$, $\Delta fbx15$::$ptrA$, $\Delta ssnF$::hph::$ssnF$::gfp	This study
AfGB66	$\Delta akuA$, $ptrA$, $^{P}gpdA$::$fbx15$::$^{T}his2A$, $\Delta ssnF$::hph::$ssnF$::gfp	This study
AfGB67	$\Delta akuA$, $\Delta nic96$::hph::$nic96$::gfp	This study
AfGB68	$\Delta akuA$, $\Delta fbx15$::$ptrA$, $\Delta nic96$::hph::$nic96$::gfp	This study
AfGB69	$\Delta akuA$, $ptrA$, $^{P}gpdA$::$fbx15$::$^{T}his2A$, $\Delta nic96$::hph::$nic96$::gfp	This study
AfGB70	$\Delta akuA$, $ptrA$, $^{P}gpdA$::gfp::$^{T}his2A$	This study
AfGB98	$\Delta akuA$, $fbx15$::rfp::$^{T}trpC$::$ptrA$, $\Delta ssnF$::$ssnF$::gfp::hph	This study
AfGB101	$\Delta akuA$, $fbx15$(S468A; S469A)::rfp::$^{T}trpC$::$ptrA$, $\Delta ssnF$::$ssnF$::gfp::hph	This study
AfGB102	$\Delta akuA$, $fbx15$(S469D)::rfp::$^{T}trpC$::$ptrA$, $\Delta ssnF$::$ssnF$::gfp::hph	This study
AfGB104	$\Delta akuA$, $fbx15$(S468D; S469D)::rfp::$^{T}trpC$::$ptrA$, $\Delta ssnF$::$ssnF$::gfp::hph	This study

Bimolecular fluorescence complementation strains

Af293.1 (FGSC# 1137)	$pyrG1$	Fungal Genetics Stock Center, Kansas City, Missouri, USA (McCluskey et al., 2010)
AfGB44	$pyrG1$, $pyrG$, $^{P}niiA$::$cyfp$::$skpA$::$^{T}niiA$, $^{P}niaD$::$nyfp$::$fbx15$::$^{T}niaD$, (pME4056 in Af293.1)	This study
AfGB45	$pyrG1$, $pyrG$, $^{P}niiA$::$cyfp$::$skpA$::$^{T}niiA$, $^{P}niaD$::$nyfp$::$sconB$::$^{T}niaD$, (pME4058 in Af293.1)	This study
AfGB93	$pyrG1$, $pyrG$, $^{P}niiA$::$cyfp$::$fbx15$::$^{T}niiA$, $^{P}niaD$::$nyfp$::$ssnF$::$^{T}niaD$, (pME4302 in Af293.1)	This study

1.2.2.1   Construction of Δfbx- and complemented strains

The construction of Δfbx strains was achieved by the replacement of the respective fbx-gene with a pyrithiamine resistance marker cassette ($ptrA$) via homologous recombina-

tion. *A. fumigatus* transformation was carried out by polyethylene glycol mediated proto-plast fusion as described (Punt and van den Hondel, 1992; Punt et al., 1987).

For the *fbx15*, *fbx23*, *sconB* and *grrA* knockout cassettes 1.5 kb 5'- and 3' UTR flan-king regions of the loci Afu3g14150 (*fbx15*), Afu4g11440 (*fbx23*), Afu2g14110 (*sconB*) and Afu1g05970n (*grrA*) were amplified from *A. fumigatus* D141 genomic DNA with oligonucleotides: (*fbx15*) Afbox15 del A/C and Afbox15 del D/F; (*fbx23*) Afbox23 del A/C and Afbox23 del D/F; (*sconB*) Afbox25 del A/C and Afbox25 del D/F; (*grrA*) AfgrrA del A/C and AfgrrA del D/F respectively. The flanking regions were fused to *ptrA*, which was amplified from pME3024 (Krappmann et al., 2006a) with OZG-(ptrA 5)/OZG-(ptrA 3). Fusion of the flanking sites with *ptrA* was achieved using fusion PCR with: (*fbx15*) Afbox15 del B/D; (*fbx23*) Afbox23 del B/D; (*sconB*) Afbox25 del B/D; (*grrA*) AfgrrA del B/D as described in detail (Bayram et al., 2008; Szewczyk et al., 2006). The resulting knockout cassettes of 4.8 kb were transformed into AfS35, generating AfGB5 (Δ*akuA*, Δ*fbx15*::*ptrA*), AfGB8 (Δ*akuA*, Δ*fbx23*::*ptrA*) and AfGB10 (Δ*akuA*, Δ*grrA*::*ptrA*).

For the generation of the complementation plasmids the genomic loci of Afu3g14150 (*fbx15*), Afu4g11440 (*fbx23*) and Afu1g05970n (*grrA*) including 1.5 kb 5'- and 3' UTR flanking sites were amplified with: (*fbx15*) Afbox15 del A/F, (*fbx23*) Afbox23 del A/F and (*grrA*) AfgrrA del A/F respectively and subcloned into *Stu*I-site of pAN7-1 (Punt et al., 1987) carrying a hygromycin resistance marker. The resulting complementation plas-mids pME3701 (*fbx15*), pME3704 (*fbx23*) and pME3706 (*grrA*) were transformed into the corresponding Δ*fbx*-strains resulting in AfGB15 (Δ*akuA*, Δ*fbx15*::*ptrA*, *fbx15*, *hph*), AfGB18 (Δ*akuA*, Δ*fbx23*::*ptrA*, *fbx23*, *hph*) and AfGB20 (Δ*akuA*, Δ*grrA*::*ptrA*, *grrA*, *hph*) respectively. Deletion and complementation of *fbx*-genes were verified by Southern hybridization.

1.2.2.2 Construction of overexpressed GFP- and TAP-tagged Fbx15 and SconB strains

To achieve *gfp*- or *tap*-tagged overexpression constructs of *fbx15* and *sconB* which were suitable for the substitution of the original loci Afu3g14150 (*fbx15*) and Afu2g14110 (*sconB*) 5' UTR flanking sites for *fbx15* and *sconB* were amplified with BJ1/Afbox15 del C and BJ10/Afbox25 del C respectively and fused to *ptrA* amplified with OZG-(ptrA 5)/BJ2 from pME3024. The resulting 5' UTR::*ptrA* modules containing a

*Kpn*I-site (before *fbx15* 5' UTR) or a *Nae*I-site (before *sconB* 5' UTR) and an *Hpa*I-site (in 3' direction after *ptrA*) were subcloned to pJET1.2 resulting in pME4042 and pME4043. Next, different modules were amplified: ^{P}*gpdA* promoter was amplified from pME3024 with BJ3/BJ4; *fbx15* was amplified from D141 genomic DNA with BJ5/BJ6 (for *gfp* tagged version) or BJ5/BJ8 (for *tap*-tagged version); *sconB* was amplified from D141 genomic DNA with BJ11/BJ12 (for *gfp*-tagged version) or BJ11/BJ15 (for *tap*-tagged version); *gfp* was amplified from pME3167 with OZG207/BJ37; *tap* was amplified from pME3154 with OZG209/BJ38; *fbx15* 3' UTR flanking region was amplified from D141 genomic DNA with BJ7/Afbox15 del F (for *gfp*-tagged version) or BJ9/Afbox15 del F (for *tap*-tagged version); *sconB* 3' UTR flanking region was amplified from D141 genomic DNA with BJ13/Afbox25 del F (for *gfp*-tagged version) or BJ16/Afbox25 del F (for *tap*-tagged version). For the *gfp*-tagged version of *fbx15* the modules ^{P}*gpdA*, BJ5/BJ6, *gfp* and BJ7/Afbox15 del F were fused by fusion PCR with BJ41/Afbox15 del E. For the *tap*-tagged version of *fbx15* the modules ^{P}*gpdA*, BJ5/BJ8, *tap* and BJ9/Afbox15 del F were fused by fusion PCR with BJ41/Afbox15 del E. The fusion PCR products were cloned into the *Hpa*I-site of pME4042 resulting in pME4044 and pME4045. For the *gfp*-tagged version of *sconB* the modules ^{P}*gpdA*, BJ11/BJ12, *gfp* and BJ13/Afbox25 del F were fused by fusion PCR with BJ41/BJ14. For the *tap*-tagged version of *sconB* the modules ^{P}*gpdA*, BJ11/BJ15, *tap* and BJ16/Afbox25 del F were fused by fusion PCR with BJ41/BJ14. The fusion PCR products were cloned into the *Hpa*I-site of pME4043 resulting in pME4046 and pME4047.

For the construction of overexpressed *fbx15::gfp* and *fbx15::tap* strains the corresponding constitutive constructs were excised from pME4044 and pME4045 by digestion with *Kpn*I and transformed into AfS35 resulting in AfGB32 (Δ*akuA*, Δ*fbx15::ptrA::*^{P}*gpdA::fbx15::gfp*) and AfGB33 (Δ*akuA*, Δ*fbx15::ptrA::*^{P}*gpdA::fbx15::tap*).

The construction of constitutively expressed *sconB::gfp* and *sconB::tap* strains was accomplished in the same fashion. Corresponding constructs were taken from pME4046 and pME4047 by digestion with *Nae*I and transformed into AfS35 resulting in AfGB34 (Δ*akuA*,   Δ*sconB::ptrA::*^{P}*gpdA::sconB::gfp*)   and   AfGB35   (Δ*akuA*, Δ*sconB::ptrA::*^{P}*gpdA::sconB::tap*). Replacement of the original locus was verified by Southern hybridization.

For the generation of constitutively expressed GFP- and TAP-tagged Fbx15(P12S) strains two parts from pME4044 or pME4045 respectively were amplified with BJ41/BJ17 and BJ20/Afbox15 del E, introducing a point mutation which results in an

exchange of proline to serine at position 12 of the Fbx15 amino acid sequence. These PCR fragments were fused together with BJ41/Afbox15 del E and subsequently cloned into *Hpa*I-site of pME4042, resulting in pME4048 and pME4049. The generation of constitutively expressed GFP- and TAP-tagged SconB (P200S) strains was carried out in the same way. First corresponding parts from pME4046 or pME4047 were amplified with BJ41/BJ19 and BJ20/BJ14 before fusing them together with BJ41/BJ14, which introduces a point mutation in the *sconB* sequence resulting in an exchange of proline to serine at position 200 of the SconB aa-sequence. The fused products were then cloned into pME4043 resulting in pME4050 and pME4051. Restriction of pME4048 – pME4051 and subsequent transformation of the tagged constructs of *fbx15* and *sconB* with the introduced point mutations was accomplished as described above, resulting in strains:

AfGB40 (Δ*akuA*, Δ*fbx15*::*ptrA*::^{P}*gpdA*::*fbx15*(P12S)::*gfp*),

AfGB41 (Δ*akuA*, Δ*fbx15*::*ptrA*::^{P}*gpdA*::*fbx15*(P12S)::*tap*),

AfGB42 (Δ*akuA*, Δ*sconB*::*ptrA*::^{P}*gpdA*::*sconB*(P200S)::*gfp*) and

AfGB43 (Δ*akuA*, Δ*sconB*::*ptrA*::^{P}*gpdA*::*sconB*(P200S)::*tap*).

1.2.2.3   Construction of *fbx15* and *gfp* overexpression strains

Overexpression of *fbx15* and *gfp* was achieved by cloning *fbx15* or *gfp* into a plasmid with constitutive ^{P}*gpdA* promoter, which was ectopically integrated into AfS35 (WT) strain. Therefore, *fbx15* was amplified from D141 gDNA with primers BJ63/BJ64 and subsequently cloned into *Mss*I-site of pSK379, resulting in pME4289. Similar, *gfp* was amplified from pME3167 with OZG207/BJ37 and cloned into *Mss*I-site of pSK379 to achieve pME4292. Both plasmids were transformed into AfS35 (WT) strain resulting in *Aspergillus* strains AfGB57 (Δ*akuA*, *ptrA*, ^{P}*gpdA*::*fbx15*::^{T}*his2A*) and AfGB70 (Δ*akuA*, *ptrA*, ^{P}*gpdA*::*gfp*::^{T}*his2A*).

1.2.2.4   Construction of Δ*ssnF*, Δ*glcA* and Δ*nimX A. fumigatus* mutants

The deletion cassettes for *ssnF* (Afu2g11840), *glcA* (Afu1g04950) and *nimX* (Afu6g07980) were constructed using the GENEART Seamless Cloning and Assembly Kit (Invitrogen). For *ssnF* deletion cassette 5'- and 3' UTR regions of the gene were amplified from D141 gDNA using oligonucleotides BJ290/BJ291 and BJ292/BJ293. The used primer introduced a 15 bp overhang on each side of the fragments that is complementary to either the recipient vector pBluescript II KS+ or the *ptrA* resistance

marker. The *ptrA* marker was amplified as shown for Δ*fbx*-constructs. All fragments were fused into *EcoR*V-site of the pBluescript II KS+ vector in a seamless cloning reaction, according to manufacturer's conditions, resulting in pME4294. The deletion cassette was cut from the plasmid with *Mss*I and transformed into AfS35 (WT). The final deletion of *ssnF* was not possible due to its essential function for *A. fumigatus*, which was proved by Heterokaryon-recue and Southern hybridization (Figure 22A/B).

For *glcA* deletion cassette, 5'- and 3' UTR flanking sites of *glcA* were amplified from WT gDNA with primer pairs BJ323/BJ324 and BJ325/BJ326 respectively. These oligonucleotides introduced a *Swa*I-restriction site followed by a 15 bp complementary overhang for pBluescript II KS+ at the 5'-end of the 5' UTR and at the 3'-end of the 3' UTR fragment. They further added a 15 bp overhang complementary to the hygromycin resistance marker cassette, which was amplified from pAN7-1 with primers BJ162/BJ167. The flanking sites and the hygromycin resistance marker were fused into *EcoR*V-site of pBluescript II KS+ in a seamless cloning reaction, leading to pME4346. The *glcA* deletion cassette was excised using *Swa*I and subsequently transformed into AfGB32 (*fbx15*::*gfp* overexpression). Like for Δ*ssnF*, Heterokaryon-rescue and Southern hybridization showed that *glcA* is essential for *A. fumigatus* (Figure 14B/C).

For the deletion of *nimX* the flanking sites of *nimX* were amplified with oligonucleotides BJ327/BJ328 (5' UTR) and BJ329/BJ330 (3' UTR). Like for Δ*glcA* deletion cassette these primers introduced 15 bp complementary overhangs for pBluescript II KS+ and the hygromycin resistance cassette from pAN7-1. All fragments were fused into pBluescript II KS+ in a seamless cloning reaction, generating pME4347. The deletion cassette was cut from pME4347 with *Swa*I and transformed into *A. fumigatus* strain AfGB32 (Fbx15::GFP overexpression). Heterokaryon-rescue and Southern hybridization supports that *nimX* is essential for *A. fumigatus* (Figure 21A/B).

1.2.2.5   Construction of GFP-tagged fusions of SsnF and Nic96

GFP-tagged fusions of SsnF and Nic96 were constructed with GENEART Seamless Cloning and Assembly Kit (Invitrogen). First a fusion cassette was created, containing *gfp* followed by a $^T trpC$ terminator sequence, which was fused to *hph* hygromycin resistance marker. For this approach *gfp* was amplified with oligonucleotides BJ168/BJ169, introducing a 15 bp overhang complementary to pBluescript II KS+ and a 15 bp overhang complementary to the $^T trpC$ terminator sequence. The $^T trpC$ sequence was amplified with

primers BJ166/BJ167 from pAN7-1. The hygromycin resistance marker was amplified from pAN7-1 as well with primers BJ164/BJ165, which inserted a 15 bp $^{T}trpC$ overhang at the 3'end and a 15 bp pBluescript II KS+ overhang at the 5'end. All fragments were fused into pBluescript II KS+ in a seamless cloning reaction, producing pME4285. The gfp::$^{T}trpC$::hph cassette was subsequently amplified from pME4285 with oligonucleotides OZG207/BJ163 and used for further fusion constructs.

To construct the GFP-fusions of SsnF and Nic96 each 5' UTR region was amplified together with the respective ORF with primer pairs BJ174/BJ175 and BJ266/BJ267 for $ssnF$ and $nic96$ respectively. These primer pairs introduced an MssI-site with a 15 bp overhang complementary to pBluescript II KS+ on the 5'end and a 15 bp gfp overhang on the 3'end, while the stop codon was eliminated. Furthermore the 3' UTR flanking regions of the respective genes were amplified with primer pairs BJ176/BJ177 and BJ268/BJ269, which introduced a 15 bp overhang for hph hygromycin resistance marker at the 5'end and an MssI-site accompanied by a 15 bp overhang of pBluescript II KS+ at the 3'end. Afterwards the single fragments including 5' UTR::ORF, gfp and 3' UTR were fused into the MssI-site of pBluescript II KS+ in a seamless cloning reaction, resulting in plasmids pME4286 and pME4291. The gfp-fusions of $ssnF$ and $nic96$ were excised from their respective plasmids and transformed into AfS35 (WT) strain, $\Delta fbx15$ mutant (AfGB5) and $fbx15$ overexpression strain (AfGB57). The obtained strains are AfGB64 ($\Delta akuA$, $\Delta ssnF$::hph::$ssnF$::gfp), AfGB65 ($\Delta akuA$, $\Delta fbx15$::$ptrA$, $\Delta ssnF$::hph::$ssnF$::gfp), AfGB66 ($\Delta akuA$, $ptrA$, $^{P}gpdA$::$fbx15$::$^{T}his2A$, $\Delta ssnF$::hph::$ssnF$::gfp), AfGB67 ($\Delta akuA$, $\Delta nic96$::hph::$nic96$::gfp), AfGB68 ($\Delta akuA$, $\Delta fbx15$::$ptrA$, $\Delta nic96$::hph::$nic96$::gfp) and AfGB69 ($\Delta akuA$, $ptrA$, $^{P}gpdA$::$fbx15$::$^{T}his2A$, $\Delta nic96$::hph::$nic96$::gfp). Successful replacement of the original gene locus by the fusion construct was verified by Southern hybridization.

1.2.2.6   Construction of RFP-tagged Fbx15 wild-type and phosphomutant fusions

For the construction of rfp-tagged variants of $fbx15$, first a plasmid containing $^{T}trpC$::$ptrA$::$fbx15$ 3' UTR was assembled. Therefore, the $^{T}trpC$ terminator was amplified from pAN7-1 with primers BJ309/BJ316, which introduced an $EcoR$V-site followed by a 15 bp pBluescript II KS+ overhang at the 5'end and a 15 bp $ptrA$ overhang at the 3'end. $ptrA$ was amplified with oligonucleotides OZG-(ptrA 5)/OZG-(ptrA 3) from pME3024 (Krappmann et al., 2006a; Wagener et al., 2008). The $fbx15$ 3' UTR flanking region was

amplified from D141 gDNA with primer pair BJ317/BJ312, introducing a 15 bp overhang for *ptrA* at the 3'end and a 15 bp overhang for pBluescript II KS+ at the 5'end. All fragments were fused together into the *EcoR*V-site of pBluescript II KS+ by using the GENEART Seamless Cloning and Assembly Kit (Invitrogen), resulting into plasmid pME4341.

For the fusion of *fbx15* with *rfp*, *fbx15* together with a 1.5 kb 5' UTR flanking region comprising the native promoter of *fbx15* was amplified with oligonucleotides BJ313/BJ318, which adds a 15 bp overhang complementary to pBluescript II KS+ at the 5'end and in addition removes the stop-codon from the *fbx15* ORF. *rfp* was amplified from pChS4 (Christoph Sasse, personal communication) with primers BJ321/BJ322, introducing 15 bp overhangs complementary to *fbx15* and ^{T}*trpC*. Both fragments were fused into the *EcoR*V-site of pME4341, within a seamless cloning reaction. This resulted in plasmid pME4342 which comprises the *fbx15*::*rfp* fusion cassette *fbx15* 5' UTR(*fbx15*)::*fbx15*::*rfp*::^{T}*trpC*::*ptrA*::3' UTR(*fbx15*), which is flanked by two *Mss*I-sites.

For the introduction of the mutated phospho-sites, which mimic a constant dephosphorylated state of Fbx15 at positions 468 and 469, a 5' UTR(*fbx15*)::*fbx15* part from pME4342 was amplified with oligonucleotides BJ313/BJ304. The second oligonucleotide introduced a mutation in the *fbx15* ORF, which leads to the S468A exchange. As a second part the rest of the *fbx15* ORF together with the *rfp*::^{T}*trpC*::3' UTR(*fbx15*) was amplified with primers BJ306/BJ312. Here the first oligonucleotide adds a 15 bp overhang complementary to the first part of the *fbx15* ORF and in addition adds two mutations, which will lead to an exchange of S468A and S469A. Now both parts were fused again into *EcoR*V-site of pBluescript II KS+ with a seamless cloning reaction, resulting in pME4345. The exchange of one or both serine residues at position 469 and 468 to aspartate to mimic a constant phosphorylation was achieved in the same way. First the 5' part of 5' UTR(*fbx15*)::*fbx15* was amplified from pME4342 with either BJ313/BJ336 leading to S469D, or BJ313/338 which leads to S468D. The second part was amplified with either BJ337/BJ312 or BJ340/BJ312 leading to *fbx15* (S469D) or *fbx15* (S468D; S469D) respectively. The fragments were fused into pBluescript II KS+ with the GENEART Seamless Cloning and Assembly Kit (Invitrogen), resulting into pME4348 (S469D) or pME4350 (S468D; S469D).

The *fbx15*::*rfp* fusion cassettes were excised from their plasmids with *Mss*I and transformed into *A. fumigatus* strain AfGB64, which carries the *ssnF*::*gfp* fusion. The genera-

ted strains are AfGB98 (Δ*akuA*, *fbx15*::*rfp*::*^TtrpC*::*ptrA*, Δ*ssnF*::*ssnF*::*gfp*::*hph*), AfGB101 (Δ*akuA*, *fbx15*(S468A; S469A)::*rfp*::*^TtrpC*::*ptrA*, Δ*ssnF*::*ssnF*::*gfp*::*hph*), AfGB102 (Δ*akuA*, *fbx15*(S469D)::*rfp*::*^TtrpC*::*ptrA*, Δ*ssnF*::*ssnF*::*gfp*::*hph*) and AfGB104 (Δ*akuA*, *fbx15*(S468D; S469D)::*rfp*::*^TtrpC*::*ptrA*, Δ*ssnF*::*ssnF*::*gfp*::*hph*). Successful replacement of the original *fbx15*-locus with the *rfp*-fusion constructs was verified with Southern hybridization and in case of the phosphomutant versions of *fbx15*::*rfp* also with sequencing.

1.2.2.7   Construction of BiFC-strains

For the construction of BiFC-plasmids *A. fumigatus skpA* (Afu5g06060) was amplified from D141 gDNA with BJ69/BJ71 and fused to *cyfp* with OZG75/BJ71. The resulting module *cyfp*::*skpA* was cloned into *Pme*I-site of pME3160 (Bayram et al., 2008) containing a bidirectional *^PniiA*/*^PniaD* nitrate inducible promoter system, resulting in pME4052. To test Fbx15/SkpA interaction *fbx15* was amplified from D141 genomic DNA with BJ66/BJ64 and subsequently fused to *nyfp* with OZG73/BJ64. The resulting module was cloned into *Swa*I-site of pME4052 resulting in pME4056. To test SconB-SkpA interaction *sconB* was amplified from D141 genomic DNA with BJ68/BJ24 and fused to *nyfp* with OZG73/BJ24. *nyfp*::*sconB* was then cloned into *Swa*I-site of pME4052 resulting in pME4058.

To examine the interaction between Fbx15 and SsnF, *fbx15* was amplified from cDNA with BJ234/BJ235 and cloned into pBluescript II KS+ resulting in pME4298. The *fbx15* cDNA was amplified from pME4298 with BJ65/BJ66, fused to *cyfp* with OZG75/BJ64 and finally cloned into *Pme*I-site of pME3160 ending with pME4301. *ssnF* was amplified from cDNA with primer-pair BJ244/BJ245 and cloned into pBluescript II KS+ resulting in pME4300. *ssnF* cDNA was then amplified from the mentioned plasmid with BJ295/BJ245 and fused to *nyfp* with OZG73/BJ245. *nyfp*::*ssnF* was then cloned into *Swa*I-site of pME4301 resulting in pME4302. pME4056, pME4058 and pME4302 were transformed into *A. fumigatus* strain Af293.1 containing a *pyrG1* mutation. The obtained transformants are AfGB44 (*pyrG1*, *pyrG*, *^PniiA*::*cyfp*::*skpA*::*^TniiA*, *^PniaD*::*nyfp*::*fbx15*::*^TniaD*), AfGB45 (*pyrG1*, *pyrG*, *^PniiA*::*cyfp*::*skpA*::*^TniiA*, *^PniaD*::*nyfp*::*sconB*::*^TniaD*) and AfGB93 (*pyrG1*, *pyrG*, *^PniiA*::*cyfp*::*fbx15*::*^TniiA*, *^PniaD*::*nyfp*::*ssnF*::*^TniaD*).

Table 3: Plasmids used in this study.

Plasmid	Description	Reference
pAN7-1	hygromycin B resistance (*hph*) vector, *amp^R*	(Punt et al., 1987)
pJET1.2	blunt Cloning Vector: CloneJET™, *amp^R*	Fermentas GmbH
pBluescript II KS+	Cloning Vector, *amp^R*	Fermentas GmbH
pSK379	pyrithiamine resistance (*ptrA*) vector including *gpdA* promoter for high expression, *amp^R*	(Wagener et al., 2008)
pME3024	pyrithiamine resistance (*ptrA*) vector, *amp^R*	(Krappmann et al., 2006a)
pME3160	expression module ^{T}*niiA*-^{P}*niiA* / ^{P}*niaD*-^{T}*niaD*, *pyrG*, *amp^R*	(Bayram et al., 2008)
pME3701	*fbx15* with 1.5 kb flanking sites in pAN7-1	(Jöhnk, 2009)
pME3704	*fbx23* with 1.5 kb flanking sites in pAN7-1	(Jöhnk, 2009)
pME3706	*grrA* with 1.5 kb flanking sites in pAN7-1	(Jöhnk, 2009)
pME4042	5' UTR (*fbx15*)::*ptrA*::3' UTR (*fbx15*) in pJET1.2	This study
pME4043	5' UTR (*sconB*)::*ptrA*::3' UTR (*sconB*) in pJET1.2	This study
pME4044	5' UTR (*fbx15*)::*ptrA*::^{P}*gpdA*::*fbx15*::*gfp*::3' UTR (*fbx15*) in pJET1.2	This study
pME4045	5' UTR (*fbx15*)::*ptrA*::^{P}*gpdA*::*fbx15*::*tap*::3' UTR (*fbx15*) in pJET1.2	This study
pME4046	5' UTR (*sconB*)::*ptrA*::^{P}*gpdA*::*sconB*::*gfp*::3' UTR (*sconB*) in pJET1.2	This study
pME4047	5' UTR (*sconB*)::*ptrA*::^{P}*gpdA*::*sconB*::*tap*::3' UTR (*sconB*) in pJET1.2	This study
pME4048	5' UTR (*fbx15*)::*ptrA*::^{P}*gpdA*::*fbx15*(P12S)::*gfp*::3' UTR (*fbx15*) in pJET1.2	This study
pME4049	5' UTR (*fbx15*)::*ptrA*::^{P}*gpdA*::*fbx15*(P12S)::*tap*::3' UTR (*fbx15*) in pJET1.2	This study
pME4050	5' UTR (*sconB*)::*ptrA*::^{P}*gpdA*::*sconB*(P200S)::*gfp*::3' UTR (*sconB*) in pJET1.2	This study
pME4051	5' UTR (*sconB*)::*ptrA*::^{P}*gpdA*::*sconB*(P200S)::*tap*::3' UTR (*sconB*) in pJET1.2	This study
pME4052	*cyfp*::*skpA* in *Pme*I-site of pME3160	This study
pME4056	*nyfp*::*fbx15* in *Swa*I-site of pME4052	This study
pME4058	*nyfp*::*sconB* in *Swa*I-site of pME4052	This study
pME4284	^{P}*gpdA*::*fbx15* in *Stu*I-site of pAN7-1	This study
pME4285	*gfp*::^{T}*trpC*::^{P}*gpdA*::*hph* in pBluescript II KS+	This study
pME4286	5' UTR (*ssnF*)::*ssnF*::*gfp*::^{T}*trpC*::^{P}*gpdA*::*hph*::3' UTR (*ssnF*) in pBluescript II KS+	This study
pME4289	*fbx15* in *Mss*I-site of pSK379	This study

Plasmid	Description	Reference
pME4291	5' UTR (*nic96*)::*nic96*::*gfp*::^{T}*trpC*::^{P}*gpdA*::*hph*::3' UTR (*nic96*) in pBluescript II KS+	This study
pME4292	*gfp* in *Mss*I-site of pSK379	This study
pME4294	5 'UTR (*ssnF*)::*ptrA*::3' UTR(*ssnF*) in pBluescript II KS+	This study
pME4298	*fbx15 cDNA* in pBluescript II KS+	This study
pME4300	*ssnF cDNA* in pBluescript II KS+	This study
pME4301	*cyfp*::*fbx15* (cDNA) in *Mss*I-site of pME3160	This study
pME4302	*nyfp*::*ssnF* (cDNA) in *Smi*I-site of pME4301	This study
pME4341	(*EcoR*V-site)::^{T}*trpC*::*ptrA*::3 'UTR (*fbx15*) in *EcoR*V-site of pBluescript II KS+	This study
pME4342	5' UTR (*fbx15*)::*fbx15*::*rfp* in *EcoR*V-site of pME4341	This study
pME4345	5' UTR (*fbx15*)::*fbx15* (S468A; S469A)::*rfp* in *EcoR*V-site of pME4341	This study
pME4346	5' UTR (*glcA*)::^{P}*gpdA*::*hph*::^{T}*trpC*::3' UTR (*glcA*) in *EcoR*V-site of pBluescript II KS+	This study
pME4347	5 'UTR (*nimX*)::^{P}*gpdA*::*hph*::^{T}*trpC*::3' UTR (*nimX*) in *EcoR*V-site of pBluescript II KS+	This study
pME4348	5 'UTR (*fbx15*)::*fbx15* (S469D)::*rfp* in *EcoR*V-site of pME4341	This study
pME4350	5 'UTR (*fbx15*)::*fbx15* (S468D; S469D)::*rfp* in *EcoR*V-site of pME4341	This study

Table 4: Oligonucleotides used in this study.

Name	Size	Sequence
OZG-(ptrA 5)	28-mer	AAT TGA TTA CGG GAT CCC ATT GGT AAC G
OZG-(ptrA 3)	29-mer	TCT TGC ATC TTT GTT TGT ATT ATA CTG TC
OZG73	21-mer	ATG GTG AGC AAG GGC GAG GAG
OZG75	25-mer	CGT GGC GAT GGA GCG CAT GAT ATA G
OZG207	21-mer	ATG GCC GAC AAG CAG AAG AAC
OZG209	27-mer	GTGGTTCATGACCTTCTGTTTCAGGTC
OZG387	24-mer	GGT GGT AGC GGT GGT ATG GTG AGC
OZG388	43-mer	GGT GGT AGC GGT GGT AAG AGA AGA TGG AAA AAG AAT TTC ATA G
HO1	21-mer	CTC TTC GAA GGC TGG ACT TGC
HO2	22-mer	GGA GAT GGC GAG GAA TGA TAC G
Afbox15 del A	24-mer	CGT GGC TCT TTA GTC GGT CAT TTG
Afbox15 del B	24-mer	GGA TAC GAT GAT GAT GGA ACC

Name	Size	Sequence
Afbox15 del C	56-mer	CAT TTC GTT ACC AAT GGG ATC CCG TAA TCA ATT GTC CAA ACT GAG AGG AAG AGA TG
Afbox15 del D	56-mer	GAA AGA CAG TAT AAT ACA AAC AAA GAT GCA AGA CGA TCC GTC CTC TCT AGT TGC AG
Afbox15 del E	22-mer	GTG TAA TGC TGC GTG CTC TAC G
Afbox15 del F	23-mer	GTC CGC CTA TCA AAC GGC TTG TG
Afbox23 del A	21-mer	CTC TTG TCA GCT CCT CGG CAG
Afbox23 del B	25-mer	CAC CTA AAC ACT CAA GTG ACA AGT G
Afbox23 del C	58-mer	CAT TTC GTT ACC AAT GGG ATC CCG TAA TCA ATT GTG AAA AAT CTT CGT CCG ATA ACA G
Afbox23 del D	56-mer	GAA AGA CAG TAT AAT ACA AAC AAA GAT GCA AGA ATA GTT TAA CGA CCT TCG TTC CC
Afbox23 del E	24-mer	CTC TAA CCG TCC GAA TGA ATA TAG
Afbox23 del F	24-mer	GGT ACA AGC TTG GTC AGA CCA CTC
Afbox25 del A	24-mer	CCT CGA TTG GCG TTC TAA TTG ACC
Afbox25 del B	23-mer	GCA TCT GCG TGT TTT CGA GGA TG
Afbox25 del C	55-mer	CAT TTC GTT ACC AAT GGG ATC CCG TAA TCA ATT AGC GGC ACT CAA CCA CTC ATC T
Afbox25 del D	58-mer	GAA AGA CAG TAT AAT ACA AAC AAA GAT GCA AGA AAG CTC CTT GAG TTG CTT TTT C T
Afbox25 del E	25-mer	GAT AGC ATC AAA GAA AGA AAC CAG G
Afbox25 del F	24-mer	GGT CTT AGT TGA GAT GCT GTC CTG
AfgrrA del A	24-mer	GCA TCC CAA GTA TTG GAT CAT CTC
AfgrrA del B	22-mer	GCT GCC TTC AGT AAG GCC AAT C
AfgrrA del C	54-mer	CAT TTC GTT ACC AAT GGG ATC CCG TAA TCA ATT TCT GGA TAG CGG GTG TGA AGC
AfgrrA del D	56-mer	GAA AGA CAG TAT AAT ACA AAC AAA GAT GCA AGA TAC CCC TCT GCT ATT CCT TCG AG
AfgrrA del E	24-mer	GTT CGA CTG CGT ATC GTC AAA GAC
AfgrrA del F	25-mer	CGG ATA TAC ACC ATG ATA TTG GTA C
BJ1	33-mer	AAA GGT ACC GGA TAC GAT GAT GAT GGA ACC TTG
BJ2	38-mer	TTG TTA ACT CTT GCA TCT TTG TTT GTA TTA TAC TGT CT
BJ3	24-mer	GAT CTT TGC CCG GTG TAT GAA ACC
BJ4	21-mer	GGT GAT GTC TGC TCA AGC GGG
BJ5	53-mer	AAC AGC TAC CCC GCT TGA GCA GAC ATC ACC ATG ACC GAC ATG AGC AAG AAC CT
BJ6	55-mer	GCC CTT GCT CAC CAT ACC ACC GCT ACC ACC CCG AAG CCA ATA TCC ATG ATT AAT G
BJ7	52-mer	ACT CAC GGC ATG GAC GAA CTG TAC AAG TAG CGA TCC GTC CTC TCT AGT TGC A

Name	Size	Sequence
BJ8	60-mer	TAT GAA ATT CTT TTT CCA TCT TCT CTT ACC ACC GCT ACC ACC CCG AAG CCA ATA TCC ATG
BJ9	52-mer	GAC GCG AAT TCC GCG GGG AAG TCA ACC TGA CGA TCC GTC CTC TCT AGT TGC A
BJ10	32-mer	AAA GCC GGC GCA TCT GCG TGT TTT CGA GGA TG
BJ11	52-mer	AAC AGC TAC CCC GCT TGA GCA GAC ATC ACC ATG GAT GCC CAT GAA CTG TCG T
BJ12	52-mer	GCC CTT GCT CAC CAT ACC ACC GCT ACC ACC GGT CTG GAA ACT GTA CAT GCG C
BJ13	56-mer	ACT CAC GGC ATG GAC GAA CTG TAC AAG TAG AAG CTC CTT TGA GTT TGC TTT TTC TT
BJ14	34-mer	TTT GCC GGC GAT AGC ATC AAA GAA AGA AAC CAG G
BJ15	52-mer	TTT CCA TCT TCT CTT ACC ACC GCT ACC ACC GGT CTG GAA ACT GTA CAT GCG C
BJ16	56-mer	GAC GCG AAT TCC GCG GGG AAG TCA ACC TGA AAG CTC CTT TGA GTT TGC TTT TTC TT
BJ17	25-mer	GCT GAT GGA GTC CAG GTT CTT GCT C
BJ18	55-mer	GAC ATG AGC AAG AAC CTG GAC TCC ATC AGC TAT GAT GTG TTC TAC CAG ATC GCT T
BJ19	23-mer	GCT GAG AGC CGT GAG GAA GTC GA
BJ20	60-mer	ATT CGT ATC GAC TTC CTC ACG GCT CTC AGC CCA GAA ATC TCT TTC AAA ATT CTA TGT TAT
BJ21	23-mer	ATG GAT GCC CAT GAA CTG TCG TT
BJ24	23-mer	TCA GGT CTG GAA ACT GTA CAT GC
BJ37	23-mer	CTA CTT GTA CAG TTC GTC CAT GC
BJ38	20-mer	TCA GGT TGA CTT CCC CGC GG
BJ63	22-mer	ATG ACC GAC ATG AGC AAG AAC C
BJ64	22-mer	GTC ACC GAA GCC AAT ATC CAT G
BJ65	52-mer	AAC GAC CTG AAA CAG AAG GTC ATG AAC CAC ATG ACC GAC ATG AGC AAG AAC C
BJ66	52-mer	AAC GTC TAT ATC ATG CGC TCC ATC GCC ACG ATG ACC GAC ATG AGC AAG AAC C
BJ67	53-mer	AAC GAC CTG AAA CAG AAG GTC ATG AAC CAC ATG GAT GCC CAT GAA CTG TCG TT
BJ68	53-mer	AAC GTC TAT ATC ATG CGC TCC ATC GCC ACG ATG GAT GCC CAT GAA CTG TCG TT
BJ69	55-mer	AAC GAC CTG AAA CAG AAG GTC ATG AAC CAC ATG ACT ACT GTT ACT CTC ACA AGC T
BJ70	55-mer	AAC GTC TAT ATC ATG CGC TCC ATC GCC ACG ATG ACT ACT GTT ACT CTC ACA AGC T
BJ71	21-mer	TTA CTC CTC GGC CCA CTC GTT

Name	Size	Sequence
BJ162	22-mer	CTA CAA CGA CCA TCA AAG TCG T
BJ163	20-mer	CTA TTC CTT TGC CCT CGG AC
BJ164	37-mer	CAC ATC TCC ACT CGA CTA CAA CGA CCA TCA AAG TCG T
BJ165	35-mer	ATC GAT AAG CTT GAT CTA TTC CTT TGC CCT CGG AC
BJ166	18-mer	AGT AGA TGC CGA CCG CGG
BJ167	20-mer	TCG AGT GGA GAT GTG GAG TG
BJ168	34-mer	CTG CAG GAA TTC GAT GGT GGT AGC GGT GGT ATG G
BJ169	37-mer	CGG TCG GCA TCT ACT CTA CTT GTA CAG TTC GTC CAT G
BJ174	45-mer	CTG CAG GAA TTC GAT GTT TAA ACA TAC TAG CTA CTA AGC CTC CTA
BJ175	33-mer	ACC ACC GCT ACC ACC GGC CGA CTC CTG TTT CGA
BJ176	35-mer	AGG GCA AAG GAA TAG GCA CAT GAT CCT CTC TCG TC
BJ177	40-mer	ATC GAT AAG CTT GAT GTT TAA ACC GCT CAG GTG CTC AGC C
BJ234	29-mer	ACT CGA GAT GAC CGA CAT GAG CAA GAA CC
BJ235	29-mer	TCT CGA GGT CAC CGA AGC CAA TAT CCA TG
BJ244	25-mer	AGA ATT CAT GGC TCA CAC TCA GCC G
BJ245	26-mer	TGA ATT CTC AGG CCG ACT CCT GTT TC
BJ256	21-mer	GGA CGG GAA GCG GAT AGA ACT
BJ257	22-mer	CAG AGG GAG CCT TGG TCA TAC A
BJ266	49-mer	CTG CAG GAA TTC GAT GTT TAA ACT GTA TTA GAG GAC ATC ATG CTA ATT T
BJ267	34-mer	ACC ACC GCT ACC ACC GTA AGC CCC GAT ATC CGC T
BJ268	38-mer	AGG GCA AAG GAA TAG TGC TTA TCA TCT GGA GTA TCT GG
BJ269	47-mer	ATC GAT AAG CTT GAT GTT TAA ACA CCT CCA GCT TCA ATC AAT TTT TC
BJ290	46-mer	CTG CAG GAA TTC GAT GTT TAA ACA TAC TAG CTA CTA AGC CTC CTA T
BJ291	32-mer	ATC CCG TAA TCA ATT TCT GCT GGC GGG AGG AC
BJ292	35-mer	AAC AAA GAT GCA AGA GCA CAT GAT CCT CTC TCG TC
BJ293	40-mer	ATC GAT AAG CTT GAT GTT TAA ACC GCT CAG GTG CTC AGC C
BJ295	48-mer	AAC GTC TAT ATC ATG CGC TCC ATC GCC ACG GCT CAC ACT CAG CCG TCG
BJ304	19-mer	CTG GGT GGG GGT CGT TGA C
BJ306	37-mer	ACG ACC CCC ACC CAG CAG CAC CAG GAG GCA GCC ACA T
BJ309	39-mer	CTG CAG GAA TTC GAT GAT ATC AGT AGA TGC CGA CCG CGG
BJ312	46-mer	ATC GAT AAG CTT GAT GTT TAA ACA CCT AGT TCA GAG ATA

Name	Size	Sequence
		TGT CCT G
BJ313	45-mer	CTG CAG GAA TTC GAT GAT GTT TAA ACT GCA TGC TGT CCA GTT GGC
BJ316	35-mer	ATC CCG TAA TCA ATT TCG AGT GGA GAT GTG GAG TG
BJ317	35-mer	AAC AAA GAT GCA AGA CGA TCC GTC CTC TCT AGT TG
BJ318	24-mer	CCG AAG CCA ATA TCC ATG ATT AAT
BJ323	43-mer	CTG CAG GAA TTC GAT ATT TAA ATT GGG AAG GTT AGA TAG GGG C
BJ324	35-mer	TGA TGG TCG TTG TAG GAC GTG CTG ATT CTC GAG AC
BJ325	39-mer	CAC ATC TCC ACT CGA GAA ATC ATA CGA GCT TTT CCA TGT
BJ326	42-mer	ATC GAT AAG CTT GAT ATT TAA ATC CCG AAG TCA GCG GGA TTG
BJ327	42-mer	CTG CAG GAA TTC GAT ATT TAA ATA GCT GTG CGC AGC AGC TTG
BJ328	32-mer	TGA TGG TCG TTG TAG GGT GGC GGT CTC CTT GC
BJ329	39-mer	CAC ATC TCC ACT CGA CTG AAA ACT TGT CAC GAC TTT TAC
BJ330	42-mer	ATC GAT AAG CTT GAT ATT TAA ATA CCG GGC CAC TTG GTA CTG
BJ336	22-mer	GTC TGA TGG GTG GGG GTC GTT G
BJ337	33-mer	CCC CAC CCA TCA GAC CCA GGA GGC AGC CAC ATC
BJ338	21-mer	GTC TGG GTG GGG GTC GTT GAC
BJ340	36-mer	GAC CCC CAC CCA GAC GAC CCA GGA GGC AGC CAC ATC

2   Methods

2.1   Cultivation of microorganisms

2.1.1   Cultivation of *Escherichia coli*

E. coli strains DH5α and MACH-1 were grown in LB-complete medium (1% tryptone, 0.5% yeast extract, 1% NaCl) at 37 °C. For solid media 2% (w/v) agar was added. Preparation of calcium competent *E. coli* cells and transformation was performed with SOB- and SOC-media according to (Hanahan et al., 1983; Inoue et al., 1990). Selective medium was achieved by using ampicillin in a final concentration of 100 µg/ml. For blue/white screening of *E. coli* colonies, which were transformed with a pBluescript II KS+ derived

vector, X-Gal (BCIG: 5-bromo-4-chloro-3-indolyl-β-D-galactopyranoside) was added to the plates in a final concentration of 40 µg/ml.

2.1.2   Cultivation of *Aspergillus fumigatus*

A. fumigatus strains were cultivated in *Aspergillus* minimal media, AMM: [1% D-glucose, 1x AspA (70 mM NaNO$_3$, 7 mM KCl, 11.2 mM KH$_2$PO$_4$, pH 5.5), 2 mM MgSO$_4$, 1x trace elements (76 µM ZnSO$_4$, 178 µM H$_3$BO$_3$, 25 µM MnCl$_2$, 18 µM FeSO$_4$, 7.1 µM CoCl$_2$, 6.4 µM CuSO$_4$, 6.2 µM Na$_2$MoO$_4$, 174 µM EDTA)] (Pontecorvo et al., 1953) at 37 °C. For selective media either pyrithiamine (100 ng/ml) or hygromycin G (150 µg/ml) were added to the media. Solid medium consisted of 2% (w/v) agar. Vegetative mycelium was obtained by inoculating 100 ml liquid AMM with 10^6-10^7 conidia, which were grown on a shaker for 18 hours at 37 °C. The grown mycelium was filtered with sterile miracloth and washed with saline (0.96% (w/v) NaCl) for further applications.

2.2   Isolation of nucleic acids

2.2.1   Extraction of genomic DNA from *A. fumigatus*

For genomic DNA (gDNA) from *A. fumigatus*, vegetative mycelium was ground in liquid nitrogen. 0.5 ml pulverized mycelium was lysed in 800 µl lysis buffer (50 mM Tris-HCl (pH 7.2), 50 mM EDTA, 3% SDS, 1% 2-mercaptoethanol) at 65 °C for one hour. gDNA was extracted with phenol and subsequently precipitated with isopropanol, containing 50 mM sodium acetate. Finally gDNA was dissolved in RNAse A containing EB-buffer (Qiagen) and stored at 4 °C.

2.2.2   Plasmid-DNA preparation

Plasmids from *E. coli* cultures were prepared with the QIAprep Spin Miniprep Kit or the QIAGEN Plasmid *Plus* Kit from Qiagen according to the manufacturers protocol. Plasmid-DNA was eluted with EB-buffer or H$_2$O and stored at -20 °C.

2.2.3   Isolation of DNA-fragments from agarose gels

DNA-bands were excised from agarose gels under low energy UVA-light ($\lambda = 366$ nm). DNA-fragments were extracted from the agarose with the QIAprep Spin Miniprep Kit from Qiagen as specified by the manufacturer. DNA-fragments were eluted in 30-50 µl H_2O or EB-buffer and stored at -20 °C.

2.2.4   RNA preparation and cDNA synthesis

RNA from vegetative mycelium was prepared with the RNeasy Plant Mini Kit from Qiagen. Mycelium was ground in liquid nitrogen and 500 mg of pulverized mycelium was lysed with 600 µl RLT-buffer that was not supplemented with β-mercaptoethanol. RNA-extraction was then performed according to manufacturer's guidelines. RNA was eluted with RNAse free H_2O and stored at -20 °C. For cDNA synthesis 0.8 µg RNA was treated with DNase and subsequently transcribed into cDNA with the QuantiTect Reverse Transcription kit from Qiagen following the manufacturer's protocol.

2.3   Molecular techniques

2.3.1   Bioinformatics

Homologous F-box proteins for *A. fumigatus* Fbx15, SconB and GrrA in other species were identified by NCBI-BLAST with blastp-algorithm (http://blast.ncbi.nlm.nih.gov/Blast.cgi) and are shown in Table 5. F-box domain of *A. fumigatus* Fbx15 was identified by amino-acid sequence analysis for Pfam-domain matches (http://pfam.sanger.ac.uk) (Finn et al., 2014). Additional Fbx15 specific motifs were identified by comparing protein sequences of Fbx15 homologs with MEME: http://meme.nbcr.net/meme/ (Bailey and Elkan, 1994). Nuclear localization sequences (NLS) were determined using the cNLS Mapper program: http://nls-mapper.iab.keio.ac.jp/cgi-bin/NLS_Mapper_form.cgi (Kosugi et al., 2009). Putative phosphorylation sites of Fbx15 primary amino acid sequence were analyzed with NetPhos 2.0 (http://www.cbs.dtu.dk/services/NetPhos) (Blom et al., 1999). Analysis of the MS2-spectra for the identification of specific phopho-sites inside identified phosphopeptides was achieved with the phosphoRS software (Taus et al., 2011).

2.3.1   Recombinant DNA methods

Generation of linear and circular DNA molecules were based on standard recombinant DNA technology protocols as described previously (Bayram et al., 2008). Oligonucleotides and plasmids used in this study are listed in Tables 3 and 4 respectively. For polymerase chain reaction (PCR) either Taq- (Fermentas) or Phusion-polymerase (Finnzymes) were used. Fusion of PCR-products was achieved by using fusion PCR protocol, which is described in detail (Szewczyk et al., 2006).

2.3.2   Southern hybridization

Southern hybridization was carried out due to standard protocols as described (Bayram et al., 2008). DNA-Probes were amplified from D141 genomic DNA with primers listed in Table 4 and either radioactive labeled with α-^{32}P-dATP from Hartmann Analytic GmbH using the DecaLabel™ DNA Labeling Kit from Thermo Scientific or chemiluminescent labeled with the Amersham Gene Images AlkPhos Direct Labeling and Detection System with CDP-Star Detection Reagent from GE Healthcare Europe GmbH. Nucleic acids were transferred to Amersham Hybond-N nylon membrane during capillary blotting and for detection either Amersham Hyperfilm MP for autoradiography or Amersham Hyperfilm ECL for chemiluminescent signals from GE Healthcare Europe GmbH were used.

2.3.3   Heterokaryon rescue

The heterokaryon rescue for the deletion of *ssnF*, *glcA* and *nimX* was carried out as described to examine whether these genes are essential for fungal growth (Osmani et al., 2006). First, conidia of primary transformants were picked and equally plated on non-selective AMM-medium and on selective AMM-medium plates containing pyrithiamine. The plates were incubated at 37 °C for 3 days. From transformants, which were still growing on the selective medium, conidia were stroked out again on selective medium. From these conidia genomic DNA was extracted and a Southern hybridization was performed.

2.3.4   Quantitative real-time PCR

The expression of *fbx15* upon oxidative stress was measured with quantitative real-time PCR using a Light Cycler 2.0 System from Roche GmbH. The total RNA from AfS35 (WT) cultures treated with 3 mM H_2O_2 for indicated time points was extracted and transcribed into cDNA. The gene expression of *fbx15* was measured from 1:10 dilutions of the cDNA samples with primer pair BJ256/BJ257 and RealMasterMix SYBR ROX 2.5x from 5 PRIME GmbH. Histone *h2A*-expression was measured with primers HO1/HO2 and used as reference.

For the expression of *gliZ* and *gliP*, cultures of AfS35 (WT), $\Delta fbx15$ and $\Delta fbx15::fbx15^+$ were grown for seven days in modified Czapek-Dox medium (3% sucrose, 1x AspA (70 mM $NaNO_3$, 7 mM KCl, 11.2 mM KH_2PO_4, pH 5.5), 2 mM $MgSO_4$, 36 µM $FeSO_4$). RNA-extraction and cDNA transcription were carried out as described above for *fbx15* expression. Real-Time PCR samples were prepared from 1:5 dilutions of the cDNA-samples using primer pairs GliZf/GliZr (*gliZ*) and GliPf/GliPr (*gliP*) in comparison to actin-expression (Afactinf/Afactinr), which were previously described by Gardiner & Howlett in 2005 with "MESA GREEN qPCR MasterMix Plus for SYBR® Assay" (Eurogentec) (Gardiner and Howlett, 2005). Gene-expressions were measured with a CFX Connect™ Real-Time System from Bio-Rad. The real-time PCR data was analyzed with $2\text{-}\Delta\Delta C_T$ method for relative quantification of gene expression (Schmittgen and Livak, 2008).

2.4   Protein methods

2.4.1   Protein extraction

Crude protein extracts from vegetative mycelia were obtained by extraction from frozen ground mycelia with B300 buffer (300 mM NaCl, 100 mM Tris-HCl pH 7.5, 10% glycerol, 1 mM EDTA, 0.1% NP-40) supplemented with 1.5 ml/L 1 M DTT, Complete Protease Inhibitor Cocktail EDTA-free (Roche), 3 ml/L 0.5 M Benzamidine, 10 ml/L phosphatase inhibitors (100 mM NaF, 50 mM NaVanadate, 800 mM β-glycerolephosphate) and 10 ml/L 100 mM PMSF.

Protein concentrations were calculated according to the method described by Bradford using the RotiQuant solution (Carl Roth GmbH & Co. KG) according to the manufacturer's conditions (Bradford, 1976).

2.4.2   Immunoblotting

For Immunoblotting experiments 100-150 μg crude protein extracts were mixed with 3x sample buffer (250 mM Tris HCl pH 6.8, 15% β-mercaptoethanol, 30% glycerol, 7% SDS, 0.3% bromphenol blue) and denatured at 95 °C for 10 min. The proteins were subsequently separated by SDS-PAGE and transferred to a nitrocellulose membrane (Whatman) by electro blotting as described previously (Christmann et al., 2013). PageRuler Prestained Protein Ladder (Fermentas) was used as molecular marker. Antibodies used for detection of fusion proteins are described in section 2.4.3. Signals were detected by enhanced chemiluminescence technique (Tesfaigzi et al., 1994) with either a Amersham Hyperfilm-P (GE Healthcare Limited) or with the Fusion SL7 system (Peqlab). For signal quantification Bio 1D imaging software (Peqlab) was used.

Protein stabilities were determined from vegetative grown cultures, which were incubated with 25 μg/ml cycloheximide for indicated time periods prior to protein extraction.

2.4.3   Antibodies used in this study

For the detection of GFP-signals α-GFP mouse antibody (SantaCruz) was used in 1:1000 dilution in TBS, containing 5% (w/v) non-fat dry milk powder. TAP signals were obtained using α-Calmodulin rabbit antibody (Millipore) in 1:2000 dilution in TBS 5% dry milk. RFP signals were detected with mouse monoclonal α-RFP [3F5] antibody (Chromotek) diluted 1:1000 in TBS 5% dry milk. Ubiquitinated proteins were detected with a custom made polyclonal α-UbiA rabbit antibody (GenScript), which was used in 1:2000 dilution in TBST (0.05% Tween-20) including 5% dry milk. Actin or tubulin, used as loading control were detected with α-Actin rabbit antibody and α-tubulin mouse antibody (Sigma-Aldrich) both diluted 1:2000 in TBS 5% dry milk. For the detection of the native Fbx15 protein from AfS35 (WT) cultures a custom made polyclonal Fbx15 rabbit antibody diluted 1:1000 in TBST (0.2% Tween-20) dry milk was applied.

Phosphorylated Fbx15-GFP protein was detected with anti-phosphoserine/threonine rabbit antibody (Abcam) diluted 1:1000 in TBST (0.05% Tween-20) containing 3% BSA. Membranes with purified Fbx15-GFP were blocked in TBS containing 3% BSA instead of 5% non-fat dry milk powder.

As second antibody peroxidase coupled rabbit anti-mouse (Jackson ImmunoResearch) or goat anti-rabbit (Invitrogen) in 1:2500 dilution in TBS 5% dry milk was used.

2.4.4 GFP- / RFP-trap

For the immunoprecipitation of GFP- or RFP-tagged proteins GFP-trap_A and RFP-trap_A agarose beads (Chromotek) were applied. Proteins were extracted from 5 ml frozen pulverized mycelium. 5 ml of protein crude extracts were incubated with 40 µl of GFP-Trap_A or RFP-Trap_A beads, respectively, which were previously equilibrated to the B300-buffer. After two hours of incubation at 4 °C the beads were washed twice with B300-buffer and transferred into a fresh 1.5 ml reaction tube. The beads were boiled in 100 µl 3x SDS-sample buffer for 10 min at 95 °C to elute the bound proteins from the beads. The extracted proteins were used directly for SDS-PAGE followed by immuno-blotting or coomassie-staining and tryptic digestion for LC-MS/MS analysis.

2.4.5 Tandem affinity purification (TAP)

Purification of TAP-tagged Fbx15, Fbx15(P12S), SconB and SconB(P200S) was performed with a modified version of the Tandem Affinity Purification (TAP) Protocol as described (Bayram et al., 2012). TAP-tagged overexpression strains were grown in liquid AMM for 24 hours at 37 °C. Mycelia was harvested and washed with 0.96% NaCl / 1% DMSO / 1% 100 mM PMSF. Crude extracts were prepared from ground mycelium with B300 buffer as described in section 2.4.1. Protein extracts were incubated with 300 µl of IgG sepharose 6 Fast Flow (GE Healthcare) for 3 hours at 4 °C on a rotary shaker. The suspension was poured onto a Poly-prep chromatography column (BioRad) and washed once with 10 ml of IPP300 (25 mM Tris-HCl pH 8.0, 300 mM NaCl, 0.1% NP-40, 2 mM DTT), once with 10 ml IPP150 (25 mM Tris-HCl pH 8.0, 150 mM NaCl, 0.1% NP-40, 2 mM DTT), and once with TEV cleavage buffer (TEV-CB: 25 ml Tris-HCl pH 8.0, 150 mM NaCl, 0.1% NP-40, 0.5 mM EDTA, 1 mM DTT). The TEV cleavage was performed with 350 U of AcTEV (Invitrogen) in 1 ml of TEV-CB at 4 °C for 12 hours. The eluate was poured into a new column containing 6 ml calmodulin binding buffer (CBB: 25 mM Tris-HCl pH 8.0, 150 mM NaCl, 1 mM Mg-acetate, 1 mM imidazole, 2 mM CaCl$_2$, 10 mM β-mercaptoethanol), 6 µl 1 M CaCl$_2$ and 300 µl of Calmodulin Affinity Resin (Agilent Technologies). The elution was repeated once with 1 ml of TEV-CB and the eluate was incubated with calmodulin beads for 2 hours at 4 °C on a rotary shaker. After incubation the beads were washed twice with CBB containing either 0.1% NP-40 or 0.02% NP-40. Proteins were eluted twice with 0.5 ml calmodulin elution buffer (CEB: 25 mM Tris-HCl pH 8.0, 150 mM NaCl, 0.02% NP-40, 1 mM Mg-acetate, 1 mM imida-

zole, 20 mM EGTA, 10 mM β-mercaptoethanol) followed by precipitation with trichloro-acetic acid (TCA) with a ratio of 1:4 for 30 minutes on ice and periodic vortexing. Proteins were pelleted by centrifugation and washed with acetone. The final pellet was resuspended in protein loading dye and separated by SDS-PAGE. The protein bands were stained with Coomassie Brilliant Blue G-Colloidal staining (Sigma).

2.4.6   Coomassie staining

Separated proteins on an SDS gel were incubated in fixing solution (7% glacial acetic acid / 40% methanol) for 1 hour. Fixed proteins were stained with Brilliant Blue G-Colloidal Concentrate (Sigma), which was diluted with 20% methanol according to manufactures specifications. Protein containing gels were destained subsequently with 10% acetic acid / 25% methanol (40 sec) and 25% methanol (2 hours).

2.4.7   Tryptic digestion of protein samples

Proteins in the coomassie-stained polyacrylamide pieces were in-gel digested with trypsin (Shevchenko et al., 1996) using "Sequencing Grade Modified Trypsin" (Promega). In brief, coomassie-stained protein bands were excised from the gel and cut into 2 mm pieces. Gel pieces were covered with acetonitrile and incubated for 10 min at room temperature. After removal of acetonitrile the remaining gel pieces were dried in a speedvac for 10 min at 50 °C. Subsequently the proteins in the gel pieces were reduced by incubation with 10 mM DTT, prepared in 100 mM NH_4HCO_3, for 1 hour at 56 °C. The DTT-solution was removed and exchanged to 55 mM iodocetamide, prepared in 100 mM NH_4HCO_3, to alkylate reduced cysteine residues. After incubation for 45 min in the dark, the gel pieces were repeatedly washed with 100 mM NH_4HCO_3 and acetonitrile and subsequently dried in a speedvac for 10 min at 50 °C. The gel pieces were then covered with trypsin-digestion buffer (Promega; prepared to manufactures specifications) and incubated on ice for 45 min, to allow the gel pieces to soak up the buffer. The remaining digestion buffer was removed and gel pieces were now covered with 20 mM NH_4HCO_3 and incubated over night at 37 °C. The reaction tubes were centrifuged for 1 min at 13000 rpm and the supernatant was collected in a new reaction tube. Gel pieces were covered with 20 mM NH_4HCO_3 and incubated for 10 min at room temperature to extract acidic peptides from the gel. After centrifugation and collection of the supernatant, re-

maining peptides were extracted from the gel pieces by 3 repeated incubation steps with 50% acetonitrile / 5% formic acid for 20 min at room temperature. The combined supernatants were subsequently dried in a speedvac and resolved in 20 µl resuspension buffer (98% H_2O, 2% acetonitrile, 0.1% formic acid) prior to LC-MS/MS analysis.

2.4.8   Tandem mass tag (TMT) labeling

Fbx15-GFP was purified from cultures before and after treatment with 3 mM H_2O_2 and run on an SDS-PAGE. After coomassie staining the proteins were in-gel digested with trypsin. Purified peptides were labeled with an isobaric mass tag using the "TMTduplex Isobaric Mass Tagging Kit" (Thermo Scientific), where Fbx15-GFP before H_2O_2 treatment was labeled with heavy TMT-127 and all time points after H_2O_2 induction were labeled with TMT-126. The labeling reaction was performed according to manufacturer's protocol with slight modifications. Both labeling reagents TMT-126 and TMT-127 (each 0.8 mg) were solved in 41 µl of acetonitrile. Subsequently, 13 µl of the TMT-127 labeling solution was added to the peptides from time point zero, while time points 20 min, 40 min and 60 min were each mixed with 13 µl of TMT-126 solution. The reactions were incubated at room temperature for 1 hour. Afterwards the labeling reaction was stopped by adding 8 µl of 5% hydroxylamine for 20 min. The peptides from time points 20, 40 and 60 min were equally mixed with the peptides from time point zero. The peptide mixtures were concentrated in a speedvac and dissolved in resuspension buffer (95% H_2O / 5% acetonitrile / 0.1% formic acid). The parameters for fragmentation during mass spectrometry were set to identify only the phosphorylated peptide of Fbx15 or two unmodified Fbx15 peptides. Specific ratios of the heavy labeled phosphopeptide were obtained from time point zero against the light labeled phosphopeptides from the other conditions. These values were quantified against the ratios of two unmodified reference peptides, which represented the overall amount of purified Fbx15.

2.4.9   LC-MS/MS protein identification

Digested peptides were separated using reversed-phase liquid chromatography with an *RSLCnano Ultimate 3000* system (Thermo Scientific) followed by mass identification with an *Orbitrap Velos Pro* mass spectrometer (Thermo Scientific). Chromatographically separated peptides were on-line ionized by nano-electrospray (nESI) using the *Nanospray*

Flex Ion Source (Thermo Scientific) at 2.4 kV and continuously transferred into the mass spectrometer. Full scans within m/z of 300-1850 were recorded by the Orbitrap-FT analyzer at a resolution of 30.000 (using m/z 445.120025 as lock mass) with parallel data-dependent top 10 MS2-fragmentation in the *LTQ Velos Pro* linear ion trap. LCMS method programming and data acquisition was performed with the software *XCalibur 2.2* (Thermo Scientific) and method/raw data validation with the program *RawMeat 2.1* (Vast Scientific). MS/MS2 data processing for protein analysis and identification was carried out with either MaxQuant quantitative proteomics software in conjunction with Perseus software for statistical analysis (Cox and Mann, 2008) or the *Proteome Discoverer 1.3* (*PD*, Thermo Scientific) and the *Discoverer Deamon Daemon 1.3* (Thermo Scientific) software using the Sequest (and/or Mascot) peptide analysis algorithm(s) and organism-specific taxon-defined protein databases extended by the most common contaminants.

2.5   Microscopy analysis

2000 conidia of respective *A. fumigatus* strains were inoculated on sterile cover slips, covered with 400 µl of liquid AMM with desired supplements. After incubation cover slips were mounted on glass slides with nail polish. For BiFC microscopy, respective strains were inoculated in 8-well borosilicate cover glass system (Thermo Scientific) containing London-medium supplemented with either (inducing) nitrate or (repressing) ammonium as stated above. For staining of nuclei, grown hyphae were incubated in liquid AMM containing either 0.1% 4',6'-diamidino-2-phenylindole, DAPI (Roth) or 0.1% Hoechst 33258 pentahydrate (Invitrogen), 20 min prior to microscopy. Fluorescence pictures were obtained from an Axiovert Observer Z1 (Zeiss) microscope equipped with a CoolSNAP ES2 (Photometrics) digital camera. All microscopy pictures were made with the SlideBook 5.0 or SlideBook 6.0 software package (Intelligent Imaging Innovations).

Quantifications of YFP-signal intensities of interaction signals for SkpA with either Fbx15 or SconB were achieved with the SlideBook 6.0 software. For quantifications the complete YFP-signal intensities of 10 hyphae with each 30 µM length incorporating 1-2 nuclei were compared to YFP-signal intensities, which were obtained from nuclear regions stained with Hoechst.

2.6   Gliotoxin measurement

The *A. fumigatus* wild-type AfS35 and Δ*fbx* strains were cultivated in 250 ml of Czapek-Dox medium, which generally promotes the production of secondary metabolites, at 28 °C for 7 days. For gliotoxin extraction, mycelium was separated from the culture supernatant by Miracloth. To the culture supernatant, 2.8 mg of 4-nitrocatechol was added as internal standard before extraction. Extraction was performed twice with 100 ml of ethyl acetate. The combined organic phases were dried with Na_2SO_4, and the solvent was removed under reduced pressure. The samples were re-dissolved in 8 ml of methanol and measured on a JASCO HPLC with DAD monitoring. For HPLC measurements, 20 μl of the concentrated sample were injected. A Nucleosil 100 (250 x 4.6 mm, 5 mm) column was used at a flow rate of 1 ml/min with the following gradient: A, H_2O, 0.1% (v/v) TFA; B, acetonitrile; start 20% B, in 20 min 65% B, after 28 min 100% B for 10 min. Gliotoxin standard elutes after 12 min and the internal standard 4-nitrocatechol elutes after 8.6 min. For quantification of gliotoxin, a calibration curve was calculated from 16 μg to 1 mg. For quantification of the internal standard, a calibration curve was calculated from 63 μg to 1 mg.

2.7   Murine virulence tests and histopathological analysis

The virulence of *A. fumigatus* Δ*fbx* mutants and the corresponding complemented strains were tested in an established murine model for invasive pulmonary aspergillosis (Liebmann et al., 2004a). In brief, female CD-1 mice were immunosuppressed with cortisone acetate (25 mg / mouse intraperitoneally; Sigma-Aldrich) on days -3 and 0. Mice were anesthetized and intranasal infected with 20 μl of a fresh suspension containing 1×10^6 conidia. A control group was mock infected with PBS to monitor the influence of the immunosuppression. The health status was monitored at least twice daily for 14 days and moribund animals (defined by severe dyspnoea and/or severe lethargy) were sacrificed. Infections were performed with a group of 10 mice for each tested strain. Lungs from euthanized animals were removed, and fixed in formalin and paraffin-embedded for histopathological analyses according to standard protocols (Schrettl et al., 2010).

2.7.1   Ethics statement

Mice were cared for in accordance with the principles outlined by the European Convention for the Protection of Vertebrate Animals Used for Experimental and Other Scientific Purposes   (European   Treaty   Series,   no.   123; http://conventions.coe.int/Treaty/en/Treaties/Html/123). All animal experiments were in compliance with the German animal protection law and were approved by the responsible Federal State authority "Thüringer Landesamt für Lebensmittelsicherheit und Verbraucherschutz" and ethics committee "Beratende Komission nach § 15 Abs. 1 Tierschutzgesetz" with the permit Reg.-Nr. 03-001/12.

III   Results

1   Molecular characterization of the F-box protein Fbx15 of *A. fumigatus*

1.1   Fbx15 is a fungal specific F-box protein conserved in Aspergilli

A. fumigatus fbx15 (Afu3g14150) corresponds to the gene of *A. nidulans* encoding F-box protein 15, which is required for development (Zeska Kress et al., 2012). cDNAs of this gene locus were sequenced and revealed that the *A. fumigatus fbx15* gene structure consists of two exons and one intron resulting in a deduced open reading frame of 655 codons for a protein with a predicted molecular mass of 75 kDa (Figure 6A). Alignments of the deduced *A. fumigatus* Fbx15 primary sequence revealed that high similarities are restricted to the Aspergilli counterparts with similarities between 72.8% and 59.8%, whereas there are significant lower similarities to Fbx15-like proteins of other filamentous fungi like *Penicillium chrysogenum* or *Neurospora crassa* with similarities of 43.6% and 24.7% respectively (Table 5). Even the F-box domain of Fbx15 is primarily conserved in Aspergilli, whereas other filamentous fungi share less similarity (Figure 6B, Table 5). The F-box domain of the deduced protein as canonical interaction site for the Skp1/A linker to the cullin scaffold of SCF E3 ubiquitin ligases is located at the very beginning of the N-terminal part of Fbx15. Homologous proteins in yeast or higher eukaryotes were not found. Bioinformatic analysis predicts two nuclear localization signals (NLS), which suggest that Fbx15 might exhibit its function in the nucleus (Figure 6B).

Most F-box proteins exhibit additional protein-protein interaction motifs, which usually serve as binding sites for their target proteins. WD40 repeats or leucine rich repeats (LRR) are typical for many F-box proteins but are absent in Fbx15. A comparative analysis of the deduced amino acid sequences of different Fbx15 homologs from filamentous fungi was performed with multiple EM for motif elicitation (MEME) (Bailey and Elkan, 1994). Two additional motifs located almost in the middle of Fbx15 are putative yet undescribed candidates for protein-protein interaction sites. Motif 1 is genus-specific and only present in Fbx15 homologs of Aspergilli. Motif 2 that is also present in different

representatives of the genus (p-value of 1.16e-57) also appeared in other fungi including *P. chrysogenum* (*p*-value: 8.94e-48) or *N. crassa* (*p*-value: 2.33e-32) (Figure 6B).
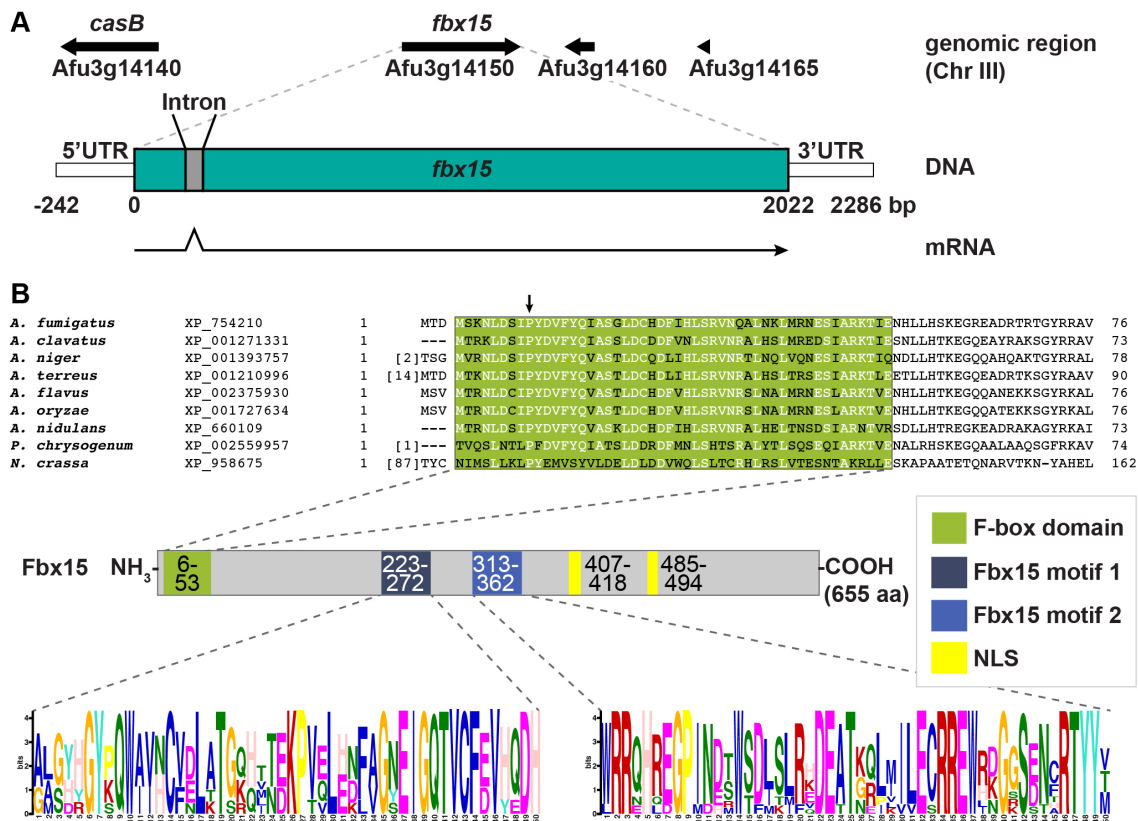
Figure 6: Structural organization of fungal specific Fbx15. (A) *fbx15* genomic locus and adjacent genes, gene structure including one intron and two exons and transcript. (B) Domain structures of the F-box protein Fbx15. *A. fumigatus* Fbx15 F-box domain was identified by bioinformatics analysis for Pfam-domain matches: http://pfam.sanger.ac.uk. ClustalW alignment of F-box domain amino acid sequences from *A. fumigatus* Fbx15 with homologues from other filamentous fungi. Highly conserved amino acids are marked white and the characteristic proline residue at position 7 of the F-box domain is indicated by an arrow. Homologous proteins in other species were identified by NCBI-BLAST with blastp-algorithm (http://blast.ncbi.nlm.nih.gov/Blast.cgi). Details about Fbx15 homologs in other species are given in Table 5. Additional Fbx15 specific motifs were identified by comparing protein sequences of Fbx15 homologs with MEME: http://meme.nbcr.net/meme/ (Bailey and Elkan, 1994). Nuclear localization sequences (NLS) were determined using the cNLS Mapper program: http://nls-mapper.iab.keio.ac.jp/cgi-bin/NLS_Mapper_form.cgi (Kosugi et al., 2009).

Table 5: NCBI-accession numbers for *A. fumigatus* F-box protein Fbx15 and their homologs in other species identified by NCBI-BLAST. Query coverage describes the percentage of the alignment, which covers the primary amino acid sequence of *A. fumigatus* Fbx15. Identity shows the degree of similarity between the identified Fbx15 homologs of other species in comparison to Fbx15 of *A. fumigatus*, which was calculated with ClustalW alignment.

F-box protein	Organism	NCBI Accession #	Query coverage	Identity
Fbx15	***A. fumigatus* Af293**	XP_754210.1	**100%**	**100%**
Fbx15	*A. clavatus* **NRRL 1**	XP_001271331.1	99%	72.8%
Fbx15	*A. terreus* **NIH2624**	XP_001210996.1	100%	69.8%
Fbx15	*A. flavus* **NRRL3357**	XP_002375930.1	100%	64.5%
Fbx15	*A. oryzae* **RIB40**	XP_001727634.1	100%	64.5%
Fbx15	*A. niger* **CBS 513.88**	XP_001393757.1	99%	64.1%
Fbx15	***A. nidulans* FGSC A4**	XP_660109.1	**88%**	**59.8%**
Fbx15	***P. chrysogenum Wisconsin 54-1255***	XP_002559957.1	99%	43.6%
Fbx15	*N. crassa* **OR74A**	XP_958675.2	99%	23.7%

1.2   Fbx15 is essential for oxidative stress resistance in *A. fumigatus*

The F-box proteins Fbx15, Fbx23 and GrrA were initially found to be enriched in *A. nidulans* mutants with a defective COP9 signalosome (Zeska Kress et al., 2012). Deletion of the fifth subunit of the CSN complex, *csnE*, moreover led to an increased oxidative stress sensitivity for *A. nidulans* mutants (Nahlik et al., 2010). We were interested whether these particular F-box proteins, which are vital for several stress response mechanisms in *A. fumigatus* (Jöhnk, 2009), might play a role for oxidative stress resistance in the pathogenic mold. Deletion mutants of *fbx15*, *fbx23* and *grrA* were grown under non-stress conditions and compared to their ability to grow under oxidative stress. Addition of 3 mM H_2O_2 causing oxidative stress completely abolished growth of the Δ*fbx15* mutant in comparison to wild type or growth under non-stress conditions. This defect could be rescued by re-introducing the original gene into the deletion mutant (Figure 7). Furthermore, hyphal development was screened under lower H_2O_2-concentrations. Even 1 mM H_2O_2, which neither had impact on wild type or the complemented strain resulted in a hyper-branched, swollen phenotype in the Δ*fbx15* strain (Figure 7C). In contrast deletion mutants of *fbx23* and *grrA* already showed abnormal colony morphology under non-stress

conditions, with decreased colony size or collapsing colony-centers respectively. This growth defect was slightly enhanced on medium containing H_2O_2 (Figure 7A/B).
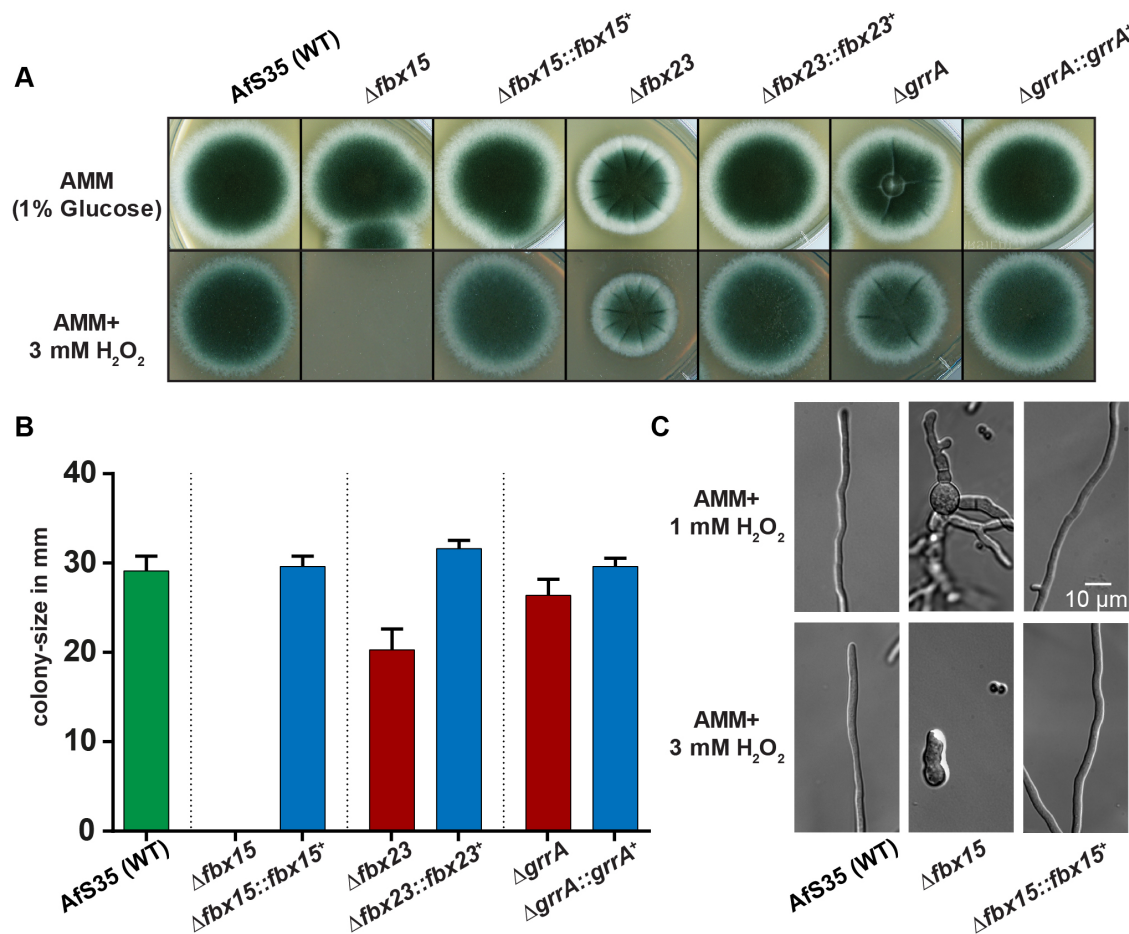
Figure 7: Fbx15 is essential for oxidative stress resistance in *A. fumigatus*. (A) *fbx* deletion mutants Δ*fbx15* (AfGB5) and to less extent Δ*fbx23* (AfGB8) and Δ*grrA* (AfGB10) showed increased oxidative stress sensitivity, provided by 3 mM H_2O_2. The growth defects could be complemented by reintroduction of the wild-type *fbx*-genes, *fbx15* (AfGB15), *fbx23* (AfGB18) and *grrA* (AfGB20), which restored the wild-type phenotype of *A. fumigatus* strain AfS35 (WT). (B) Quantification of colony diameter for AfS35 (WT), Δ*fbx* and complemented strains from A. Colony diameters were measured after 3 days of incubation at 37 °C. All growth tests were repeated 10 times due to instability of H_2O_2 in solid media plates. (C) Light microscopy pictures of hyphal development for AfS35 (WT), Δ*fbx15* and complemented strains under different H_2O_2-concentrations. Δ*fbx15* showed a hyperbranched phenotype with swollen hyphae already at low H_2O_2 concentrations.

Together with the previous results these data suggest that the three F-box proteins Fbx23, GrrA and Fbx15 are part of a general stress response in *A. fumigatus* caused by multiple environmental stressors. The impact of the strain lacking Fbx15 suggests that this protein plays a key role in the fungal stress response.

1.3   Oxidative stress transiently induces *fbx15* expression

H_2O_2 mediated oxidative stress provided drastic effects on the $\Delta fbx15$ mutant strain. Comparison of an *fbx15* overexpression mutant with the wild type revealed no growth differences under oxidative stress conditions, indicating that overexpression of *fbx15* does not provide additional protection against oxidative stress (Figure 8A). The comparison of the *fbx15* promoter regions of various homologs from different filamentous fungi with multiple EM for motif elicitation (MEME) (Bailey and Elkan, 1994) revealed a common DNA-motif comprising 10 nucleotides. The consensus sequence 5'-(A/T)GAGCC(T/G)CA(A/T) is located 259 bp upstream from the translational start codon of the *A. fumigatus fbx15* open reading frame (Figure 8B). According to the YEASTERACT database, which represents a repository for transcription factors and their target genes in *S. cerevisiae* (Teixeira et al., 2014), this DNA motif acts as binding site for Crz1. CrzA, the C2H2-type zinc finger transcription factor that resembles Crz1 in Aspergilli, regulates cellular tolerance to high external calcium and manganese concentrations (Soriani et al., 2008). However, possible targets of CrzA had been analyzed by comparison of transcriptional profiles of *A. fumigatus* wild type and a $\Delta crzA$ mutant strain (Soriani et al., 2010) and *fbx15* was not among the target genes identified for CrzA. In addition, the $\Delta fbx15$ mutant was not affected by 200 mM $CaCl_2$ as it is described for the $\Delta crzA$ mutant and only showed a slightly reduced colony growth on medium containing 10 mM $MnCl_2$ (Figure 8C). Therefore, there might be an additional, so far not identified transcriptional regulator, which binds the 10 bp motif and supports *fbx15* transcript formation.

The exposure to oxidative stress was analyzed as a possible external signal, which triggers changes in *fbx15* gene expression in *A. fumigatus*. Fungal cultures were exposed to 3 mM H_2O_2 and harvested at different time points within a 120 min period. RNAs were isolated and *fbx15* transcript levels were determined with real-time PCR (RT-PCR). A rapid increase of *fbx15* expression was already observed in the first 20 min reaching its maximum peak at 40 min with a 14-fold increased gene expression. Afterwards the expression decreased to a basal level, which is approximately 4-fold increased compared to the non-induced expression. Proteins from the same samples were extracted to test whether the changes in *fbx15* transcript levels are also reflected on protein level. Fbx15 was visualized after immunoblotting by incubation with a polyclonal Fbx15 specific antibody. The general abundance of Fbx15 was very low. A three-fold increase of Fbx15 pro-

tein amounts was measured, starting after 40 min of H_2O_2 exposure mirroring the increased gene expression on the protein level with a delay of 20 min (Figure 8D).
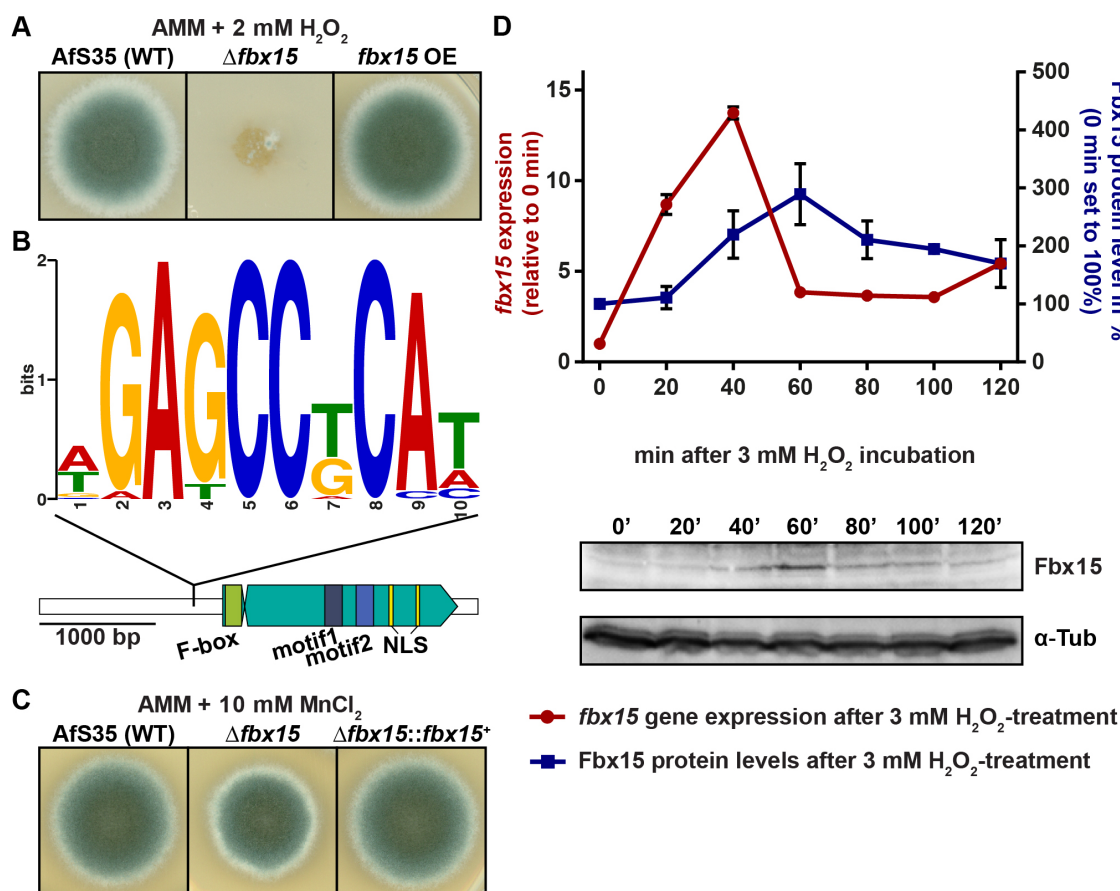
Figure 8: Oxidative stress transiently induces *fbx15* expression. (A) Overexpression of *fbx15* in strain AfGB57 does not affect the oxidative stress response. (B) Putative promoter binding element of *fbx15*, located 259 bp upstream from the translational start codon. The promoter element was discovered with MEME: http://meme.nbcr.net/meme/ (Bailey and Elkan, 1994), by comparing promoter sequences of *fbx15* homologs from filamentous fungi. This conserved DNA-motif serves as a binding site for the C2H2-type zinc finger transcription factor Crz1p in yeast, which is responsible for fungal calcium tolerance. (C) The Δ*fbx15* mutant showed a slightly smaller colony-size on calcium-stress (10 mM MnCl₂) containing AMM medium compared to AfS35 (WT) and complemented strain, indicating a CrzA independent regulation of *fbx15* expression. (D) Expression pattern for *fbx15* upon oxidative stress. AfS35 (WT) cultures were exposed to 3 mM H_2O_2 and harvested after indicated time-points. *fbx15* gene expression was determined by real-time PCR, whereas protein amounts were measured using western hybridization of the crude extracts with an Fbx15-specific antibody. Real-time expression patterns were normalized against *h2A* expression, whereas Fbx15 protein levels were normalized and quantified against tubulin levels. A rapid increase in *fbx15* gene expression was already observed in the first 20 minutes of H_2O_2 exposure, which is reflected with a short delay on the protein level.

These data suggest that the Fbx15 protein levels are increased as part of an adaptation response towards oxidative stress. The shared promoter site in *fbx15* related to genes of different fungi suggests that the control of the expression of all these genes might be conserved between different species.

1.4   Fbx15 is primarily localized in the nucleus

Bioinformatics analysis of Fbx15 predicts two nuclear localization sites, which suggest a nuclear function. A similar situation is found for the conserved *A. fumigatus* F-box protein SconB, which also possesses two nuclear localization signals, and was used as control. SconB from *A. nidulans* and related proteins, as SCON2 in *N. crassa* or Met30 in yeast, act as negative regulators of sulfur metabolite repression (Natorff et al., 2003; Piłsyk et al., 2007) and are essential for viability (Brzywczy et al., 2011; Chandrasekaran and Skowyra, 2008; Petroski and Deshaies, 2005). In previous works, it has been shown by heterokaryon assay and Southern hybridization, that the corresponding gene in *A. fumigatus*, *sconB*, is essential as well, indicating its conserved role in the fungal kingdom (Jöhnk, 2009).

GFP-tagged versions for Fbx15 and SconB were constructed to compare their subcellular localizations. The constitutive *gpdA* promoter drove the gene expression of both GFP-tagged F-box proteins. The fusion constructs replaced the original locus by homologous recombination, which was verified by Southern hybridization. Constitutively expressed GFP-tagged Fbx15 or SconB are both functional during normal growth conditions (AMM, growth at 37 °C) as well as under oxidative stress provided by 3 mM H_2O_2. Growth and colony morphology were similar to wild type under these conditions (Figure 9A). Fluorescence microscopy revealed that Fbx15-GFP and SconB-GFP fusion proteins are primarily co-localized with DAPI visualizing the nuclei. Only small subpopulations of both proteins remain in the cytoplasm (Figure 9B). These data suggest a predominant nuclear molecular function for both F-box proteins, Fbx15 and SconB, in *A. fumigatus*.
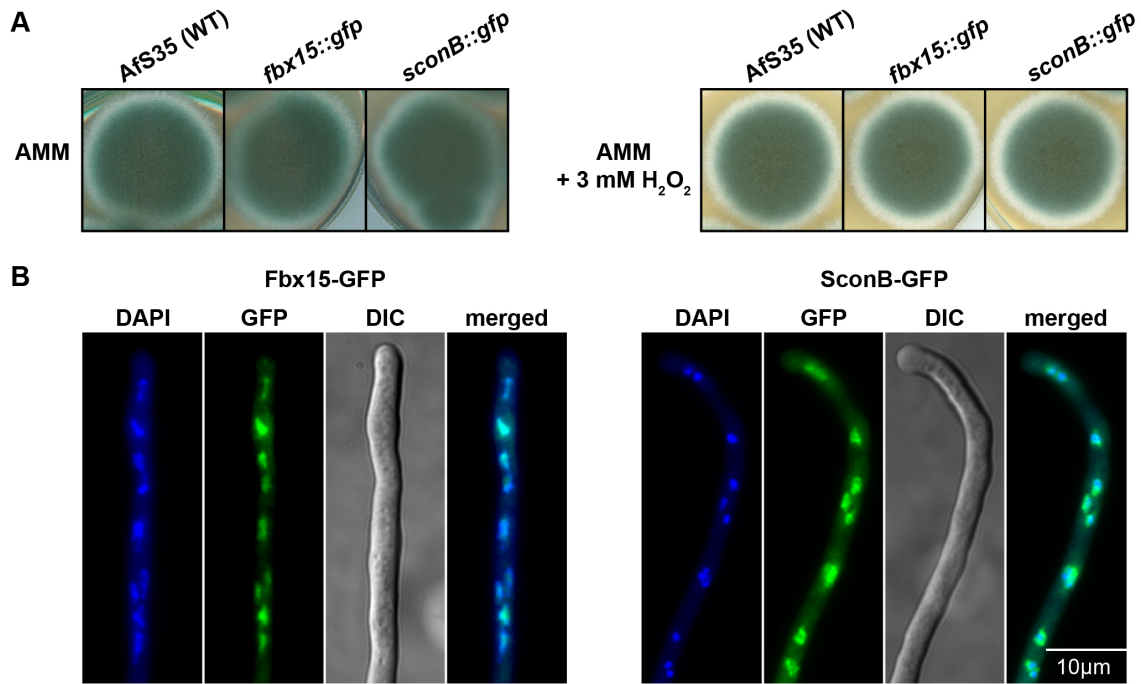
Figure 9: Fbx15-GFP fusion protein localizes primarily to the nucleus. (A) Phenotypical comparison of AfS35 (WT) with strains, constitutively expressing GFP-fusion proteins of F-box proteins Fbx15 (AfGB32) and SconB (AfGB34) under normal and oxidative stress conditions. The expression of GFP-fusion proteins showed no altered colony morphology compared to wild type, thus confirming their functionality. (B) Fluorescence microscopy of strains expressing GFP-fusions of either Fbx15 or SconB under constitutive promoter revealed a predominantly nuclear localization for both F-box proteins. Nuclei were visualized with DAPI.

1.5   Fbx15 is more stable than F-box protein SconB

F-box proteins are the interchangeable subunits of SCF complexes. They are often less stable than cullin-1/A or the adaptor Skp1/A. Instability of F-box proteins often correlates with efficient recruitment of these proteins into SCF complexes (Zhou and Howley, 1998). We compared the protein stability of the two nuclear F-box proteins Fbx15 and SconB of *A. fumigatus*. The yeast SconB homolog, Met30 had been described as a short-lived protein (Pashkova et al., 2010). Vegetative cultures of the constitutively expressed *A. fumigatus fbx15::gfp* and *sconB::gfp* strains were treated with cycloheximide (CHX) to inhibit protein synthesis and to follow the decrease in protein levels over time. Protein extracts of different time points after CHX treatment were used for immunoblotting with anti-GFP antibody. Fbx15 is a stable protein with a half-life of more than 90 min in comparison to 40 min for SconB (Figure 10).

KNLDSI**P**YDVFYQIASGLDCHDFIHLSRVNQALNKLMRNESIARKTIE

6-53

NH₃- ...... -COOH
(899 aa / 102.4 kDa)

Fbx15-GFP + CHX

| 0' | 20' | 40' | 60' | 80' | 100' | 120' |

130 kDa—
100 kDa—
α-GFP

α-Tub

DFLTAL**P**PEISFKILCYLDTTSLCKAAQVSRRWRALADDDVVWHRMCE

194-241

NH₃- ...... -COOH
(940 aa / 105 kDa)

SconB-GFP + CHX

| 0' | 20' | 40' | 60' | 80' | 100' | 120' |

130 kDa—
100 kDa—
α-GFP

α-Tub
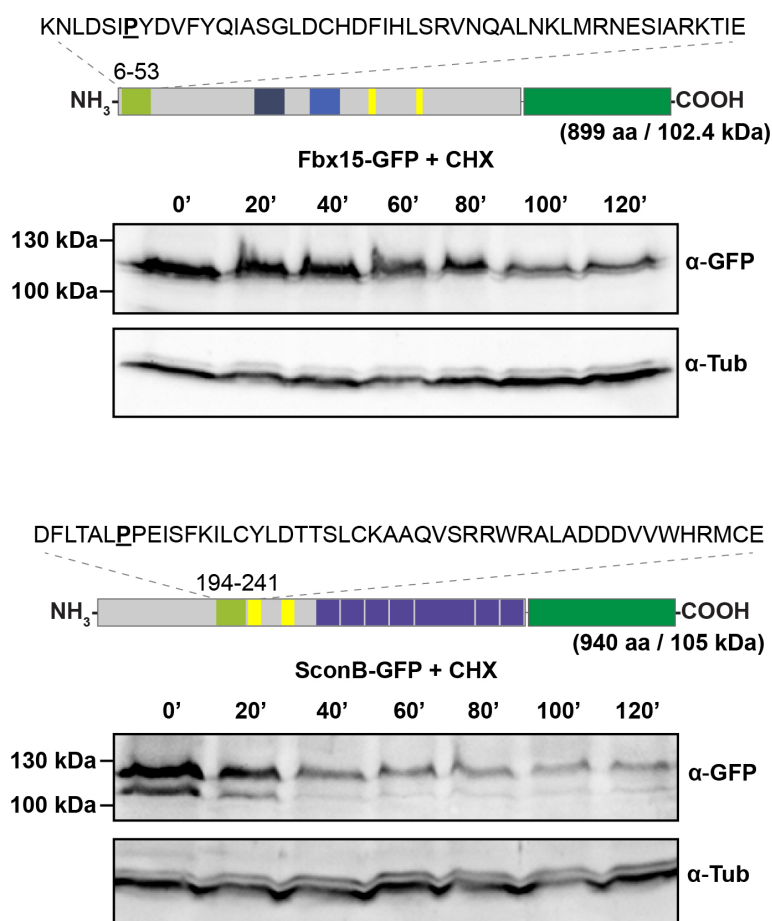
Figure 10: Fbx15 is a stable F-box protein. Protein stability assays of GFP-tagged Fbx15 and SconB. Structure of the GFP-fusion proteins of Fbx15 and SconB are shown with their respective domains and their predicted molecular weight of 102.4 and 105 kDa. The 48 amino acid sequences of their respective F-box domains with the characteristic proline residue at position seven of the F-box domain are highlighted. Respective strains AfGB32 and AfGB34 were incubated in AMM for 18 hours and then shifted to 25 µg/ml cycloheximide containing AMM for two hours. Crude protein extracts were prepared from cultures every 20 min. Immunoblottings were prepared using GFP and tubulin antibody as control. Protein stability was determined by signal quantification relatively to the tubulin-signal. Fbx15-GFP showed a higher stability compared to SconB-GFP.

A highly conserved proline residue at position seven of the F-box domain is important for efficient F-box protein recruitment into functional SCF complexes and is often combined with a prepended leucine residue (Schmidt et al., 2009). Both F-box proteins, Fbx15 and SconB, carry this highly conserved proline residue at position 7 of their respective F-box domains (Figure 10). We examined whether there is a difference in stabilization between Fbx15 and SconB when the connection between the F-box protein and Skp1/A as connecting subunit to SCF E3 ubiquitin ligases is weakened. Mutant alleles for both F-box proteins were constructed with codon substitutions where conserved proline residues at position 12 in Fbx15 or position 200 in SconB were replaced by serines and

the corresponding genes were constitutively expressed as GFP fusions at the original locus (Figure 11B). Growth tests under normal or oxidative stress conditions mediated by 3 mM H_2O_2 suggested that all mutant alleles are as functional as the corresponding wild-type genes (Figure 11A). Protein stabilities after incubation with cycloheximide revealed only for the P200S variant of SconB an increased stability in comparison to wild type, whereas the corresponding P12S Fbx15 variant and the wild-type version exhibit similar protein stabilities (Figure 11B/C).

These data demonstrate that Fbx15 is a particular stable F-box protein and that this stability is independent of the presence or absence of the proline residue, which supports incorporation into SCF-complexes.
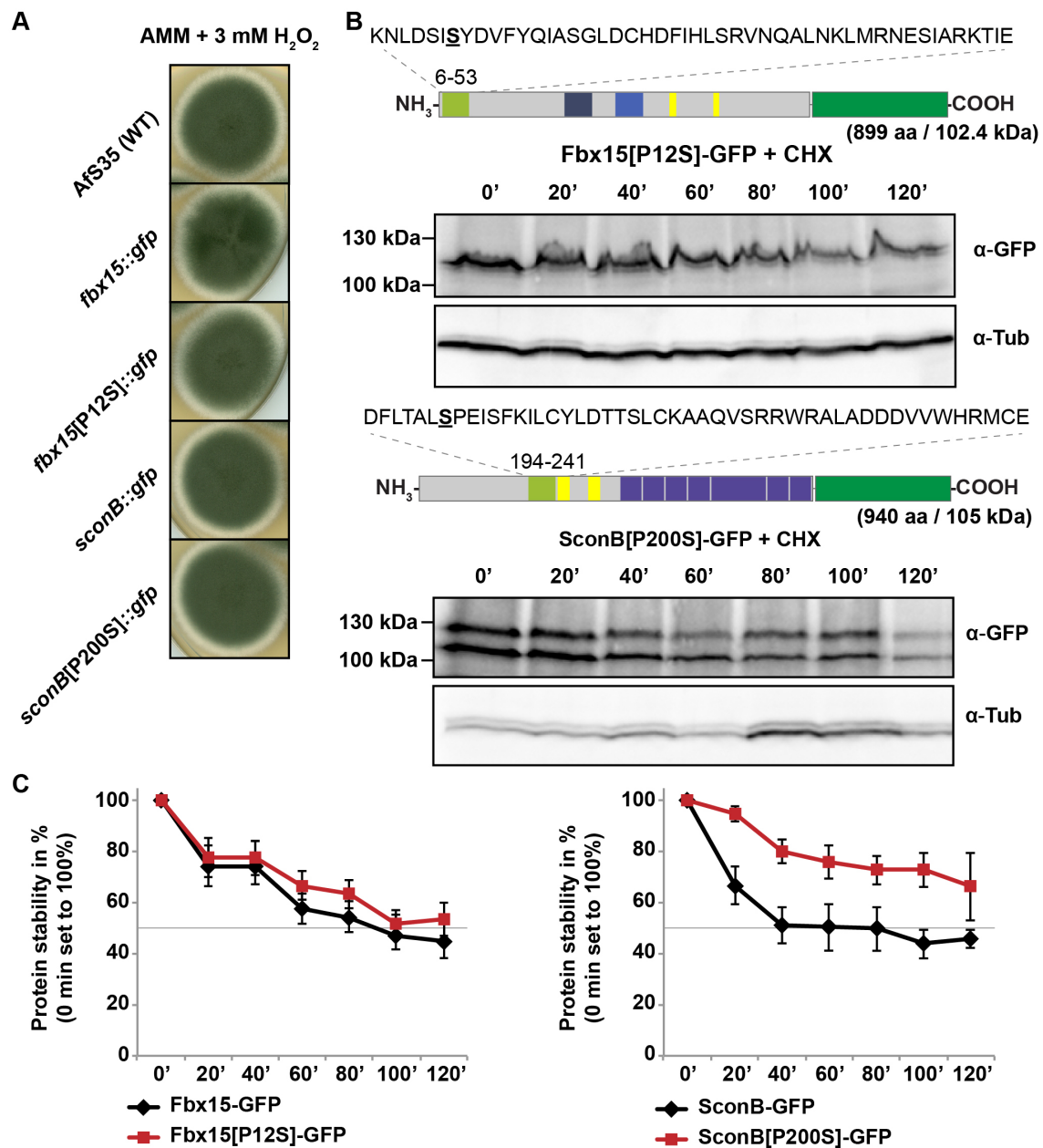
Figure 11: Fbx15 stability is not influenced by mutations in the codons for the F-box domain. (A) F-box-GFP fusion strains were tested for their viability under oxidative stress conditions in comparison to the wild type. 5 x 10³ conidia of AfS35 wild type and the GFP-fusion strains were spotted on an aspergillus minimal medium (AMM) plate, supplemented with 3 mM H_2O_2 and grown for four days at 37 °C. (B) Protein stability assay for GFP-fusions of Fbx15 (AfGB40) and SconB (AfGB42) after replacement of the conserved proline residue at position 7 of the respective F-box domains by a serine. The protein stability of Fbx15 was not affected by the exchange of the conserved proline residue inside the F-box domain. In contrast, the protein stability of SconB[P200S] was drastically increased compared to wild-type SconB. (C) Quantifications of protein levels from Fbx15-GFP and SconB-GFP in comparison to their proline mutant versions. Fbx15 showed high protein stability with a half-life of 90 min, which was independent of the presence or absence of the proline-residue in the F-box domain. In contrast SconB is a short-lived protein with a half-life of approximately 40 min. SconB stability was substantially increased after exchange of its conserved proline residue at position 200, leading to a half-life of more than two hours.

1.6   Fbx15 is phosphorylated during vegetative growth under non-stress conditions

Fbx15 is primarily nuclear but has a significant cytoplasmatic subpopulation. Different cellular localization of proteins can coincide with different posttranslational phosphorylations. Bioinformatic analysis of the deduced amino acid sequence of Fbx15 with NetPhos 2.0 (http://www.cbs.dtu.dk/services/NetPhos) (Blom et al., 1999) predicts in total 15 serine, 11 threonine and 4 tyrosine residues as putative phosphorylation sites (score value between 0 and 1; cutoff value >0.5: Figure 12).
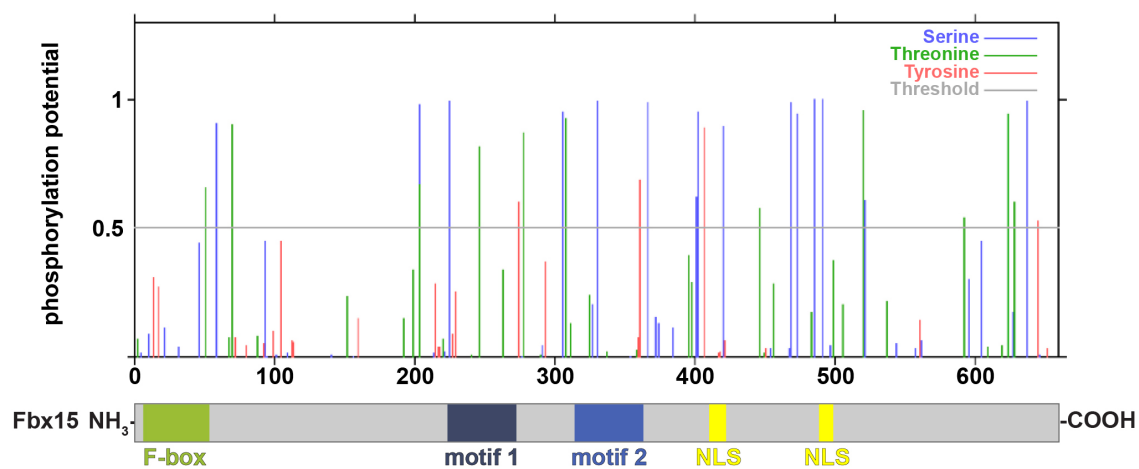
Figure 12: Fbx15 contains 30 putative phosphorylation sites. Putative phosphorylation sites inside the primary amino acid sequence of Fbx15. Phosphorylation sites on serine, threonine and tyrosine residues were determined with NetPhos 2.0 (http://www.cbs.dtu.dk/services/NetPhos). Phosphorylation probability was provided with score-values from 0-1, whereas the cutoff value for potential phosphosites was set to 0.5.

It was analyzed, whether Fbx15 before or after induction with H_2O_2 is subject to phosphorylation. With mass-spectrometry of purified Fbx15-TAP fusions, we were able to identify a phosphopeptide of Fbx15, which carried a single phosphorylation (Figure 13). Analysis of the MS2-spectra of this phosphopeptide with the phosphoRS software (Taus et al., 2011) revealed serine residues 468 and 469 as potential phosphorylation sites with a probabilities of 45.5% each, whereas Ser473 only showed a low probability of 8.9%. Bioinformatic analysis of the primary amino-acid sequence of Fbx15 with NetPhos 2.0 supports Ser469 with a high score value of 0.988, whereas Ser468 had a low score value of 0.029 and therefore is unlikely to be phosphorylated (Figure 12). In contrast no phosphorylated peptides were identified for purified Fbx15-GFP fusions when the cells were grown under oxidative stress conditions.
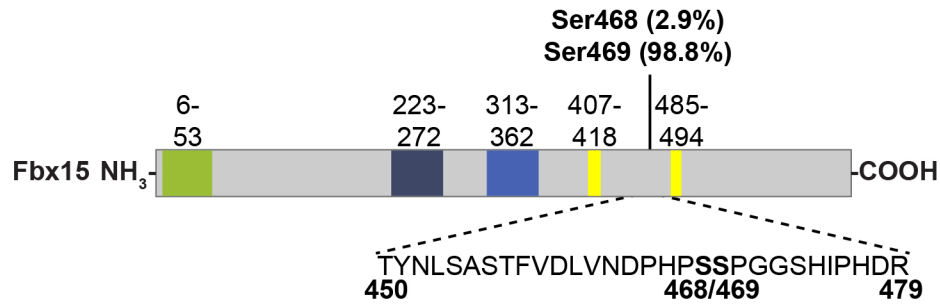
Figure 13: Fbx15 phosphopeptide identified under non-stress conditions. Phosphorylated peptide of Fbx15, which was determined using TAP-purification of Fbx15-TAP coupled with LC-MS/MS identification. Phosphorylation probabilities based on NetPhos 2.0 are given.

In summary, Fbx15 was found to be phosphorylated during vegetative growth under non-stress conditions and is preferentially single phosphorylated on Ser468 or Ser469 (Ser468/469). In contrast, no phosphorylation of cellular Fbx15 could be detected after oxidative stress.

1.7   Fbx15 interacts with the GlcA/BimG phosphatase and is dephosphorylated during oxidative stress

Fbx15 is phosphorylated during normal vegetative growth but unphosphorylated during oxidative stress. This suggests that a phosphatase is activated by oxidative stress, which uses phosphorylated Fbx15 as potential substrate. GFP-traps with Fbx15-GFP followed by LC-MS/MS identification were performed to analyze whether phosphatases can be recruited by Fbx15 as putative interacting proteins. The phosphatase GlcA was identified as Fbx15 interacting partner (Figure 14A). The *A. nidulans* GlcA homolog BimG has been characterized as major protein phosphatase 1, which is associated with thermotolerance, hyphal morphology and cell cycle control (Borgia, 1992; Fox et al., 2002). The *bimG* gene of *A. nidulans* is essential (Son and Osmani, 2009) and transformation of a *glcA* deletion cassette in an *A. fumigatus* strain expressing *fbx15::gfp* under constitutive promoter verified in a heterokaryon rescue and subsequent Southern hybridization (Figure 14B/C) that the situation is similar and *glcA* is essential for *A. fumigatus*.
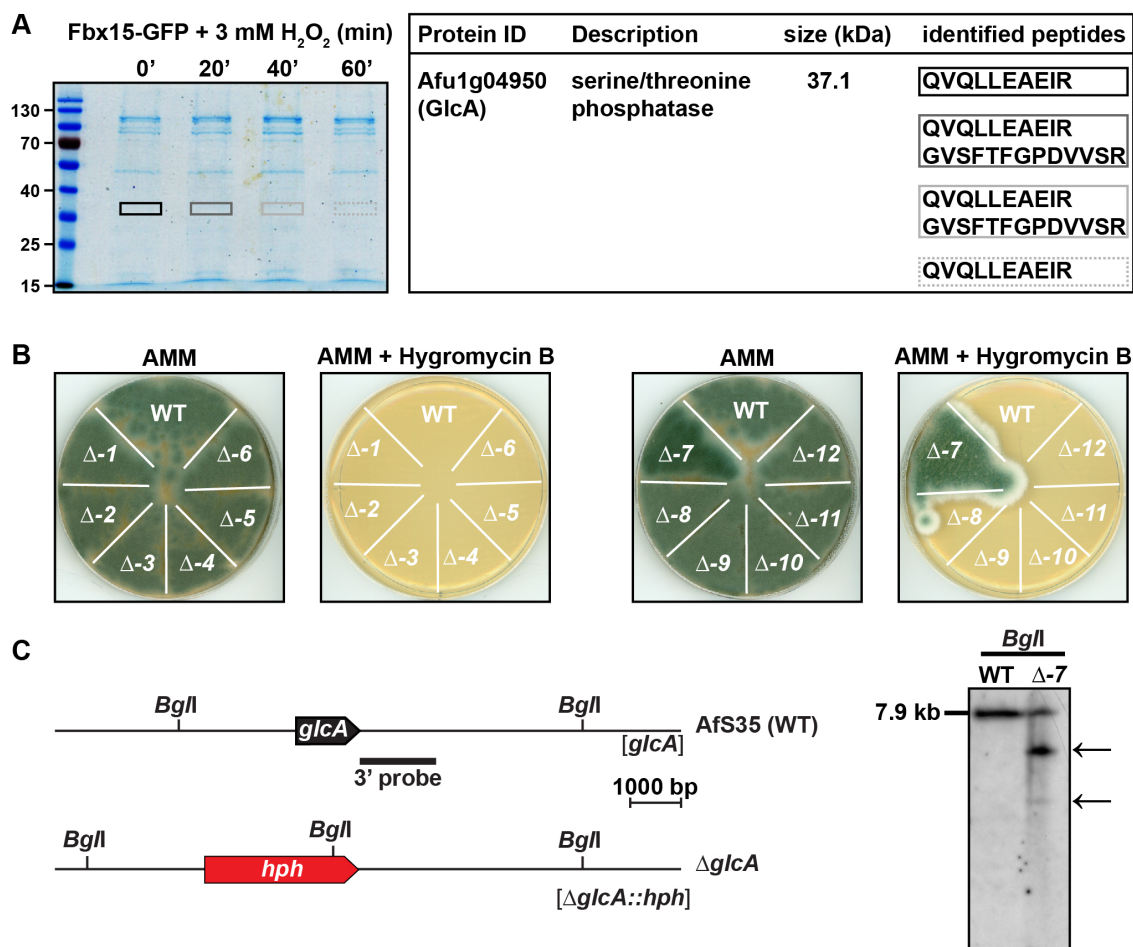
Figure 14: Fbx15 interacts with the essential phosphatase GlcA/BimG. (A) Coomassie-stained SDS-gel of purified Fbx15-GFP before and after oxidative stress. The phosphatase GlcA was identified with LC-MS/MS for all stages of oxidative stress induction. Identified peptides for GlcA are shown in the table corresponding to the respective rectangles in the Coomassie-gel. (B) Heterokaryon rescue assay for primary transformants of ΔglcA. From 12 primary transformants only one was able to propagate on selective medium containing hygromycin B. (C) Southern hybridization of ΔglcA-7 mutant. In addition to the WT band for *glcA*, which complies with the restriction map shown at the left, the ΔglcA-7 mutant showed two additional bands confirming an ectopic integration of the marker cassette, indicated by arrows.

The co-purified phosphatase GlcA suggests that there might be cellular dephosphorylation of Fbx15 during stress. Therefore, the phosphorylation pattern of Fbx15 in response to oxidative stress was further examined. Strains expressing Fbx15-GFP under the constitutive *gpdA* promoter were grown in liquid cultures and subjected to oxidative stress by adding 3 mM H_2O_2 for different durations. Fbx15-GFP from these cultures was purified using GFP-trap and treated with an antibody against phosphorylated Ser/Thr residues. The rate of dephosphorylation was quantified against the overall amount of Fbx15-GFP, determined by an anti-GFP antibody (Figure 15A). A rapid dephosphorylation of 40% of the overall amount Fbx15 upon oxidative stress was observed. These results indicate that

Fbx15, which is phosphorylated during vegetative growth, becomes dephosphorylated in a stress-dependent manner.
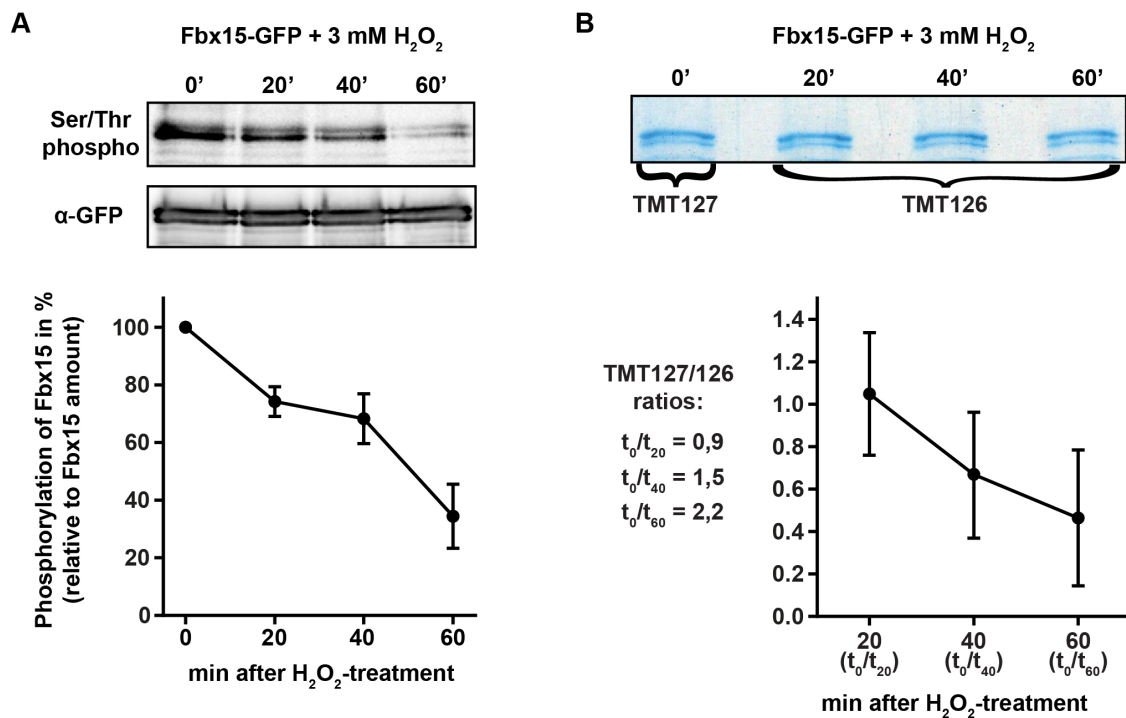
Figure 15: Fbx15 gets dephosphorylated on Ser468/469 upon oxidative stress. (A) Immunoblotting of purified Fbx15-GFP before and after 3 mM H_2O_2 treatment with an antibody against phosphorylated Ser- and Thr-residues. The rapid dephosphorylation of Fbx15 was quantified against the overall amount of Fbx15, which is represented in the graph. (B) Coomassie stained SDS gel of GFP-trap-purified Fbx15-GFP before and after incubation with 3 mM H_2O_2. After tryptic digestion, peptides were differentially labeled with TMT isobaric mass labeling reagent. Peptides from time point 0' (without H_2O_2, heavy label), were then equally mixed with peptides from time points 20, 40 or 60 min (light labeled) respectively, followed by LC-MS/MS, which were focused on the identification of the previously identified Fbx15 phosphopeptide. Ratios of the TMT reporter-ion intensities for the MS2-spectra of the phosphopeptide are given, while the graph on the right represents the reciprocal values of these ratios quantified against the ratios of two unmodified Fbx15 reporter peptides, which confirmed the specific dephosphorylation of S468 or S469 upon oxidative stress.

The Fbx15 dephosphorylation site from cultures treated with H_2O_2 was localized after Fbx15-GFP enrichment and separation on a coomassie-stained SDS-PAGE (Figure 15B). In-gel digestion with trypsin and subsequent TMT isobaric mass tag labeling (Thompson et al., 2003) was performed with TMT127 for the untreated culture and TMT126 for all time points of the H_2O_2 treated cultures, respectively. The sample of time point zero was individually mixed with all other time points and analyzed by LC-MS/MS. The parameters for fragmentation during mass spectrometry were set to identify only the phosphory-

lated peptide of Fbx15, which was previously identified. Specific ratios of the heavy labeled phosphopeptide were obtained from time point zero against the light labeled phosphopeptides from the other conditions. These values were quantified against the ratios of two unmodified reference peptides of Fbx15, which represented the overall amount of purified Fbx15. The reciprocal values of these ratios are decreasing, and corroborate that the specific dephosphorylation of Fbx15 happens at the above-mentioned Ser468/469 site where presumably Ser469 is preferred (Figure 15B).

These results further support that Fbx15, which becomes phosphorylated at Ser468/469 under non-stress conditions, will be dephosphorylated when cells encounter oxidative stress. The Fbx15 interacting protein GlcA/BimG, which is an essential phosphatase, is an interesting candidate enzyme, which might catalyze this reaction.

1.8   Dephosphorylation of Fbx15 shifts the interaction with Skp1/A from the cytoplasm into the nucleus

The canonical function of F-box proteins is their ability to form ubiquitinating SCF ligase complexes. The high stability of Fbx15 even without integration into SCF-complexes is an unusual feature. Nevertheless, Fbx15 seems to be stable without binding to SCF-complexes. It was examined whether Fbx15 is able to interact *in vivo* with Skp1/A as the adaptor for the integration of F-box proteins into E3 SCF ubiquitin ligases. *A. fumigatus* Fbx15 interaction to SkpA was compared to the corresponding interaction of SconB. Native *fbx15* or *sconB* were fused to the N-terminal part and *skpA* to the C-terminal part of eYFP and expressed by the nitrate inducible promoter for b̲imolecular f̲luorescence c̲omplementation (BiFC). Both F-box protein fusions produced an YFP-signal, supporting interactions between the F-box proteins and SkpA (Figure 16A). Signal intensities were quantified and demonstrated that the YFP-signal for SconB is almost exclusively colocalized with the DAPI stained nuclei, whereas Fbx15 interacts with SkpA primarily in the subpopulation outside of the nucleus (74%) and to a lower extent in the nuclei (26%) (Figure 16B).
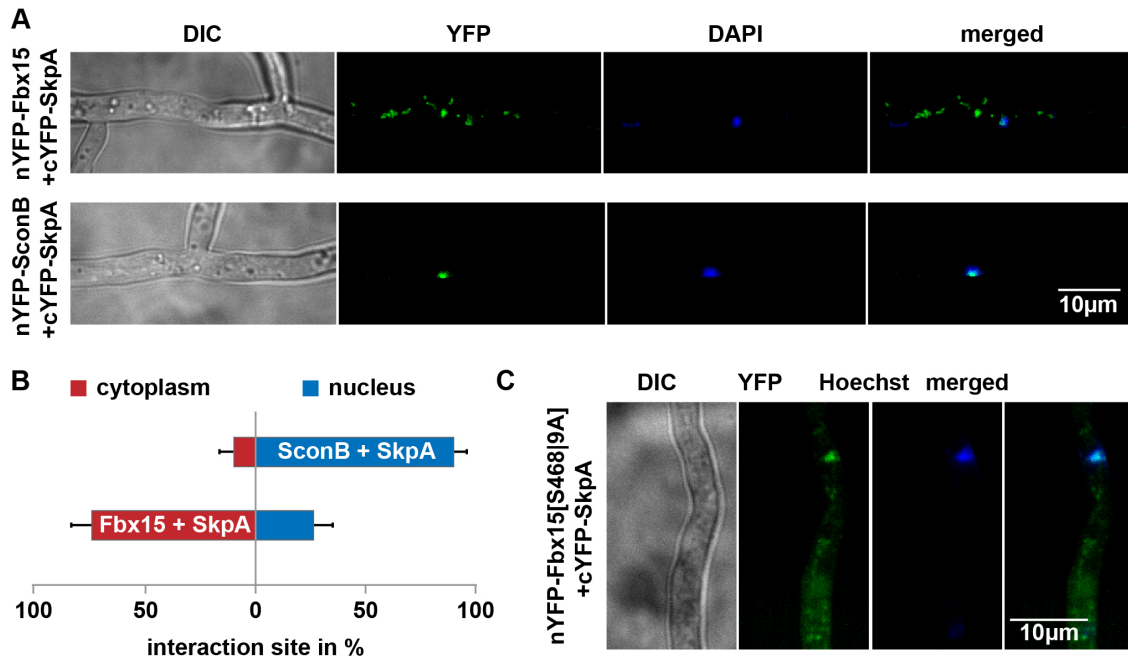
Figure 16: Fbx15 dephosphorylation shifts the interaction with SkpA from the cytoplasm to the nucleus. (A) Bimolecular fluorescence complementation (BiFC) assays. nYFP-Fbx15 and nYFP-SconB fusion proteins interact with cYFP-SkpA in strains AfGB44 and AfGB45, respectively. Nuclear SconB-SkpA interaction is dominant, whereas Fbx15 and SkpA interacted more in the cytoplasm than in the nucleus. (B) Quantification of YFP-intensities according to their subcellular localization in 10 hyphae for each F-box protein. Whereas almost all interaction between SconB and SkpA took place in the nucleus (>90%), the interaction site of Fbx15 with SkpA was observed primarily in the cytoplasm (74%) with smaller fractions in the nucleus (26%). (C) Bimolecular fluorescence complementation (BiFC) of constantly dephosphorylated Fbx15[S468|9A] with SkpA in strain AfGB120. The interaction was primarily observed in the nucleus, stained with Hoechst.

Fbx15 interacted with Skp1/A primarily in the cytoplasm, whereas the bulk of Fbx15 could be localized in the nucleus. It was further investigated whether the phosphorylation of Fbx15 is an important factor for the localization of the interaction with the Skp1/A SCF adaptor. The Fbx15 serine codons of wild-type positions S468 and S469 were replaced to alanine residues to mimic a constant dephosphorylated Fbx15[S468|9A]. The modified *fbx15*[S468|9A] was fused to the N-terminal part of split-eYFP, whereas the adaptor *skpA* was fused to the C-terminal eYFP for bimolecular fluorescence complementation. Expression of both fusion genes resulted in a reconstituted eYFP molecule, which gave a clear signal in the nucleus, which was stained with Hoechst (Figure 16C).

These results corroborate an important function of the phosphorylation state of Fbx15 for the interaction with the SCF-adaptor protein Skp1/A. Thus dephosphorylated Fbx15 potentially forms SCF-complexes in the nucleus. Since under vegetative growth condi-

tions the Fbx15-Skp1/A interaction in the nucleus is very limited, nuclear dephosphory-lated Fbx15 might be rare.

1.9   Phosphorylated and unphosphorylated Fbx15-Skp1/A heterodimers can interact with cullin 1/A

Fbx15 phosphorylation or dephosphorylation depends on the environmental conditions. The impact of the phosphorylation state of Fbx15 on its ability to interact with SCF-complexes was analyzed. The respective serine residue of wild-type position S469 was replaced to aspartate to mimic a constant phosphorylation resulting in Fbx15[S469D] and compared to the unphosphorylated Fbx15 version, where both S468 and S469 were exchanged to alanine residues to mimic a constant dephosphorylated Fbx15[S468|9A]. Both constructs and the wild-type gene were expressed under the native promoter as Fbx15-RFP fusions. An immunoblotting of crude extracts from cultures expressing the respective Fbx15-RFP fusions before and after induction with 3 mM H_2O_2 revealed that all fusion proteins were more abundant after oxidative stress exposure (Figure 17A).

   RFP-trap for the wild-type Fbx15 as well as the phosphomutant versions was per-formed after stress induction with 3 mM H_2O_2 to yield a sufficient amount of co-purified proteins. Co-purified proteins were identified with LC-MS/MS with a focus on the subu-nits of the SCF-ligase machinery. Further analysis included MaxQuant quantitative prote-omic software in conjunction with Perseus software for statistical analysis (Cox and Mann, 2008). Besides Fbx15 or its phosphovariants, the other SCF core components SkpA or CulA were identified, independently of the phosphorylation-state of Fbx15 (Fig-ure 17B/C). This indicates that the phosphorylated as well as the unphosphorylated Fbx15 is able to connect through SkpA to CulA.
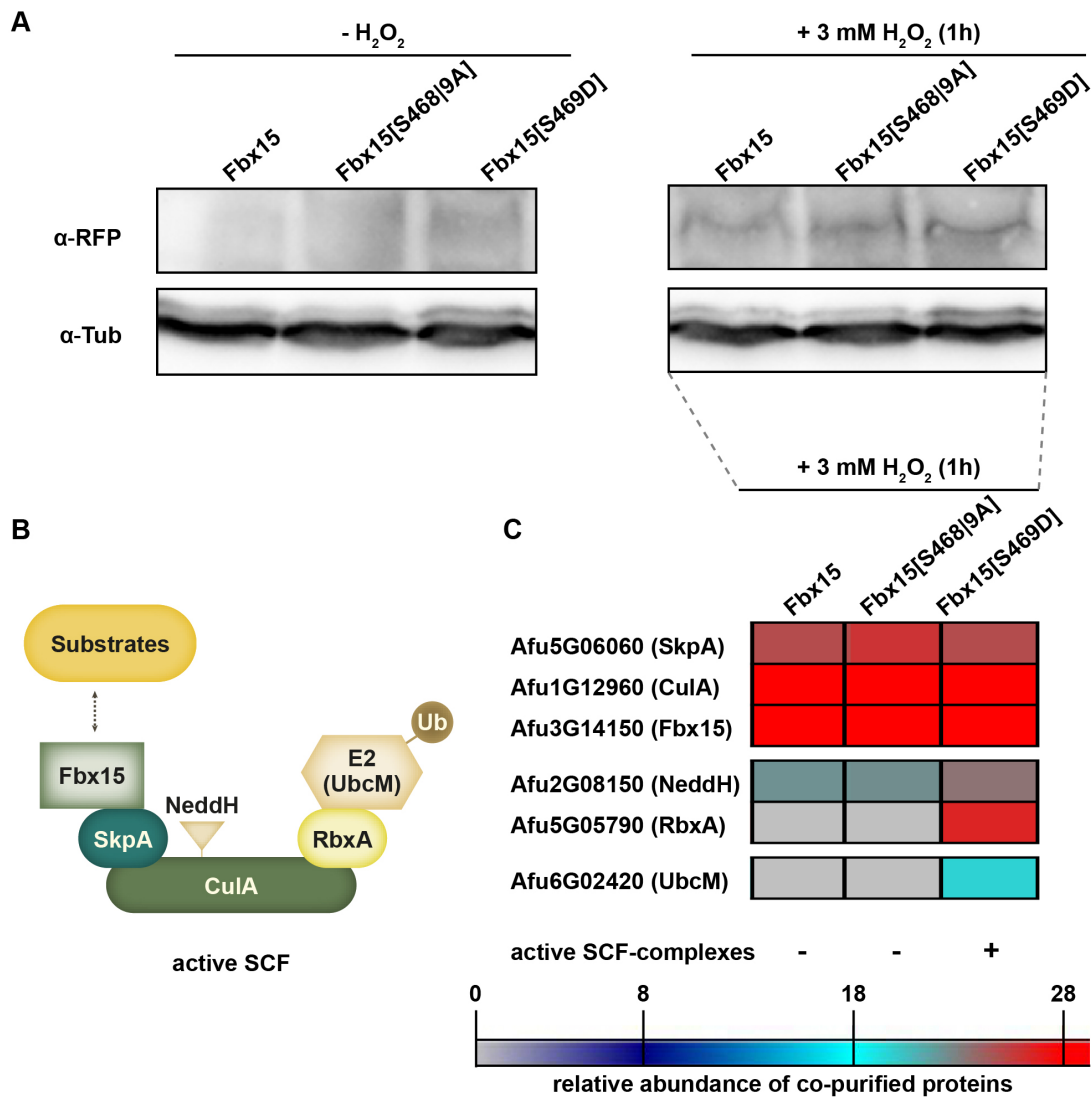
Figure 17: Phosphorylated or unphosphorylated Fbx15 can interact with SkpA and CulA. (A) Immunohybridization of protein crude extracts from RFP-tagged wild-type Fbx15-RFP (AfGB98) and phosphomutant versions of Fbx15, which mimic either a constant unphosphorylated state Fbx15[S468|9A]-RFP (AfGB101) or a constant phosphorylation Fbx15[S469D]-RFP (AfGB102), before and after oxidative stress induction with 3 mM H_2O_2. RFP-tagged Fbx15 levels were significantly increased after stress induction. (B) Scheme of an active SCF-complex. CulA is neddylated in order to bind to the SkpA-F-box heterodimer and the E2-linker protein RbxA. In a final step F-box specific substrates are bound to the F-box protein, while the linker protein RbxA recruits the respective E2-enzyme with the activated ubiquitin, which is ultimately transferred to the target substrate. (C) Heatmap of co-purified proteins for RFP-tagged Fbx15 and phosphomutant versions of Fbx15 after oxidative stress. Different subunits of the SCF-complex are shown, which were quantified with relative Label-free quantification using MaxQuant/Perseus software. The SCF-core subunits were co-purified with all versions of Fbx15 independent of the Fbx15 phosphorylation state. SCF-subunits NeddH and RbxA, which are required for an active E3 ligase, with addition of the ubiquitin-conjugating E2-enzyme UbcM are especially present for co-purifications with the constantly phosphorylated Fbx15 version, Fbx15[S469D].

Activation of SCF-ligases is a highly dynamic process and requires the RING protein RbxA for the interaction with the E2 ubiquitin-conjugating enzyme and the covalent modification of the cullin by the ubiquitin like protein NEDD8/NeddH (Figure 17B). For the native Fbx15, which is presumably dephosphorylated at S468/469 after oxidative stress as well as the artificial unphosphorylated Fbx15[S468|9A] only the cullin associated modifier NeddH could be co-purified, whereas the RbxA linker protein and an E2 enzyme were absent in our co-purifications (Figure 17C).

In contrast the Fbx15 variant, where we introduced a negatively charged aspartate to mimic a constant phosphorylation state was able to co-purify all SCF-subunits, necessary to form an active SCF-complex. The SCF-activator NeddH, which was also co-purified for the unphosphorylated versions of Fbx15, was more abundant in co-purifications for the constant phosphorylated Fbx15[S469D]. In addition the SCF-components RbxA and the E2-enzyme UbcM, were only purified for the version of Fbx15 that mimics a constant phosphorylation, indicating that the assembly of a functional SCF-ligase including the ubiquitin-carrying E2-enzyme can be promoted by the phosphorylation of Fbx15 on Ser469 (Figure 17C).

The cellular ubiquitination pattern of the $\Delta fbx15$ mutant, wild type and the *fbx15* overexpression strain were compared before and after induction with H_2O_2. Neither the ubiquitination pattern nor the general protein composition of the $\Delta fbx15$ strain was significantly altered in comparison to the wild type or the *fbx15* overexpression strain (Figure 18).

Taken together our results suggest that independent of the phosphorylation state, Fbx15 is able to interact with the SCF-core components SkpA and CulA. However, a difference towards the activation of the canonical SCF^{Fbx15} E3 ligase complex could be observed, suggesting that the phosphorylated Fbx15 is primarily incorporated into active SCF-complexes. Furthermore, the fact that both general protein patterns and ubiquitin patterns of cellular proteins were not significantly changed, propose few specific substrates for SCF^{Fbx15} ligases rather than a broad spectrum of targets.
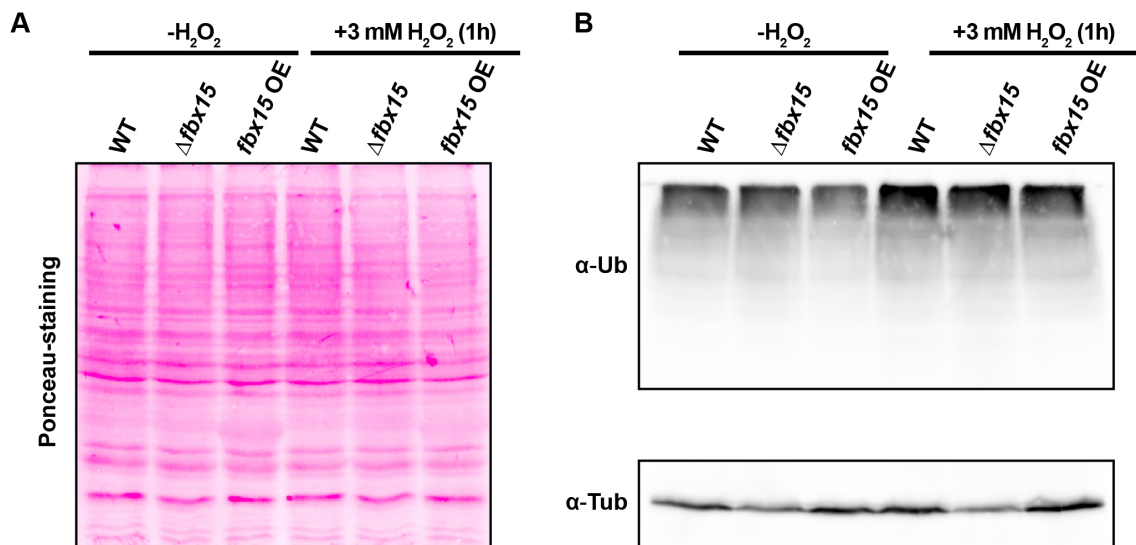
Figure 18: Fbx15 plays minor roles for protein ubiquitination and/or degradation.
(A) 50 µg protein crude extract from AfS35 (WT), Δ*fbx15* and Δ*fbx15*::*fbx15*⁺ before and
after incubation with 3 mM H₂O₂, blotted to a Ponceau S-stained nitrocellulose-
membrane showed no major differences in the cellular protein pattern. (B) Immunoblot of
50 µg protein crude extract from AfS35 (WT), Δ*fbx15* and Δ*fbx15*::*fbx15*⁺ before and
after induction with 3 mM H₂O₂ incubated with anti-ubiquitin antibody. The cellular
ubiquitination-pattern was not significantly altered in the Δ*fbx15* mutant compared to
AfS35 (WT) or complemented strain. Anti-tubulin antibody was used as loading control.

2 Identification of Fbx15 target proteins

2.1 Fbx15-TAP recruits three CSN subunits and proteins involved in transcription, translation, signal transduction, morphology and metabolism

Fbx15 could interact with the SCF-core components SkpA and CulA, but the formation of
active SCF-complexes seems to be a dynamic process, which is promoted by the phos-
phorylation of Fbx15. We were interested whether Fbx15 might act as a substrate adaptor
for SCF^{Fbx15} complexes.

Additional potential interacting proteins for Fbx15 were identified by using the highly
sensitive t̲andem-a̲ffinity-p̲urification (TAP) method, which has been customized to fit
Aspergillus specific requirements (Bayram et al., 2012). The F-box proteins Fbx15 and
SconB as a control were fused to TAP-tags under the constitutive *gpdA* promoter. We
added mutated variants of *fbx15* and *sconB* to the comparative TAP enrichment analysis,
where we exchanged the conserved proline codon of the F-box domain into a serine,
which might weaken the F-box binding to SkpA and allow a screening for SCF-

independent interaction partners. The expression of the fusion proteins was monitored by immunoblotting with crude protein extracts from vegetative cultures using anti-calmodulin and anti-tubulin antibody as a control (Figure 19). Besides detecting some unspecific proteins above the expected signal, the anti-calmodulin antibody recognized several bands below the full sized fusion proteins, which were much more prominent for SconB fusion proteins, corroborating that SconB is subject to rapid degradation, whereas Fbx15 is a much more stable F-box protein.
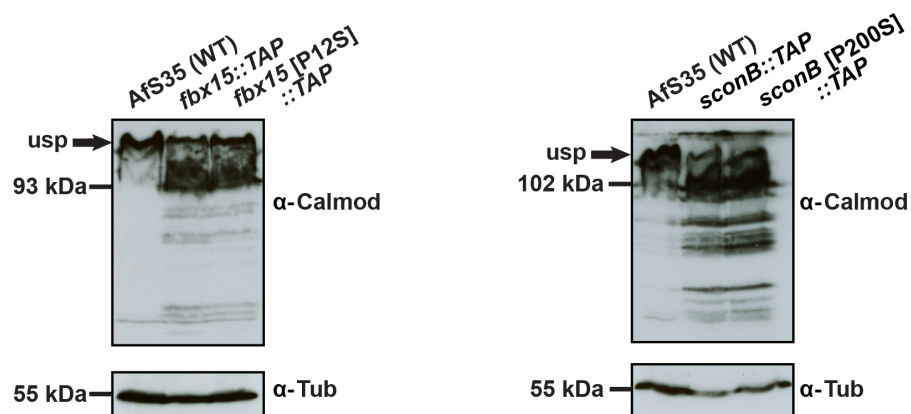
Figure 19: Fbx15-TAP is more stable than SconB-TAP. Immunoblotting of strains expressing C-terminal TAP-tagged versions of either wild type or mutated F-box proteins Fbx15 (AfGB33 and AfGB41) and SconB (AfGB35 and AfGB43). Constitutively expressed TAP-tagged proteins were visualized by α-calmodulin antibody. Unspecific proteins (usp) recognized by the α-calmodulin antibody are indicated. α-tubulin antibody was used as control. Several bands below the full size proteins were especially observed for SconB-TAP fusions indicating their rapid degradation compared to Fbx15-TAP variants.

Proteins recruited by the TAP-tagged fusion proteins of *A. fumigatus* were enriched and identified by mass spectrometry. AfS35 (WT) was used as control to exclude unspecific bound proteins (Figure 20). With the SconB-TAP as control we were able to co-purify the transcriptional activator MetR, which is a known target of SCF$^{\text{SconB}}$ E3 ligases (Brzywczy et al., 2011; Chandrasekaran and Skowyra, 2008) and therefore, demonstrates the functionality of the TAP-purification.
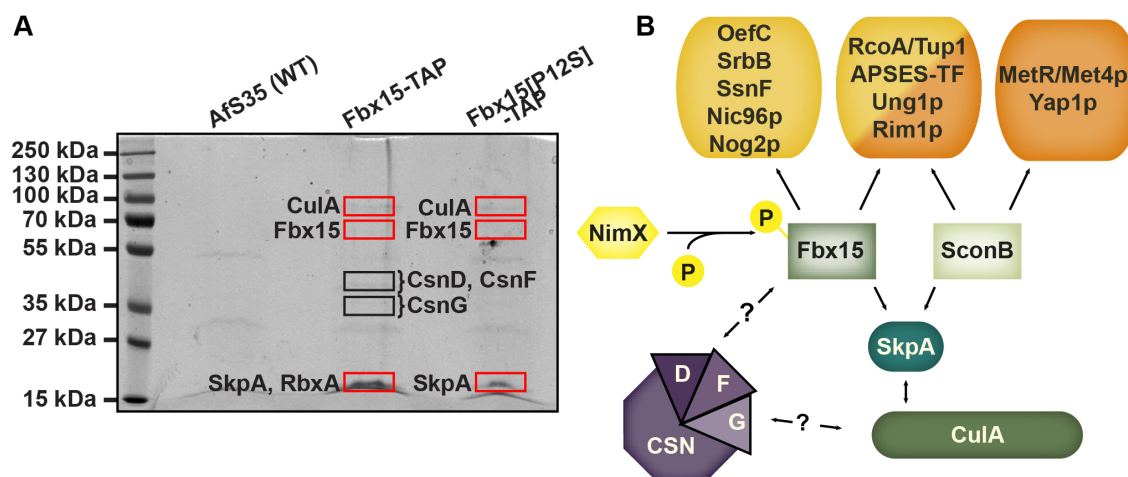
Figure 20: Fbx15-TAP recruited a total of 38 proteins during tandem affinity purification. (A) Coomassie stained SDS-gel of tandem affinity purifications for Fbx15-TAP and Fbx15[P12S]-TAP. Purifications with protein crude extract of the AfS35 (WT) were used as a control. Co-purified proteins were identified with LC-MS/MS and are listed in Table 6. Indicated by red rectangles are proteins of the SCF-ligase complex, which were co-purified with the respective F-box proteins. Black rectangles showed the estimated size of co-purified CSN-subunits. (B) Scheme of a subset of interacting proteins of Fbx15 and SconB based on LC-MS/MS identifications of co-purified proteins. Shown are presumably nuclear proteins, which are either exclusively found for each F-box protein or which were found for both. Furthermore, co-purified components of the SCF-ligase machinery, including three CSN subunits and the cyclin-dependent kinase NimX with a potential function for Fbx15 phosphorylation are shown.

38 putative interaction partners of the Fbx15-TAP fusions could be identified. Only 22 proteins were purified from the SconB-TAP fusions (Table 6). From these, 11 proteins were identified for both F-box proteins.

Both F-box proteins were able to co-purify the SCF-core subunits CulA and SkpA, whereas the subunits required for the activation of the respective SCF-complex, namely NeddH and RbxA were not found during our TAP-purifications. In contrast, the native Fbx15 was able to co-purify three COP9 signalosome (CSN) subunits, which were absent for SconB. The CSN complex functions as regulator for SCF-complex assembly by deneddylation of the cullin subunit. Since SconB is known to build functional SCF-complexes, these results indicate that both F-box proteins can interact within SCF-core complexes, whereas the interactions with the activating subunits of the SCF-ligase are rather dynamic. Furthermore, the presence of three CSN subunits for native Fbx15 co-purifications might reflect a highly dynamic assembly/disassembly of Fbx15 incorporating SCF complexes, which is rather stable in SCF^{SconB} complexes.

Table 6: Putative interacting proteins of Fbx15 and SconB. Putative interaction partners of *A. fumigatus* Fbx15 and SconB, which were co-purified with TAP-tagged versions of Fbx15 and SconB in either wild type or mutated form Fbx15[P12S]/SconB[P200S]. Homologous proteins in *S. cerevisiae* with a known function are given in brackets. Criteria for interacting proteins was that they had to appear at least twice in two independent purifications for each F-box protein. An exception is CulA which was found only once for SconB, indicated with an asterisk. Amount of independent co-purifications are given. Proteins, which were identified for both F-box proteins are shaded in grey.

A. fumigatus	Protein description	Co-purified with:			
		Fbx15	Fbx15 [P12S]	SconB	SconB [P200S]
SCF-subunits & related proteins					
AFUA_1G12960; CulA	SCF ubiquitin ligase subunit	3	3	1*	-
AFUA_5G06060; SkpA	SCF ubiquitin ligase subunit	3	2	2	2
AFUA_4G10350; UbiD	Polyubiquitin	1	2	1	1
AFUA_4G10780 (Tom1)	ubiquitin-protein ligase	1	1	1	1
AFUA_8G05500; CsnD	COP9 signalosome subunit	3	-	-	-
AFUA_5G07260; CsnF	COP9 signalosome subunit	2	-	-	-
AFUA_4G12630; CsnG	COP9 signalosome subunit	3	-	-	-
Transcription factors & nuclear proteins					
AFUA_3G09670; OefC	C6 transcription factor	1	1	-	-
AFUA_4G03460; SrbB	bHLH transcription factor, involved in hypoxia and virulence	1	1	-	-
AFUA_4G04720 (Nic96)	nuclear pore protein	0	2	-	-
AFUA_4G08930	Putative nucleolar GTPase	1	1	-	-
AFUA_2G11840; SsnF	Transcriptional corepressor (SsnF/Ssn6)	1	1	-	-
AFUA_6G05150; RcoA	Transcriptional corepressor (RcoA/Tup1)	1	1	-	2
AFUA_5G11390	APSES transcription factor, putative	2	3	1	2

A. fumigatus	Protein description	Co-purified with:			
		Fbx15	Fbx15 [P12S]	SconB	SconB [P200S]
AFUA_2G06140	uracil DNA N-glycosylase activity, DNA repair	1	1	1	1
AFUA_5G07890 (Rim1)	single-stranded DNA binding protein	3	1	1	1
AFUA_4G06530; MetR	bZIP transcription factor	-	-	-	2
AFUA_6G09930 (Yap1)	bZIP transcription factor, putative	-	-	1	2
RNA processing					
AFUA_3G06440 (Prp21)	Splicing factor with U2 snRNP localization	1	2	-	-
AFUA_5G04420 (Cus1)	Splicing factor with U2 snRNP localization	1	1	-	-
AFUA_6G08610 (Tgs1)	RNA trimethylguanosine synthase, role in 7-methylguanosine cap hypermethylation	2	-	-	-
AFUA_5G09670	RNase III domain protein	1	1	-	-
AFUA_7G05810 (Mrd1)	Putative ribonucleoprotein, nucleic acid binding	1	1	-	-
AFUA_2G04940 (Pbp2)	mRNA binding, role in telomere maintenance	-	-	1	1
AFUA_6G04330 (Ecm16)	RNA helicase, maturation of SSU-rRNA	-	-	1	1
Ribosomal proteins					
AFUA_1G05990 (Rpl16A)	60S ribosomal protein	2	1	-	-
AFUA_2G04130 (Rps11A)	40S ribosomal protein	2	1	-	-
AFUA_2G01830	Protein with putative ribosomal activity	1	1	-	-
Signal-transduction					
AFUA_1G11730; ArfA	GTPase activity, role in ER/Golgi transport	1	1	-	-
AFUA_2G07600	GTP binding, signal recognition activity	1	1	-	-
AFUA_6G07980; NimX	Cyclin-dependent serine/threonine kinase	1	1	-	-

A. fumigatus	Protein description	Co-purified with:			
		Fbx15	**Fbx15 [P12S]**	**SconB**	**SconB [P200S]**
AFUA_6G06750	14-3-3 family protein; predicted gene pair with ArtA	2	1	-	2
AFUA_2G03290; ArtA	14-3-3 family protein; predicted gene pair with AFUA_6G06750	-	-	1	2
AFUA_3G09550; CmkB	Calcium/calmodulin dependent protein kinase	-	-	-	2
AFUA_5G04130; PhoA	Putative cyclin-dependent protein kinase	-	-	1	2
Metabolic enzymes					
AFUA_1G12800 (Idh2)	Putative NADPH isocitrate dehydrogenase	1	1	-	-
AFUA_2G04520 (Adh4)	Protein with metal ion binding domains, oxidoreductase activity	1	1	-	-
AFUA_2G10920; EchA	Putative enoyl-CoA hydratase/isomerase family protein, role in beta oxidation of fatty acids	1	1	-	-
AFUA_3G08660; IdpA	Putative isocitrate dehydrogenase	1	1	-	-
AFUA_6G10660; AclA	Putative ATP citrate lyase subunit	2	-	-	-
AFUA_3G11070; PdaC	Putative pyruvate decarboxylase	1	1	1	1
AFUA_1G06960 (Pda1)	Pyruvate dehydrogenase complex subunit alpha	-	-	1	1
AFUA_1G15640	Domains with predicted carbon-sulfur lyase activity	-	-	1	1
Fungal morphology					
AFUA_4G08770	Protein with putative microtubule binding activity	2	1	-	-
AFUA_5G03080; AspC	Septin, role in cell polarity and hyphal growth	2	2	1	1
AFUA_1G08850; AspD	Septin, localizes to long tubular structures within hyphae and to newly formed septa	-	-	1	2

A. fumigatus	Protein description	Co-purified with:			
		Fbx15	Fbx15 [P12S]	SconB	SconB [P200S]
Unknown function					
AFUA_1G09610	Conserved hypothetical protein	2	1	-	-
AFUA_3G13930	Conserved hypothetical protein	2	1	-	-
AFUA_2G10860	Domains with predicted zinc ion binding activity	-	-	1	1

Based on their putative function and common origin with yeast proteins the co-purified proteins could be divided into subclasses. The predominant nuclear localization of Fbx15 is consistent with several nuclear proteins, which were recruited by Fbx15. Among them we found two transcriptional regulators (SsnF/Ssn6p, OefC), a putative DNA binding protein, a nuclear GTPase and the nuclear pore protein Nic96. (Figure 20B, Table 6). In addition, Fbx15 recruited four putative nuclear proteins, which were also found in TAP-purification with SconB (Figure 20B, Table 6). These proteins included two transcriptional regulators (RcoA/Tup1 and a putative APSES transcription factor), an enzyme involved in DNA repair and a single strand DNA binding protein. The fact that both, Fbx15 and SconB, recruited these proteins might reflect a tight control by more than one F-box protein. Furthermore, we could identify five proteins with a putative role in RNA processing and RNA maturation.

Four potential Fbx15 interaction partners exhibit a putative role in signal transduction pathways. Among them we found the cyclin-dependent serine/threonine kinase NimX/Cdc28p, which is required for the coordinated control of cell cycle arrest and conidiophore morphology in the model *A. nidulans* (Ye et al., 1999). We were interested whether NimX is responsible for the phosphorylation of Fbx15, instead of being an Fbx15 directed target. We tried to replace the native *nimX* genomic locus with a hygromycin resistance cassette in a background strain that constitutively expresses GFP-tagged Fbx15 to examine its effect on Fbx15 phosphorylation. But similar to the phosphatase GlcA, NimX seems to be an essential protein for *A. fumigatus* as we could show with heterokaryon rescue assays (Figure 21).
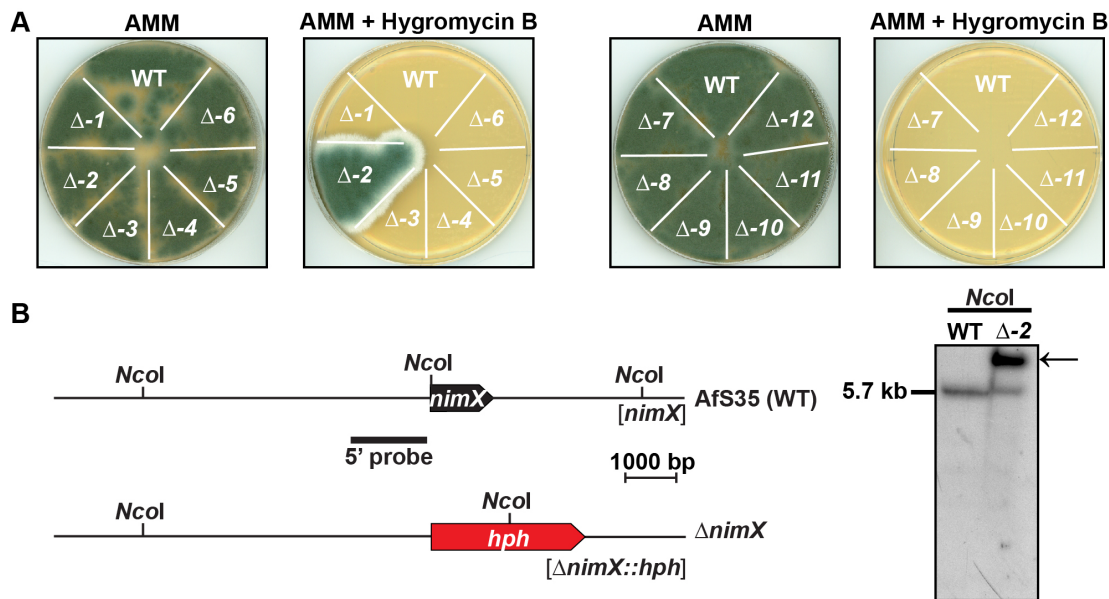
Figure 21: The cyclin dependent Ser/Thr kinase NimX is essential for *A. fumigatus*. (A) Heterokaryon rescue assay for 12 primary Δ*nimX* transformants. Conidia of primary transformants were plated equally on non-selective AMM and selective minimal medium containing hygromycin B. Only Δ*nimX* mutant 2 was able to grow on the selective medium, indicating that *nimX* is essential for *A. fumigatus*. (B) The Southern hybridization for Δ*nimX-2* mutant in comparison with the wild type verified an ectopic integration of the hygromycin B resistance cassette in addition to the wild-type locus of *nimX*, indicated with an arrow.

Another class of proteins, which were co-purified with Fbx15 are metabolic enzymes, which are required for the first steps of citrate cycle, the beta-oxidation of fatty acids and an enzyme with putative oxidoreductase activity. The interaction with these enzymes might reflect the severe growth defects, which were observed for Δ*fbx15* mutant on various carbon sources (Jöhnk, 2009).

Finally, we were able to identify two potential Fbx15 interaction partners, which might play a role in hyphal morphology. Especially the septin AspC, which is required for cell polarity and hyphal growth, might coincide with the hyperbranched swollen hyphae, which were observed for the Δ*fbx15* mutant under oxidative stress conditions (Figure 7C).

In summary, we were able to co-purify several possible target proteins for Fbx15, whose putative functions are in agreement with Fbx15 localization or Δ*fbx15*-related growth defects. In addition, the co-purification of three CSN-subunits for the native Fbx15 protein suggests a highly dynamic assembly/disassembly of SCF^{Fbx15} E3 ligases. An interesting aspect of the comparison between co-purified proteins of both F-box proteins, was their ability to co-purify RcoA/Tup1, which is part of the conserved transcrip-

tional co-repressor complex RcoA/Tup1-SsnF/Ssn6, whereas only Fbx15 could also co-purify the SsnF/Ssn6 part of the co-repressor complex.

2.2   Interaction of Fbx15 with SsnF/Ssn6 does not change the stability of the co-repressor subunit

The F-box proteins SconB and Fbx15 were both able to recruit RcoA/Tup1 in a TAP-enrichment. In contrast, only Fbx15 co-purified the SsnF/Ssn6p adaptor, which is necessary for the RcoA/Tup1 transcriptional repression domain to interact with various DNA-binding proteins (García-Sánchez et al., 2005). A homo-tetramer of the RcoA/Tup1 repressor subunits is connected to one SsnF/Ssn6p adaptor protein, which binds to a DNA-binding protein that escorts the repressor complex to the target genes. The corresponding SsnF encoding gene of the model *A. nidulans* is essential for growth, whereas the yeast counterpart Ssn6p is dispensable (García et al., 2008; Smith and Johnson, 2000). Transformation of a deletion cassette of *ssnF* resulted in six slowly growing transformants, of which only three were able to propagate on selective medium. Heterokaryon rescue and subsequent Southern analysis indicated that *ssnF* is not only essential for *A. nidulans* but also for *A. fumigatus* (Figure 22A/B).
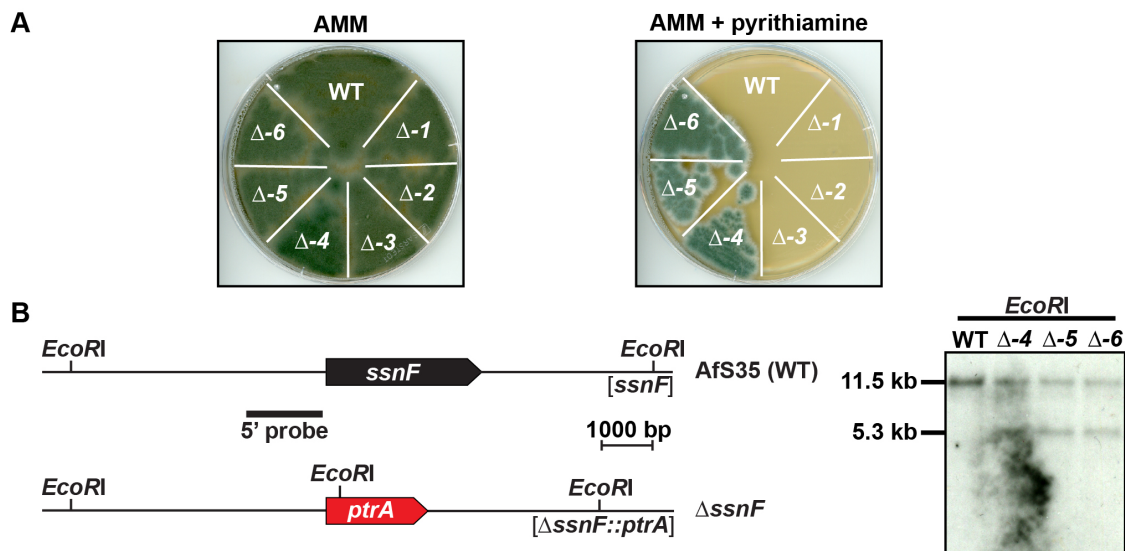
Figure 22: The co-repressor complex subunit SsnF is essential for *A. fumigatus*. (A) Heterokaryon rescue assay for primary transformants of Δ*ssnF*. Primary transformants were equally plated on AMM and selective medium containing pyrithiamine. Transformants Δ*ssnF 4-6* were still growing on selective medium and were further analyzed by Southern. (B) Restriction map of AfS35 (WT) and Δ*ssnF* genomic loci with cutting sites for *EcoR*I used for Southern. Southern hybridization of Δ*ssnF* mutants 4-6 showed in addition to the WT band at 11.5 kb a band at 5.3 kb indicating an ectopic integration of the Δ*ssnF* deletion cassette.

The yeast Ssn6-Tup1 co-repressor complex affects the expression of 7% of all genes with emphasis on stress responses (Proft and Struhl, 2002; Smith and Johnson, 2000). It was analyzed whether Fbx15, which is required for stress response of *A. fumigatus*, physically interacts with SsnF. We used BiFC and observed a fluorescence signal of the reassembled YFP under non-stress conditions due to the direct interaction of Fbx15 and SsnF. The interaction took place primarily in the cytoplasm, which was often located close to the nuclei (Figure 23).
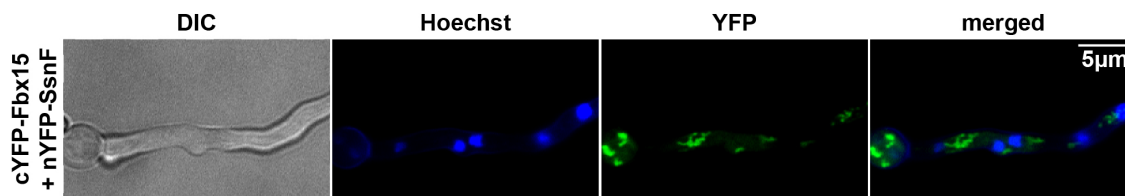
Figure 23: Fbx15 interacts with SsnF primarily in the cytoplasm. Bimolecular fluorescence complementation (BiFC) of Fbx15 and SsnF. cYFP-Fbx15 and nYFP-SsnF fusion proteins were interacting primarily in the cytoplasm, with close proximity to the nucleus.

The interaction of Fbx15 with both adaptor proteins SkpA and SsnF was primarily located in the cytoplasm. We were interested if SsnF is a substrate for an SCF^{Fbx15}-complex for ubiquitination and subsequent proteasomal degradation. SsnF-GFP fusions were constructed under native promoter, transformed into *A. fumigatus* wild type, Δ*fbx15* and *fbx15* overexpression strain backgrounds. The different Fbx15 levels in these cells did not change SsnF stability in CHX-protein stability assays (Figure 24A). Similarly, the amount of SsnF-GFP in wild type and *fbx15* deletion background did not change in the absence or presence of 3 mM H_2O_2 (Figure 24B). We analyzed if SsnF is ubiquitinated in an Fbx15 dependent manner. We purified SsnF-GFP with GFP-trap from wild type and Δ*fbx15* backgrounds before and after oxidative stress. The purified protein was probed with an anti-ubiquitin antibody and re-probed with an anti-GFP antibody as loading control. Independent of Fbx15 or the presence or absence of H_2O_2, no significant ubiquitin signal was visible for the purified SsnF-GFP (Figure 24C).
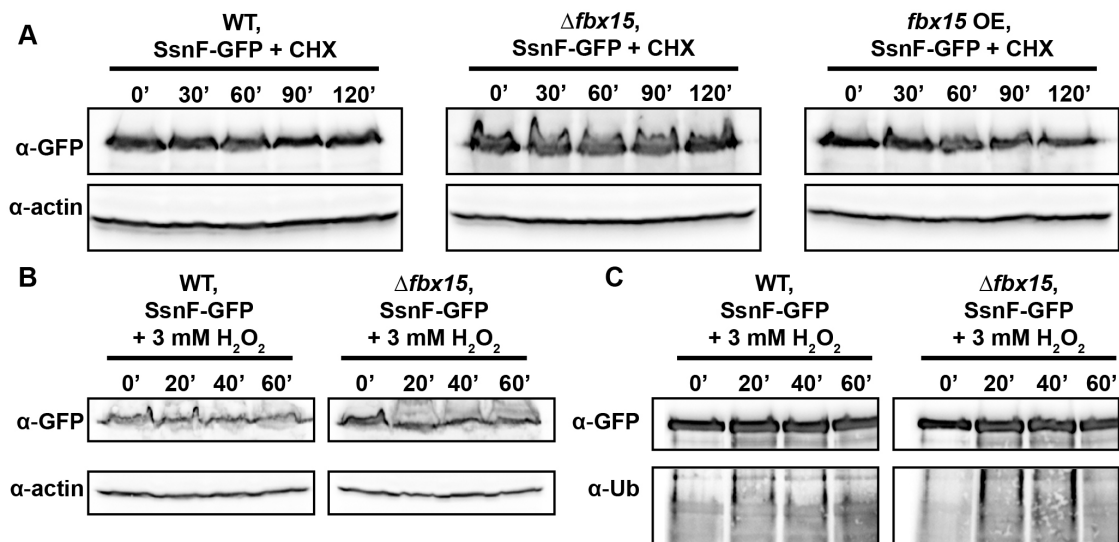
Figure 24: Fbx15 is not required for SsnF stability control. (A) Protein stability assays of SsnF-GFP in either *fbx15* wild type (AfGB64), Δ*fbx15* (AfGB65) or *fbx15* overexpression (AfGB66) backgrounds with cultures exposed to cycloheximide (CHX). SsnF-stability was not influenced in an Fbx15 dependent way. (B) Immunoblotting of SsnF-GFP in either wild type or Δ*fbx15* background before and after incubation with 3 mM H_2O_2. SsnF amount was not influenced by either treatment with H_2O_2 or in an Fbx15 dependent manner. (C) SsnF-GFP was purified from cultures with GFP-trap from either wild type or Δ*fbx15* background before and after H_2O_2-stress induction. Immunoblotting of the purified SsnF-GFP with anti-ubiquitin antibody showed no Fbx15 specific ubiquitination of SsnF.

These data indicate that SsnF is not a significant substrate of an active SCF^{Fbx15} E3 ubiquitin ligase complex and rather suggests an additional cytoplasmic function of the physical interaction of Fbx15 and SsnF.

2.3   Fbx15 is required for nuclear localization of SsnF and interacts with SsnF in the nucleus upon stress

The cellular interaction of Fbx15 with SkpA shifted from the cytoplasm into the nucleus upon oxidative stress. The cellular localization of Fbx15-SsnF interaction also took place in the cytoplasm under non-stress conditions. We analyzed the interaction of an Fbx15 mutant, which mimics the constant dephosphorylated state, Fbx15[S468|9A], with SsnF using BiFC. A reconstituted YFP-signal, facilitated by the interaction of nYFP-Fbx15[S468|9A] with cYFP-SsnF could be observed, which demonstrates their ability to interact (Figure 25). However, in contrast to wild-type Fbx15, which interacts with SsnF in the cytoplasm (Figure 23), the dephosphorylated mutant version Fbx15[S468|9A] interacted primarily in the nucleus.
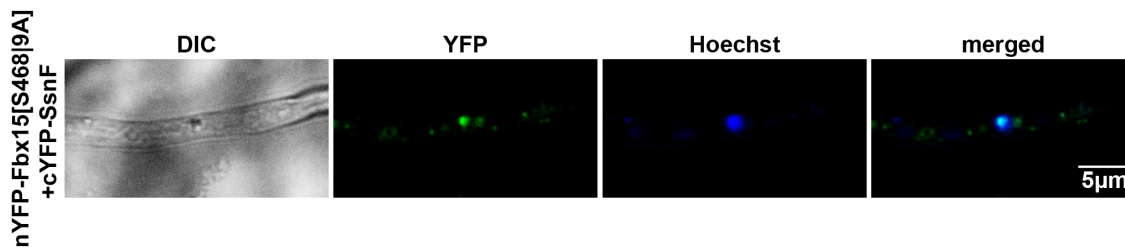
Figure 25: Dephosphorylated Fbx15 interacts with SsnF in the nucleus. BiFC-assay of constantly dephosphorylated nYFP-Fbx15[S468|9A] with cYFP-SsnF in strain AfGB121. A reconstituted YFP-signal, facilitated by the interaction of Fbx15[S468|9A] and SsnF could be observed primarily in the nucleus.

The cellular localization of SsnF as a function of Fbx15 was analyzed. We compared the localization of SsnF-GFP in *fbx15* wild type and deletion mutant. Strains were grown in minimal medium and hyphal nuclei were stained with Hoechst. SsnF-GFP could be clearly localized to the nucleus in wild-type background. The deletion of *fbx15* led to an enrichment of SsnF at nuclear pore complexes suggesting that the nuclear import is blocked (Figure 26).
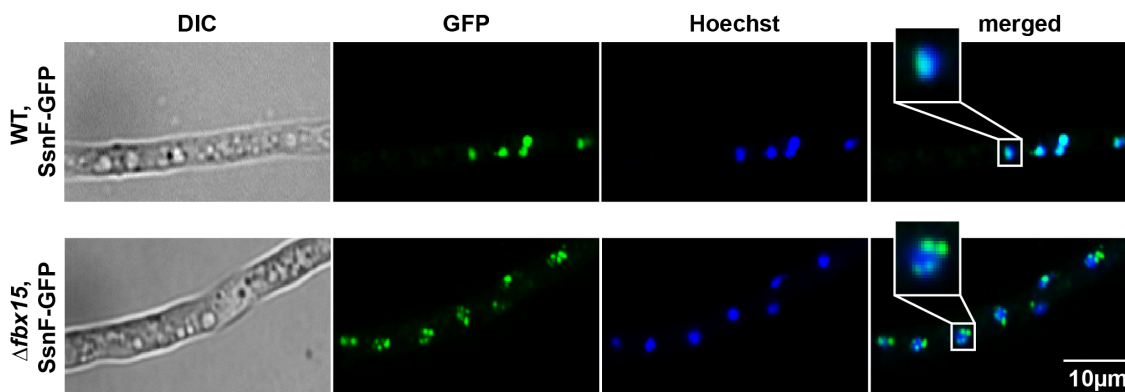
Figure 26: Fbx15 is required for nuclear localization of SsnF. Fluorescence microscopy of SsnF-GFP in either wild type or Δ*fbx15* background. Strains were grown in minimal medium and hyphal nuclei were stained with Hoechst. In Δ*fbx15* background SsnF-GFP was localized to the periphery of the nuclei, whereas in the wild-type background SsnF-GFP could be clearly localized inside the nuclei.

Since the phosphorylation state of Fbx15 is an important determinant for its cellular interaction site with SkpA, it was analyzed whether dephosphorylation of Fbx15 is involved in SsnF nuclear localization. We analyzed the localization of SsnF-GFP in the presence of different Fbx15 phosphomutants. Strains harboring the SsnF-GFP fusion and RFP-tagged versions of either the wild-type Fbx15, the constant dephosphorylated Fbx15[S468|9A] or the constant phosphorylated Fbx15[S469D] were grown in liquid minimal medium under non-stress conditions and examined under the fluorescence microscope, where nuclei

were stained with Hoechst. In *fbx15* wild type as well as in the *fbx15* mutant that mimics a constant phosphorylation, SsnF-GFP could be localized in the nucleus, whereas in the unphosphorylated Fbx15[S468|9A] mutant SsnF accumulated at the nuclear envelop (Figure 27, left panel). We further tested the localization of SsnF-GFP under oxidative stress conditions. The strains were grown as mentioned, but before microscopy the grown mycelia were shifted to medium containing 3 mM H_2O_2 and incubated for one hour. Here we observed no nuclear SsnF-GFP in *fbx15* wild type as well as in the unphosphorylated Fbx15[S468|9A] mutant. Contrastingly, SsnF-GFP in the Fbx15 phosphomutant, which mimics a constant phosphorylated state Fbx15[S469D] SsnF-GFP was still localized to the nucleus (Figure 27, right panel).
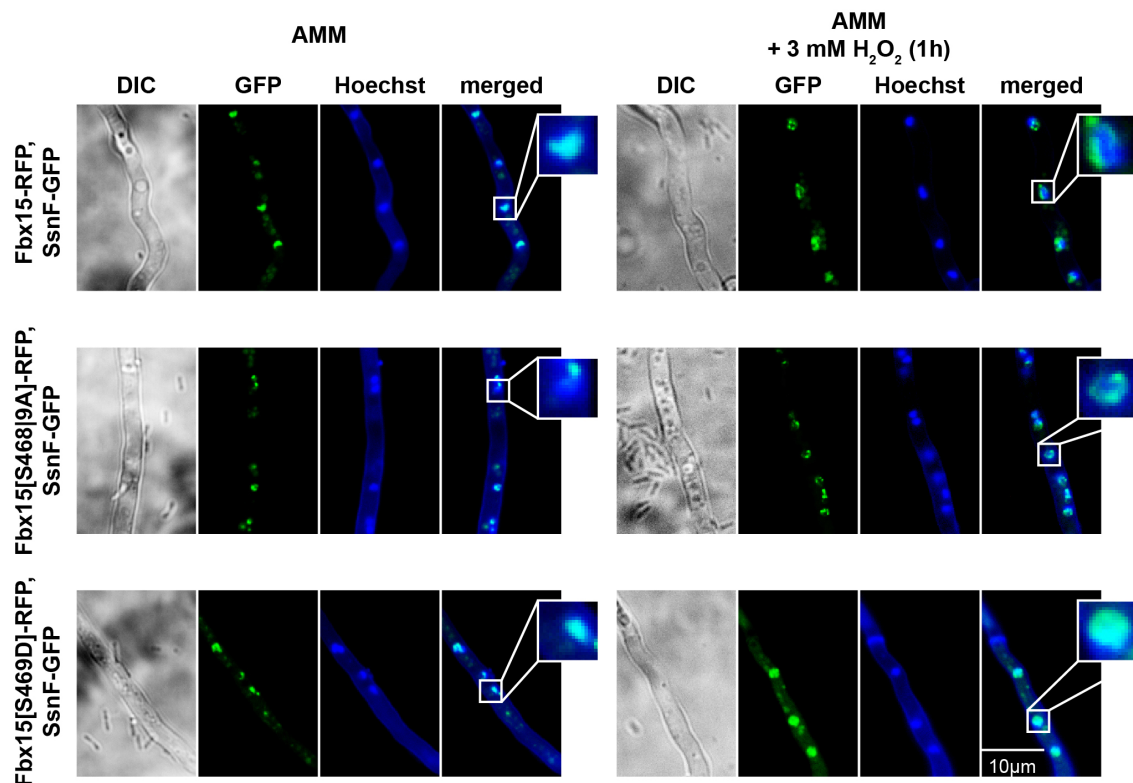
Figure 27: SsnF localization upon stress depends on the phosphorylation state of Fbx15. Microscopic analysis of SsnF-GFP in wild-type Fbx15-RFP (AfGB98), dephosphorylated Fbx15[S468|9A]-RFP (AfGB101) and S469 phosphorylated Fbx15[S469D]-RFP (AfGB102) backgrounds before and after H_2O_2-treatment. SsnF-GFP is displayed in green, whereas Nuclei were stained with Hoechst and are shown in blue. Under normal growth conditions SsnF could be localized in the nucleus in wild type and constant phosphorylated Fbx15[S469D] mutant, whereas nuclear entry of SsnF-GFP was blocked in the Fbx15[S468|9A] background. Upon oxidative stress, the dephosphorylation of Fbx15 blocks the nuclear entry of SsnF, which is resembled in the unphosphorylated Fbx15[S468|9A] mutant. In the phosphomutant with constantly phosphorylated Fbx15[S469D] SsnF-GFP was able to enter the nucleus even after H_2O_2-treatment.

These data demonstrates that Fbx15 is a vital part for the nuclear localization of SsnF under non-stress conditions. Under oxidative stress conditions the dephosphorylated Fbx15 interacts with SsnF primarily in the nucleus, which finally results in an exclusion of SsnF from the nucleus. Thus, it could be concluded that the phosphorylation of Fbx15 under non-stress conditions supports the nuclear import of SsnF, whereas the dephosphorylation of Fbx15 during stress leads to a cytoplasmic accumulation of SsnF.

2.4   Fbx15 does not change stability or ubiquitination pattern of nuclear pore protein Nic96

The co-repressor subunit SsnF is not able to enter the nucleus in the Δ*fbx15* mutant background. Therefore, a potential ubiquitinating function of SCF^{Fbx15} E3 ligase complexes towards the nuclear pore protein Nic96, which was discovered during TAP-purification, could be a reasonable function to promote nuclear transport control. The native *nic96* genomic locus in *fbx15* wild type or deletion background was replaced by a *gfp*-tagged *nic96* construct to analyze possible Fbx15 dependent effects on Nic96. Fluorescence microscopy revealed a localization of Nic96 at the periphery of the nucleus. The localization pattern of Nic96 was not changed in the Δ*fbx15* background (Figure 28). However, the localization pattern of Nic96 resembled the localization of SsnF in the *fbx15* deletion background, which seemed to get sucked at the nuclear pore (Figure 26).
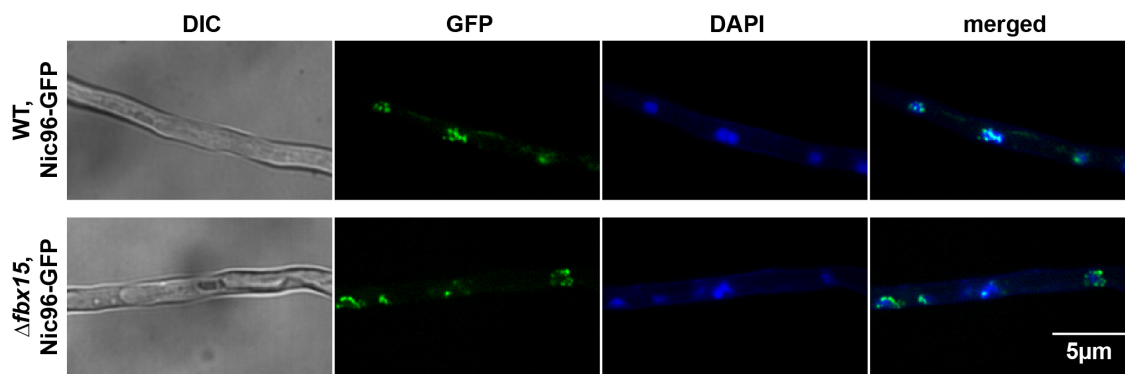
Figure 28: Nuclear pore protein Nic96 is located at the nuclear envelop independent of Fbx15. Fluorescence microscopy of Nic96-GFP in either WT or Δ*fbx15* background. Nuclei were stained with DAPI. Nic96-GFP could be detected at the periphery of the nuclei independent of the presence or absence of Fbx15.

Therefore, it was analyzed whether Nic96 might be ubiquitinated in an Fbx15 dependent manner upon oxidative stress. GFP-pull-downs of Nic96 in either *fbx15* wild type or

deletion strains before and after induction with H_2O_2 were subjected to western hybridization with ubiquitin specific antibody. Although an ubiquitin signal for Nic96 could be observed, the signal was not significantly changed upon oxidative stress exposure or in an Fbx15 dependent way (Figure 29). This suggests a Nic96 independent function of SsnF nuclear transport control for Fbx15 upon stress.
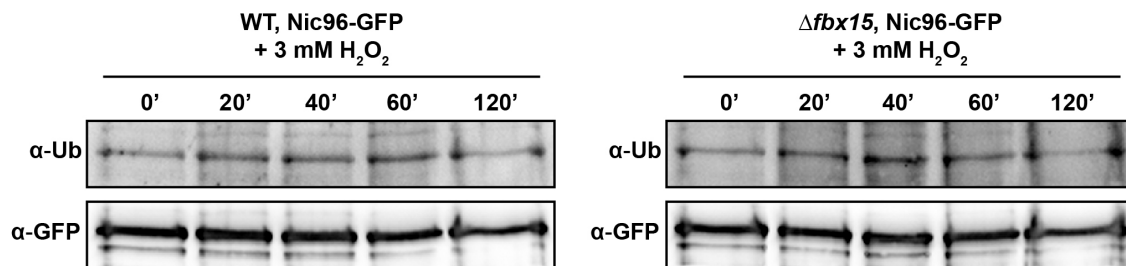
Figure 29: Nic96 is ubiquitinated independent of oxidative stress or Fbx15. GFP-trap pull-down of Nic96-GFP in either WT or Δ*fbx15* background before and after H_2O_2-treatment followed by immunoblotting. Purified Nic96-GFP of respective conditions was incubated with anti-ubiquitin antibody, but no Fbx15 dependent ubiquitination pattern could be detected. Blotting membranes were subsequently incubated with anti-GFP antibody indicating equal amounts of purified Nic96-GFP.

3 Fbx15 acts as suppressor for gliotoxin production and is essential for virulence of *A. fumigatus*

3.1 Fbx15 is required for the repression of gliotoxin biosynthesis

A group of genes, which are usually repressed during normal fungal growth, are secondary metabolite genes. It was further shown that defects in the CSN-regulated ubiquitination machinery have a tremendous effect on secondary metabolite production (Gerke and Braus, 2014). It was analyzed whether the deletion of *fbx* genes in *A. fumigatus* might lead to an altered expression of secondary metabolites. A potent immunosuppressive mycotoxin in *A. fumigatus* is gliotoxin, which is considered as one of multiple virulence factors of this pathogen (Scharf et al., 2012). Gliotoxin production of the Δ*fbx15* mutant was determined by high-performance liquid chromatography (HPLC) and compared with the production levels of wild type, Δ*fbx23* and Δ*grrA* strains. The gliotoxin production of Δ*fbx15* increased more than 4-fold compared to wild type (Figure 30A). In addition HPLC-chromatograms revealed two more metabolites produced by AfS35 (WT) with retention times (t) = 9.5 min and (t) = 11.2 min, which were elevated, whereas one me-

tabolite with retention time (t) = 6.5 min was significantly reduced in the mutant compared to wild type (Figure 30B). The gliotoxin level produced by Δ*fbx23* was two times elevated compared to wild type displaying a less pronounced effect on secondary metabolite production compared to Δ*fbx15* (Figure 30A/B). In contrast, the Δ*grrA* strain showed no alteration in gliotoxin production levels but an overall decreased metabolite production compared to the wild type (Figure 30A/B).
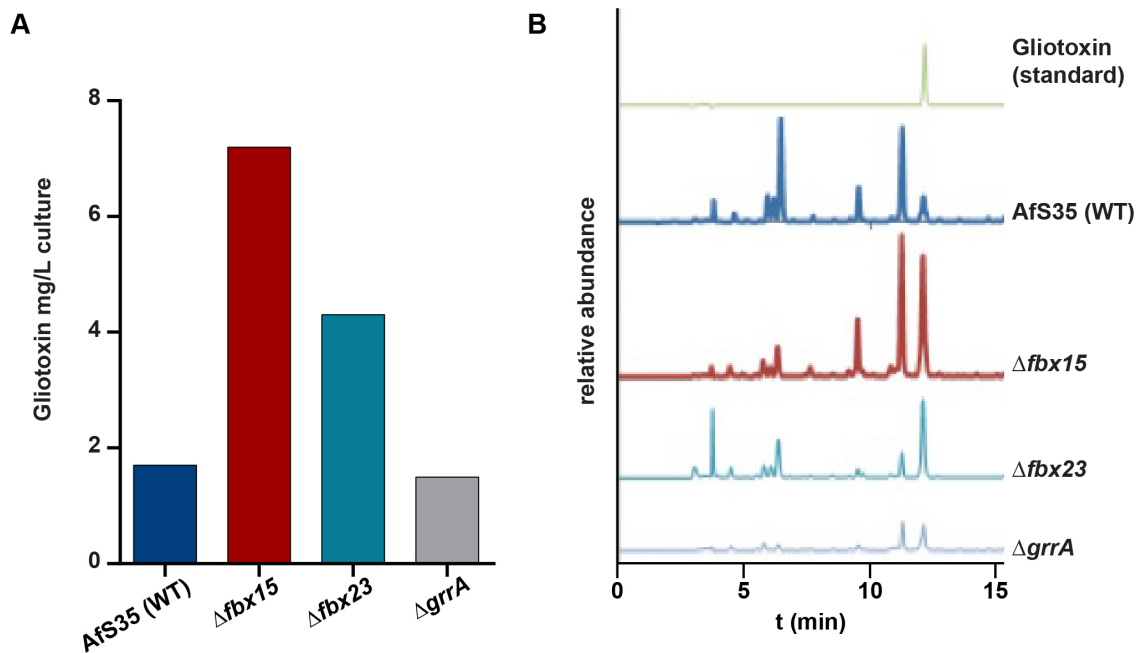
Figure 30: Fbx15 represses gliotoxin biosynthesis. (A) The gliotoxin production of Δ*fbx15* mutant strain was analyzed with HPLC and compared to AfS35 (WT) and deletion strains Δ*fbx23* and Δ*grrA*. The Δ*fbx15* strain showed more than four fold-increased gliotoxin production compared to the wild type, while the amount of gliotoxin produced by Δ*fbx23* was 2x increased. (B) HPLC chromatograms for organic extracts of AfS35 (WT) and Δ*fbx*-strains, indicating an altered secondary metabolism with elevated gliotoxin production levels for Δ*fbx15* and Δ*fbx23* compared to wild type. In contrast the Δ*grrA* mutant showed a generally decreased secondary metabolite production compared to the wild type.

Since SsnF is not able to enter the nucleus in the Δ*fbx15* mutant, we were interested if the de-repression of gliotoxin production in the Δ*fbx15* strain is already initiated at the transcriptional level. We analyzed the expression of *gliZ*, which encodes a transcriptional activator that has been shown to drive the expression of *gli*-genes encoded in the gliotoxin gene cluster and *gliP*, encoding the non-ribosomal peptide synthetase GliP with a key role in gliotoxin biosynthesis (Bok et al., 2006; Kupfahl et al., 2006). We determined the expression of *gliZ* and *gliP* in AfS35 (WT), Δ*fbx15* and the complemented strain with quantitative real-time (qRT) PCR. While the expression of *gliZ* in the Δ*fbx15* mutant was not

significantly changed compared to wild type and complemented strain, *gliP*-expression of the Δ*fbx15* strain was increased by almost three times in comparison to the wild type (Figure 31).
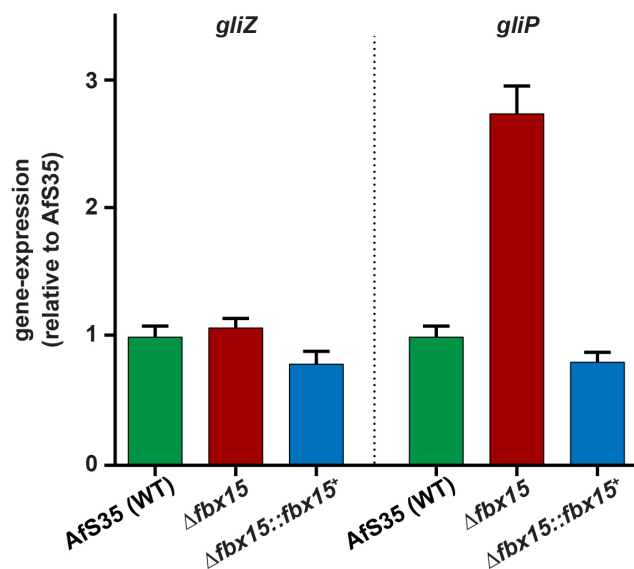
Figure 31: Fbx15 is required for *gliP* repression. *gliZ* and *gliP* expression determined with real-time PCR. The Δ*fbx15* mutant showed a nearly 3-fold increased *gliP* expression compared to wild type and complemented strain, while the expression of *gliZ* was not influenced in the mutant.

These results suggest a prominent function for F-box proteins in secondary metabolite production. Especially Fbx15 and to lesser degree Fbx23 are involved in the repression of gliotoxin production and other metabolites, whereas GrrA might support a more general induction of secondary metabolite production. Furthermore, RT-PCR showed that the repression of gliotoxin biosynthesis mediated by Fbx15, already starts at the transcriptional level, by repressing the expression of *gliP*.

3.2 Fbx15 is essential for virulence in a mouse model of aspergillosis

It was analyzed whether there is a connection between the observed defects in various stress responses and the increased gliotoxin production levels of the Δ*fbx15* mutant and its virulence. Virulence of the Δ*fbx15* mutant was analyzed in comparison to wild type, Δ*fbx23* and Δ*grrA* strains in an established murine model of invasive pulmonary aspergillosis (IPA) (Liebmann et al., 2004a). This model uses cortisone acetate for immunosup-

pression of CD-1 mice, which in contrast to neutropenic mice, enables to screen for the effect of altered gliotoxin production on virulence (Kwon-Chung and Sugui, 2009).

Mice infected with AfS35 (WT) and complemented strains displayed normal mortality rates within 14 days (Figure 32). The survival of mice treated with Δ*fbx23* or Δ*grrA* was not significantly changed compared to wild type or complemented strains, although the Δ*fbx23* strain displayed a slightly increased virulence (p = 0.03) in direct comparison to the wild type. This suggests that the observed defects of the corresponding mutant strains in stress conditions like temperature or oxidative stress sensitivity are not of major relevance in the tested model.
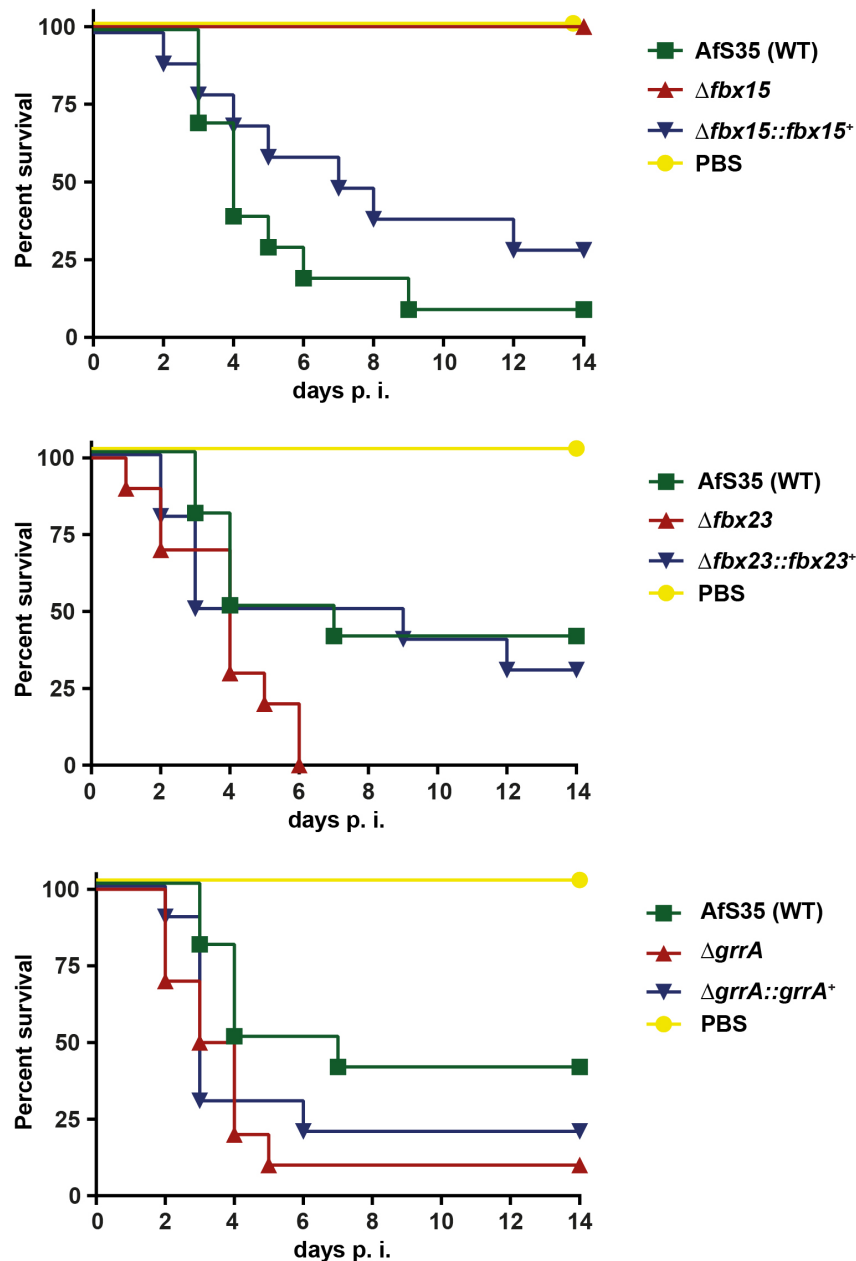
Figure 32: Fbx15 is essential for virulence. Survival rates of CD-1 mice (n=10), which were immunosuppressed with cortisone acetate and infected intranasal with 1x 10^6 conidia of the respective strains. A control group was mock infected with PBS and survival was monitored twice daily for 14 days. The Δ*fbx15*-infected mice did not show any symptom and looked the same as PBS-treated mice, whereas mice infected with AfS35 (WT) and complemented strains showed normal mortality rates within 14 days. Survival of mice infected with Δ*fbx23* displayed slightly attenuated virulence (p=0.03) compared to wild type, whereas the survival for Δ*grrA* mutants did not show significant difference in contrast to wild type and complemented strain.

As previously shown, virulence tests revealed that the Δ*fbx15* mutant completely lost its virulence (Figure 32) (Jöhnk, 2009). The Δ*fbx15*-infected mice did not show any symptoms and had the same clinical appearance as the mock-infected control group, trea-

ted with <u>p</u>hosphate <u>b</u>uffered <u>s</u>aline (PBS). Consequently, histopathology analysis of the infected lung tissue was consistent with the survival rates. Mice infected with either AfS35 (WT) or complemented strains showed fungal hyphae surrounded by tissue necrosis and extensive immune cell infiltration. While moderate immune cell infiltrates were also found in the lungs of mice infected with the Δ*fbx15* mutant, no fungal hyphae could be detected, suggesting that the fungus was cleared at an early stage of infection, probably due to innate immune responses characterized by increased temperature and elevated levels of oxidative stress (Figure 33).
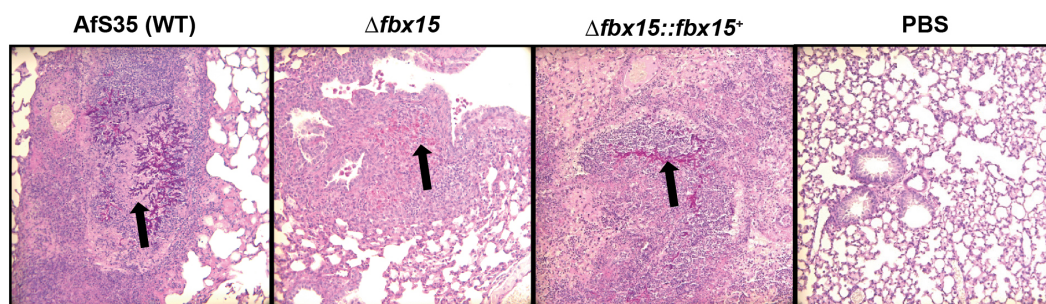
Figure 33: Infected lung tissue revealed no fungal persistence for Δ*fbx15* infected mice. Histopathology of lung tissue from mice infected with AfS35 (WT), Δ*fbx15*, Δ*fbx15::fbx15*[+] and PBS control using PAS staining (hyphae stained pink). Black arrows indicate infection sites. The infection site of Δ*fbx15* was already cleared, while the lung tissue of AfS35 (WT) and Δ*fbx15::fbx15*[+] infected mice displayed hyphal growth.

These data suggest that Fbx15 enables *A. fumigatus* to adapt to several stress conditions like fever or oxidative stress during innate immune response and therefore plays a crucial role during infection and development in the host. We could further conclude that the increased amount of gliotoxin, produced by the Δ*fbx15* strain, was not able to rescue the mutant from being cleared.

3.3   Fbx15 is a potential drug target

Fbx15 plays a crucial role for *A. fumigatus* infection of immunocompromised mice and thus might be used as a potential target for antifungal drugs. Previous reports have demonstrated that monoclonal immunoglobulins, which are targeting *A. fumigatus* cell wall components have an protective function against murine aspergillosis (Casadevall and Pirofski, 2007; Chaturvedi et al., 2005). Therefore, in an initial experiment, the polyclonal antibody against Fbx15 was analyzed for its ability to suppress fungal growth under oxi-

dative stress conditions. *A. fumigatus* wild-type conidia were precultured in the presence and absence of the Fbx15 antibody and then transferred to solid medium with and without 3 mM H_2O_2. The effect of the Fbx15 antibody was compared to growth defects of the Δ*fbx15* mutant and wild-type conidia, which were grown in the presence of a GFP antibody. The preincubation with either anti Fbx15 or anti GFP antibody had no effect on the growth on non-stress conditions, thus resembling the colony morphology of the wild type or the Δ*fbx15* mutant (Figure 34). Under oxidative stress conditions, the preincubation of the wild type with the Fbx15 antibody completely abolished its growth, which was identical to the Δ*fbx15* mutant. The preincubation with the GFP antibody also led to a slight growth impairment under oxidative stress conditions, indicating that the GFP antibody reacts with some components of *A. fumigatus* oxidative stress response pathways (Figure 34).
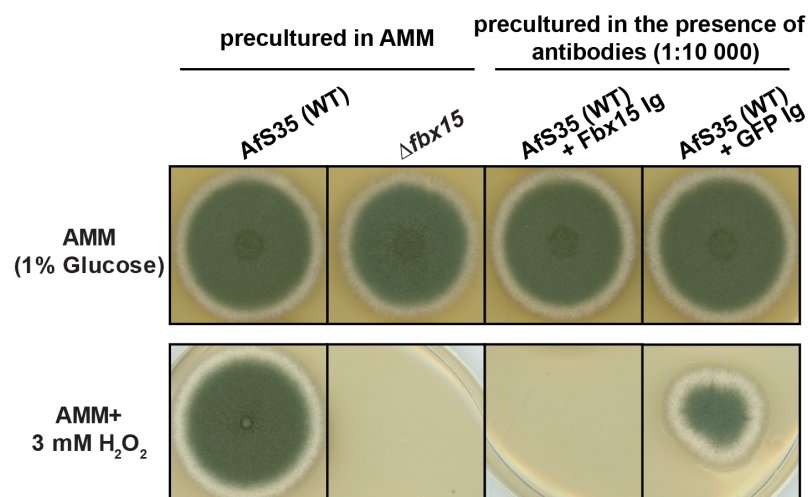
Figure 34: Fbx15 is a potential antifungal drug target. AfS35 (WT) conidiospores were preincubated in AMM for 12 hours either in the presence or absence of 0.1 µg/ml antibodies against Fbx15 and GFP as control. Germinated mycelium was then transferred to solid media plates with and without 3 mM H_2O_2. AfS35 (WT), which was preincubated with in the presence of the Fbx15 antibody, were not able to grow under oxidative stress conditions and resembled Δ*fbx15* phenotype, whereas the preincubation with the GFP antibody only led to slight growth defects on AMM containing H_2O_2.

The complete growth impairment of *A. fumigatus* wild type under oxidative stress in the presence of an Fbx15 specific antibody indicates that Fbx15 might serve as potent antifungal drug target.

IV   Discussion

Aspergillus fumigatus is the most prevalent cause for pulmonary infections in immuno-compromised patients. Virulence contributing factors, like high thermo- and oxidative stress tolerance, toxic metabolites and a versatile metabolism have been identified and probably act together to allow *A. fumigatus* to colonize the host tissue (McCormick et al., 2010). We have identified the fungal-specific F-box protein Fbx15, which plays a key role in stress response and secondary metabolism. Fbx15 can act as part of an SCF E3 ubiquitin ligase complex, but as a second function also is a vital part of the cellular transcriptional regulation by controlling the nuclear transport of the transcriptional repressor adaptor SsnF. Both functions are modulated by increased transcription and phosphorylation upon external stressors. The dual function of Fbx15 is essential for the virulence of *A. fumigatus*, which makes it an attractive target for antifungal drugs.

1   The molecular mechanism of Fbx15 mediated stress response

1.1   Fbx15 highlights multiple roles for F-box proteins

This work highlights a dual function of Fbx15, which can interact within SCF complexes but in addition is also crucial for the nuclear localization control of the transcriptional co-repressor subunit SsnF. Though F-box proteins are generally considered as adaptor subunits for SCF E3 ligase complexes with an ubiquitinating function towards their substrates only few ubiquitinated targets have been identified for them. Moreover, around 12% of the human F-box proteins exhibit SCF-independent functions (Nelson et al., 2013). An example for an F-box protein with additional SCF-independent functions is the human Fbh1/Fbxo18, which exhibits a helicase domain and is involved in DNA maintenance and repair. It also assembles into SCF-complexes, but no ubiquitinated target proteins were identified so far (Kim et al., 2004). Another prominent example is the human F-box protein Fbxo7. It assembles into SCF-complexes and so far three ubiquitinated targets of SCF^{Fbxo7} have been identified, among them two additional E3 ligases. In addition Fbxo7 has SCF-independent roles in regulation of the cell cycle, proteasomal activity and mitophagy (Nelson et al., 2013). These examples together with our findings for *A. fumigatus*

Fbx15 emphasize the multiple roles of F-box proteins in cellular integrity beyond its ca-
nonical function as SCF-substrate adaptors.

1.2   The phosphorylated form of Fbx15 promotes SCF^{Fbx15} assembly during non-stress conditions

Most studies about the dynamics of CRLs and specifically for SCF complexes were fo-
cused on neddylation/deneddylation cycles of the cullin scaffold and the cullin-CAND
interaction, which promotes the exchange of substrate adaptors (Figure 35) (Choo et al.,
2011; Duda et al., 2008; Olma and Dikic, 2013; Pierce et al., 2013; Schmidt et al., 2009).
In addition traditional concepts of SCF-directed substrate recognition are usually based
on the modification of the target protein. Different small motifs called degrons are the
recognition sites for F-box proteins, which are subject to covalent modification by phos-
phorylation and glycosylation (Skaar et al., 2013). However, recent studies have shown
that the regulation of CRL activities is rather complex, incorporating additional factors,
dimerization of substrate adaptors or whole CRL complexes (Figure 35). The fact that an
inhibition of Nedd8 conjugation to cullins does not result in decreased amounts of CRL
complexes further suggests additional control mechanisms (Lee et al., 2011; Merlet et al.,
2009). A recent study focused on posttranslational modifications of human Fbx4 and its
target substrate cyclin D1, which promotes G1/S cell-cycle transition by activation of
cyclin-dependent kinases. They showed that not only the substrate but also Fbx4 has to be
phosphorylated in order to activate SCF^{Fbx4} E3 ligase activity. Phosphorylation of Fbx4
triggers the interaction of Fbx4 with the 14-3-3ε phosphoserine/threonine binding protein,
which in turn promotes the dimerization of Fbx4. The dimerization of Fbx4 substantially
increases its ubiquitinating activity towards cyclin D1 (Barbash et al., 2011; Li and Hao,
2010).
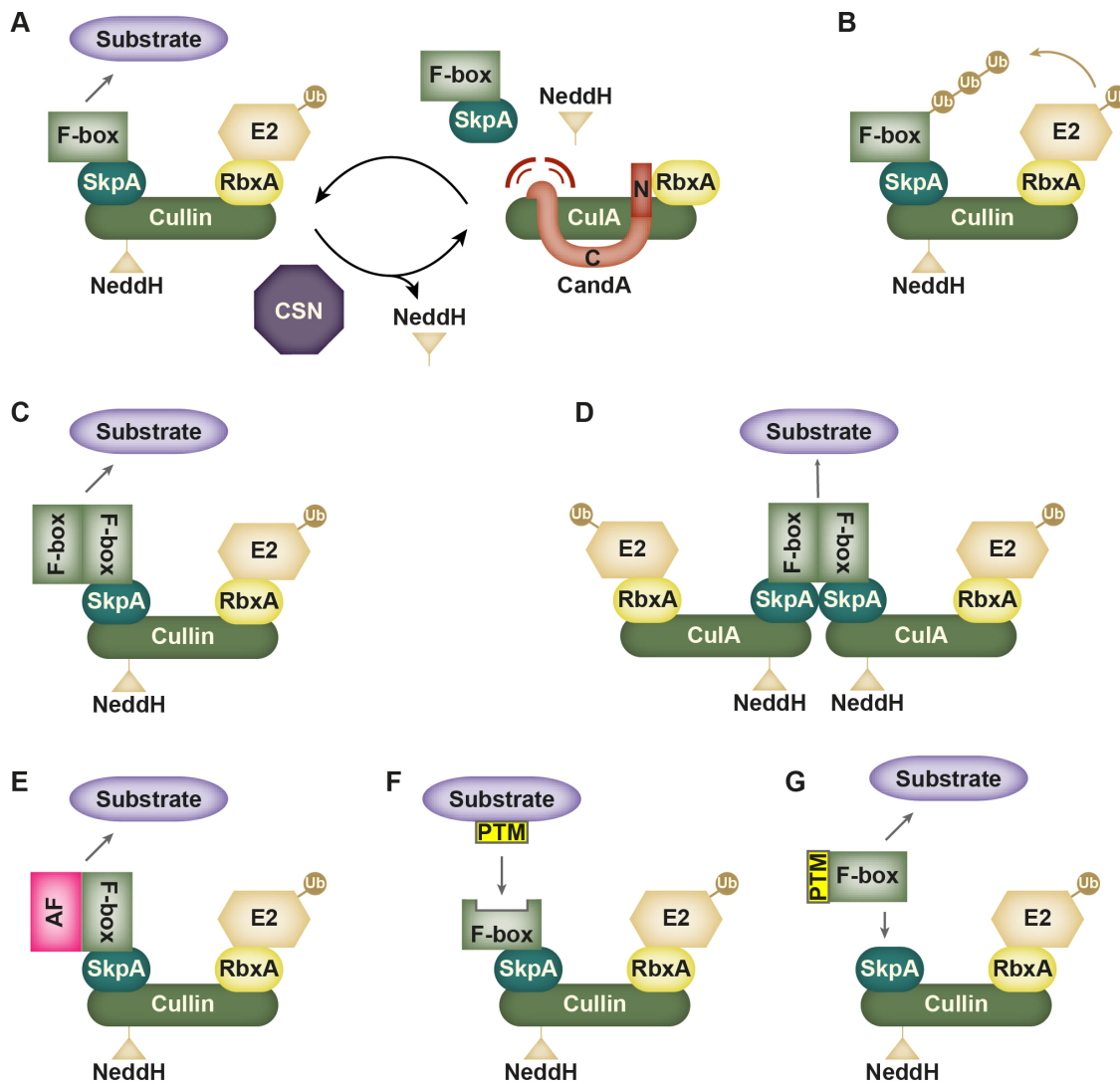
Figure 35: Mechanisms of Cullin RING ligase regulation. (A) CRL assembly/disassembly cycles through the CSN deneddylase. The CSN removes the ubiquitin-like modifier NeddH from the Cullin, leading to the dissociation of the CRL substrate adaptor. This is accompanied by the binding of CandA to the Cullin subunit, further inhibiting the binding of substrate adaptors. (B) Autoregulatory mechanism through the ubiquitination of substrate adaptors within their own CRL. (C) Stimulation of CRL activity by dimerization of substrate adaptors, or hole CRLs (D), which allows conformational variability or ubiquitination on multiple lysine acceptor sites at the substrate. (E) CRL activation by additional activating factors (AF) that bind to the substrate recognition subunit. (F) Posttranslational modifications (PTM) of the substrate like glycosylation or phosphorylation, which allows the binding to the substrate adaptor subunit in CRLs. (G) Posttranslational modifications of the substrate adaptor, which allows either substrate recognition or CRL assembly.

During this work Fbx15 was also found to be phosphorylated on either Ser468 or Ser469 with an effect towards its interaction within SCF^{Fbx15} complexes. Only Fbx15 mutations, which mimic a constant phosphorylation were able to pull-down all subunits required for an active SCF^{Fbx15} E3 ligase complex. This effect emphasizes an important

role for posttranslational modifications of substrate adaptor subunits in CRLs, which are required to modulate their activities. Moreover, one of the Fbx15 interacting proteins, which were identified with TAP-purification, was the so far uncharacterized 14-3-3 family protein AFUA_6G06750, which might modulate its function as it was previously shown for 14-3-3ε-Fbx4 interaction.

1.3   Comparison of F-box proteins Fbx15 and SconB

The molecular function of Fbx15 was analyzed in comparison to the well-characterized F-box protein Met30/SconB. Met30 from *S. cerevisiae* is one of three F-box proteins, which have been studied thoroughly in the recent years, thus making it a model F-box protein. It is a highly conserved protein with seven WD40 repeats in addition to the F-box domain and a crucial part of the <u>s</u>ulfur <u>m</u>etabolite <u>r</u>epression (SMR) system, which is analog to the carbon catabolite repression system. It was originally thought that the presence of methionine in the medium activates SCF^{Met30} ligases, which target the transcriptional activator of genes for the uptake and biosynthesis of sulfur containing compounds, Met4, for proteasomal degradation. However, more recent studies have shown that Met4 stability is not changed upon K48-linked ubiquitination, but turned into a resting inactive state. Moreover Met4 itself can become part of SCF$^{Met30/Met4}$ ubiquitin ligases, which recruit Met4 co-factors for ubiquitination and subsequent degradation (Figure 36) (Ouni et al., 2010; Tyrrell et al., 2010). The transcription of *MET30* itself is also under the control of Met4, thus providing a feedback regulation of SCF^{Met30} activity (Brunson et al., 2004; Chandrasekaran and Skowyra, 2008; Rouillon et al., 2000). A feature of Met30, which was also observed for yeast F-box proteins Grr1 and Cdc4, was their intrinsic instability due to an autocatalytic mechanism. These F-box proteins get ubiquitinated and targeted for degradation within their own SCF complexes (Galan and Peter, 1999; Pashkova et al., 2010). This effect could also be observed for SconB of *A. fumigatus*, where the instability of SconB could be reduced by a mutation in the F-box domain, resulting in impaired SkpA binding efficiency. In contrast, Fbx15 showed high stability independent of SCF incorporation, suggesting a different mode of F-box protein control. This also provides some evidence that the general properties of F-box containing proteins are quite diverse and should not be limited to standard functions, discovered for a few model F-box proteins.

In comparison little is known about the Met30 homologs in filamentous fungi. But similar to Met30, SconB and SCON2 of *A. nidulans* and *N. crassa* are negative regulators for sulfur assimilation by targeting the Met4 homologous central transcriptional activators MetR and CYS3 for degradation (Kumar and Paietta, 1998; Natorff et al., 1998). However, this function only seems to be partial conserved, since *N. crassa* mutants, where the F-box domain of SCON2 was exchanged to the respective F-box domain of Met30 from yeast, showed an intermediate phenotype between functional and impaired SCON2 (Kumar and Paietta, 1998). Since SconB in *A. nidulans* and *A. fumigatus* are essential proteins, an additional function for SconB beside SMR has been proposed. A recent study has shown that beyond sulfur metabolism genes also genes required for stress responses, signal transduction and energy metabolism are upregulated in *A. nidulans sconB* mutants, which provided increased stress resistance for these mutants (Sieńko et al., 2014). In addition Met4 is also activated by oxidative stress response and cell division (Chandrasekaran and Skowyra, 2008). The results for SconB co-purifications of this work also suggest additional functions for SconB, since beside MetR also a transcriptional activator for oxidative stress response, Yap1, was found as potential target for SCF^{SconB} ligases. By comparison of proteomes from wild type and Δ*yap1* strains several putative target genes of Yap1 have been identified, including antioxidant proteins and heat shock proteins (Lessing et al., 2007). Our results indicate a interdepend role for Fbx15 and SconB for various stress responses, which is linked to sulfur metabolism through SconB, rather than independent functions though they are controlled in entirely different ways.
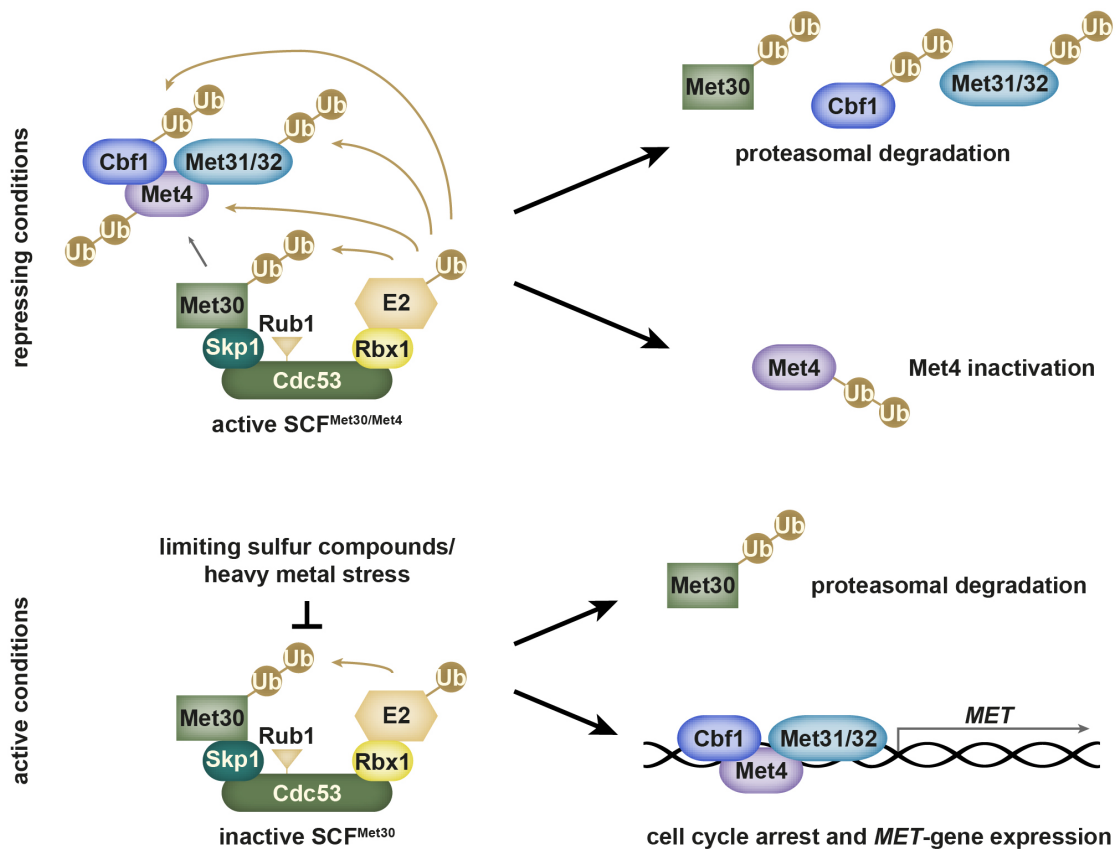
Figure 36: Current model of SCF^{Met30} mediated ubiquitination. Under repressing conditions with sufficient amounts of sulfur compounds the SCF^{Met30} ligase complex ubiquitinates the transcriptional activator Met4 leading to its inactivation. Furthermore the SCF^{Met30} target Met4 recruits its co-activators Cbf1, Met31 and Met32 to the ligase complex, resulting in their ubiquitination and subsequent degradation. Under active conditions limiting sulfur compounds and/or heavy metal stress inhibits the ubiquitin ligase activity of the SCF^{Met30} complex, leading to the transcriptional activation of Met4 target genes, including *MET30*. However, under both conditions Met30 seems to be ubiquitinated and subject to proteasomal degradation.

1.4   Putative target proteins of SCF^{Fbx15} ligase complexes

Fbx15 was initially co-purified for *A. nidulans* NeddH, suggesting its functionality in SCF^{Fbx15} (Zeska Kress et al., 2012). The co-purification experiments of this work provide further evidence that Fbx15 is a component of ubiquitinating SCF E3 ligases, since impaired SnnF localization in Fbx15 phosphomutants are only partially responsible for the defects in stress responses, observed for the Δ*fbx15* mutant. 27 putative interacting proteins were exclusively identified for Fbx15, whereas another 11 of them were also found for the well-described F-box protein SconB. Interestingly, only the native Fbx15 was able to co-purify three subunits of the COP9 signalosome (CSN), which were absent for

SconB or a modified Fbx15 version with diminished SkpA binding abilities. The CSN complex functions as a regulator for the SCF-complex assembly by deneddylation of the CulA-subunit. This process is thought to be necessary for the exchange and stability of the F-box substrate adaptors inside SCFs (Dubiel, 2009; Enchev et al., 2012; Wei et al., 2008). This suggests a tight regulation of SCF[Fbx15] complexes, which results in the increased stability of Fbx15 compared to SconB, where no CSN subunits could be co-purified. Indeed, it was shown for *A. nidulans* that a functional CSN is required for the stability of Fbx15 (Zeska Kress et al., 2012). However, it remains to be elusive whether the CSN-subunits were co-purified by Fbx15 as a direct interaction partner or as part of a CSN-SCF[Fbx15] super complex.

Based on the predominantly nuclear localization of Fbx15 several putative nuclear target proteins could be identified. A promising target protein for Fbx15 is the bHLH transcription factor SrbB. SrbB belongs to the fungal <u>s</u>terol <u>r</u>egulatory <u>e</u>lement <u>b</u>inding protein family (SREBP), which is required for hypoxia adaptation (Hughes et al., 2005; Todd et al., 2006a). The deletion of *fbx15* in *A. fumigatus* led to an elevated secondary metabolite production, an effect which is also present in Δ*srbB* mutants. Moreover SREBP proteins in the human pathogenic fungi *Cryptococcus neoformans* and *A. fumigatus* have an attenuating effect on pathogenicity, when deleted (Chun et al., 2007; Chung et al., 2014). Therefore, SrbB might be a potential target for Fbx15 and growth tests for the Δ*fbx15* mutant under hypoxic conditions would provide further evidence, whether Fbx15 is involved in growth during oxygen limitations, which is resembled in infected host tissues.

Another interesting candidate for Fbx15 targeting is the yet uncharacterized APSES transcription factor AFUA_5G11390, which was also co-purified with SconB, indicating a tight control of this protein by two different F-box proteins. Transcription factors of the APSES family are characterized by a fungal specific <u>b</u>asic <u>h</u>elix-<u>l</u>oop-<u>h</u>elix (bHLH) DNA-binding domain and have been described as key regulators for fungal development and virulence (Ramírez-Zavala and Domínguez, 2008; Zhao et al., 2014). StuA of *A. nidulans* is one of the founding members of the APSES family, which is required for asexual and sexual development. During sexual development StuA also triggers the expression of the catalase-peroxidase gene *cpeA* (Scherer et al., 2002; Wu and Miller, 1997). The deletion of the corresponding gene in *A. fumigatus* resulted in severely impaired production of asexual conidia, impaired secondary metabolism and hypersensitivity against oxidative stress (Sheppard et al., 2005). Like StuA, AFUA_5G11390 contains

only one APSES domain and both transcription factors belong to evolutionary similar groups (Zhao et al., 2014). Thus the APSES transcription factor AFUA_5G11390 might also be involved in developmental processes that are linked to secondary metabolism and/or oxidative stress tolerance, which makes it an interesting target protein for Fbx15 and SconB.

Another putative nuclear target protein of Fbx15 was the transcription factor OefC, which regulates asexual development in *A. nidulans* (Lee et al., 2005). The overexpression of *oefC* resulted in a phenotype with fluffy white mycelium, while asexual conidiation was completely abolished. It is possible that an increased stabilization of OefC in Δ*fbx15* mutants during stress leads to the drastically reduced conidiospore formation, which was observed under various stress conditions.

Further nuclear proteins, which were co-purified with Fbx15 were either not characterized so far or belong to the RNA processing category that often bears false positive candidates. However they might also be controlled in an Fbx15 mediated fashion, allowing a broad spectrum of affected pathways.

During co-purifications Fbx15 has recruited the kinase NimX and the phosphatase GlcA. These essential proteins probably play a role in the posttranslational modification of Fbx15 itself. However, these proteins might also be potential targets for Fbx15, since F-box proteins have been reported to play an ubiquitinating role in signal transduction, such as Grr1 form *S. cerevisiae*, which is responsible for the ubiquitination and subsequent degradation of the serine/threonine kinase Ime2 (Purnapatre et al., 2005).

1.4   Phosphorylated Fbx15 is required for nuclear localization of SsnF

Fbx15 plays a crucial role for adaptive responses to environmental changes and general stress response mechanisms in *A. fumigatus* whereas during non-stress conditions *fbx15* is dispensable for normal growth. This correlates with the expression patterns of *fbx15* gene transcription and translation, which demonstrated that Fbx15 becomes really abundant not before stress induction. Contrastingly, the presence of Fbx15, although under low expression levels, is required for the nuclear localization of the transcriptional co-repressor subunit SsnF during non-stress conditions (Figure 37). SsnF is part of the conserved fungal transcriptional co-repressor complex, which is well known as Ssn6(Cyc8)-Tup1 from yeast. Ssn6-Tup1 mediated gene repression affects at least 334 genes during normal

growth conditions, which are part of a multitude of developmental, metabolic and stress response pathways in yeast (Asada et al., 2015; Green and Johnson, 2004). Whereas Tup1 functions as the repressing subunit in this complex, which is able to mediate gene repression also in the absence of Ssn6p, Ssn6p mainly acts as an adaptor between a tetramer of Tup1 and additional DNA-binding proteins that cause sequence specificity (Chujo et al., 2015; Liu and Karmarkar, 2008; Roy et al., 2013). The fact that Tup1 alone is able to promote transcriptional repression (Merhej et al., 2015), might explain the ability of the Δ*fbx15* mutant to grow under normal conditions, where SsnF is not able to reach the nuclear target sites. However, the Ssn6-Tup1 counterparts in the filamentous fungi *A. nidulans* (SsnF/RcoA) and *N. crassa* (RCM-1/RCO-1) seem to have more specific functions since the deletions of *rcoA* or *rco-1* respectively have a tremendous influence on sexual/asexual development and secondary metabolite production, whereas glucose repression is only slightly affected (Hicks et al., 2001; Todd et al., 2006b). The Δ*rcoA* phenotype is very similar to *A. nidulans* Δ*fbx15* mutant strains, which are also blocked in both developmental pathways and showed an impaired secondary metabolism (Zeska Kress et al., 2012). Thus Fbx15 mediated transcriptional regulation due to nuclear localization control of SsnF might be a conserved mechanism in filamentous fungi.

The DNA binding protein that associates with Ssn6 specifies the genomic site, where Ssn6-Tup1 mediated repression is initiated (Hanlon et al., 2011; Merhej et al., 2015; Smith and Johnson, 2000). In this context the DNA-binding protein Rim1, which was co-purified for Fbx15, is an interesting candidate for SsnF-RcoA target specificity. Rim1 has an activating function for *IME1* expression. Ime1 in turn is a positive regulator of meiosis in yeast that gets phosphorylated by Ime2, which targets Ime1 for proteasomal degradation during vegetative growth (Guttmann-Raviv et al., 2002; Su and Mitchell, 1993). Interestingly *IME1* transcript levels are elevated in *SSN6* or *TUP1* mutants, suggesting a loss of repressing function (Mizuno et al., 1998). These findings indicate that Rim1 might serve as specific SsnF binding protein, which targets SsnF-RcoA to specific genomic regions.

The Δ*fbx15* mutant strains, which result in decreased nuclear SsnF levels are impaired during stress but similar to wild type under non-stress conditions. The RcoA counterparts in yeast (Tup1) and higher eukaryotes (Groucho/TLE) are known to mediate its repressing function through a variety of mechanisms including histone deacetylation by recruiting histone deacetylases, chromatin rearrangements through nucleosome packaging, modification of RNA polymerase II activity and simply by competing with

transcriptional activators (Asada et al., 2015; Fleming et al., 2014; Paul et al., 2015; Roy et al., 2013). These mechanisms are not only involved in repressing functions but sometimes are also required for transcriptional activation. It has been shown that the Ssn6-Tup1 co-repressor is also able to recruit histone acetylases to repressed promoter target sites, which enables a rapid de-repression of the respective target genes (Desimone and Laney, 2010). Another example is the transcriptional repressor Sko1, which inhibits hyperosmotic stress response genes in conjunction with Ssn6-Tup1. During osmotic stress Sko1 is phosphorylated, which turns it into a transcriptional activator, recruiting SAGA and SWI/SNF chromatin remodeling complexes to the respective promoter sites. During this activation Tup1 plays an important role for the recruitment of SAGA and SWI/SNF, thus being a vital part of transcriptional activation (Proft and Struhl, 2002). Probably the lack of de-repression/activation of stress response genes in the Δ*fbx15* mutant led to serious defects in stress response, whereas normal growth is not affected.

1.5 Dephosphorylation of Fbx15 is required for nuclear clearance of SsnF

During stress conditions Fbx15 becomes rapidly dephosphorylated, presumably by the essential protein phosphatase 2A catalytic subunit GlcA/BimG (Figure 37). GlcA belongs to the serine/threonine phosphatases and shares homology with the yeast protein phosphatase 1 (PP1) catalytic subunit Glc7 (Winkelströter et al., 2015). *GLC7* is essential for yeast as well, but conditional mutant alleles of *GLC7* could be connected to defects in adaptive functions like temperature tolerance, glucose repression, amino acid starvation, cell morphology and DNA damage repair, which are reminiscent to the growth defects of the Δ*fbx15* mutant on the respective conditions (Andrews and Stark, 2000; Hu et al., 2012; Stark, 1996; Zeska Kress et al., 2012). The dephosphorylation of Fbx15 on Ser468/Ser469 finally led to cytoplasmic accumulation of SsnF, whereas nuclear SsnF was cleared.
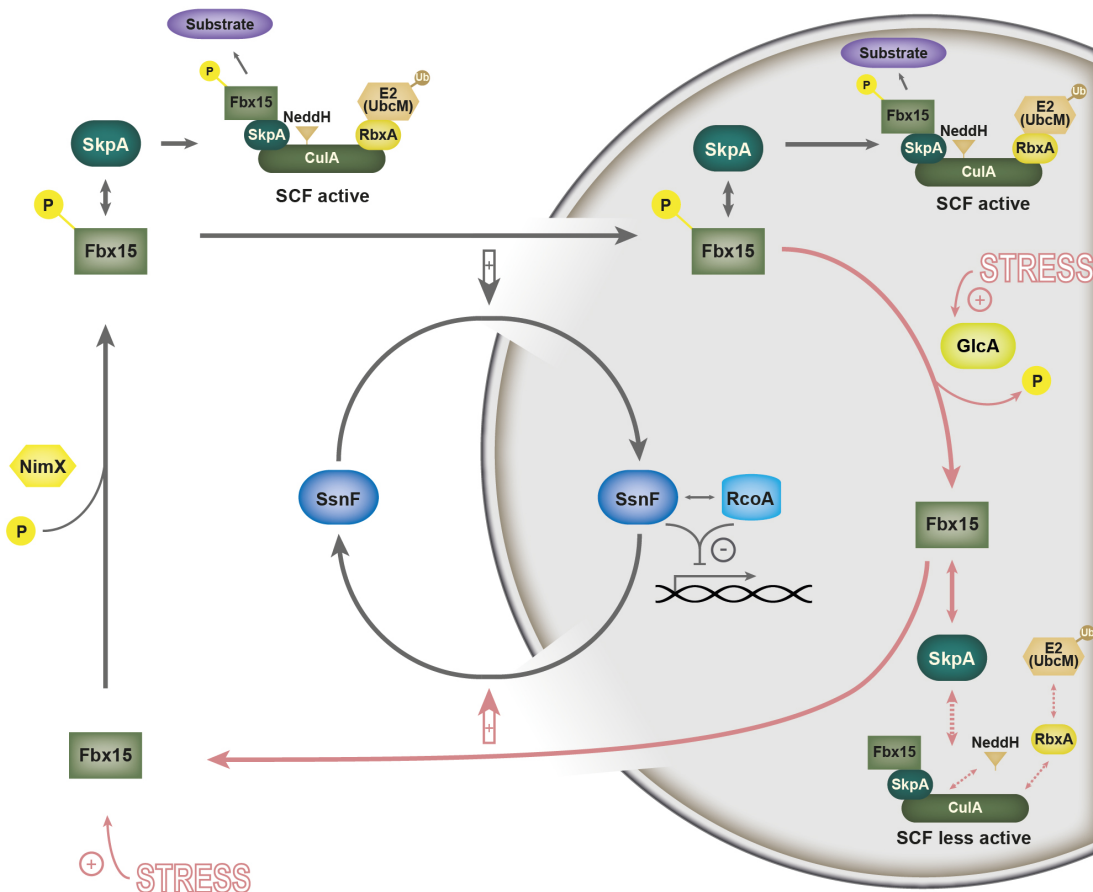
Figure 37: Model for Fbx15 function and localization during vegetative growth and stress response in *A. fumigatus*. During vegetative growth a significant part of Fbx15 is phosphorylated, potentially by the cyclin-dependent kinase NimX. Most of this phosphorylated Fbx15 is transported together with the transcriptional repressor adaptor SsnF into the nucleus. In the nucleus SsnF forms a functional co-repressor complex with a tetramer of RcoA, which interacts with DNA binding proteins for the repression of stress and secondary metabolite target genes. The small fraction of cytoplasmic as well as the larger fraction of nuclear phosphorylated Fbx15 can be integrated into active SCF^{Fbx15} E3 ubiquitin ligases. Grey arrows reflect the situation of phosphorylated Fbx15 under vegetative growth conditions. Fbx15 interacts with the phosphatase GlcA and becomes dephosphorylated and produced in higher levels under stress conditions (red arrows). Dephosphorylated Fbx15 can be integrated into less active nuclear SCF complexes. Dephosphorylated Fbx15 results in less SsnF in the nucleus, which can be caused by a reduced import or an enhanced export of the co-repressor from the nucleus or a combination of both. Reduced nuclear SsnF results in the de-repression of stress response and secondary metabolite genes like *gliP*.

One possibility for the Fbx15-dependent nuclear clearance of SsnF is of course the ubiquitin mediated proteasomal degradation of SsnF. However, SsnF was not found to be ubiquitinated and the overall cellular pool of SsnF appeared to be stable independent of external stress or Fbx15. Therefore, ubiquitin-dependent degradation of SsnF seems un-likely. However, previous studies have shown that some E3 ubiquitin ligases can directly

interact with the regulatory particle of the proteasome and thus are able to transfer target proteins to the proteasome for degradation (Xie and Varshavsky, 2002). A similar scenario could be responsible for selective nuclear degradation of SsnF, where dephosphorylated Fbx15 incorporates into inactive SCF-core complexes, which have the potential to carry specific target substrates such as SsnF directly to the proteasome. This is also supported by the fact that dephosphorylated Fbx15 interacts with SkpA primarily in the nucleus by forming inactive SCF^{Fbx15} core complexes.

Another possibility for the reduction of nuclear SsnF upon external stress might be a reduced nuclear import or an Fbx15-dependent nuclear export mechanism. The data from this work indicates a combination of both mechanisms, since SsnF seemed to be stuck at nuclear pore complexes upon stress, in an Fbx15-dependent manner. In addition, an Fbx15 dependent SsnF-export mechanism might facilitate the rapid nuclear clearance of SsnF, while the cellular pool of SsnF remains stable.

Both phosphorylated and dephosphorylated Fbx15 are able to interact with SsnF. The difference between both phosphorylation states of Fbx15 is the cellular interaction site. Under normal growth conditions the primarily phosphorylated version of Fbx15 seems to interact with SsnF predominantly in the cytoplasm, indicating a cargo function for the nuclear import of SsnF, which is released in the nucleus. Stoichiometric abundances of Fbx15 and SsnF were not balanced after all, especially under non-stress conditions, further arguing against stable Fbx15-SsnF complexes. In addition a potential ubiquitinating function of Fbx15 towards the <u>n</u>uclear <u>p</u>ore <u>c</u>omplex (NPC) subunit Nic96, which was co-purified during our TAP-tag pull-downs, might be a reasonable function for SCF^{Fbx15}-ligase complexes to promote nuclear transport control. Although the localization of SsnF-GFP in $\Delta fbx15$ background and the localization of Nic96-GFP shared some similarities, no Fbx15-specific or stress-dependent changes in the ubiquitination pattern for Nic96 could be observed. However, the nuclear pore complex is a massive multi-protein complex composed of 30 different NPC-proteins, which are arranged in multiples and finally reach a molecular mass between 66 and 125 MDa (Dokudovskaya et al., 2007; Grossman et al., 2012). In 2012 Hayakawa *et al.* showed that approximately half of the NPC-proteins in yeasts are ubiquitinated, but not necessarily targeted for proteasomal degradation (Bailey and Elkan, 1994; Hayakawa et al., 2012). It might be possible that Fbx15 plays a role in NPC-protein ubiquitination, which targets NPC-proteins in close proximity to Npc96 and thereby promotes a more general nuclear transport control.

Under stress conditions Fbx15 expression is induced. In addition stress leads to the dephosphorylation of Fbx15, which then seems to interact with SsnF primarily in the nucleus, finally resulting in reduced SsnF amounts in the nucleus. This could imply a nuclear export function, where Fbx15 acts as a cargo receptor for SsnF (Figure 37).

1.6   The phosphorylation state of Fbx15 might determine its nuclear/cytoplasmic localization

Fbx15 interacts not only with the SsnF adaptor for transcriptional repressors but also with the adaptor protein SkpA, which bridges Fbx15 into SCF E3 ubiquitin ligase complexes. Similar to the interaction with SsnF the interaction between Fbx15 and SkpA was not disturbed due to the dephosphorylation of Fbx15 upon oxidative stress, but rather shifted from the cytoplasm to the nucleus. The identified phosphorylation site of Fbx15, Ser469 with Ser468 as an alternative, putatively redundant phospho-acceptor, is located between both nuclear localization sites (NLS). So, phosphorylation/dephosphorylation events on Fbx15 Ser468/469 might determine nuclear import/export of Fbx15 by rearranging the NLSs rather than protein-binding specificity. The localization pattern of Fbx15 seems to have a major influence on the nuclear localization of SsnF, but disturbed localization patterns of SsnF in constantly unphosphorylated *fbx15* mutants resulted only in an intermediate phenotype. This suggests a second mechanism for Fbx15, which is required for complete stress tolerance in *A. fumigatus*. This is presumably based on the canonical function of Fbx15 as part of an SCF E3 ligase complex. The formation of active SCF^{Fbx15} ligase complexes was promoted in *fbx15* mutants, which mimic a constant phosphorylation, which further suggests an ubiquitinating function of Fbx15-carrying SCF ligases during non-stress conditions. Since Fbx15 abundance under non-stress conditions is very low and overall ubiquitin-patterns of the cellular pool of proteins were not significantly changed between wild type and Δ*fbx15* mutants, the putative target(s) of SCF^{Fbx15} are presumably highly specific.

2   The development – virulence connection in fungi

2.1   Fbx15 bridges a connection between fungal development and virulence

Fbx15 was initially discovered as a developmental regulator in the model organism *A. nidulans*, where the deletion of *fbx15* resulted in a complete block in sexual and asexual development (Zeska Kress et al., 2012). In contrast, the *fbx15* deletion mutant in the opportunistic pathogen *A. fumigatus* did not display a developmental defect, but emerges as key regulator for stress response and virulence. Several virulence factors of *A. fumigatus*, like mycotoxin production, oxidative stress resistance and nutritional versatility are linked to developmental control mechanisms, which were identified in the closely related non-pathogenic *A. nidulans*. An example is the fungal-specific velvet protein VeA, which acts as a light dependent negative regulator for asexual development in *A. nidulans* (Bayram et al., 2008; Terfrüchte et al., 2014). Contrastingly deletion of *veA* in *A. fumigatus* does not exhibit a light dependent regulation of development and affected asexual sporulation only under specific growth conditions. Instead VeA acts as a positive regulator for secondary metabolite production (Dhingra et al., 2012; 2013; Krappmann et al., 2005).

Another example is the recently identified VeA-dependent transcription factor MtfA, which is required for asexual and sexual development in *A. nidulans* and further controls the production of several secondary metabolites (Ramamoorthy et al., 2013). In contrast, a deletion mutant of its counterpart in *A. fumigatus* has a minor effect on asexual development and secondary metabolite production, but showed an attenuated virulence in a Galleria model of infection (Smith and Calvo, 2014). A stress factor *A. fumigatus* has to cope with, either if it grows on decaying organics like compost or in the human host, is oxidative stress due to reactive oxygen species (ROS), which are caused by environmental conditions or human immune cells. *A. fumigatus* has a huge arsenal of antioxidant enzymes such as catalases and superoxide dimutases, which have been shown to be dispensable for virulence (Lambou et al., 2010; Paris et al., 2003b). However, another antioxidant mechanism, the thioredoxin redox regulation pathway, based on thioredoxin A (TrxA) and a thioredoxin reductase (TrxR), has been shown to play an essential role in asexual and sexual development in *A. nidulans* (Thön et al., 2007). In contrast the deletion of the *trxA* homolog *aspf29* in *A. fumigatus* did not result in any obvious developmental defects. However, *A. fumigatus* possesses five putative

thioredoxins and a functional block of these led to a drastic reduction of hyphal survival in the presence of neutrophils (Leal et al., 2012).

Together with the results of this work these phenomena emphasize a connection between developmental regulators of non-pathogenic fungi and their role for virulence in fungal pathogens. Therefore, a closer look at the functions of conserved developmental regulators such as the recently discovered chitin synthases CHS-7 and ChsA with crucial roles for development in *N. crassa* and *A. nidulans* respectively (Fajardo-Somera et al., 2015), might unravel new so far unknown virulence determinants in fungal pathogens.

2.2   Fbx15-dependent regulation of VeA

VeA is a fungal specific key regulatory protein, which coordinates development and secondary metabolism in response to light. VeA belongs to the velvet family of proteins that were thoroughly studied in the model organism *A. nidulans* (Bayram and Braus, 2012). VeA bridges another velvet protein VelB and the global regulator of secondary metabolism LaeA as part of the heterotrimeric velvet complex, which promotes sexual development and secondary metabolism during darkness in *A. nidulans* (Bayram et al., 2008). While sexual development is initiated in darkness, VelB also forms an additional heterodimeric complex with the velvet protein VosA that inhibits asexual propagation (Figure 38) (Sarikaya Bayram et al., 2010). Velvet counterparts in a variety of fungi have been described with regulatory functions for development, hyphal morphology, secondary metabolism and virulence (Bayram and Braus, 2012; Beyhan et al., 2013; Calvo, 2008; López-Berges et al., 2013). Although the regulatory mechanisms, driven by the velvet family proteins share huge amount of similarity between different fungal species, they also have distinct roles during their respective developmental pathways (Calvo, 2008). Whereas the velvet proteins VeA, VelB and VosA are essential for sexual development and the repression of conidiation in *A. nidulans* during darkness their counterparts in *A. fumigatus* are required to maintain vegetative growth, while asexual development is downregulated (Figure 38) (Park et al., 2012).
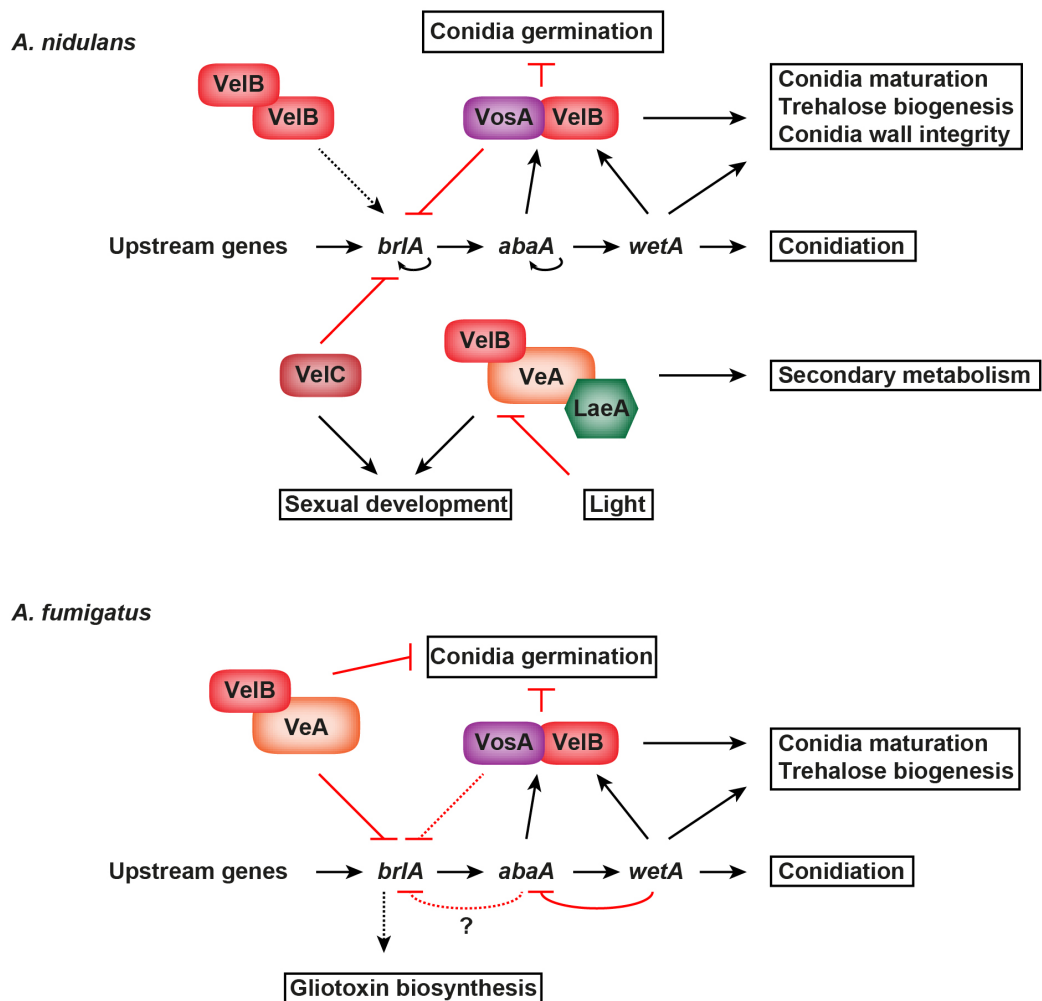
Figure 38: Velvet regulated control of development in *A. nidulans* and *A. fumigatus*. In *A. nidulans* the central velvet regulator VeA is primarily involved in the promotion of sexual development and secondary metabolism as part of heterodimeric (VeA-VelB) or heterotrimeric (VeA-VelB-LaeA) complexes, which are repressed by light. This is supported by VelC, which also suppresses asexual development by inhibiting expression of *brlA*. VelB can also form homodimers that promote asexual development, whereas VelB-VosA heterodimers inhibit asexual development and thus conferring feedback regulation of *brlA* expression. In contrast the velvet regulators in *A. fumigatus* are primarily involved in maintaining normal vegetative growth, while asexual development is downregulated. Modified after Park et al., 2012.

Although this study did not reveal a direct control mechanism of Fbx15 towards regulatory proteins of the velvet family since they were not found for Fbx15 co-purifications, there is some evidence that there might be an interdependent connection. Fbx15 of *A. nidulans* was described with a crucial role for both developmental pathways as well as for secondary metabolism (Zeska Kress et al., 2012). This resembles to some extant the phenotypic characteristics of *veA* mutant strains, which were impaired in sexual development and the production of the mycotoxin sterigmatocystin (Gerke and Braus, 2014; Kato

et al., 2003; Kim et al., 2002). This work has shown that Fbx15 in *A. fumigatus* is specifically required for oxidative stress response, gliotoxin production and virulence, whereas Fbx15 is dispensable for normal growth. Similar, Δ*veA* mutants of *A. fumigatus* showed normal growth under standard conditions but impaired gliotoxin production levels, though they were lower than in the wild type. However oxidative stress response or virulence was not influenced by the loss of *veA*, suggesting a broad range of Fbx15 controlled downstream targets, including VeA.

A direct hint of a possible Fbx15 controlled regulation of VeA comes from *A. nidulans*, where it has been shown that the Tup1 counterpart RcoA is required for both developmental pathways as well as for the production of secondary metabolites (Hicks et al., 2001). It was further shown that multicopy integration of *rcoA* into a *veA1* background strain, which is characterized by reduced sexual development, could restore the *veA*⁺ (wild type) phenotype with normal sexual and asexual development. In contrast different expression levels of *veA* in a Δ*rcoA* background were not able to rescue the mutant from impaired sexual development, indicating that *veA* is a downstream target of RcoA (Todd et al., 2006b).

The RcoA interacting protein SsnF is controlled by Fbx15. Therefore, a misregulated, RcoA mediated transcriptional repression in the Δ*fbx15* mutant might affect the transcriptional profile of *veA*, which is particularly upregulated during developmental pathways.

3   Fungal F-box proteins and virulence in fungi

3.1   Fbx15 is a true virulence factor

Virulence factors of pathogenic microorganisms are characterized by their potential to contribute to virulence without affecting the normal lifestyle. It has been argued, whether *A. fumigatus* possesses unique virulence factors, as they are described for professional pathogens like pathogenic *Yersinia* spp. (Cornelis, 2002; Reuter et al., 2012) or if the pathogenicity of *A. fumigatus* is just the result of its evolutionary background as a saprophyte. Several mechanisms, which enable *A. fumigatus* to colonize its natural habitat like heat tolerance, extracellular proteases, secondary metabolite production or oxidative stress resistance, are thought to be virulence determinants, but deletion of specific genes involved in these mechanisms often had only minor or no effect on pathogenicity

(Karkowska-Kuleta et al., 2009; Latgé, 2001; Rhodes, 2006; Tomee and Kauffman, 2000). Therefore, it was already suggested to focus more on the host instead of the pathogen in order to understand the pathogenicity of *A. fumigatus* (Tekaia and Latgé, 2005).

However, the fact that single gene deletions not necessarily result in mutant strains with reduced pathogenicity might not reflect that the mechanism where these particular genes are involved in, is not part of the virulence determination. A good example is the resistance to oxidative stress, which is considered to protect *A. fumigatus* from innate immune responses of macrophages and neutrophils, which are characterized by the excessive production of ROS (Braem et al., 2015; Cramer et al., 2011; Leal et al., 2012). The deletion of either conidial or mycelial catalases resulted in similar phenotypes as for the wild type, when incubated with murine alveolar macrophages, leading to the assumption that oxidative stress defense might be dispensable for pathogenicity (Dagenais and Keller, 2009; Paris et al., 2003b). But in fact *A. fumigatus* incorporates a multitude of oxidative stress resistance mechanisms, ranging from catalases, superoxide dismutases and peroxidases to more distant mechanisms like the rodlet layer of conidia and secondary metabolites such as melanins and gliotoxin, which might be sufficient to bypass a single defect (Brandon et al., 2015). Therefore, it is reasonable that the lack one specific enzyme might not necessarily result in a strain with reduced virulence, although the general oxidative stress resistance of *A. fumigatus* still contributes to its pathogenicity.

Oxidative stress response is only one of several mechanisms, which are thought to contribute to the virulence of *A. fumigatus*. With Fbx15 a true virulence factor was identified, which plays a crucial role for multiple stress response mechanisms involved in pathogenicity. Remarkably, Fbx15 is not required for normal growth, which is characteristic for true virulence factors. Interestingly, the deletion of *fbx15* led to increased amounts of the immunocompromising mycotoxin gliotoxin, which is also considered as a virulence factor. However, deletion mutants in the gliotoxin biosynthetic pathway did not exhibit a consistent phenotype in terms of pathogenicity. Whereas some groups claim that loss of gliotoxin biosynthesis led to reduced pathogenicity in a mouse model of aspergillosis, others demonstrated that gliotoxin has no effect on virulence (Bok et al., 2006; Kupfahl et al., 2006). The results from this work endorse the assumption that gliotoxin plays a minor role for host colonization, whereas multiple stress response pathways under the control of Fbx15 are sufficient for pathogenicity.

3.2   Fungal F-box proteins have a diverse role in pathogenicity

Most fungal F-box proteins, which have been studied today, were described initially in
S. cerevisiae and a substantial part of our current knowledge of SCF-functionality derives
from studies in the baker's yeast. The genome of *S. cerevisiae* encodes 22 F-box proteins
with Cdc4 and Grr1 as the best characterized so far. SCF^{Cdc4} ligases for instance have
been accounted for the turnover of several target proteins, which are involved in various
processes like cell-cycle control, morphology, nutrient- and calcium-sensing and thereby
emphasize the vast diversity of molecular mechanisms, which can be connected to a sin-
gle F-box protein (Table 7) (Finley et al., 2012; Jonkers and Rep, 2009). However, these
mechanisms are only partially conserved between fungal species. An SCF^{Cdc4} target pro-
tein, which is required for pseudohyphal growth in *S. cerevisiae* is the transcription factor
Tec1 (Chou et al., 2004). The Cdc4 homolog in the human pathogenic yeast *Candida
albicans* is also involved in a switch from yeast-like to hyphal growth, which is required
for pathogenicity. But in contrast to baker's yeast no elevated Tec1 levels were observed
in Δ*cdc4* mutants of *C. albicans* (Atir-Lande et al., 2005; Chin et al., 2013).

Only few studies have been made for F-box proteins in filamentous fungi and most of
them concentrate on homologs of Grr1 from yeast, which is responsible for a variety of
cellular functions like cell-cycle regulation, morphology, amino-acid sensing and the con-
trol of glucose repression (Benanti et al., 2007; Finley et al., 2012; Guo et al., 2015; Skaar
et al., 2009). Similar to the deletion of *GRR1* in *S. cerevisiae*, which leads to a stabiliza-
tion of G1 cyclins Cln1 and Cln2, resulting in continuous pseudohyphal growth (Flick
and Johnston, 1991; Kishi and Yamao, 1998; Loeb et al., 1999), the deletion of *GRR1* in
C. albicans results in the stabilization of G1 cyclins Ccn1 and Cln3 and thus triggers a
constitutive pseudohyphal growth (Butler et al., 2006; Li et al., 2006). The Grr1 counter-
part in the pathogenic yeast *Cryptococcus neoformans*, Fbp1, was shown to be essential
for sexual development as well, but also plays a crucial role for pathogenicity. But in con-
trast to the yeasts *S. cerevisiae* and *C. albicans*, *C. neoformans* Δ*fbp1* mutants showed a
specific sensitivity against cell-membrane stress, whereas glucose sensing and carbon
catabolite repression was not influenced (Liu et al., 2011).

Table 7: F-box proteins in fungal pathogens. Fungal F-box proteins and their homologs with a verified or proposed role for pathogenicity. Most studies were carried out on homologous proteins of *S. cerevisiae* Cdc4 and Grr1, which are also included. Homologous proteins to Fbx15 of *A. fumigatus* were identified by NCBI-BLAST search and display similarities to Fbx15 of 24-32%, similar to Fbx15 homolog in *N. crassa* (see also Table 5).

	fungal species	F-box proteins and their homologs in fungal pathogens (F-box directed functions are indicated in brackets)			
Yeast Model	*S. cerevisiae*	**Cdc4**	**Grr1**	NP	NP
Human Pathogens	*C. albicans*	**Cdc4** (pseudohyphal growth)	**Grr1** (pseudohyphal growth)	NP	NP
	C. neo-formans	CNAG_00693 (NA)	**Fbp1** (virulence, development & cell membrane stress)	NP	NP
	A. fumigatus	Afu6g13030 (NA)	**GrrA** (slightly impaired stress response, no effect on virulence)	**Fbx15** (stress response & virulence)	NP
Plant Pathogens	*F. gramine-arum*	FG02237 (NA)	**Fbp1** (development & virulence)	FG10047 (NA)	**Frp1** (development, slightly impaired in CCR & virulence)
	F. oxysporum	FOXG_03818 (NA)	**Fbp1** (invasive growth & virulence)	FOXG_05359 (NA)	**Frp1** (CCR & virulence)
	B. cinerea	Bcin08g06680 (NA)	Bcin10g01220.1 (NA)	Bcin14g02740 (NA)	**Frp1** (development, dispensable for CCR & virulence)
	M. oryzae	MGG_08345 (NA)	**MoGrr1** (development, stress response & virulence)	MGG_00768 (NA)	MGG_06351 (NA)

NP: not present; NA: not analyzed; CCR: carbon catabolite expression

The Grr1 homolog in *A. nidulans*, GrrA, was shown to have a specific role during meiosis, since Δ*grrA* mutants were blocked at the last step of ascospore formation during sexual development but otherwise resemble the wild-type phenotype (Krappmann et al., 2006a). Although *grrA* is able to complement the Δ*grr1* phenotype in yeast, both Grr1 homologs have distinct functions within their species, for the reason that *S. cerevisiae* Δ*grr1* mutants are still able to form asci with mature ascospores (Purnapatre et al., 2005). GrrA shares similar functionalities with Fbp1, the Grr1 homolog of the plant pathogenic fungi *Fusarium graminearum* and *Fusarium oxysporum*. The deletion of *FBP1* led to a loss of virulence for both fungi (Han et al., 2007; Miguel-Rojas and Hera, 2013; 2016). Like Δ*grrA* mutants of *A. nidulans* loss of *FBP1* in *F. graminearum*, which also is a homothallic fungus, results in a loss of sexual reproduction. However, Δ*fbp1* mutants of *F. graminearum* were not able to produce any fruiting bodies thus displaying a more drastic effect on sexual development. Another characteristic, which distinguishes Fbp1 from its counterparts in yeast and *A. nidulans*, is the fact that *FBP1* of *F. graminearum* can only partially complement the Δ*grr1* phenotype in *S. cerevisiae*. Although defects in the glucose repression system as well as in the suppression of pseudohyphal growth could be restored, the sporulation defects were not complemented by heterologous expression of *FBP1* in *S. cerevisiae* Δ*grr1* mutants (Han et al., 2007). More recently also the Grr1 equivalent of *Magnaporthe oryzae*, another plant pathogenic fungus, which causes rice blast disease has been characterized as MoGrr1 with essential roles for asexual development, oxidative stress response and pathogenicity (Guo et al., 2015).

These examples present the importance of Grr1 homologs for virulence of a variety of pathogenic fungi. However, the function of Grr1 seems only partially to be conserved between fungal species. During this work it has been shown that the Grr1 homolog of *A. fumigatus*, GrrA, has only minor effects on external stresses and is not required for virulence in a mouse model of invasive pulmonary aspergillosis. These results further indicate that conserved fungal F-box proteins do not necessarily resemble the same functionality for different species. This is further corroborated by a study on the filamentous fungi specific F-box protein Frp1 in different plant pathogenic fungi. Whereas the deletion of *FRP1* in *Fusarium oxysporum* led to a loss of pathogenicity, *F. graminearum* Δ*frp1* mutants were only impaired during root infection, but no negative effect on infection capabilities of *Botrytis cinerea* could be observed (Duyvesteijn et al., 2005; Jonkers et al., 2011). Thus it might be worth to examine the distinct functions of F-box proteins in

different pathogenic fungi in order to identify new mechanisms, which are connected to virulence.

3.3 Fbx15 as potential antifungal drug target

Fbx15 in *A. fumigatus* is a unique F-box protein, specific to filamentous fungi. It is especially conserved in Aspergilli, whereas other filamentous fungi share only distant evolutionary relationship (Figure 39). This might provide opportunity for future drug design against *A. fumigatus* infections by targeting fungal specific Fbx15. Although novel antifungal agents are improving the chances of recovery for infected patients, the treatment of invasive aspergillosis is still based on aggressive antifungal drugs, which are also toxic to eukaryotic host cells (Denning, 1998; Kuiper and Ruijgrok, 2009; Lamoth et al., 2016). This disadvantage is aggravated by the fact that an increasing number of *A. fumigatus* species were found to be resistant against the commonly used medical triazoles (Cramer, 2016; Smith and Kauffman, 2012; Snelders et al., 2009). Due to the fungal specificity of Fbx15, this F-box protein might be a potential drug target, excluding the risk of cross-reactions with human proteins. In contrast to novel drugs, which target the general ubiquitin proteasomal degradation machinery by inhibiting their core components, such as Nedd8-activating enzyme, the SCF-adaptor SkpA or the proteasome, and thus providing therapeutic chances for cancer, neurodegenerative diseases and immune deficiencies, a drug against Fbx15 would not affect the ubiquitin-proteasome system itself, but instead offer a highly specific inhibitor for fungal dissemination during life threatening aspergillosis (Mandel et al., 2012; Schwartz and Ciechanover, 2009; Soucy et al., 2009). Furthermore Fbx15 bears the potential to identify new virulence determining factors, which can be used for advanced drug design. The results from the tandem affinity purification of Fbx15 provide a good basis for the identification of new virulence traits in *A. fumigatus*.
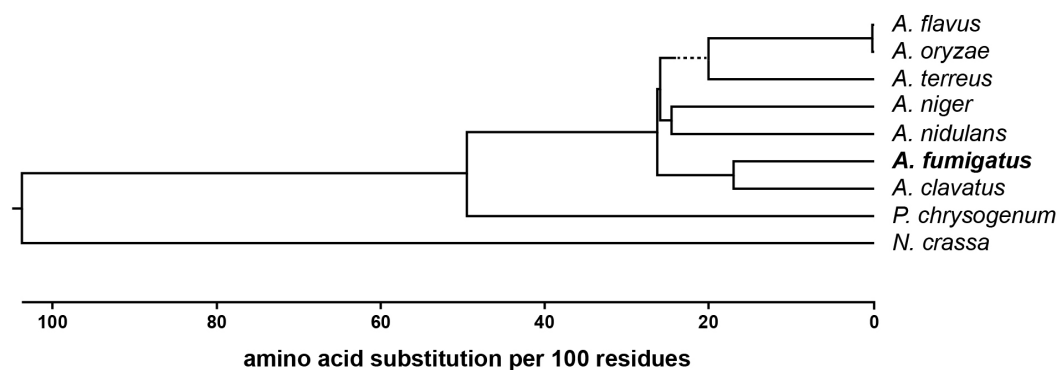
Figure 39: Phylogenetic tree of Fbx15 homologs from different filamentous fungi.
Evolutionary relationships between Fbx15 homologs of different filamentous fungi were
calculated by multiple sequence alignment of their amino acid sequences with ClustalW
(see also Figure 6B and Table 5). The length between each pair of branches represents the
distance between pairs. The dotted line indicates a negative branch length. Fbx15 is high-
ly conserved among Aspergilli, whereas it shows only distant relationship with Fbx15
homologs of other filamentous fungi.

4   Outlook and Conclusion

The results from this work indicate a dual function for Fbx15 in *A. fumigatus*, which is on
one hand required for transcriptional regulation through the localization control of the
transcriptional co-repressor subunit SsnF but also interacts within SCF E3 ligase
complexes. However, it remains unclear whether these mechanisms are connected to each
other. The fact that *A. fumigatus* Fbx15 phosphomutants, which prohibit the nuclear entry
of SsnF, are only partially impaired in oxidative stress tolerance suggests an additional
role of Fbx15, presumably as part of ubiquitinating SCF^{Fbx15} complexes. It would be
interesting to follow up the results from the tandem affinity purifications, to see whether
Fbx15 has an ubiquitinating role for any of the potential candidates. This would not only
provide a better picture for the molecular mechanisms behind Fbx15 mediated stress
tolerance, but might in addition reveal new insights into general fungal stress responses,
since most of the candidates have not been characterized so far.

The effect of Fbx15 towards transcriptional repression has been demonstrated by the
increased expression of *gliP* in the Δ*fbx15* mutant. This is presumably the result of the
cytoplasmic accumulation of SsnF. Ssn6-Tup1 mediated repression affects almost 3% of
the genes in *S. cerevisiae* with implications for development, nutrient sensing and stress
response. The comparison of whole cell RNA transcript levels between wild type, Δ*fbx15*
mutant and a strain with *ssnF* under a switchable promoter, since *ssnF* is essential, would

allow to determine the direct influence of Fbx15 on transcriptional repression though its interaction with SsnF. This might also provide new insights towards secondary metabolism control, which is severely impaired in the Δ*fbx15* mutant. Moreover several new, so far uncharacterized stress response and virulence factors as well as developmental regulators could be unraveled by the identification of Fbx15-SsnF controlled genes.

The dual function of Fbx15 plays an essential role for virulence of *A. fumigatus* in a mouse model of invasive pulmonary aspergillosis. A preliminary test with polyclonal antibodies against Fbx15 revealed the potential of Fbx15 as antifungal drug target. However, it has to be shown whether these antibodies really have the potential to interact with the intracellular Fbx15 and thus might lead to an accumulation of Fbx15 or the block of specific binding sites. The antifungal potential during infection of this antibody could be further analyzed by treatment of immunocompromised mice, which were infected with *A. fumigatus* wild-type conidia. Another possibility to produce an antifungal drug that targets *A. fumigatus* Fbx15 would be the screening of purified Fbx15 against a library of small peptides for possible interactions with Fbx15. Small peptides have several advantages in comparison to antibodies. They are very small with a molecular mass below 10 kDa, which allows a more efficient distribution. In addition they are easily synthesized and bear the potential to be rapidly modified to ensure high specificity.

Taken together, with this work Fbx15 was identified as a crucial regulator for stress response and virulence in *A. fumigatus*. By targeting the nuclear import of the transcriptional co-repressor SsnF upon oxidative stress, Fbx15 links oxidative stress response to a global transcriptional regulation on chromatin level. Furthermore, Fbx15 provides a promising target for drug development, since it is a fungal specific protein distinct from the otherwise highly conserved components of the SCF E3 ligase machinery.

References

Abad, A., Fernández-Molina, J.V., Bikandi, J., Ramírez, A., Margareto, J., Sendino, J., Hernando, F.L., Pontón, J., Garaizar, J., and Rementeria, A. (2010). What makes *Aspergillus fumigatus* a successful pathogen? Genes and molecules involved in invasive aspergillosis. **Rev Iberoam Micol** *27*, 155–182.

Adav, S.S., Ravindran, A., and Sze, S.K. (2015). Quantitative proteomic study of *Aspergillus fumigatus* secretome revealed deamidation of secretory enzymes. **J Proteomics** *119*, 154–168.

Agarwal, R., Chakrabarti, A., Shah, A., Gupta, D., Meis, J.F., Guleria, R., Moss, R., Denning, D.W., ABPA complicating asthma ISHAM working group (2013). Allergic bronchopulmonary aspergillosis: Review of literature and proposal of new diagnostic and classification criteria. **Clin Exp Allergy** *43*, 850–873.

Agoston, Z., and Schulte, D. (2009). Meis2 competes with the Groucho co-repressor Tle4 for binding to Otx2 and specifies tectal fate without induction of a secondary midbrain-hindbrain boundary organizer. **Development** *136*, 3311–3322.

Aguirre, J., Ríos-Momberg, M., Hewitt, D., and Hansberg, W. (2005). Reactive oxygen species and development in microbial eukaryotes. **Trends Microbiol** *13*, 111–118.

Aimanianda, V., Bayry, J., Bozza, S., Kniemeyer, O., Perruccio, K., Elluru, S.R., Clavaud, C., Paris, S., Brakhage, A.A., Kaveri, S.V., et al. (2009). Surface hydrophobin prevents immune recognition of airborne fungal spores. **Nature** *460*, 1117–1121.

Alkhayyat, F., Chang Kim, S., and Yu, J.-H. (2015). Genetic control of asexual development in *Aspergillus fumigatus*. **Adv Appl Microbiol** *90*, 93–107.

Amarsaikhan, N., and Templeton, S.P. (2015). Co-recognition of β-glucan and chitin and programming of adaptive immunity to *Aspergillus fumigatus*. **Front Microbiol** *6*, 344.

Amich, J., Dümig, M., O'Keeffe, G., Binder, J., Doyle, S., Beilhack, A., and Krappmann, S. (2016). Exploring sulfur assimilation of *Aspergillus fumigatus* reveals biosynthesis of sulfur-containing amino acids as a virulence determinant. **Infect Immun**, IAI.01124-15.

Andrews, P.D., and Stark, M.J. (2000). Type 1 protein phosphatase is required for maintenance of cell wall integrity, morphogenesis and cell cycle progression in *Saccharomyces cerevisiae*. **J Cell Sci** *113*, 507–520.

Araujo, R., and Rodrigues, A.G. (2004). Variability of germinative potential among pathogenic species of *Aspergillus*. **J Clin Microbiol** *42*, 4335–4337.

Aravind, L., and Koonin, E.V. (2000). The U box is a modified RING finger - a common domain in ubiquitination. **Curr Biol** *10*, R132–R134.

Ardley, H.C., and Robinson, P.A. (2005). E3 ubiquitin ligases. **Essays Biochem** *41*, 15–30.

Asada, R., Takemata, N., Hoffman, C.S., Ohta, K., and Hirota, K. (2015). Antagonistic controls of chromatin and mRNA start site selection by Tup family corepressors and the CCAAT-binding factor. **Mol Cell Biol** *35*, 847–855.

Ashida, H., Kim, M., and Sasakawa, C. (2014). Exploitation of the host ubiquitin system by human bacterial pathogens. **Nat Rev Microbiol** *12*, 399–413.

Atir-Lande, A., Gildor, T., and Kornitzer, D. (2005). Role for the SCF^{CDC4} ubiquitin ligase in *Candida albicans* morphogenesis. **Mol Biol Cell** *16*, 2772–2785.

Bai, C., Sen, P., Hofmann, K., Ma, L., Goebl, M., Harper, J.W., and Elledge, S.J. (1996). *SKP1* connects cell cycle regulators to the ubiquitin proteolysis machinery through a novel motif, the F-Box. **Cell** *86*, 263–274.

Bailey, T.L., and Elkan, C. (1994). Fitting a mixture model by expectation maximization to discover motifs in biopolymers. **Proc Int Conf Intell Syst Mol Biol** *2*, 28–36.

Barbash, O., Lee, E.K., and Diehl, J.A. (2011). Phosphorylation-dependent regulation of SCF^{Fbx4} dimerization and activity involves a novel component, 14-3-3ε. **Oncogene** *30*, 1995–2002.

Bayram, Ö., and Braus, G.H. (2012). Coordination of secondary metabolism and development in fungi: the velvet family of regulatory proteins. **FEMS Microbiol Rev** *36*, 1–24.

Bayram, Ö., Bayram, Ö.S., Valerius, O., Jöhnk, B., and Braus, G.H. (2012). Identification of protein complexes from filamentous fungi with tandem affinity purification. **Humana Press** *944*, 191–205.

Bayram, Ö., Feussner, K., Dumkow, M., Herrfurth, C., Feussner, I., and Braus, G.H. (2016). Changes of global gene expression and secondary metabolite accumulation during light-dependent *Aspergillus nidulans* development. **Fungal Genet Biol** *87*, 30–53.

Bayram, Ö., Krappmann, S., Ni, M., Bok, J.W., Helmstaedt, K., Valerius, O., Braus-Stromeyer, S., Kwon, N.-J., Keller, N.P., Yu, J.-H., et al. (2008). VelB/VeA/LaeA complex coordinates light signal with fungal development and secondary metabolism. **Science** *320*, 1504–1506.

Bayry, J., Aimanianda, V., Guijarro, J.I., Sunde, M., and Latgé, J.-P. (2012). Hydrophobins - unique fungal proteins. **PLoS Pathog** *8*, e1002700.

Beckmann, E.A., Köhler, A.M., Meister, C., Christmann, M., Draht, O.W., Rakebrandt, N., Valerius, O., and Braus, G.H. (2015). Integration of the catalytic subunit activates deneddylase activity *in vivo* as final step in fungal COP9 signalosome assembly. **Mol Microbiol** *97*, 110–124.

Beever, R.E., and Dempsey, G.P. (1978). Function of rodlets on the surface of fungal spores. **Nature** *272*, 608–610.

Benanti, J.A., Cheung, S.K., Brady, M.C., and Toczyski, D.P. (2007). A proteomic screen reveals SCF^{Grr1} targets that regulate the glycolytic-gluconeogenic switch. **Nat Cell Biol** *9*, 1184–1191.

Beyhan, S., Gutierrez, M., Voorhies, M., and Sil, A. (2013). A temperature-responsive network links cell shape and virulence traits in a primary fungal pathogen. **PLoS Biol** *11*, e1001614.

Bhabhra, R., and Askew, D.S. (2005). Thermotolerance and virulence of *Aspergillus fumigatus*: role of the fungal nucleolus. **Med Mycol** *43 Suppl 1*, S87–S93.

Bhattacharyya, S., Yu, H., Mim, C., and Matouschek, A. (2014). Regulated protein turnover: snapshots of the proteasome in action. **Nat Rev Mol Cell Biol** *15*, 122–133.

Blom, N., Gammeltoft, S., and Brunak, S. (1999). Sequence and structure-based prediction of eukaryotic protein phosphorylation sites. **J Mol Biol** *294*, 1351–1362.

Bohlin, C., Praestgaard, E., Baumann, M.J., Borch, K., Praestgaard, J., Monrad, R.N., and Westh, P. (2013). A comparative study of hydrolysis and transglycosylation activities of fungal β-glucosidases. **Appl Microbiol Biotechnol** *97*, 159–169.

Bok, J.W., Balajee, S.A., Marr, K.A., Andes, D., Nielsen, K.F., Frisvad, J.C., and Keller, N.P. (2005). LaeA, a regulator of morphogenetic fungal virulence factors. **Eukaryot Cell** *4*, 1574–1582.

Bok, J.W., Chung, D., Balajee, S.A., Marr, K.A., Andes, D., Nielsen, K.F., Frisvad, J.C., Kirby, K.A., and Keller, N.P. (2006). GliZ, a transcriptional regulator of gliotoxin biosynthesis, contributes to *Aspergillus fumigatus* virulence. **Infect Immun** *74*, 6761–6768.

Borgia, P.T. (1992). Roles of the *orlA*, *tsE*, and *bimG* genes of *Aspergillus nidulans* in chitin synthesis. **J Bacteriol** *174*, 384–389.

Bosu, D.R., and Kipreos, E.T. (2008). Cullin-RING ubiquitin ligases: global regulation and activation cycles. **Cell Div** *3*, 7.

Bradford, M.M. (1976). A rapid and sensitive method for the quantitation of microgram quantities of protein utilizing the principle of protein-dye binding. **Anal Biochem** *72*, 248–254.

Braem, S.G.E., Rooijakkers, S.H.M., van Kessel, K.P.M., de Cock, H., Wösten, H.A.B., van Strijp, J.A.G., and Haas, P.-J.A. (2015). Effective neutrophil phagocytosis of *Aspergillus fumigatus* is mediated by classical pathway complement activation. **J Innate Immun** *7*, 364–374.

Brakhage, A.A., and Langfelder, K. (2002). Menacing Mold: the molecular biology of *Aspergillus fumigatus*. **Annu Rev Microbiol** *56*, 433–455.

Brandon, M., Howard, B., Lawrence, C., and Laubenbacher, R. (2015). Iron acquisition and oxidative stress response in *Aspergillus fumigatus*. **BMC Syst Biol** *9*, 19.

Braus, G.H., Sasse, C., and Krappmann, S. (2006). Amino acid acquisition, cross-pathway control, and virulence in *Aspergillus*. **Med Mycol** *44*, 91–94.

Braus, G.H., Irniger, S., and Bayram, Ö. (2010). Fungal development and the COP9 signalosome. **Curr Opin Microbiol** *13*, 672–676.

Bruneau, J.M., Magnin, T., Tagat, E., Legrand, R., Bernard, M., Diaquin, M., Fudali, C., and Latgé, J.P. (2001). Proteome analysis of *Aspergillus fumigatus* identifies glyco-sylphosphatidylinositol-anchored proteins associated to the cell wall biosynthesis. **Electrophoresis** *22*, 2812–2823.

Brunson, L.E., Dixon, C., Kozubowski, L., and Mathias, N. (2004). The amino-terminal portion of the F-Box protein Met30p mediates its nuclear import and assimilation into an SCF complex. **J Biol Chem** *279*, 6674–6682.

Brzywczy, J., Kacprzak, M.M., and Paszewski, A. (2011). Novel mutations reveal two important regions in *Aspergillus nidulans* transcriptional activator MetR. **Fungal Genet Biol** *48*, 104–112.

Busch, S., Eckert, S.E., Krappmann, S., and Braus, G.H. (2003). The COP9 signalosome is an essential regulator of development in the filamentous fungus *Aspergillus nidulans*. **Mol Microbiol** *49*, 717–730.

Busch, S., Schwier, E.U., Nahlik, K., Bayram, O., Helmstaedt, K., Draht, O.W., Krapp-mann, S., Valerius, O., Lipscomb, W.N., and Braus, G.H. (2007). An eight-subunit COP9 signalosome with an intact JAMM motif is required for fungal fruit body formation. **Proc Natl Acad Sci USA** *104*, 8089–8094.

Butler, D.K., All, O., Goffena, J., Loveless, T., Wilson, T., and Toenjes, K.A. (2006). The *GRR1* gene of *Candida albicans* is involved in the negative control of pseudohyphal morphogenesis. **Fungal Genet Biol** *43*, 573–582.

Calvo, A.M. (2008). The VeA regulatory system and its role in morphological and chemical development in fungi. **Fungal Genet Biol** *45*, 1053–1061.

Cardozo, T., and Pagano, M. (2004). The SCF ubiquitin ligase: Insights into a molecular machine. **Nat Rev Mol Cell Biol** *5*, 739–751.

Casadevall, A., and Pirofski, L.-A. (2007). Antibody-mediated protection through cross-reactivity introduces a fungal heresy into immunological dogma. **Infect Immun** *75*, 5074–5078.

Chandrasekaran, S., and Skowyra, D. (2008). The emerging regulatory potential of SCF^{Met30}-mediated polyubiquitination and proteolysis of the Met4 transcriptional activator. **Cell Div** *3*, 11.

Chang, Y.C., Tsai, H.-F., Karos, M., and Kwon-Chung, K.J. (2004). *THTA*, a thermotolerance gene of *Aspergillus fumigatus*. **Fungal Genet Biol** *41*, 888–896.

Chaturvedi, A.K., Kavishwar, A., Shiva Keshava, G.B., and Shukla, P.K. (2005). Monoclonal immunoglobulin G1 directed against *Aspergillus fumigatus* cell wall glycoprotein protects against experimental murine aspergillosis. **Clin Diagn Lab Immunol** *12*, 1063–1068.

Chauhan, N., Latgé, J.-P., and Calderone, R. (2006). Signalling and oxidant adaptation in *Candida albicans* and *Aspergillus fumigatus*. **Nat Rev Microbiol** *4*, 435–444.

Chen, G., and Courey, A.J. (2000). Groucho/TLE family proteins and transcriptional repression. **Gene** *249*, 1–16.

Chen, Z.J., and Sun, L.J. (2009). Nonproteolytic functions of ubiquitin in cell signaling. **Molecular Cell** *33*, 275–286.

Chin, C., Lai, W.-C., Lee, T.-L., Tseng, T.-L., and Shieh, J.-C. (2013). Dissection of the *Candida albicans* Cdc4 protein reveals the involvement of domains in morphogenesis and cell flocculation. **J Biomed Sci** *20*, 97.

Choo, Y.Y., Boh, B.K., Lou, J.J.W., Eng, J., Leck, Y.C., Anders, B., Smith, P.G., and Hagen, T. (2011). Characterization of the role of COP9 signalosome in regulating cullin E3 ubiquitin ligase activity. **Mol Biol Cell** *22*, 4706–4715.

Chou, S., Huang, L., and Liu, H. (2004). Fus3-regulated Tec1 degradation through SCF^{Cdc4} determines MAPK signaling specificity during mating in yeast. **Cell** *119*, 981–990.

Christianson, J.C., and Ye, Y. (2014). Cleaning up in the endoplasmic reticulum: ubiquitin in charge. **Nat Struct Mol Biol** *21*, 325–335.

Christmann, M., Schmaler, T., Gordon, C., Huang, X., Bayram, Ö., Schinke, J., Stumpf, S., Dubiel, W., and Braus, G.H. (2013). Control of multicellular development by the physically interacting deneddylases DEN1/DenA and COP9 signalosome. **PLoS Genet** *9*, e1003275.

Chua, Y.S., Boh, B.K., Ponyeam, W., and Hagen, T. (2011). Regulation of Cullin RING E3 ubiquitin ligases by CAND1 *in vivo*. **PLoS ONE** *6*, e16071.

Chujo, M., Yoshida, S., Ota, A., Murata, K., and Kawai, S. (2015). Acquisition of the ability to assimilate mannitol by *Saccharomyces cerevisiae* through dysfunction of the general corepressor Tup1-Cyc8. **Appl Environ Microbiol** *81*, 9–16.

Chun, C.D., Liu, O.W., and Madhani, H.D. (2007). A link between virulence and homeostatic responses to hypoxia during infection by the human fungal pathogen *Cryptococcus neoformans*. **PLoS Pathog** *3*, e22.

Chung, D., Barker, B.M., Carey, C.C., Merriman, B., Werner, E.R., Lechner, B.E., Dhingra, S., Cheng, C., Xu, W., Blosser, S.J., et al. (2014). ChIP-seq and *in vivo* transcriptome analyses of the *Aspergillus fumigatus* SREBP SrbA reveals a new regulator of the fungal hypoxia response and virulence. **PLoS Pathog** *10*, e1004487.

Clague, M.J., Heride, C., and Urbé, S. (2015). The demographics of the ubiquitin system. **Trends Cell Biol** *25*, 417–426.

Cornelis, G.R. (2002). The *Yersinia* Ysc-Yop "Type III" weaponry. **Nat Rev Mol Cell Biol** *3*, 742–752.

Cox, J., and Mann, M. (2008). MaxQuant enables high peptide identification rates, individualized p.p.b.-range mass accuracies and proteome-wide protein quantification. **Nat Biotechnol** *26*, 1367–1372.

Cramer, R.A. (2016). In vivo veritas: *Aspergillus fumigatus* proliferation and pathogenesis - conditionally speaking. **Virulence** *7*, 7–10.

Cramer, R.A., Rivera, A., and Hohl, T.M. (2011). Immune responses against *Aspergillus fumigatus*: What have we learned? **Curr Opin Infect Dis** *24*, 315–322.

da Silva Ferreira, M.E., Kress, M.R.V.Z., Savoldi, M., Goldman, M.H.S., Härtl, A., Heinekamp, T., Brakhage, A.A., and Goldman, G.H. (2006). The *akuB*^{KU80} mutant deficient for nonhomologous end joining is a powerful tool for analyzing pathogenicity in *Aspergillus fumigatus*. **Eukaryot Cell** *5*, 207–211.

Dagenais, T.R.T., and Keller, N.P. (2009). Pathogenesis of *Aspergillus fumigatus* in invasive aspergillosis. **Clin Microbiol Rev** *22*, 447–465.

Davie, J.K., Edmondson, D.G., Coco, C.B., and Dent, S.Y.R. (2003). Tup1-Ssn6 interacts with multiple class I histone deacetylases *in vivo*. **J Biol Chem** *278*, 50158–50162.

Debeaupuis, J.P., Sarfati, J., Chazalet, V., and Latgé, J.P. (1997). Genetic diversity among clinical and environmental isolates of *Aspergillus fumigatus*. **Infect Immun** *65*, 3080–3085.

Denning, D.W. (1998). Invasive aspergillosis. **Clin Infect Dis** *26*, 781–803.

DeRisi, J.L., Iyer, V.R., and Brown, P.O. (1997). Exploring the metabolic and genetic control of gene expression on a genomic scale. **Science** *278*, 680–686.

Desimone, A.M., and Laney, J.D. (2010). Corepressor-directed preacetylation of histone H3 in promoter chromatin primes rapid transcriptional switching of cell-type-specific genes in yeast. **Mol Cell Biol** *30*, 3342–3356.

Dhingra, S., Andes, D., and Calvo, A.M. (2012). VeA regulates conidiation, gliotoxin production, and protease activity in the opportunistic human pathogen *Aspergillus fumigatus*. **Eukaryot Cell** *11*, 1531–1543.

Dhingra, S., Lind, A.L., Lin, H.-C., Tang, Y., Rokas, A., and Calvo, A.M. (2013). The fumagillin gene cluster, an example of hundreds of genes under *veA* control in *Aspergillus fumigatus*. **PLoS ONE** *8*, e77147.

Dokudovskaya, S., Veenhoff, L.M., Zhang, W., Kipper, J., Devos, D., Suprapto, A., Karni-Schmidt, O., Williams, R., Chait, B.T., Sali, A., et al. (2007). The molecular architecture of the nuclear pore complex. **Nature** *450*, 695–701.

Dolan, S.K., O'Keeffe, G., Jones, G.W., and Doyle, S. (2015). Resistance is not futile: Gliotoxin biosynthesis, functionality and utility. **Trends Microbiol** *23*, 419–428.

Dubiel, W. (2009). Resolving the CSN and CAND1 paradoxes. **Molecular Cell** *35*, 547–549.

Duda, D.M., Borg, L.A., Scott, D.C., Hunt, H.W., Hammel, M., and Schulman, B.A. (2008). Structural insights into NEDD8 activation of cullin-RING ligases: Conformational control of conjugation. **Cell** *134*, 995–1006.

Duyvesteijn, R.G.E., Van Wijk, R., Boer, Y., Rep, M., Cornelissen, B.J.C., and Haring, M.A. (2005). Frp1 is a *Fusarium oxysporum* F-box protein required for pathogenicity on tomato. **Mol Microbiol** *57*, 1051–1063.

Dyer, P.S., and O'Gorman, C.M. (2012). Sexual development and cryptic sexuality in fungi: insights from *Aspergillus* species. **FEMS Microbiol Rev** *36*, 165–192.

Emri, T., Szarvas, V., Orosz, E., Antal, K., Park, H., Han, K.-H., Yu, J.-H., and Pócsi, I. (2015). Core oxidative stress response in *Aspergillus nidulans*. **BMC Genomics** *16*, 478.

Enchev, R.I., Schreiber, A., Beuron, F., and Morris, E.P. (2010). Structural insights into the COP9 signalosome and its common architecture with the 26S proteasome lid and eIF3. **Structure** *18*, 518–527.

Enchev, R.I., Scott, D.C., da Fonseca, P.C.A., Schreiber, A., Monda, J.K., Schulman, B.A., Peter, M., and Morris, E.P. (2012). Structural basis for a reciprocal regulation between SCF and CSN. **Cell Rep** *2*, 1–12.

Ene, I.V., and Bennett, R.J. (2014). The cryptic sexual strategies of human fungal pathogens. **Nat Rev Microbiol** *12*, 239–251.

Fajardo-Somera, R.A., Jöhnk, B., Bayram, Ö., Valerius, O., Braus, G.H., and Riquelme, M. (2015). Dissecting the function of the different chitin synthases in vegetative growth and sexual development in *Neurospora crassa*. **Fungal Genet Biol** *75*, 30–45.

Finley, D., Ulrich, H.D., Sommer, T., and Kaiser, P. (2012). The ubiquitin-proteasome system of *Saccharomyces cerevisiae*. **Genetics** *192*, 319–360.

Finn, R.D., Bateman, A., Clements, J., Coggill, P., Eberhardt, R.Y., Eddy, S.R., Heger, A., Hetherington, K., Holm, L., Mistry, J., et al. (2014). Pfam: The protein families database. **Nucleic Acids Res** *42*, D222–D230.

Fleming, A.B., Beggs, S., Church, M., Tsukihashi, Y., and Pennings, S. (2014). The yeast Cyc8-Tup1 complex cooperates with Hda1p and Rpd3p histone deacetylases to robustly repress transcription of the subtelomeric *FLO1* gene. **Biochim Biophys Acta** *1839*, 1242–1255.

Flick, J.S., and Johnston, M. (1991). *GRR1* of *Saccharomyces cerevisiae* is required for glucose repression and encodes a protein with leucine-rich repeats. **Mol Cell Biol** *11*, 5101–5112.

Flipphi, M., Sun, J., Robellet, X., Karaffa, L., Fekete, E., Zeng, A.-P., and Kubiecek, C.P. (2009). Biodiversity and evolution of primary carbon metabolism in *Aspergillus nidulans* and other Aspergillus spp. **Fungal Genet Biol** *46 Suppl 1*, S19–S44.

Fox, H., Hickey, P.C., Fernández-Abalos, J.M., Lunness, P., Read, N.D., and Doonan, J.H. (2002). Dynamic distribution of BIMG[PP1] in living hyphae of *Aspergillus* indicates a novel role in septum formation. **Mol Microbiol** *45*, 1219–1230.

Frisvad, J.C., and Larsen, T.O. (2016). Extrolites of *Aspergillus fumigatus* and other pathogenic species in *Aspergillus* section *Fumigati*. **Front Microbiol** *6*, 1485.

Frisvad, J.C., Rank, C., Nielsen, K.F., and Larsen, T.O. (2009). Metabolomics of *Aspergillus fumigatus*. **Med Mycol** *47 Suppl 1*, S53–S71.

Galagan, J.E., Calvo, S.E., Cuomo, C., Ma, L.-J., Wortman, J.R., Batzoglou, S., Lee, S.-I., Baştürkmen, M., Spevak, C.C., Clutterbuck, J., et al. (2005). Sequencing of *Aspergillus nidulans* and comparative analysis with *A. fumigatus* and *A. oryzae*. **Nature** *438*, 1105–1115.

Galan, J.M., and Peter, M. (1999). Ubiquitin-dependent degradation of multiple F-box proteins by an autocatalytic mechanism. **Proc Natl Acad Sci USA** *96*, 9124–9129.

García, I., Mathieu, M., Nikolaev, I., Felenbok, B., and Scazzocchio, C. (2008). Roles of the *Aspergillus nidulans* homologues of Tup1 and Ssn6 in chromatin structure and cell viability. **FEMS Microbiol Lett** *289*, 146–154.

García-Sánchez, S., Mavor, A.L., Russell, C.L., Argimon, S., Dennison, P., Enjalbert, B., and Brown, A.J.P. (2005). Global roles of Ssn6 in Tup1- and Nrg1-dependent gene regulation in the fungal pathogen, *Candida albicans*. **Mol Biol Cell** *16*, 2913–2925.

Gardiner, D.M., and Howlett, B.J. (2005). Bioinformatic and expression analysis of the putative gliotoxin biosynthetic gene cluster of *Aspergillus fumigatus*. **FEMS Microbiol Lett** *248*, 241–248.

Gazendam, R.P., van Hamme, J.L., Tool, A.T.J., Hoogenboezem, M., van den Berg, J.M., Prins, J.M., Vitkov, L., van de Veerdonk, F.L., van den Berg, T.K., Roos, D., et al. (2016). Human neutrophils use different mechanisms to kill *Aspergillus fumigatus* conidia and hyphae: Evidence from phagocyte defects. **J Immunol** *196*, 1272–1283.

Georgiadou, S.P., and Kontoyiannis, D.P. (2012). Concurrent lung infections in patients with hematological malignancies and invasive pulmonary aspergillosis: How firm is the *Aspergillus* diagnosis? **J Infect** *65*, 262–268.

Gerke, J., and Braus, G.H. (2014). Manipulation of fungal development as source of novel secondary metabolites for biotechnology. **Appl Microbiol Biotechnol** *98*, 8443–8455.

Gerke, J., Bayram, Ö., Feussner, K., Landesfeind, M., Shelest, E., Feussner, I., and Braus, G.H. (2012). Breaking the silence: Protein stabilization uncovers silenced biosynthetic gene clusters in the fungus *Aspergillus nidulans*. **Appl Environ Microbiol** *78*, 8234–8244.

Glickman, M.H., and Ciechanover, A. (2002). The ubiquitin-proteasome proteolytic pathway: Destruction for the sake of construction. **Physiol Rev** *82*, 373–428.

Gounalaki, N., Tzamarias, D., and Vlassi, M. (2000). Identification of residues in the TPR domain of Ssn6 responsible for interaction with the Tup1 protein. **FEBS Lett** *473*, 37–41.

Grant, C.M., Luikenhuis, S., Beckhouse, A., Soderbergh, M., and Dawes, I.W. (2000). Differential regulation of glutaredoxin gene expression in response to stress conditions in the yeast *Saccharomyces cerevisiae*. **Biochim Biophys Acta** *1490*, 33–42.

Green, S.R., and Johnson, A.D. (2004). Promoter-dependent roles for the Srb10 cyclin-dependent kinase and the Hda1 deacetylase in Tup1-mediated repression in *Saccharomyces cerevisiae*. **Mol Biol Cell** *15*, 4191–4202.

Grossman, E., Medalia, O., and Zwerger, M. (2012). Functional architecture of the nuclear pore complex. **Annu Rev Biophys** *41*, 557–584.

Gu, Z.C., and Enenkel, C. (2014). Proteasome assembly. **Cell Mol Life Sci** *71*, 4729–4745.

Guo, M., Gao, F., Zhu, X., Nie, X., Pan, Y., and Gao, Z. (2015). MoGrr1, a novel F-box protein, is involved in conidiogenesis and cell wall integrity and is critical for the full virulence of *Magnaporthe oryzae*. **Appl Microbiol Biotechnol** *99*, 8075–8088.

Guttmann-Raviv, N., Martin, S., and Kassir, Y. (2002). Ime2, a meiosis-specific kinase in yeast, is required for destabilization of its transcriptional activator, Ime1. **Mol Cell Biol** *22*, 2047–2056.

Hagiwara, D., Suzuki, S., Kamei, K., Gonoi, T., and Kawamoto, S. (2014). The role of AtfA and HOG MAPK pathway in stress tolerance in conidia of *Aspergillus fumigatus*. **Fungal Genet Biol** *73*, 138–149.

Han, Y.-K., Kim, M.-D., Lee, S.-H., Yun, S.-H., and Lee, Y.-W. (2007). A novel F-box protein involved in sexual development and pathogenesis in *Gibberella zeae*. **Mol Microbiol** *63*, 768–779.

Hanahan, D., Ramamoorthy, V., Kaever, A., Gerke, J., Sabatini, L., Landesfeind, M., Fanning, S., Menant, A., Feussner, K., Praefcke, G.J.K., et al. (1983). Studies on transformation of *Escherichia coli* with plasmids. **J Mol Biol** *166*, 557–580.

Hanahan, D., Lim, F.Y., Vogt, N., Eddy, S.R., Smith, J.A., Shlezinger, N., Madhani, H.D., Smith, R.L., Cramer, R.A., Chia, A.J.L., et al. (1985). DNA cloning: A practical approach. **IRL Press**.

Hanlon, S.E., Rizzo, J.M., Tatomer, D.C., Lieb, J.D., and Buck, M.J. (2011). The stress response factors Yap6, Cin5, Phd1, and Skn7 direct targeting of the conserved corepressor Tup1-Ssn6 in *S. cerevisiae*. **PLoS ONE** *6*, e19060.

Hayakawa, A., Babour, A., Sengmanivong, L., and Dargemont, C. (2012). Ubiquitylation of the nuclear pore complex controls nuclear migration during mitosis in *S. cerevisiae*. **J Cell Biol** *196*, 19–27.

He, C., and Klionsky, D.J. (2009). Regulation mechanisms and signaling pathways of autophagy. **Annu Rev Genet** *43*, 67–93.

Hedayati, M.T., Azimi, Y., Droudinia, A., and Mousavi, B. (2015). Prevalence of chronic pulmonary aspergillosis in patients with tuberculosis from Iran. **Eur J Clin Microbiol Infect Dis** *34*, 1759–1765.

Heinekamp, T., Thywißen, A., Macheleidt, J., Keller, S., Valiante, V., and Brakhage, A.A. (2012). *Aspergillus fumigatus* melanins: Interference with the host endocytosis pathway and impact on virulence. **Front Microbiol** *3*, 440.

Helmstaedt, K., Schwier, E.U., Christmann, M., Nahlik, K., Westermann, M., Harting, R., Grond, S., Busch, S., and Braus, G.H. (2011). Recruitment of the inhibitor Cand1 to the cullin substrate adaptor site mediates interaction to the neddylation site. **Mol Biol Cell** *22*, 153–164.

Hicks, J., Lockington, R.A., Strauss, J., Dieringer, D., Kubicek, C.P., Kelly, J., and Keller, N. (2001). RcoA has pleiotropic effects on *Aspergillus nidulans* cellular development. **Mol Microbiol** *39*, 1482–1493.

Hillmann, F., Novohradská, S., Mattern, D.J., Forberger, T., Heinekamp, T., Westermann, M., Winckler, T., and Brakhage, A.A. (2015). Virulence determinants of the human pathogenic fungus *Aspergillus fumigatus* protect against soil amoeba predation. **Environ Microbiol** *17*, 2858–2869.

Hirsch, C., Gauss, R., Horn, S.C., Neuber, O., and Sommer, T. (2009). The ubiquitylation machinery of the endoplasmic reticulum. **Nature** *458*, 453–460.

Hoffmann, B., Valerius, O., Andermann, M., and Braus, G.H. (2001). Transcriptional autoregulation and inhibition of mRNA translation of amino acid regulator gene *cpcA* of filamentous fungus *Aspergillus nidulans*. **Mol Biol Cell** *12*, 2846–2857.

Hohl, T.M., and Feldmesser, M. (2007). *Aspergillus fumigatus*: Principles of pathogenesis and host defense. **Eukaryot Cell** *6*, 1953–1963.

Horn, F., Heinekamp, T., Kniemeyer, O., Pollmächer, J., Valiante, V., and Brakhage, A.A. (2012). Systems biology of fungal infection. **Front Microbiol** *3*, 108.

Hu, K., Li, W., Wang, H., Chen, K., Wang, Y., and Sang, J. (2012). Shp1, a regulator of protein phosphatase 1 Glc7, has important roles in cell morphogenesis, cell cycle progression and DNA damage response in *Candida albicans*. **Fungal Genet Biol** *49*, 433–442.

Hua, Z., and Vierstra, R.D. (2011). The cullin-RING ubiquitin-protein ligases. **Annu Rev Plant Biol** *62*, 299–334.

Hughes, A.L., Todd, B.L., and Espenshade, P.J. (2005). SREBP pathway responds to sterols and functions as an oxygen sensor in fission yeast. **Cell** *120*, 831–842.

Huibregtse, J.M., Scheffner, M., Beaudenon, S., and Howley, P.M. (1995). A family of proteins structurally and functionally related to the E6-AP ubiquitin-protein ligase. **Proc Natl Acad Sci USA** *92*, 2563–2567.

Inoue, H., Nojima, H., and Okayama, H. (1990). High efficiency transformation of *Escherichia coli* with plasmids. **Gene** *96*, 23–28.

Jonkers, W., and Rep, M. (2009). Lessons from fungal F-Box proteins. **Eukaryot Cell** *8*, 677–695.

Jonkers, W., van Kan, J.A.L., Tijm, P., Lee, Y.-W., Tudzynski, P., Rep, M., and Michielse, C.B. (2011). The *FRP1* F-box gene has different functions in sexuality, pathogenicity and metabolism in three fungal pathogens. **Mol Plant Pathol** *12*, 548–563.

Jöhnk, B. (2009). Comparison of the model organism *Aspergillus nidulans* and opportunistic pathogen *Aspergillus fumigatus* F-box protein encoding genes. Diploma thesis, **Georg-August-Universität, Göttingen**.

Karkowska-Kuleta, J., and Kozik, A. (2015). Cell wall proteome of pathogenic fungi. **Acta Biochim Pol** *62*, 339–351.

Karkowska-Kuleta, J., Rapala-Kozik, M., and Kozik, A. (2009). Fungi pathogenic to humans: Molecular bases of virulence of *Candida albicans*, *Cryptococcus neoformans* and *Aspergillus fumigatus*. **Acta Biochim Pol** *56*, 211–224.

Kato, N., Brooks, W., and Calvo, A.M. (2003). The expression of sterigmatocystin and penicillin genes in *Aspergillus nidulans* is controlled by *veA*, a gene required for sexual development. **Eukaryot Cell** *2*, 1178–1186.

Kim, H., Han, K., Kim, K., Han, D., Jahng, K., and Chae, K. (2002). The *veA* gene activates sexual development in *Aspergillus nidulans*. **Fungal Genet Biol** *37*, 72–80.

Kim, J.-H., Kim, J., Kim, D.-H., Ryu, G.-H., Bae, S.-H., and Seo, Y.-S. (2004). SCF^{hFBH1} can act as helicase and E3 ubiquitin ligase. **Nucleic Acids Res** *32*, 2287–2297.

Kirkin, V., McEwan, D.G., Novak, I., and Dikic, I. (2009). A role for ubiquitin in selective autophagy. **Molecular Cell** *34*, 259–269.

Kishi, T., and Yamao, F. (1998). An essential function of Grr1 for the degradation of Cln2 is to act as a binding core that links Cln2 to Skp1. **J Cell Sci** *111*, 3655–3661.

Kleiger, G., and Mayor, T. (2014). Perilous journey: A tour of the ubiquitin-proteasome system. **Trends Cell Biol** *24*, 352–359.

Komander, D., and Rape, M. (2012). The ubiquitin code. **Annu Rev Biochem** *81*, 203–229.

Kosugi, S., Hasebe, M., Tomita, M., and Yanagawa, H. (2009). Systematic identification of cell cycle-dependent yeast nucleocytoplasmic shuttling proteins by prediction of composite motifs. **Proc Natl Acad Sci USA** *106*, 10171–10176.

Krappmann, S., and Braus, G.H. (2005). Nitrogen metabolism of *Aspergillus* and its role in pathogenicity. **Med Mycol** *43 Suppl 1*, S31–S40.

Krappmann, S. (2006). Tools to study molecular mechanisms of *Aspergillus* pathogenicity. **Trends Microbiol** *14*, 356–364.

Krappmann, S., Bayram, Ö., and Braus, G.H. (2005). Deletion and allelic exchange of the *Aspergillus fumigatus veA* locus via a novel recyclable marker module. **Eukaryot Cell** *4*, 1298–1307.

Krappmann, S., Bignell, E.M., Reichard, U., Rogers, T., Haynes, K., and Braus, G.H. (2004). The *Aspergillus fumigatus* transcriptional activator CpcA contributes significantly to the virulence of this fungal pathogen. **Mol Microbiol** *52*, 785–799.

Krappmann, S., Jung, N., Medic, B., Busch, S., Prade, R.A., and Braus, G.H. (2006a). The *Aspergillus nidulans* F-box protein GrrA links SCF activity to meiosis. **Mol Microbiol** *61*, 76–88.

Krappmann, S., Sasse, C., and Braus, G.H. (2006b). Gene targeting in *Aspergillus fumigatus* by homologous recombination is facilitated in a nonhomologous end- joining-deficient genetic background. **Eukaryot Cell** *5*, 212–215.

Kuiper, L., and Ruijgrok, E.J. (2009). A review on the clinical use of inhaled amphotericin B. **J Aerosol Med Pulm Drug Deliv** *22*, 213–227.

Kumar, A., and Paietta, J.V. (1998). An additional role for the F-box motif: Gene regulation within the *Neurospora crassa* sulfur control network. **Proc Natl Acad Sci USA** *95*, 2417–2422.

Kupfahl, C., Heinekamp, T., Geginat, G., Ruppert, T., Härtl, A., Hof, H., and Brakhage, A.A. (2006). Deletion of the *gliP* gene of *Aspergillus fumigatus* results in loss of gliotoxin production but has no effect on virulence of the fungus in a low-dose mouse infection model. **Mol Microbiol** *62*, 292–302.

Kwon-Chung, K.J., and Sugui, J.A. (2009). What do we know about the role of gliotoxin in the pathobiology of *Aspergillus fumigatus*? **Med Mycol** *47 Suppl 1*, S97–S103.

Kwon-Chung, K.J., and Sugui, J.A. (2013). *Aspergillus fumigatus* - what makes the species a ubiquitous human fungal pathogen? **PLoS Pathog** *9*, e1003743.

Lamarre, C., Ibrahim-Granet, O., Du, C., Calderone, R., and Latgé, J.-P. (2007). Characterization of the *SKN7* ortholog of *Aspergillus fumigatus*. **Fungal Genet Biol** *44*, 682–690.

Lambou, K., Lamarre, C., Beau, R., Dufour, N., and Latgé, J.-P. (2010). Functional analysis of the superoxide dismutase family in *Aspergillus fumigatus*. **Mol Microbiol** *75*, 910–923.

Lamoth, F., Juvvadi, P.R., and Steinbach, W.J. (2016). Advances in *Aspergillus fumigatus* pathobiology. **Front Microbiol** *7*, 43.

Latgé, J.P. (1999). *Aspergillus fumigatus* and aspergillosis. **Clin Microbiol Rev** *12*, 310–350.

Latgé, J.P. (2001). The pathobiology of *Aspergillus fumigatus*. **Trends Microbiol** *9*, 382–389.

Leal, S.M., Vareechon, C., Cowden, S., Cobb, B.A., Latgé, J.-P., Momany, M., and Pearlman, E. (2012). Fungal antioxidant pathways promote survival against neutrophils during infection. **J Clin Invest** *122*, 2482–2498.

Lee, B.-Y., Han, S.-Y., Choi, H.G., Kim, J.H., Han, K.-H., and Han, D.-M. (2005). Screening of growth- or development-related genes by using genomic library with inducible promoter in *Aspergillus nidulans*. **J Microbiol** *43*, 523–528.

Lee, I.R., Morrow, C.A., and Fraser, J.A. (2013). Nitrogen regulation of virulence in clinically prevalent fungal pathogens. **FEMS Microbiol Lett** *345*, 77–84.

Lee, J.E., Sweredoski, M.J., Graham, R.L.J., Kolawa, N.J., Smith, G.T., Hess, S., and Deshaies, R.J. (2011). The steady-state repertoire of human SCF ubiquitin ligase complexes does not require ongoing Nedd8 conjugation. **Mol Cell Proteomics** *10*, M110.006460.

Lessing, F., Kniemeyer, O., Wozniok, I., Loeffler, J., Kurzai, O., Haertl, A., and Brakhage, A.A. (2007). The *Aspergillus fumigatus* transcriptional regulator AfYap1 represents the major regulator for defense against reactive oxygen intermediates but is dispensable for pathogenicity in an intranasal mouse infection model. **Eukaryot Cell** *6*, 2290–2302.

Li, J.-M., and Jin, J. (2012). CRL ubiquitin ligases and DNA damage response. **Front Oncol** *2*, 29.

Li, L., Stoeckert, C.J., and Roos, D.S. (2003). OrthoMCL: Identification of ortholog groups for eukaryotic genomes. **Genome Res** *13*, 2178–2189.

Li, W.J., Wang, Y.M., Zheng, X.D., Shi, Q.M., Zhang, T.T., Bai, C., Li, D., Sang, J.L., and Wang, Y. (2006). The F-box protein Grr1 regulates the stability of Ccn1, Cln3 and Hof1 and cell morphogenesis in *Candida albicans*. **Mol Microbiol** *62*, 212–226.

Li, Y., and Hao, B. (2010). Structural basis of dimerization-dependent ubiquitination by the SCF^{Fbx4} ubiquitin ligase. **J Biol Chem** *285*, 13896–13906.

Liebmann, B., Mühleisen, T.W., Müller, M., Hecht, M., Weidner, G., Braun, A., Brock, M., and Brakhage, A.A. (2004a). Deletion of the *Aspergillus fumigatus* lysine biosynthesis gene *lysF* encoding homoaconitase leads to attenuated virulence in a low-dose mouse infection model of invasive aspergillosis. **Arch Microbiol** *181*, 378–383.

Liebmann, B., Müller, M., Braun, A., and Brakhage, A.A. (2004b). The cyclic AMP-dependent protein kinase A network regulates development and virulence in *Aspergillus fumigatus*. **Infect Immun** *72*, 5193–5203.

Lind, A.L., Wisecaver, J.H., Smith, T.D., Feng, X., Calvo, A.M., and Rokas, A. (2015). Examining the evolution of the regulatory circuit controlling secondary metabolism and development in the fungal genus *Aspergillus*. **PLoS Genet** *11*, e1005096.

Liu, T.-B., Wang, Y., Stukes, S., Chen, Q., Casadevall, A., and Xue, C. (2011). The F-Box protein Fbp1 regulates sexual reproduction and virulence in *Cryptococcus neoformans*. **Eukaryot Cell** *10*, 791–802.

Liu, Z., and Karmarkar, V. (2008). Groucho/Tup1 family co-repressors in plant development. **Trends Plant Sci** *13*, 137–144.

Loeb, J.D., Kerentseva, T.A., Pan, T., Sepulveda-Becerra, M., and Liu, H. (1999). *Saccharomyces cerevisiae* G1 cyclins are differentially involved in invasive and pseudohyphal growth independent of the filamentation mitogen-activated protein kinase pathway. **Genetics** *153*, 1535–1546.

López-Berges, M.S., Hera, C., Sulyok, M., Schäfer, K., Capilla, J., Guarro, J., and Di Pietro, A. (2013). The velvet complex governs mycotoxin production and virulence of *Fusarium oxysporum* on plant and mammalian hosts. **Mol Microbiol** *87*, 49–65.

Machida, M., Asai, K., Sano, M., Tanaka, T., Kumagai, T., Terai, G., Kusumoto, K.-I., Arima, T., Akita, O., Kashiwagi, Y., et al. (2005). Genome sequencing and analysis of *Aspergillus oryzae*. **Nature** *438*, 1157–1161.

Mandel, S.A., Fishman-Jacob, T., and Youdim, M.B.H. (2012). Targeting Skp1, an ubiquitin E3 ligase component found decreased in sporadic parkinson's disease. **Neurodegener Dis** *10*, 220–223.

McCluskey, K., Wiest, A., and Plamann, M. (2010). The Fungal Genetics Stock Center: A repository for 50 years of fungal genetics research. **J Biosci** *35*, 119–126.

McCormick, A., Loeffler, J., and Ebel, F. (2010). *Aspergillus fumigatus*: Contours of an opportunistic human pathogen. **Cell Microbiol** *12*, 1535–1543.

Meister, C., Kolog Gulko, M., Köhler, A.M., and Braus, G.H. (2015). The devil is in the details: comparison between COP9 signalosome (CSN) and the LID of the 26S proteasome. **Curr Genet** *62*, 129–136.

Merhej, J., Delaveau, T., Guitard, J., Palancade, B., Hennequin, C., Garcia, M., Lelandais, G., and Devaux, F. (2015). Yap7 is a transcriptional repressor of nitric oxide oxidase in yeasts, which arose from neofunctionalization after whole genome duplication. **Mol Microbiol** *96*, 951–972.

Merlet, J., Burger, J., Gomes, J.-E., and Pintard, L. (2009). Regulation of cullin-RING E3 ubiquitin-ligases by neddylation and dimerization. **Cell Mol Life Sci** *66*, 1924–1938.

Miao, Y., Liu, D., Li, G., Li, P., Xu, Y., Shen, Q., and Zhang, R. (2015). Genome-wide transcriptomic analysis of a superior biomass-degrading strain of *A. fumigatus* revealed active lignocellulose-degrading genes. **BMC Genomics** *16*, 459.

Miguel-Rojas, C., and Hera, C. (2013). Proteomic identification of potential target proteins regulated by the SCF^{Fbp1}-mediated proteolysis pathway in *Fusarium oxysporum*. **Mol Plant Pathol** *14*, 934–945.

Miguel-Rojas, C., and Hera, C. (2016). The F-box protein Fbp1 functions in the invasive growth and cell wall integrity mitogen-activated protein kinase (MAPK) pathways in *Fusarium oxysporum*. **Mol Plant Pathol** *17*, 55–64.

Mizuno, T., Nakazawa, N., Remgsamrarn, P., Kunoh, T., Oshima, Y., and Harashima, S. (1998). The Tup1-Ssn6 general repressor is involved in repression of *IME1* encoding a transcriptional activator of meiosis in *Saccharomyces cerevisiae*. **Curr Genet** *33*, 239–247.

Monia, B.P., Ecker, D.J., Jonnalagadda, S., Marsh, J., Gotlib, L., Butt, T.R., and Crooke, S.T. (1989). Gene synthesis, expression, and processing of human ubiquitin carboxyl extension proteins. **J Biol Chem** *264*, 4093–4103.

Nahlik, K., Dumkow, M., Bayram, Ö., Helmstaedt, K., Busch, S., Valerius, O., Gerke, J., Hoppert, M., Schwier, E., Opitz, L., et al. (2010). The COP9 signalosome mediates transcriptional and metabolic response to hormones, oxidative stress protection and cell wall rearrangement during fungal development. **Mol Microbiol** *78*, 964–979.

Natorff, R., Piotrowska, M., and Paszewski, A. (1998). The *Aspergillus nidulans* sulphur regulatory gene *sconB* encodes a protein with WD40 repeats and an F-box. **Mol Gen Genet** *257*, 255–263.

Natorff, R., Sieńko, M., Brzywczy, J., and Paszewski, A. (2003). The *Aspergillus nidulans metR* gene encodes a bZIP protein which activates transcription of sulphur metabolism genes. **Mol Microbiol** *49*, 1081–1094.

Nelson, D.E., Randle, S.J., and Laman, H. (2013). Beyond ubiquitination: The atypical functions of Fbxo7 and other F-box proteins. **Open Biol** *3*, 130131.

Ng, C.H., Akhter, A., Yurko, N., Burgener, J.M., Rosonina, E., and Manley, J.L. (2015). Sumoylation controls the timing of Tup1-mediated transcriptional deactivation. **Nat Commun** *6*, 6610.

Nierman, W.C., Pain, A., Anderson, M.J., Wortman, J.R., Kim, H.S., Arroyo, J., Berriman, M., Abe, K., Archer, D.B., Bermejo, C., et al. (2005). Genomic sequence of the pathogenic and allergenic filamentous fungus *Aspergillus fumigatus*. **Nature** *438*, 1151–1156.

O'Gorman, C.M., Fuller, H.T., and Dyer, P.S. (2009). Discovery of a sexual cycle in the opportunistic fungal pathogen *Aspergillus fumigatus*. **Nature** *457*, 471–474.

Olma, M.H., and Dikic, I. (2013). Cullins getting undressed by the protein exchange factor Cand1. **Cell** *153*, 14–16.

Osmani, A.H., Oakley, B.R., and Osmani, S.A. (2006). Identification and analysis of essential *Aspergillus nidulans* genes using the heterokaryon rescue technique. **Nat Protoc** *1*, 2517–2526.

Ouni, I., Flick, K., and Kaiser, P. (2010). A transcriptional activator is part of an SCF ubiquitin ligase to control degradation of its cofactors. **Molecular Cell** *40*, 954–964.

Owens, R.A., Durairaj, G., Hammel, S., Chen, B.B., Sheridan, K.J., Busby, T.M., Jones, G.W., Cardozo, T., Lahudkar, S., Christmann, M., et al. (2014). A proteomic approach to investigating gene cluster expression and secondary metabolite functionality in *Aspergillus fumigatus*. **PLoS ONE** *9*, e106942.

Palaiomylitou, M., Tartas, A., Vlachakis, D., Tzamarias, D., and Vlassi, M. (2008). Investigating the structural stability of the Tup1-interaction domain of Ssn6: Evidence for a conformational change on the complex. **Proteins** *70*, 72–82.

Paris, S., Debeaupuis, J.-P., Crameri, R., Carey, M., Charlès, F., Prévost, M.C., Schmitt, C., Philippe, B., and Latgé, J.-P. (2003a). Conidial hydrophobins of *Aspergillus fumigatus*. **Appl Environ Microbiol** *69*, 1581–1588.

Paris, S., Wysong, D., Debeaupuis, J.-P., Shibuya, K., Philippe, B., Diamond, R.D., and Latgé, J.-P. (2003b). Catalases of *Aspergillus fumigatus*. **Infect Immun** *71*, 3551–3562.

Park, C.-W., and Ryu, K.-Y. (2014). Cellular ubiquitin pool dynamics and homeostasis. **BMB Rep** *47*, 475–482.

Park, H.S., Bayram, Ö., Braus, G.H., Kim, S.C., and Yu, J.-H. (2012). Characterization of the *velvet* regulators in *Aspergillus fumigatus*. **Mol Microbiol** *86*, 937–953.

Parnell, E.J., and Stillman, D.J. (2011). Shields up: The Tup1-Cyc8 repressor complex blocks coactivator recruitment. **Genes Dev** *25*, 2429–2435.

Pashkova, N., Gakhar, L., Winistorfer, S.C., Yu, L., Ramaswamy, S., and Piper, R.C. (2010). WD40 repeat propellers define a ubiquitin-binding domain that regulates turnover of F Box proteins. **Molecular Cell** *40*, 433–443.

Paul, E., Zhu, Z.I., Landsman, D., and Morse, R.H. (2015). Genome-wide association of mediator and RNA polymerase II in wild-type and mediator mutant yeast. **Mol Cell Biol** *35*, 331–342.

Perez-Nadales, E., Nogueira, M.F.A., Baldin, C., Castanheira, S., Ghalid, El, M., Grund, E., Lengeler, K., Marchegiani, E., Mehrotra, P.V., Moretti, M., et al. (2014). Fungal model systems and the elucidation of pathogenicity determinants. **Fungal Genet Biol** *70*, 42–67.

Perrin, R.M., Fedorova, N.D., Bok, J.W., Cramer, R.A., Wortman, J.R., Kim, H.S., Nierman, W.C., and Keller, N.P. (2007). Transcriptional regulation of chemical diversity in *Aspergillus fumigatus* by LaeA. **PLoS Pathog** *3*, e50.

Petroski, M.D., and Deshaies, R.J. (2005). Function and regulation of cullin-RING ubiquitin ligases. **Nat Rev Mol Cell Biol** *6*, 9–20.

Pierce, N.W., Lee, J.E., Liu, X., Sweredoski, M.J., Graham, R.L.J., Larimore, E.A., Rome, M., Zheng, N., Clurman, B.E., Hess, S., et al. (2013). Cand1 promotes assembly of new SCF complexes through dynamic exchange of F Box proteins. **Cell** *153*, 206–215.

Piłsyk, S., Natorff, R., Sieńko, M., and Paszewski, A. (2007). Sulfate transport in *Aspergillus nidulans*: A novel gene encoding alternative sulfate transporter. **Fungal Genet Biol** *44*, 715–725.

Pontecorvo, G., Roper, J.A., and Forbes, E. (1953). Genetic recombination without sexual reproduction in *Aspergillus niger*. **J Gen Microbiol** *8*, 198–210.

Proft, M., and Struhl, K. (2002). Hog1 kinase converts the Sko1-Cyc8-Tup1 repressor complex into an activator that recruits SAGA and SWI/SNF in response to osmotic stress. **Molecular Cell** *9*, 1307–1317.

Punt, P.J., and van den Hondel, C.A. (1992). Transformation of filamentous fungi based on hygromycin B and phleomycin resistance markers. **Meth Enzymol** *216*, 447–457.

Punt, P.J., Oliver, R.P., Dingemanse, M.A., Pouwels, P.H., and van den Hondel, C.A. (1987). Transformation of *Aspergillus* based on the hygromycin B resistance marker from *Escherichia coli*. **Gene** *56*, 117–124.

Purnapatre, K., Gray, M., Piccirillo, S., and Honigberg, S.M. (2005). Glucose inhibits meiotic DNA replication through SCF^{Grr1p}-dependent destruction of Ime2p kinase. **Mol Cell Biol** *25*, 440–450.

Ramamoorthy, V., Dhingra, S., Kincaid, A., Shantappa, S., Feng, X., and Calvo, A.M. (2013). The putative C2H2 transcription factor MtfA is a novel regulator of secondary metabolism and morphogenesis in *Aspergillus nidulans*. **PLoS ONE** *8*, e74122.

Rambach, G., Blum, G., Latgé, J.-P., Fontaine, T., Heinekamp, T., Hagleitner, M., Jeckström, H., Weigel, G., Würtinger, P., Pfaller, K., et al. (2015). Identification of *Aspergillus fumigatus* surface components that mediate interaction of conidia and hyphae with human platelets. **J Infect Dis** *212*, 1140–1149.

Ramírez-Zavala, B., and Domínguez, Á. (2008). Evolution and phylogenetic relationships of APSES proteins from *Hemiascomycetes*. **FEMS Yeast Res** *8*, 511–519.

Reichard, U., Büttner, S., Eiffert, H., Staib, F., and Rüchel, R. (1990). Purification and characterisation of an extracellular serine proteinase from *Aspergillus fumigatus* and its detection in tissue. **J Med Microbiol** *33*, 243–251.

Reuter, S., Thomson, N.R., and McNally, A. (2012). Evolutionary dynamics of the *Yersinia enterocolitica* complex. **Adv Exp Med Biol** *954*, 15–22.

Rhodes, J.C. (2006). *Aspergillus fumigatus*: Growth and virulence. **Med Mycol** *44 Suppl 1*, S77–S81.

Rizzo, J.M., Mieczkowski, P.A., and Buck, M.J. (2011). Tup1 stabilizes promoter nucleosome positioning and occupancy at transcriptionally plastic genes. **Nucleic Acids Res** *39*, 8803–8819.

Rocchi, S., Reboux, G., and Millon, L. (2015). Azole resistance with environmental origin: What alternatives for the future? **J Mycol Med** *25*, 249–256.

Rogov, V., Dötsch, V., Johansen, T., and Kirkin, V. (2014). Interactions between autophagy receptors and ubiquitin-like proteins form the molecular basis for selective autophagy. **Molecular Cell** *53*, 167–178.

Rouillon, A., Barbey, R., Patton, E.E., Tyers, M., and Thomas, D. (2000). Feedback-regulated degradation of the transcriptional activator Met4 is triggered by the SCF^{Met30} complex. **Embo J** *19*, 282–294.

Roy, A., Shin, Y.J., Cho, K.H., and Kim, J.-H. (2013). Mth1 regulates the interaction between the Rgt1 repressor and the Ssn6-Tup1 corepressor complex by modulating PKA-dependent phosphorylation of Rgt1. **Mol Biol Cell** *24*, 1493–1503.

Samar, D., Kieler, J.B., and Klutts, J.S. (2015). Identification and deletion of *Tft1*, a predicted glycosyltransferase necessary for cell wall β-1,3;1,4-glucan synthesis in *Aspergillus fumigatus*. **PLoS ONE** *10*, e0117336.

Sarikas, A., Hartmann, T., and Pan, Z.-Q. (2011). The cullin protein family. **Genome Biol** *12*, 220.

Sarikaya Bayram, Ö., Bayram, Ö., Feussner, K., Kim, J.-H., Kim, H.-S., Kaever, A., Feussner, I., Chae, K.-S., Han, D.-M., Han, K.-H., et al. (2014). Membrane-bound methyltransferase complex VapA-VipC-VapB guides epigenetic control of fungal development. **Dev Cell** *29*, 406–420.

Sarikaya Bayram, Ö., Bayram, Ö., Valerius, O., Park, H.S., Irniger, S., Gerke, J., Ni, M., Han, K.-H., Yu, J.-H., and Braus, G.H. (2010). LaeA control of velvet family regulatory proteins for light-dependent development and fungal cell-type specificity. **PLoS Genet** *6*, e1001226.

Sasse, C., Bignell, E.M., Hasenberg, M., Haynes, K., Gunzer, M., Braus, G.H., and Krappmann, S. (2008). Basal expression of the *Aspergillus fumigatus* transcriptional activator CpcA is sufficient to support pulmonary aspergillosis. **Fungal Genet Biol** *45*, 693–704.

Scharf, D.H., Brakhage, A.A., and Mukherjee, P.K. (2015). Gliotoxin- bane or boon? **Environ Microbiol**, doi:10.1111/1462-2920.13080.

Scharf, D.H., Heinekamp, T., Remme, N., Hortschansky, P., Brakhage, A.A., and Hertweck, C. (2012). Biosynthesis and function of gliotoxin in *Aspergillus fumigatus*. **Appl Microbiol Biotechnol** *93*, 467–472.

Scheffner, M., Nuber, U., and Huibregtse, J.M. (1995). Protein ubiquitination involving an E1-E2-E3 enzyme ubiquitin thioester cascade. **Nature** *373*, 81–83.

Scherer, M., Wei, H., Liese, R., and Fischer, R. (2002). *Aspergillus nidulans* catalase-peroxidase gene (*cpeA*) is transcriptionally induced during sexual development through the transcription factor StuA. **Eukaryot Cell** *1*, 725–735.

Schmaler-Ripcke, J., Sugareva, V., Gebhardt, P., Winkler, R., Kniemeyer, O., Heinekamp, T., and Brakhage, A.A. (2009). Production of pyomelanin, a second type of melanin, via the tyrosine degradation pathway in *Aspergillus fumigatus*. **Appl Environ Microbiol** *75*, 493–503.

Schmidt, M.W., Mcquary, P.R., Wee, S., Hofmann, K., and Wolf, D.A. (2009). F-Box-directed CRL complex assembly and regulation by the CSN and CAND1. **Molecular Cell** *35*, 586–597.

Schmittgen, T.D., and Livak, K.J. (2008). Analyzing real-time PCR data by the comparative C_T method. **Nat Protoc** *3*, 1101–1108.

Schoberle, T.J., Svahn, K.S., Leiter, É., Liu, T.-B., Nguyen-Coleman, C.K., Helmstaedt, K., Hughes, M., Kosugi, S., Herold, J., Culp, D.W., et al. (2014). A novel C2H2 transcription factor that regulates *gliA* expression interdependently with GliZ in *Aspergillus fumigatus*. **PLoS Genet** *10*, e1004336.

Schrettl, M., and Haas, H. (2011). Iron homeostasis - Achilles' heel of *Aspergillus fumigatus*? **Curr Opin Microbiol** *14*, 400–405.

Schrettl, M., Beckmann, N., Varga, J., Heinekamp, T., Jacobsen, I.D., Jöchl, C., Moussa, T.A., Wang, S., Gsaller, F., Blatzer, M., et al. (2010). HapX-mediated adaption to iron starvation is crucial for virulence of *Aspergillus fumigatus*. **PLoS Pathog** *6*, e1001124.

Schrettl, M., Bignell, E., Kragl, C., Sabiha, Y., Loss, O., Eisendle, M., Wallner, A., Arst, H.N., Haynes, K., and Haas, H. (2007). Distinct roles for intra- and extracellular siderophores during *Aspergillus fumigatus* infection. **PLoS Pathog** *3*, e128.

Schuster-Böckler, B., Schultz, J., and Rahmann, S. (2004). HMM logos for visualization of protein families. **BMC Bioinformatics** *5*, 7.

Schwartz, A.L., and Ciechanover, A. (2009). Targeting proteins for destruction by the ubiquitin system: Implications for human pathobiology. **Annu Rev Pharmacol Toxicol** *49*, 73–96.

Sekiya, T., and Zaret, K.S. (2007). Repression by Groucho/TLE/Grg proteins: Genomic site recruitment generates compacted chromatin *in vitro* and impairs activator binding *in vivo*. **Molecular Cell** *28*, 291–303.

Sheppard, D.C., Doedt, T., Chiang, L.Y., Kim, H.S., Chen, D., Nierman, W.C., and Filler, S.G. (2005). The *Aspergillus fumigatus* StuA protein governs the up-regulation of a discrete transcriptional program during the acquisition of developmental competence. **Mol Biol Cell** *16*, 5866–5879.

Shevchenko, A., Wilm, M., Vorm, O., and Mann, M. (1996). Mass spectrometric sequencing of proteins from silver-stained polyacrylamide gels. **Anal Chem** *68*, 850–858.

Shin, K.-S., Kim, Y.H., and Yu, J.-H. (2015). Proteomic analyses reveal the key roles of BrlA and AbaA in biogenesis of gliotoxin in *Aspergillus fumigatus*. **Biochem Biophys Res Commun** *463*, 428–433.

Sieńko, M., Natorff, R., Skoneczny, M., Kruszewska, J., Paszewski, A., and Brzywczy, J. (2014). Regulatory mutations affecting sulfur metabolism induce environmental stress response in *Aspergillus nidulans*. **Fungal Genet Biol** *65*, 37–47.

Skaar, J.R., Pagan, J.K., and Pagano, M. (2009). SnapShot: F box proteins I. **Cell** *137*, 1160–1160.e1161.

Skaar, J.R., Pagan, J.K., and Pagano, M. (2013). Mechanisms and function of substrate recruitment by F-box proteins. **Nat Rev Mol Cell Biol** *14*, 369–381.

Smith, J.A., and Kauffman, C.A. (2012). Pulmonary fungal infections. **Respirology** *17*, 913–926.

Smith, R.L., and Johnson, A.D. (2000). Turning genes off by Ssn6-Tup1: A conserved system of transcriptional repression in eukaryotes. **Trends Biochem Sci** *25*, 325–330.

Smith, T.D., and Calvo, A.M. (2014). The *mtfA* transcription factor gene controls morphogenesis, gliotoxin production, and virulence in the opportunistic human pathogen *Aspergillus fumigatus*. **Eukaryot Cell** *13*, 766–775.

Snelders, E., Huis In t Veld, R.A.G., Rijs, A.J.M.M., Kema, G.H.J., Melchers, W.J.G., and Verweij, P.E. (2009). Possible environmental origin of resistance of *Aspergillus fumigatus* to medical triazoles. **Appl Environ Microbiol** *75*, 4053–4057.

Son, S., and Osmani, S.A. (2009). Analysis of all protein phosphatase genes in *Aspergillus nidulans* identifies a new mitotic regulator, Fcp1. **Eukaryot Cell** *8*, 573–585.

Soriani, F.M., Malavazi, I., Savoldi, M., Espeso, E., Dinamarco, T.M., Bernardes, L.A.S., Ferreira, M.E.S., Goldman, M.H.S., and Goldman, G.H. (2010). Identification of possible targets of the *Aspergillus fumigatus* CRZ1 homologue, CrzA. **BMC Microbiol** *10*, 12.

Soriani, F.M., Malavazi, I., da Silva Ferreira, M.E., Savoldi, M., Zeska Kress, von, M.R., de Souza Goldman, M.H., Loss, O., Bignell, E., and Goldman, G.H. (2008). Functional characterization of the *Aspergillus fumigatus* CRZ1 homologue, CrzA. **Mol Microbiol** *67*, 1274–1291.

Soucy, T.A., Smith, P.G., Milhollen, M.A., Berger, A.J., Gavin, J.M., Adhikari, S., Brownell, J.E., Burke, K.E., Cardin, D.P., Critchley, S., et al. (2009). An inhibitor of NEDD8-activating enzyme as a new approach to treat cancer. **Nature** *458*, 732–736.

Spruck, C., Strohmaier, H., Watson, M., Smith, A.P., Ryan, A., Krek, T.W., and Reed, S.I. (2001). A CDK-independent function of mammalian Cks1: Targeting of SCF^{Skp2} to the CDK inhibitor p27^{Kip1}. **Molecular Cell** *7*, 639–650.

Stark, M.J. (1996). Yeast protein serine/threonine phosphatases: Multiple roles and diverse regulation. **Yeast** *12*, 1647–1675.

Steinbach, W.J. (2013). Are we there yet? Recent progress in the molecular diagnosis and novel antifungal targeting of *Aspergillus fumigatus* and invasive aspergillosis. **PLoS Pathog** *9*, e1003642.

Stromnaes, O., and Garber, E.D. (1963). Heterocaryosis and the parasexual cycle in *Aspergillus fumigatus*. **Genetics** *48*, 653–662.

Su, S.S., and Mitchell, A.P. (1993). Molecular characterization of the yeast meiotic regulatory gene *RIM1*. **Nucleic Acids Res** *21*, 3789–3797.

Sueiro-Olivares, M., Fernandez-Molina, J.V., Abad-Diaz-de-Cerio, A., Gorospe, E., Pascual, E., Guruceaga, X., Ramirez-Garcia, A., Garaizar, J., Hernando, F.L., Margareto, J., et al. (2015). *Aspergillus fumigatus* transcriptome response to a higher temperature during the earliest steps of germination monitored using a new customized expression microarray. **Microbiol** *161*, 490–502.

Sugareva, V., Härtl, A., Brock, M., Hübner, K., Rohde, M., Heinekamp, T., and Brakhage, A.A. (2006). Characterisation of the laccase-encoding gene *abr2* of the dihydroxynaphthalene-like melanin gene cluster of *Aspergillus fumigatus*. **Arch Microbiol** *186*, 345–355.

Svahn, K.S., Göransson, U., Chryssanthou, E., Olsen, B., Sjölin, J., and Strömstedt, A.A. (2014). Induction of gliotoxin secretion in *Aspergillus fumigatus* by bacteria-associated molecules. **PLoS ONE** *9*, e93685.

Szewczyk, E., Nayak, T., Oakley, C.E., Edgerton, H., Xiong, Y., Taheri-Talesh, N., Osmani, S.A., Oakley, B.R., and Oakley, B. (2006). Fusion PCR and gene targeting in *Aspergillus nidulans*. **Nat Protoc** *1*, 3111–3120.

Tao, L., and Yu, J.-H. (2011). AbaA and WetA govern distinct stages of *Aspergillus fumigatus* development. **Microbiol** *157*, 313–326.

Taus, T., Köcher, T., Pichler, P., Paschke, C., Schmidt, A., Henrich, C., and Mechtler, K. (2011). Universal and confident phosphorylation site localization using phosphoRS. **J Proteome Res** *10*, 5354–5362.

Teixeira, M.C., Monteiro, P.T., Guerreiro, J.F., Gonçalves, J.P., Mira, N.P., Santos, dos, S.C., Cabrito, T.R., Palma, M., Costa, C., Francisco, A.P., et al. (2014). The YEASTRACT database: An upgraded information system for the analysis of gene and genomic transcription regulation in *Saccharomyces cerevisiae*. **Nucleic Acids Res** *42*, D161–D166.

Tekaia, F., Lazcano, A., and Dujon, B. (1999). The genomic tree as revealed from whole proteome comparisons. **Genome Res** *9*, 550–557.

Tekaia, F., and Latgé, J.-P. (2005). *Aspergillus fumigatus*: Saprophyte or pathogen? **Curr Opin Microbiol** *8*, 385–392.

Terfrüchte, M., Joehnk, B., Fajardo-Somera, R., Braus, G.H., Riquelme, M., Schipper, K., and Feldbrügge, M. (2014). Establishing a versatile Golden Gate cloning system for genetic engineering in fungi. **Fungal Genet Biol** *62*, 1–10.

Tesfaigzi, J., Smith-Harrison, W., and Carlson, D.M. (1994). A simple method for reusing western blots on PVDF membranes. **BioTechniques** *17*, 268–269.

Texari, L., Dieppois, G., Vinciguerra, P., Contreras, M.P., Groner, A., Letourneau, A., and Stutz, F. (2013). The nuclear pore regulates *GAL1* gene transcription by controlling the localization of the SUMO protease Ulp1. **Molecular Cell** *51*, 807–818.

Thompson, A., Schäfer, J., Kuhn, K., Kienle, S., Schwarz, J., Schmidt, G., Neumann, T., Johnstone, R., Mohammed, A.K.A., and Hamon, C. (2003). Tandem mass tags: A novel quantification strategy for comparative analysis of complex protein mixtures by MS/MS. **Anal Chem** *75*, 1895–1904.

Thön, M., Al-Abdallah, Q., Hortschansky, P., and Brakhage, A.A. (2007). The thioredoxin system of the filamentous fungus *Aspergillus nidulans*: Impact on development and oxidative stress response. **J Biol Chem** *282*, 27259–27269.

Todd, B.L., Stewart, E.V., Burg, J.S., Hughes, A.L., and Espenshade, P.J. (2006a). Sterol regulatory element binding protein is a principal regulator of anaerobic gene expression in fission yeast. **Mol Cell Biol** *26*, 2817–2831.

Todd, R.B., Hynes, M.J., and Andrianopoulos, A. (2006b). The *Aspergillus nidulans rcoA* gene is required for *veA*-dependent sexual development. **Genetics** *174*, 1685–1688.

Tomee, J.F., and Kauffman, H.F. (2000). Putative virulence factors of *Aspergillus fumigatus*. **Clin Exp Allergy** *30*, 476–484.

Tyrrell, A., Flick, K., Kleiger, G., Zhang, H., Deshaies, R.J., and Kaiser, P. (2010). Physiologically relevant and portable tandem ubiquitin-binding domain stabilizes polyubiquitylated proteins. **Proc Natl Acad Sci USA** *107*, 19796–19801.

Tzamarias, D., and Struhl, K. (1994). Functional dissection of the yeast Cyc8-Tup1 transcriptional co-repressor complex. **Nature** *369*, 758–761.

Valiante, V., Macheleidt, J., Föge, M., and Brakhage, A.A. (2015). The *Aspergillus fumigatus* cell wall integrity signaling pathway: drug target, compensatory pathways, and virulence. **Front Microbiol** *6*, 325.

Voigt, O., and Pöggeler, S. (2013). Autophagy genes *Smatg8* and *Smatg4* are required for fruiting-body development, vegetative growth and ascospore germination in the filamentous ascomycete *Sordaria macrospora*. **Autophagy** *9*, 33–49.

Wagener, J., Echtenacher, B., Rohde, M., Kotz, A., Krappmann, S., Heesemann, J., and Ebel, F. (2008). The putative α-1,2-mannosyltransferase AfMnt1 of the opportunistic fungal pathogen *Aspergillus fumigatus* is required for cell wall stability and full virulence. **Eukaryot Cell** *7*, 1661–1673.

Wang, D., Sun, J., Yu, H.-L., Li, C.-X., Bao, J., and Xu, J.-H. (2012). Maximum saccharification of cellulose complex by an enzyme cocktail supplemented with cellulase from newly isolated *Aspergillus fumigatus* ECU0811. **Appl Biochem Biotechnol** *166*, 176–186.

Wang, H., Wang, L., Erdjument-Bromage, H., Vidal, M., Tempst, P., Jones, R.S., and Zhang, Y. (2004). Role of histone H2A ubiquitination in polycomb silencing. **Nature** *431*, 873–878.

Watson, A.D., Edmondson, D.G., Bone, J.R., Mukai, Y., Yu, Y., Du, W., Stillman, D.J., and Roth, S.Y. (2000). Ssn6-Tup1 interacts with class I histone deacetylases required for repression. **Genes Dev** *14*, 2737–2744.

Watson, I.R., Irwin, M.S., and Ohh, M. (2011). NEDD8 pathways in cancer, Sine Quibus Non. **Cancer Cell** *19*, 168–176.

Wei, N., Chamovitz, D.A., and Deng, X.W. (1994). Arabidopsis COP9 is a component of a novel signaling complex mediating light control of development. **Cell** *78*, 117–124.

Wei, N., Serino, G., and Deng, X.-W. (2008). The COP9 signalosome: More than a protease. **Trends Biochem Sci** *33*, 592–600.

Winkelströter, L.K., Bom, V.L.P., de Castro, P.A., Ramalho, L.N.Z., Goldman, M.H.S., Brown, N.A., Rajendran, R., Ramage, G., Bovier, E., Reis, dos, T.F., et al. (2015). High osmolarity glycerol response PtcB phosphatase is important for *Aspergillus fumigatus* virulence. **Mol Microbiol** *96*, 42–54.

Wong, K.H., and Struhl, K. (2011). The Cyc8-Tup1 complex inhibits transcription primarily by masking the activation domain of the recruiting protein. **Genes Dev** *25*, 2525–2539.

Wu, J., and Miller, B.L. (1997). *Aspergillus* asexual reproduction and sexual reproduction are differentially affected by transcriptional and translational mechanisms regulating *stunted* gene expression. **Mol Cell Biol** *17*, 6191–6201.

Wurzer, B., Zaffagnini, G., Fracchiolla, D., Turco, E., Abert, C., Romanov, J., and Martens, S. (2015). Oligomerization of p62 allows for selection of ubiquitinated cargo and isolation membrane during selective autophagy. **eLife** *4*.

Wyatt, T.T., Wösten, H.A.B., and Dijksterhuis, J. (2013). Fungal spores for dispersion in space and time. **Adv Appl Microbiol** *85*, 43–91.

Xie, Y., and Varshavsky, A. (2002). UFD4 lacking the proteasome-binding region catalyses ubiquitination but is impaired in proteolysis. **Nat Cell Biol** *4*, 1003–1007.

Ye, X.S., Lee, S.L., Wolkow, T.D., McGuire, S.L., Hamer, J.E., Wood, G.C., and Osmani, S.A. (1999). Interaction between developmental and cell cycle regulators is required for morphogenesis in *Aspergillus nidulans*. **Embo J** *18*, 6994–7001.

Ye, Y., and Rape, M. (2009). Building ubiquitin chains: E2 enzymes at work. **Nat Rev Mol Cell Biol** *10*, 755–764.

Yu, J.-H. (2010). Regulation of development in *Aspergillus nidulans* and *Aspergillus fumigatus*. **Mycobiology** *38*, 229–237.

Zeska Kress, von, M.R., Harting, R., Bayram, Ö., Christmann, M., Irmer, H., Valerius, O., Schinke, J., Goldman, G.H., and Braus, G.H. (2012). The COP9 signalosome counteracts the accumulation of cullin SCF ubiquitin E3 RING ligases during fungal development. **Mol Microbiol** *83*, 1162–1177.

Zhang, C., Meng, X., Wei, X., and Lu, L. (2016). Highly efficient CRISPR mutagenesis by microhomology-mediated end joining in *Aspergillus fumigatus*. **Fungal Genet Biol** *86*, 47–57.

Zhao, Y., Su, H., Zhou, J., Feng, H., Zhang, K.-Q., and Yang, J. (2014). The APSES family proteins in fungi: Characterizations, evolution and functions. **Fungal Genet Biol** *81*, 271–280.

Zhou, H., Hu, H., Zhang, L., Li, R., Ouyang, H., Ming, J., and Jin, C. (2007). *O*-mannosyltransferase 1 in *Aspergillus fumigatus* (AfPmt1p) is crucial for cell wall integrity and conidium morphology, especially at an elevated temperature. **Eukaryot Cell** *6*, 2260–2268.

Zhou, P., and Howley, P.M. (1998). Ubiquitination and degradation of the substrate recognition subunits of SCF ubiquitin-protein ligases. **Molecular Cell** *2*, 571–580.

Curriculum vitae

Bastian Jöhnk

Birth date

January 5, 1980, in Eckernförde, Germany

School education

1986–1990	Elementary school
	Albert-Schweizer-Grundschule, Eckernförde
1990–1999	High school
	Integrierte Gesamtschule, Eckernförde
	School leaving exam: Abitur
1999-2000	Civilian service at Commit-cbf Mainz, Germany
	Personal assistant to people with severe disabilities
2000-2001	International experience
	6 months in Thailand

Higher education

2001-2009	Studies in biology, Georg-August-University Göttingen
	Diploma, Biology (major: Microbiology, minor: Chemistry and Human Genetics)
	Diploma thesis: "Comparison of the model organism *Aspergillus nidulans* and opportunistic pathogen *Aspergillus fumigatus* F-box protein encoding genes"
since 2010	PhD studies, Georg-August-University Göttingen
	Since 2010, I am a PhD-student at the Department of Microbiology and Genetics of Prof. Dr. Gerhard H. Braus, where I continue my work on F-box proteins in the opportunistic human pathogen *Aspergillus fumigatus*.

Awards

Poster award 2011:

"Interplay between protein degradation, oxidative stress response, polar growth and virulence in the pathogen *A. fumigatus*"

Presented at the Annual Conference of the Association for General and Applied Microbiology, VAAM, April 3-6, 2011, Karlsruhe, Germany.

Young Investigator Award for a Poster presentation:

"Analysis of the F-box protein encoding genes of the opportunistic human pathogen *Aspergillus fumigatus*"

Presented at the 4ths FEBS Advanced Lecture Course: "Human Fungal Pathogens, HFP", May 7-13, 2011, La Colle sur Loup, France.

Publications

Jöhnk, B., Bayram, Ö., Valerius, O., Heinekamp, T., Jacobsen, I.D., and Braus, G.H. (2016) SCF ubiquitin ligase F-box protein Fbx15 controls nuclear co-repressor localization, stress response and virulence of the human pathogen *Aspergillus fumigatus*. Under review.

Fajardo-Somera, R.A., **Jöhnk, B.**, Bayram, Ö., Valerius, O., Braus, G.H., and Riquelme, M. (2015) Dissecting the function of the different chitin synthases in vegetative growth and sexual development in *Neurospora crassa*. Fungal Genet Biol *75*, 30-45.

Terfrüchte, M., **Joehnk, B.**, Fajardo-Somera, R., Braus, G.H., Riquelme, M., Schipper, K., and Feldbrügge, M. (2014) Establishing a versatile Golden Gate cloning system for genetic engineering in fungi. Fungal Genet Biol *62*, 1-10.

Bayram, Ö., Bayram, Ö.S., Valerius, O., **Jöhnk, B.**, and Braus G.H. (2012) Identification of protein complexes from filamentous fungi with tandem affinity purification. Humana Press *944*, 191-205.

List of Oral and Poster Presentations

B. Jöhnk, Ö. Bayram, T. Heinekamp, A. A. Brakhage and G. H. Braus (2011), Poster

"Interplay between protein degradation, oxidative stress response, polar growth and virulence in the pathogen *A. fumigatus*"

Presented at the Annual Conference of the Association for General and Applied Microbiology, VAAM, April 3-6, 2011, Karlsruhe, Germany.

B. Jöhnk, Ö. Bayram, T. Heinekamp, A. A. Brakhage and G. H. Braus (2011), Poster

"Analysis of the F-box protein encoding genes of the opportunistic human pathogen *Aspergillus fumigatus*"

Presented at the 4ths FEBS Advanced Lecture Course: "Human Fungal Pathogens, HFP", May 7-13, 2011, La Colle sur Loup, France.

B. Jöhnk, Ö. Bayram, O. Valerius, T. Heinekamp, A. A. Brakhage and G. H. Braus (2012), Poster

"Analysis of the F-box protein encoding genes of the opportunistic human pathogen *Aspergillus fumigatus*"

Presented at the Annual Conference of the Association for General and Applied Microbiology, VAAM, March 18-21, 2012, Tübingen, Germany.

B. Jöhnk and G. H. Braus (2012), Talk

"Impact of F-box-proteins on fungal oxidative stress response and polar growth"

Presented at the Second Workshop Germany Mexico, Determinants of Polarized Growth and Development in Filamentous Fungi, DFG-CONACyT Research Unit 1334, May 31-June 2, 2012, Mexico City, Mexico.

B. Jöhnk, Ö. Bayram, O. Valerius, T. Heinekamp, A. A. Brakhage and G. H. Braus (2012), Poster

"Analysis of the F-box protein encoding genes of the opportunistic human pathogen *Aspergillus fumigatus*"

Presented at the Annual Conference of the Association for General and Applied Microbiology, VAAM, March 18-21, 2012, Tübingen, Germany.

B. Jöhnk, Ö. Bayram, O. Valerius, T. Heinekamp, I. D. Jacobsen, A. A. Brakhage and G. H. Braus (2013), Talk

"F-box protein 15 (Fbx15) links virulence of *Aspergillus fumigatus* to protein degradation and stress response"

Presented at the Tenth International *Aspergillus* Meeting, Asperfest, March 11-12, 2013, Asilomar Conference Grounds, Pacific Grove, CA, USA.

B. Jöhnk, Ö. Bayram, O. Valerius, T. Heinekamp, I. D. Jacobsen, A. A. Brakhage and G. H. Braus (2013), Poster

"F-box protein 15 (Fbx15) links virulence of *Aspergillus fumigatus* to protein degradation and stress response"

Presented at the 27th Fungal Genetics Conference, March 12-17, 2013, Asilomar Conference Grounds, Pacific Grove, CA, USA.

B. Jöhnk, Ö. Bayram, O. Valerius, T. Heinekamp, I. D. Jacobsen, A. A. Brakhage and G. H. Braus (2013), Talk

"F-box protein 15 (Fbx15) links virulence of *Aspergillus fumigatus* to protein degradation and stress response"

Presented at the CICESE Seminar, Center for Scientific Research and Higher Education at Ensenada, Department of Microbiology, March 20, 2013, Ensenada, Baja California, Mexico.

B. Jöhnk, Ö. Bayram, O. Valerius, T. Heinekamp, I. D. Jacobsen, A. A. Brakhage and G. H. Braus (2013), Talk

"F-box protein 15 (Fbx15) links virulence of *Aspergillus fumigatus* to protein degradation and stress response"

Presented at the XI IFB Conference, September 29-October 3, 2013, Karlsruhe, Germany.

B. Jöhnk (2014), Talk

"GFP-immunoprecipitation (GFP-trap)"

Presented at the First International Workshop, Determinants of Polarized Growth and Development in Fungi, Cinvestav / LANGEBIO, October 3-17, 2014, Irapuato, Mexico.

B. Jöhnk, Ö. Bayram, O. Valerius, T. Heinekamp, I. D. Jacobsen and G. H. Braus (2015), Talk

"The F-box protein Fbx15 of *Aspergillus fumigatus* controls nuclear transport of the transcriptional co-repressor SsnF/Ssn6p upon oxidative stress"

Presented at the 49th DMykG Scientific Conference, September 16-19, 2015, Jena, Germany.

B. Jöhnk, Ö. Bayram, O. Valerius, T. Heinekamp, I. D. Jacobsen and G. H. Braus (2015), Talk

"The F-box protein Fbx15 of *Aspergillus fumigatus* controls nuclear transport of the transcriptional co-repressor SsnF/Ssn6p upon oxidative stress"

Presented at the 11th Molecular Biology of Fungi Conference, October 7-9, 2015, Berlin, Germany.

Acknowledgements